Carl von Ossietzky Universität Oldenburg

Department für Informatik
Fakultät II – Informatik, Wirtschafts- und Rechtswissenschaften

Multi-objective Blackstart of an impaired ICT-reliant Renewable Energy System

Von der Fakultät für Informatik, Wirtschafts- und Rechtswissenschaften der Carl von Ossietzky Universität Oldenburg zur Erlangung des Grades und Titels

Doktorin der Naturwissenschaften (Dr. rer. nat.)

angenommene Dissertation von

Frau Sanja Stark

geboren am 10. März 1991 in Bremen

Gutachter:

Prof. Dr. Sebastian Lehnhoff
Fakultät II – Informatik, Wirtschafts- und Rechtswissenschaften,
Carl von Ossietzky Universität Oldenburg

Weitere Gutachter:

Prof. Dr.-Ing. Reinhard German
Lehrstuhl für Informatik 7 (Rechnernetze und Kommunikationssysteme),
Friedrich-Alexander-Universität Erlangen-Nürnberg

Tag der Disputation: 09. Januar 2025

Abstract

A blackstart is a set of procedures to restore the electrical power system after a blackout without external resources. Since a widespread blackout severely impacts our daily lives, rapid power system restoration is critical. By introducing advanced information and communication technologies (ICT) into distribution grids, distributed energy resources (DERs) can support existing restoration approaches, e.g., by creating island grids in the distribution system. Finding the optimal composition of an island grid is a complex optimization problem that an intelligent automated restoration service can solve. The role of the ICT system is to support this restoration service by providing monitoring and control functions. However, due to their interdependencies, a blackout in the power system would also affect the ICT system. In this case, a distributed restoration service – executed by a Multi-Agent System (MAS) – can be more effective than a centralized approach.

While agent-based restoration algorithms are already a popular concept in the literature, the power and ICT systems interdependencies during a blackstart with a MAS have yet to be considered. This PhD project aims to fill this gap by developing an agent-based restoration algorithm that restores power and ICT systems in parallel. The restoration process is regarded as a multi-objective optimization problem and both the restored load and ICT should be maximized. Using a co-simulation platform, the algorithm is evaluated using different interconnected power and ICT scenarios. Specifically, the effect of considering ICT restoration as a separate objective is studied by comparing a version of the algorithm with ICT (MOO3) and without (MOO2).

Abstract (German)

Ein Schwarzstart ist ein Verfahren zur Wiederherstellung der Stromversorgung nach einem Blackout. Da ein großflächiger Stromausfall gravierende Folgen hat, ist ein schneller Wiederaufbau des Stromnetzes entscheidend. Mit Hilfe von neuen Informations- und Kommunikationstechnologien (IKT) in Verteilungsnetzen können dezentrale Energieanlagen (DEA) die bestehenden Wiederaufbaukonzepte unterstützen, z. B. durch Inselnetze im Verteilungsnetz. Der Aufbau eines Inselnetzes ist ein komplexes Optimierungsproblem, bei dessen Lösung intelligente Algorithmen unterstützen können. Die Rolle des IKT-Systems besteht in diesem Fall darin, diese Algorithmen durch die Bereitstellung von Überwachungs- und Steuerungsfunktionen zu unterstützen. Aufgrund der wechselseitigen Abhängigkeiten würde sich ein Stromausfall jedoch auch auf das IKT-System auswirken. In diesem Fall kann ein verteilter Netzwiederaufbau - ausgeführt von einem Multiagentensystem (MAS) - effektiver sein als ein zentraler Ansatz.

Agentenbasierter Netzwiederaufbau wurde in der Literatur schon an vielen Stellen untersucht, doch die wechselseitigen Abhängigkeiten zwischen Strom- und IKT Systemen während eines Schwarzstarts wurden bisher noch nicht berücksichtigt. Daher soll in dieser Dissertation ein agentenbasierter Algorithmus zum Netzwiederaufbau entwickelt werden, der Strom- und IKT-Systeme parallel wiederherstellt. Der Wiederaufbau wird als ein multikriterielles Optimierungsproblem betrachtet, bei dem sowohl die wiederhergestellte Last als auch die Kommunikation maximiert werden sollen. Unter Verwendung einer Co-Simulationsplattform wird der Algorithmus anhand verschiedener Strom- und IKT-Szenarien bewertet. Insbesondere werden die Auswirkungen von IKT in der Zielfunktion untersucht, indem Versionen des Algorithmus mit IKT (MOO3) und ohne (MOO2) verglichen werden.

Acknowledgement

Diese Dissertation wäre ohne die Unterstützung, Ermutigung und Zusammenarbeit vieler Menschen nicht möglich gewesen, denen ich an dieser Stelle meinen herzlichen Dank aussprechen möchte.

Mein besonderer Dank gilt meinem Doktorvater, Herrn Prof. Dr. Sebastian Lehnhoff, für seine fachliche Unterstützung und sein konstruktives Feedback während der gesamten Promotionszeit. Ich habe seine stets wertschätzende und offene Kommunikation sehr geschätzt und konnte mich jederzeit mit Fragen an ihn wenden. Ebenso danke ich meinem Zweitgutachter, Herrn Prof. Dr.-Ing. Reinhard German, dessen wertvolle Anmerkungen mir geholfen haben, zentrale Aspekte meiner Arbeit weiter zu schärfen. Mein Dank gilt auch den weiteren Mitgliedern meiner Prüfungskommission, Frau Prof. Dr.-Ing. Astrid Nieße als Vorsitzende sowie Frau Dr.-Ing. Frederike Bruns.

Während meiner Promotion war ich im Forschungsbereich Energie am OFFIS – Institut für Informatik in Oldenburg tätig. Mein besonderer Dank gilt den Leitenden meiner Forschungsgruppe *Distributed Artificial Intelligence (DAI)*, Dr. Stefanie Holly und Dr. Martin Tröschel. Vor allem Stefanie hat mir nicht nur den Rücken freigehalten, damit ich mich auf meine Dissertation konzentrieren konnte, sondern hat mir auch geholfen, das Ziel nicht aus den Augen zu verlieren - besonders auf den letzten Metern. Ihre Motivation und ihr Zuspruch waren mir eine große Unterstützung. Ebenso danke ich meinen Kolleginnen und Kollegen in der DAI-Gruppe für den fachlichen Austausch und die stets angenehme und freundliche Arbeitsatmosphäre. Ein besonderer Dank gilt auch Dr. Jörg Bremer, dessen wertvolle Diskussionen und fachlicher Input mir immer wieder geholfen haben, die richtigen nächsten Schritte zu finden. Meiner Projektpartnerin Anna Volkova von der Universität Passau danke ich für die inspirierende und angenehme Zusammenarbeit. Ihre Expertise war ein wesentlicher Beitrag zu dieser Arbeit, und unsere gemeinsame Forschung hat mir stets große Freude bereitet.

Meiner Familie und meinen Freunden danke ich von Herzen für ihre Geduld und ihre beständige Unterstützung auf diesem Weg. Sie haben mir geholfen, die richtige Balance zwischen Forschung und Erholung zu finden, und mir gezeigt, wie wichtig es ist, auch in intensiven Phasen Pausen einzulegen und den Kopf freizubekommen.

Mein besonderer Dank gilt meinem Mann, Dr.-Ing. Anand Narayan. Unsere unzähligen inhaltlichen Diskussionen – sei es während der Arbeitszeit, bei Spaziergängen oder beim Sonntagsfrühstück – sowie sein Trost und seine liebevolle Motivation in schwierigen und frustrierenden Momenten waren für mich von unschätzbarem Wert. Ohne ihn hätte ich diese Dissertation sicher nicht erfolgreich abgeschlossen.

Diese Arbeit wurde gefördert durch die Deutsche Forschungsgemeinschaft (DFG) – Projektnummer 360475113 – als Teil des Schwerpunktprogrammes DFG SPP 1984 - Hybride und multimodale Energiesysteme: Systemtheoretische Methoden für die Transformation und den Betrieb komplexer Netze.

Contents

1 Introduction

Nearly all systems relevant to a modern society's safety, health, and economy, such as food and water, information and communication technologies (ICT), or transportation, depend on the power system. Therefore, the power system is considered a safety-critical infrastructure.

While most critical customers, such as hospitals and central communication nodes, have an emergency power supply, it only lasts about 8+ hours [11]. This means that especially wide-area (e.g., several states in Germany) and long-lasting (e.g., several days to weeks) blackouts can have disastrous effects, as presented for example by the *Büro für Technikfolgen-Abschätzung beim Deutschen Bundestag – TAB* (Office of Technology Assessment at the German Bundestag) in a study from 2011 [79]. The study vividly describes how the problems that would occur immediately after a blackout – from traffic chaos due to failed traffic lights to people stuck in elevators to trains at a standstill – would evolve into severe constraints on society. These include fuel shortages as gas pumps fail, the shutdown of all rail and air travel, the unavailability of drinking water, and drastic shortages of critical staple foods.

Fortunately, blackouts of this magnitude are very rare today. In many cases, the power system's contingency measures are sufficient to resolve unstable system states without causing a complete blackout. If a blackout can not be prevented, all transmission system operators (TSOs) have adequate restoration plans and are well prepared due to regular training. The restoration process usually starts at the transmission level, using a generator with blackstart capability or a generator in island mode to energize a first line, thereby providing power to more generators. When sufficient power is available, loads at the distribution level are reconnected. Distributed energy resources (DER) are typically switched off so that the lower voltage grid can be treated as a mere load, and the possible uncertain feed-in of DER does not have to be considered [110]. The whole process is manually coordinated by the TSO in the area where the blackout occurred. As a last step, the resulting island grid must be synchronized with the rest of the interconnected system [100].

This preparation makes the probability of a major blackout very low, especially in Europe. In 2016, the median SAIDI (System Average Interruption Duration Index) across all European countries was only 76 minutes, including exceptional events (see [21] for a detailed comparison between the countries).

1.1 Blackouts in the Power System

However, even with reliable grid infrastructure and a well-prepared restoration concept, the total restoration time can still be long enough to cause serious problems. Table 1.1 shows examples of past major European blackouts and their respective restoration times. It can be seen that the time required to restore a power grid after a major blackout ranges from just two hours to several days or even weeks. The reason for the long restoration often lies in the necessary repair work of the infrastructure, for example, in the case of the Münsterland blackout from 2005, where heavy snowfall destroyed overhead power lines.

Tab. 1.1.: Overview of past blackouts

Year	Area	Customers not served	Restoration Time	Reference
2003	Italy	56 Million	Up to 18h	[5]
2003	Denmark and Sweden	5 Million	7 hours	[55]
2005	Münsterland	250.000	Up to 6 weeks	[87]
2006	Germany, France, Italy, Belgium, Spain, and Portugal	15 Million	2 hours	[99]
2007	Netherlands	50.000	3 days	[41]
2015	Netherlands	1 Million	5 hours	[105]
2015	Ukraine	225.000	Up to 6 hours	[6]

When analyzing the root causes of blackouts, natural disasters like the snowstorm in the Münsterland blackout are among the most common. Figure 1.1 summarizes causes for power outages by occurrence for 140 worldwide outage data from 1965 to 2012 taken from [9]. It can be seen that most blackouts are caused by either equipment failure or natural disasters. For this kind of root cause, it is possible to use conventional risk management to measure and evaluate the probability of different events leading to a blackout and prepare the system accordingly.

However, the distribution of these root causes may change in the future. The energy transition is making the power system more complex. The increase of renewables in the grid leads to an increase in the diversity of generation, geographical diversity,

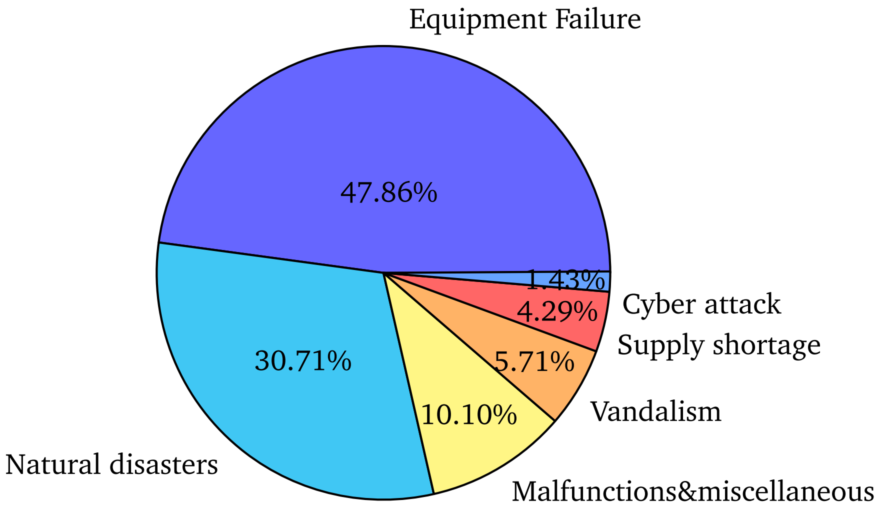

Fig. 1.1.: Causes for power outages from [9]

rising demand and changing consumption patterns, and a growing strain on electricity grids [3]. At the same time, the digitalization of the energy system is progressing, leading to increased automation and communication, especially in the distribution grid. Both these developments lead to new risk factors that can potentially increase the risk for wide-area, long-lasting blackouts in the future [3].

1.2 Island Grids and Automated Restoration

At the same time, both decarbonization and digitalization also bring certain advantages that allow the development of new concepts to reduce the duration of blackouts. The future digitalized power system, especially the distribution grid, will have specific characteristics that support so-called islanding: The creation of small, balanced island grids within the power system that can help to reduce the outage time for (critical) customers. These characteristics include large numbers of DER, battery storages, grid-forming converters, remote-controllable switches, and advanced ICT for monitoring and control [12]. In July 2024, the four German TSOs published a document to supplement the previous list of grid restoration measures [1]. It explicitly includes specific measures for implementing island grids in the distribution grid, showing the relevance of this concept in the near future.

Since it has to be assumed that there is not enough generation to serve all the loads, a decision must be made on which nodes to connect. The optimal island grid formation depends on numerous constraints, such as the current distribution of demand and supply, the limitations of power system equipment, or potential faults in power system infrastructure, thus resulting in a complex optimization problem [64]. The step-wise reconnection of nodes defines the restoration problem, which belongs to the NP-hard complexity class [62] and has the following properties [110]:

- Combinatorial (due to the large number of switching elements)
- Nonlinear (due to the nonlinear nature of power flow constraints)
- Non-differentiable (because any change in a switch status may change the values of objectives and constraints, meaning two solutions that differ in one switching operation can have completely different fitness values)
- Constrained (because of radiality and the operational voltage and current restrictions)
- Multi-objective (for example, maximizing the amount of restored load and minimizing the number of switching operations)

Solving this complex optimization problem is an essential part of blackstarting an island grid, as it is the first step before the technical blackstarting process (starting generators, re-connecting grid parts) can be conducted.

Automated restoration algorithms can help solve the problem and coordinate the large number of DER during the restoration process. This requires careful coordination between the different elements, which is enabled by the advanced ICT infrastructure in the distribution system. A popular approach to solve this problem in an automated manner is to use an agent-based restoration algorithm. Here, different relevant parts of the power system are represented by individual software agents that exchange information via messages and work together to organize a restoration process (see, for example, [29], [61], [66], [84], [92], [108]). Compared to a fully centralized approach, distributed MAS can solve optimization problems with reduced communication requirements due to their distributed information sharing that does not rely on a central controller [97]. These Multi-Agent Systems (MAS) can be organized in different architectures, e.g., hybrid centralized-decentralized [29], hierarchical [66] or fully decentralized [61], depending on how exactly the power system is to be represented. Many different optimization approaches are possible, such as rule-based [92], consensus-based [108], or heuristic [84]. Typically, the focus is on challenges from the power system side, such as balancing load and generation and dealing with transient effects during restoration while assuming the ICT system is fully functional.

1.3 Challenges and Research Gap

While some parts of the communication infrastructure might have emergency power, a certain level of impairment still has to be expected in the blackout areas, leaving parts of the grid uncontrollable [103]. This is especially relevant in the case of a wide-area blackout, where medium and low voltage distribution grids would likely use public cellular communication networks to exchange information and send control commands to power system equipment [30], [66]. The weak points in this public communication infrastructure are the base stations, which only work as long as the installed backup battery power is available – if there is any [80]. Combined with the potential for rapid battery discharge due to increased communications network load, base stations may only operate for a few minutes or hours without power. It is, therefore, reasonable to assume that the communications infrastructure would be (at least partially) unavailable or degraded during a wide-area blackout. Thus, the power system and the ICT system must be restored in a complementary manner. This results in a new objective for the restoration process, namely the rapid restoration of the ICT system to gain more observation and control over other parts of the network and to support the restoration of the power system.

Some approaches already consider a certain level of impairment in the ICT system for their MAS design and ensure robustness against link failures and message loss, proving that agents can work with limited communication [29], [30], [59], [66], [108]. However, the focus here is only on the failures in the ICT system. It does not consider the restoration of the ICT infrastructure itself, nor how the restoration of the ICT can support the restoration of the power system. Power system restoration is highly dependent on the ICT system since only those parts of the network that are reachable by communication can be considered in the restoration process. In addition, unstable communication can increase the uncertainty of the variables in the restoration process. An automated restoration process comes with specific Quality of Service (QoS) requirements that, if not met, can reduce the algorithm's success or block it altogether. Conversely, power system restoration positively affects the interdependent ICT infrastructure by supplying power to critical ICT nodes and improving connectivity. This is also confirmed in [7], where the authors use a central optimization approach to show how independent restoration of power and ICT system leads to improper utilization of resources. They conclude that a restoration process should always consider the interdependencies by including ICT in the objective function and the constraints.

As stated before, power system restoration is known to be a multi-objective optimization (MOO) problem. Different objectives – apart from load restoration – have already been considered in different multi-agent-based approaches, e.g., minimizing the number of switching operations and maximizing the likelihood of the success of the restoration process (in case of uncertainty) [91]. However, the active restoration of the ICT system has not yet been included in the objective function. Therefore, a multi-agent-based approach that solves the multi-objective restoration problem, including ICT in the objective function, is missing. This algorithm can be used to study the interdependencies between power and ICT during restoration and evaluate the efficiency of a parallel restoration process.

It should be noted that this is only relevant under the assumption that a) there is not enough generation to restore all loads and therefore, it is necessary to select which nodes to restore, and b) load restoration and ICT restoration are conflicting objectives, i.e., critical ICT infrastructure elements are not necessarily connected to those PS nodes that have the highest load anyway. In addition, it requires an iterative restoration process that not only performs a single restoration step but continually attempts to extend existing island networks with the newly restored additional communications infrastructure.

1.4 Research Questions and Artefacts

The main research question of this thesis is **How to blackstart an ICT-reliant distribution system with high DER penetration using MAS?**. "Blackstart" means that the grid is in a total blackout state, and initially, no already functioning island is available. The term "ICT-reliant" emphasizes that the restoration process and the control of the resulting islanded grid require communication. The term "distribution system" defines the grid level on which this thesis focuses and distinguishes it from the restoration process of a transmission grid. With "high DER penetration," it is clear that this thesis assumes a future grid structure with a large number of generation devices in the distribution grid, which is a prerequisite for the blackstart process to work. Finally, "MAS" defines the method used in this thesis.

This research question is divided into several subquestions. Specifically, this thesis investigates the hypothesis *that the overall performance (in terms of total restored load) of an agent-based restoration algorithm in distribution networks can be improved by considering ICT as a separate objective in the optimization problem*. Figure 1.2

gives an overview of the research questions and the resulting artifacts, which will be explained in the following:

RQ-1 **How to formulate the multi-objective optimization problem considering the ICT system (impairment and restoration)?** The answer to this research question is the formalization of the multi-objective island grid restoration problem, specifically considering an ICT performance value for each resulting island grid. This performance value has to capture the level of ICT impairment in the grid and improve with the restoration of the ICT system until the best possible value (= the full restoration of the ICT system) is reached.

RQ-2 **How to design the MAS considering ICT impairment?** This research question focuses on the architecture of the MAS that will coordinate the restoration process. Potential negative effects on the restoration algorithm due to the ICT impairment need to be considered in the architecture design.

RQ-3 **How to implement the optimization problem in the designed MAS?** This research question now combines the results from RQ-1 and RQ-2. It aims to design and develop a restoration algorithm based on the developed architecture capable of solving the formulated optimization problem.

RQ-4 **How to test and validate the developed MAS using a co-simulation framework?** Finally, a large part of this thesis will be to test the developed restoration algorithm and study the hypothesis. This will be done with empirical methods, such as executing the algorithm in a simulation model of the defined use case to observe the algorithm's behavior in a realistic environment. This requires an adequate simulation environment.

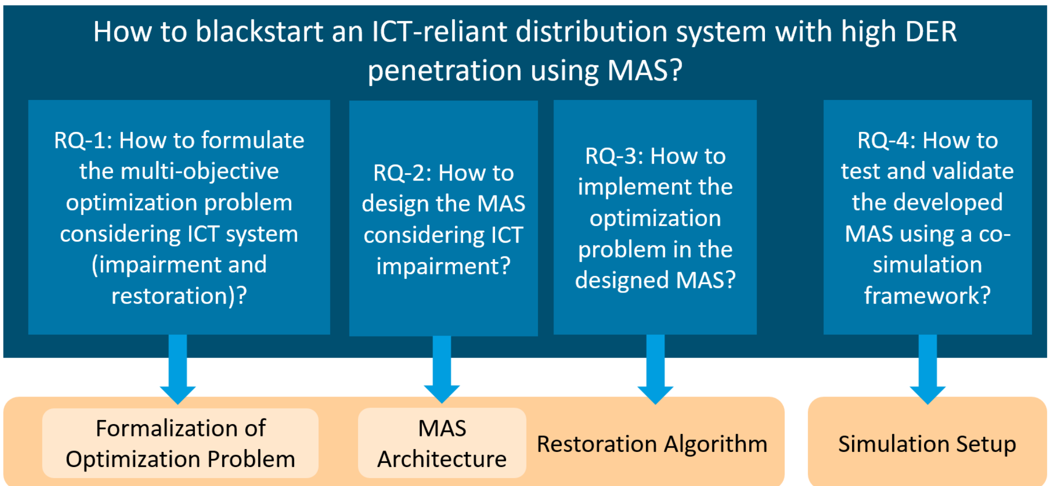

Fig. 1.2.: Overview of research questions and artifacts

The two main artifacts that will be developed to answer the research questions are 1) the agent-based restoration algorithm and 2) the simulation setup. A set of functional requirements is defined, which should be satisfied by the artifacts.

The restoration algorithm should:

FR-1 **Restore a distribution grid from blackout state by solving the optimization problem using a heuristic.** The first part of this requirement is derived from the scenario described in the motivation: A long-lasting, wide-area blackout that leaves the distribution system without power and small, local island systems should be used to restart parts of the system and serve customers until the overall restoration process can be performed. The underlying assumption is that not all nodes can be connected (due to generation constraints). Therefore, a choice must be made regarding which nodes to connect, resulting in an optimization problem. The second part describes the method chosen to perform the restoration, namely agent-based heuristics. Agents are used to have a fully distributed recovery process that is not susceptible to single points of failure. Heuristics are chosen because the solution space can become very large depending on the number of flexible elements in the network. This makes an exhaustive search infeasible, especially since power system restoration is time-critical and should be performed as quickly as possible. Therefore, finding a valid solution in a short time is more important than finding the optimal solution, making heuristics a good method choice. The heuristic chosen for this work is the Combinatorial Optimization Heuristic for Distributed Agents (COHDA) [43]. COHDA was originally developed for day-ahead planning of active power provisioning and has already been proven to converge, terminate, and be robust to unsteady communication networks and different network topologies (see [43]). This makes it a reliable approach to the restoration problem. It should be noted that the goal of this work is neither to compare different methods for distributed restoration nor – after choosing heuristics as a method – to compare different heuristics to find the optimal one.

FR-2 **Be fault-tolerant (impaired ICT system).** This requirement is one of the key aspects of the motivation and the considered use case. While most MAS-based restoration algorithms in the literature assume a fully functional ICT system, the developed algorithm should consider that not all agents are available and that ICT availability changes during the restoration process. The details of what ICT impairment means for the restoration algorithm and how it is considered will be defined later in this thesis.

FR-3 Consider the ICT system in the optimization problem. This is another key aspect of the motivation and is also necessary to investigate the hypothesis. It is assumed that ICT is critical for load restoration, while at the same time the optimal island configuration in terms of ICT restoration and load restoration may be different. Therefore, ICT restoration must be considered as an equal objective. This includes the development of a concept for measuring ICT performance and requires the restoration algorithm to have multi-objective problem-solving.

FR-4 Consider multiple voltage levels (hierarchical structure). This requirement is derived from the scenario of a distribution grid, where at least MV and LV have to be considered, potentially also HV for larger islands. This hierarchical structure has to be reflected in the restoration algorithm.

The simulation setup should:

FR-5 Co-simulate the MAS with power and communication system. Co-simulation allows the use of well-established tools and can simplify the creation of a simulation setup. Therefore, the method of co-simulation was chosen for the evaluation. This requirement also defines which systems should be part of the scenario's co-simulation environment.

FR-6 Consider all relevant characteristics of the systems needed for evaluation in the context of a simplified scenario. This requirement defines that the use of abstracted scenarios is allowed as long as those characteristics relevant to the evaluation are still present. For example, since the focus is on planning the restoration process and finding the optimal island rather than executing the restoration process, a steady-state simulation of the power system is sufficient. Therefore, the first step to fulfill this requirement must be to identify relevant characteristics. This includes especially the relevant interdependencies between the different systems.

FR-7 Consider the interdependencies of power and communication system during restoration. This requirement could be considered part of the previous requirement since the interdependencies are one of the relevant characteristics. However, since it is the most critical aspect of the investigated use case, it is listed as a separate requirement. This includes not only modeling the impact of the blackout on the ICT system but also considering the potential negative impact of the degraded ICT system on the power system and, therefore, on the restoration algorithm.

FR-8 **Provide sufficient logging results needed for evaluation.** This requirement is self-explanatory. The first step is to define which logging results are necessary for the evaluation and then see how these can be collected from the simulation.

Finally, **non-functional requirements (NFR)** have been defined, following the classification of evaluation criteria from [46]. Here, evaluation criteria are categorized into zeroth-order, first-order, and higher-order criteria with different properties. While zeroth-order criteria yield a yes-no answer and are independent of any scenario configuration, first-order criteria provide scalar quantifies and are the outcome of an experiment. Higher-order criteria are measured in higher-order quantities such as vectors or matrices and describe the interdependencies between different scenario instances and first-order criteria. The developed algorithm should have the following non-functional requirements:

Zeroth-Order Criteria:

NRF-1 **Guaranteed Convergence:** This describes the ability of the algorithm to find a valid solution for the given problem in a finite amount of time after it has been started [46]. The heuristic COHDA used in this Thesis has already been formally shown to converge. However, this convergence proof must also be applied to any changes or extensions made in this algorithm.

NRF-2 **Extensibility:** This defines whether it is possible to extend the algorithm and include new objectives or constraints.

First-Order Criteria:

NRF-3 **Effectiveness:** This describes the quantification of the restoration algorithm to reach its goal – in this case, how much load can be restored. Considering ICT is also part of the objective, the amount of restored ICT can also be measured here.

NRF-4 **Efficiency:** This describes the resource requirements of the restoration algorithm and can refer to both restoration time as well as communication complexity. To measure the concrete restoration time, an evaluation under realistic circumstances is necessary with agents running as distributed processes to get a realistic estimate. As this was not possible, the focus here is on communication complexity on the one hand and "restoration steps" on the other, meaning how many times the restoration process has to be repeated before the final result is reached.

Higher-Order Criteria:

NRF-5 Robustness: This measures the influence of different levels of ICT disturbances on the two first-order criteria. The focus here is on the initially impaired ICT system and less on additional disturbances during restoration.

NRF-6 Scalability: Here, effectiveness and efficiency parameters are measured for different grid sizes.

1.5 Limitations and Assumptions for Blackstart Scenarios

The blackstart of an island grid is a highly complex process with many aspects to consider. The island grid's stability must be maintained during and after the restoration process. An island grid can be defined as "stable if, after being subjected to a disturbance, all state variables recover to (possibly new) steady-state values which satisfy operational constraints, and without the occurrence of involuntary load shedding." [32]. In this case, a disturbance can be changes in load or set-point adjustments. Compared to bulk power systems, island grids face the following challenges with regard to stability [32]:

1. **Smaller system size**: Island grids could be created in medium or even low voltage and reach from large networks of tens of MW down to small networks of just hundreds of kW. The smaller the island grid, the more difficult it is to keep stable.
2. **Higher uncertainty**: With fewer loads, load forecasting becomes more difficult and could even be 100% wrong (for example, if the island grid is in the low voltage level). Moreover, due to the small grid area, the RES in the island grid are highly correlated and can show fast variation in their generation behavior.
3. **Lower system inertia**: System inertia plays an important role in frequency stability. With low inertia, even small deviations in load and generation can cause instabilities.
4. **Higher R/X ratio of the feeders**: Due to the short size of the feeders in island grids, the mathematical relationships between the power system parameters (voltage, angles, power flows) are different from the conventional grids.
5. **Limited short-circuit capacity**: The short-circuit capacity of power system equipment describes the maximum fault current it can sustain for a definite time period before the faulted section gets isolated.

This thesis specifically focuses on the role of ICT in power system restoration and how it can improve the restoration process to consider ICT restoration as part of the optimization problem. Therefore, several assumptions and limitations have been defined to reduce the complexity and define the borders of this thesis.

- The focus is only on **restoration planning** and not the technical blackstart process with the starting of units, timed switching, synchronization of island grids, etc.
- Following this, the system is expected to be in **steady-state**, meaning transient effects are not considered, and there is no dynamic simulation.
- All **technical requirements** for the blackstart process on the distribution level are assumed to be in place. This includes, for example, the availability of blackstart capable units, from which the restoration process is started, and which also have island operation capability to keep the island grid stable (see definition in [100]).
- The primary constraint considered for the restoration is the balance of demand and supply in an island grid. **Bus voltage and line loading limits are not considered** in the constraints.
- The **ICT system** is assumed to be built in a way that **allows a stepwise restoration process**. This requires the ability to communicate with power system nodes outside the initial island grid – nodes still in a blackout state – to extend existing island grids and potentially activate further parts of the ICT system. If communication is always available only between nodes that are part of an active island, it is never possible to restore more than the initially connected nodes because no information is available from outside the already existing communication island.
- The **forecast** of load and generation is assumed to be **accurate**. While uncertainty is a highly relevant topic in the context of DER coordination, especially during restoration, it is not the focus of this thesis.
- There are **no persisting faults in either ICT or power system**. The exact cause of the blackout is not considered, and it is assumed that all failures in both power and communication systems are either already taken care of or have not occurred in the to-be-restored island grid. This also includes cyber attacks; it is assumed that the **agents are not compromised**.

1.6 Methodology and Thesis Structure

To develop the two artifacts and answer the research questions systematically, the Smart Grid Algorithm Engineering (SGAE) process was used [75]. It starts with a conceptualizing phase and then goes into a cycle of designing, analyzing, implementing, experimenting, and evaluating, which can be reiterated several times if necessary. Figure 1.3 shows the SGAE process and maps the chapters of this thesis to the different SGAE phases. Light and dark blue circles mark the chapters in which the artifacts are described and the different FRs and NFRs are discussed.

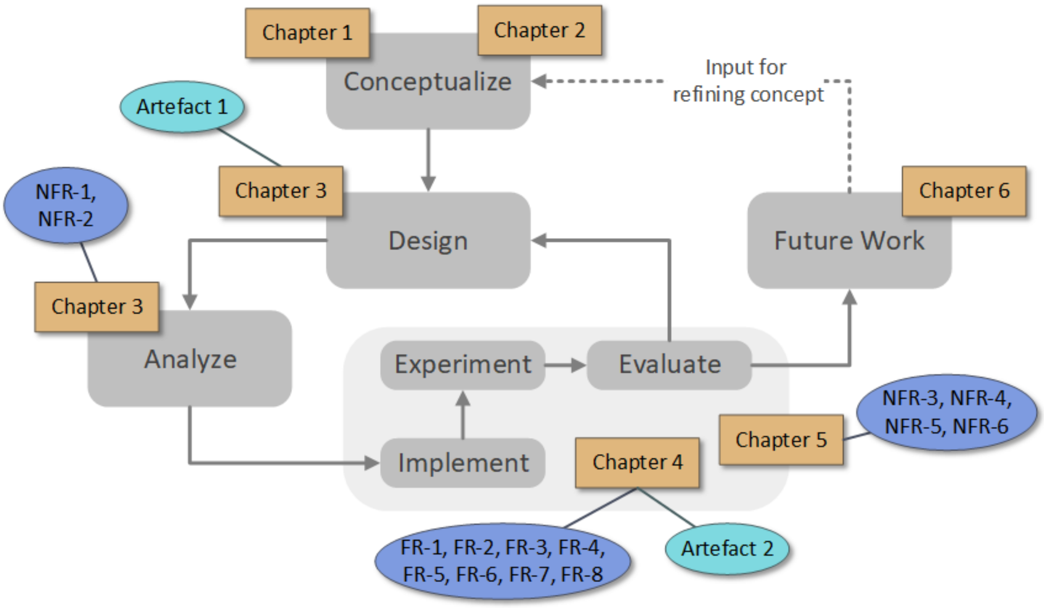

Fig. 1.3.: Overview of methodology after SGAE [75] and thesis structure

Chapter 1 (the current chapter) and **Chapter 2** correspond to the *conceptualization phase*. While this chapter defines the general problem, research gap, hypothesis, and research questions, Chapter 2 describes the fundamentals and related work more thoroughly. This includes the current and future blackstart process, island grid restoration, the behavior of ICT during emergencies, automated island grid restoration approaches, and an introduction to COHDA, the heuristic used in this thesis. This information is relevant for the design of the scenarios later on.

Chapter 3 corresponds mostly to the *design phase* and goes on to describe the first artifact. Using the information from Chapter 2, the concrete scenario is defined for which the restoration algorithm will be developed. Subsequently, referring to the different research questions, the agent architecture and optimization problem are defined and combined into the full restoration algorithm. Following this, the results of the *analyze phase* are also presented in Chapter 3 by formally proving the algorithm's convergence and showing its extensibility, thereby discussing NFRs 1 and 2.

Chapter 4 now covers all three *implement phase*, *experiment phase* and *evaluate phase* for a proof of concept. The focus here is on showing the fulfillment of the FRs and introducing artifact 2, the co-simulation setup used for all evaluations. Chapter 4 describes one evaluation with only single-objective optimization and one with multi-objective optimization and discusses the results.

Chapter 5 presents the extended multi-objective evaluation, using larger scenarios and focussing on the remaining NFRs as well as discussing the hypothesis in depth. Again, all three phases of implementation, experimentation, and evaluation are passed through.

Chapter 6 finally does not correspond to any of the original phases of SGAE but provides a summary of the thesis, a look at the influence of design choices on the results, and a detailed discussion of possibilities for future work, which could feed into a new conceptualization phase.

1.7 Acknowledgement and Collaborative Work

This work was funded by the Deutsche Forschungsgemeinschaft (DFG, German Research Foundation) — project number 360475113 – as part of the priority program DFG SPP 1984 - Hybrid and Multimodal Energy Systems: System theory methods for the transformation and operation of complex networks.

The research project was done in collaboration with Anna Volkova from the University of Passau, whose focus was to investigate the restoration problem from the perspective of the ICT system. The definition of the blackstart-capable system architecture – especially the definition of the ICT scenario – and the evaluation of the single-objective algorithm have been done in collaboration.

2 Fundamentals and Related Work

This chapter presents the topics discussed in this thesis: Blackstart, distribution grid restoration with island grids and ICT in emergencies. The focus of this thesis is mainly on the European or German grid. Therefore, descriptions of the current or future grid structure, the blackstart processes, or the communication infrastructure are either based directly on the ENTSO-E network codes[1] or on research that focuses on these grids. Following the background sections, related work on automated island network restoration is presented to analyze the research gap in more detail. Finally, COHDA, the heuristic used for the restoration algorithm, is introduced.

2.1 Blackstart of Power Systems

The power system is defined to be in a blackout state when "the operation of part or all of the transmission system is terminated" [100]. To return the system to a normal state, it goes through the restoration state, where the sole objective is to restore the system to operation. This section explains how power system restoration is performed nowadays and provides an outlook on how this process needs to be adapted for the future power system.

2.1.1 Present-day Power System Restoration

Power system restoration aims to restore as much load as possible while maintaining normal frequency and voltage levels. Any deviation of these parameters from their nominal values can cause the system to go back into blackout state. There are two main principles of restoration: *Bottom-up* and *top-down* [100]. While the top-down process relies on external power sources from neighboring TSOs, the bottom-up process relies on blackstart capable units in the TSO's grid area. In the following, the focus is on this bottom-up approach. The careful coordination of this blackstart

[1] https://www.entsoe.eu/network_codes

is a critical and complex process and requires a sequence of coordinated actions [100]. System operators already consider restoration while designing a grid, define restoration plans and regularly train for emergencies in simulations. The restoration process can be divided into four steps, which are explained below [53].

Step 1: Preparation of the system. Before the actual restoration begins, the TSOs have to prepare the network. Since all steps in the restoration process are coordinated from the control room, the control room's functionalities must still be available in case of a blackout. Therefore, the control room is required to have backup functions as well as an emergency power supply for all main functions such as remote control, telecommunication, and computer installations [100]. This also includes other control systems in the field that are required for the restoration process, such as SCADA/EMS systems and load frequency control equipment.

An essential task is identifying and isolating the faulty areas to ensure they are not inadvertently reconnected to the grid, which could cause the protection to trip again. This requires knowledge of the cause of the outage, whether it was equipment failure, human error, natural disaster, etc. [53]. Other important information is the state of the generators, the load on the grid before the blackout, and estimates of how it might differ immediately after restoration. Information is exchanged between different TSOs mainly via telephone communication, designed to be robust against blackouts to ensure high availability [100]. The network is then separated by switching operations to create a clearly defined, observable network area [83]. The goal is a horizontal separation (all switches between the control area and neighboring control areas are opened) and a vertical separation (switches between underlying voltage levels are opened). By separating the MV from the HV network, the MV network is divided into sufficiently small sub-networks that can later be energized in a single restoration step.

Due to their uncertain and fluctuating power feed-in, DER units are typically disconnected during grid restoration and reconnected only when the system is in a stable state [11]. In Europe, the "Network Code on Requirements for Generators"[2] defines the specific behavior of DER in the event of a blackout, which can vary depending on the size and connected voltage level. For disconnection, over- and underfrequency thresholds are defined at which the DER should automatically disconnect from the grid. As of 2012, these thresholds must differ between different DERs so that not all DERs in the same grid area are disconnected simultaneously but gradually (§11 Paragraph 1 SysStabV). For reconnection after a blackout, as of 2017, only generating units below 1 MW connected to 110 kV or less are allowed

[2] http://data.europa.eu/eli/reg/2016/631/oj

to reconnect automatically to the grid (§13 Paragraph 7 Commission Regulation (EU) 2016/631), while units with a capacity of 1 MW or more require approval of the TSO (§14 Paragraph 4 Commission Regulation (EU) 2016/631). DERs with automatic reconnection use the frequency value to identify the allowed reconnection time. This behavior can be used to prevent automatic reconnection during the restoration process by initially setting a higher frequency setpoint and only reducing the frequency below 50.2Hz when the restoration is complete [11].

Step 2: Rebuilding the Transmission System. Many power plants require a large amount of energy to start up from a shutdown state, which they would draw from the functioning grid during normal operation. When this energy is unavailable due to a blackout, power plants are needed that can operate despite the lack of power supply to provide the initial generation for restoration. Some power plants can ramp down their production to the point where they produce precisely the amount of power they need for their own most critical functions. They can increase their output from this state when consumers are added to the grid or energy is required to start another power plant. However, they can only stay in this state for a few hours, requiring a fast restoration process [83]. In the case of nuclear power plants, backup power is also crucial for safety reasons since a failure of the cooling system, for example, can have serious consequences. Other power plants have a so-called blackstart capability: They can be started from a shutdown state without an external power supply, such as hydroelectric or compressed air storage power plants, or with the help of small emergency power sources, such as batteries or diesel generators [53]. Blackstart-capable units also include islanding capability, which means they can regulate frequency and voltage in the isolated operation of a grid segment and also specify setpoints [100].

In this step, the focus is not yet on supplying loads but on providing power to elements critical to further restoration, such as other generating units or auxiliary power supplies for substations and control centers [53]. Therefore, blackstart-capable units or units in self-supply mode are started and gradually used to supply neighboring units. Plants in self-supply mode are synchronized with the blackstart-capable units and can also proceed to restore the transmission network [83].

Step 3: Restore the loads. When enough generation is available in the transmission network, load restoration in the distribution network can be started. Especially at the early stages of restoration, overvoltages are a common problem due to the Ferranti effect. Several measures can be taken to prevent overvoltages, such as minimizing the number of circuits switched in, operating generators at minimum voltage levels, or adjusting transformer taps [53]. Another challenge is the communication between the transmission and distribution grid. The substations in the distribution network might have less backup power capacity than in the transmission grid or not be remote-controllable, requiring staff to operate switches to re-connect parts of the grid manually [53]. This can delay the whole restoration process.

In this step, it is essential to ensure there is enough generation to supply all the loads and perform restoration slowly. If the load is picked up too fast without the power plants being able to increase generation, the frequency drops, and the system collapses again [53].

Step 4: Synchronisation with other island grids. This requires placing system synchronization equipment at strategic points in the grid from which two adjacent disconnected parts can be synchronized. A *synchronization leader* is defined to coordinate the synchronization of voltage and frequency and the subsequent reconnection of two islands [100].

2.1.2 Future Power System Restoration

According to the IPCC Sixth Assessment Report, the global energy system is the largest source of CO2 emissions in the world [50]. To limit global warming to below $2°C$, changing how energy is provided and used is essential. Several scenarios have been defined as to what the future energy system might look like. Figure 2.1 compares the global energy mix in 2019 with two potential future scenarios [20]. As can be seen, the share of renewable generation, such as solar, wind, and biomass, increases, while conventional generation from coal and oil decreases. Incorporating large amounts of fluctuating energy from PV and wind requires storing large amounts of energy (e.g., batteries or hydrogen storage) and flexibility from demand-side response [20]. Widespread electrification of end users, such as electric vehicles, and more efficient energy use are changing the load patterns. In addition, more loads will be controllable and can provide positive balancing power. Home battery storage should also be included in the restoration process.

While the previously described restoration process has been successful in past blackouts, the evolution of the power grid towards more DER and increased penetration of renewables introduces new challenges. Strategies for restoring the grid after a blackout need to be adapted to consider the specificities of renewables in terms of grid stability. In today's restoration process, the generation capacities offered by DER are not used in case of blackout due to the inability to handle the fluctuating behavior. In future power systems, on the other hand, renewables and DER must be

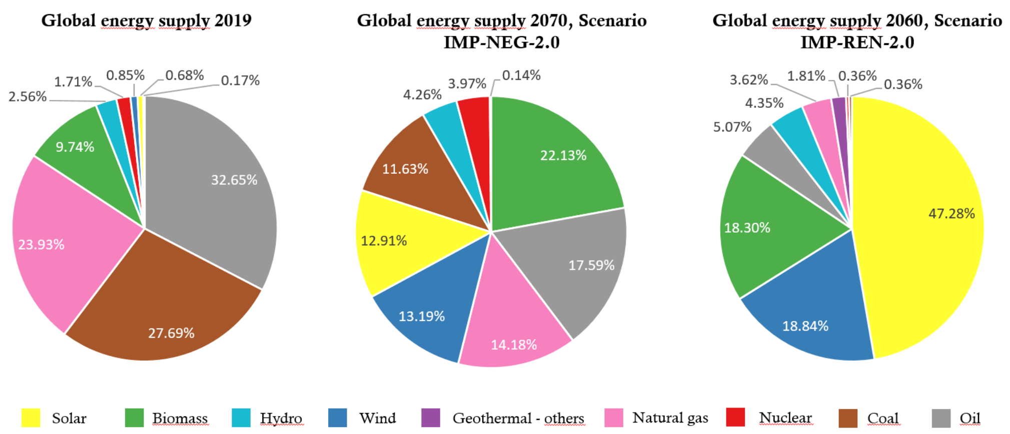

Fig. 2.1.: Comparison of energy-mix for the global energy supply of 2019 and two net-zero scenarios [20]

considered as an active part of the restoration process to make up for the reduction of large conventional power plants such as coal and nuclear. Several technical adaptions are necessary to enable the units to fulfill this task.

For example, switching from synchronous to inverter-based generators reduces system inertia, an essential component of system stability. The system inertia partially absorbs changes in load or generation before the primary control reserve kicks in. The lack of inertia makes frequency control more difficult, especially in a blackstart scenario. To mitigate this problem, new generating units in Germany must be equipped with virtual inertia, and existing units at the EHV level are being retrofitted with fast frequency response [2]. These measures have already largely compensated for the loss of instantaneous reserves due to the retirement of large conventional power plants. The authors in [35] examined how wind turbines could have helped avoid the blackout in Flensburg, Germany, on January 9, 2019, using virtual inertia and primary frequency control. The blackout was initially caused by a cable failure that disconnected Flensburg from the Danish and the German grid, leaving the islanded area with a large power surplus and triggering protection systems, which resulted in a blackout. While virtual inertia alone would not have been sufficient to keep the frequency below the 51.5 Hz threshold, wind turbines combined with primary frequency control would have been able to effectively balance the power in the grid, at least in scenarios where wind turbines generate a large portion of the power.

Another general challenge with renewable resources is the availability of generation in the case of the so-called "Dunkelflaute" ("dark doldrums"), a time in which no energy can be created by wind or solar power. For countries bordering the North and Baltic Sea areas, these events can occur several times a year and last at least a day [60]. However, the correlation coefficients of Dunkelflaute events for neighboring countries appear to be only moderate, suggesting that in an interconnected power system, the effects of these events can be mitigated by pooling wind and PV generation [60]. Together with a carefully designed energy mix that also includes controllable generation and energy storages and reduced energy demand through, for example, more efficient building insulation and demand response, it should be possible to manage these extreme weather events [22]. The concepts used in normal operation can also be used during system restoration.

The National Grid ESO (electricity system operator for Great Britain) has commissioned an investigation on the blackstart capability of non-traditional technologies to restore the GB power system [73]. These include large and small wind power, solar PV power, battery storage, industrial and commercial demand side response, synchronous DER (e.g., biomass), and electric vehicles. They conclude that, except for EVs, all investigated technologies have the necessary characteristics and capabilities to support a blackstart and system restoration. Especially by co-locating battery storage with wind and solar PV, the blackstart capability of these units can be improved. There are already technical solutions for most of the problems, but upgrading the system costs money, and this requires proper incentives, ideally through the market. Table 2.1 summarizes several problems and their solutions when using DER for blackstart.

Tab. 2.1.: Problems and potential solutions for using DER in grid restoration according to [73]

Problem	**Solution**
Uncertainty of resource availability of battery storage	Market-driven incentives to ensure minimum level of state of charge for batteries
Uncertainty of resource availability of wind and solar	Better modeling and forecasting tools
Blackstart capability	several technical solutions are already available (e.g., equipping unit with auxiliary power supply for blackstart purposes)
Grid-forming capability needed to create voltage signal	Upgrading units with grid-forming inverters and necessary software
The resilience of the communications infrastructure	Upgrade infrastructure to meet the necessary resilience requirements, either on the wider communications network or individually at each unit

Apart from the technical side, DERs generally work on a much smaller scale than conventional power plants, which must be considered when setting technical requirements. The grid code should be adapted accordingly, e.g., by reducing the size of demand blocks, which the generating units should be able to pick up while controlling frequency and voltage, or by reducing the time for which the blackstart service should be kept available. In general, the authors in [73] conclude that "none of the technical barriers which exist are insurmountable; they only require appropriate commercial and regulatory support to ensure these can be addressed to the benefit of all."

As a significant amount of renewables will be at the distribution level, the role of the Distribution System Operator (DSO) in the restoration process will have to change. This means a key factor for a successful future restoration process is clearly defining roles, responsibilities, and interfaces between TSOs and DSOs. In their white paper published in 2022, the four German TSOs have described their goal for network restoration in 2030, considering the effects of the energy transition [2]. They emphasize that in the future restoration plan, TSOs will continue to be the initiators and coordinators of the restoration process and bear the main responsibility in their respective control areas. The aim will be to reconnect the different grid control areas as early as possible in the restoration process to optimally distribute the available generation flexibility and increase grid stability within Germany and with the neighbors in the European interconnected grid.

The job of the DSOs is only to prepare their grids to serve the restoration process as best as possible and to be ready for any requests for defined load or generation coming from the TSOs. This includes (1) splitting the grid into suitably large areas, (2) monitoring and forecasting the behavior of load, and (3) controlling and forecasting the behavior of DER and controllable loads. The necessary technical requirements, such as blackout-resistant communication with the DER, have to be installed by the DSOs. During the restoration, the DSOs then aggregate the load and generation from their grid area and offer the flexibilities to the overlying TSO, who decides, based on this information, how much load and generation is needed for the next restoration step. According to [2], the ability for a blackstart on the DSO level can be installed under specific technical circumstances as a requirement from the TSO to the DSO if it suits the overall restoration strategy, but would be the exception.

It becomes clear that digitalization is a key element of many solutions for future system restoration with DER and will, therefore, be an integral part of the future energy system. Digitalization may also include the use of new control interfaces and tools. For example, in [42], the authors present a new control center interface for communication tasks and interactions during grid restoration, along with associated restoration tools to relieve and support both TSOs and DSOs during system restoration. This includes an awareness tool that visualizes essential system information from neighboring grids and a decision support tool for resynchronizing or assisting neighboring SOs after a blackout.

The authors in [19] go one step further and describe an integrated decision support tool for distribution system restoration that uses advanced technologies to increase situational awareness and focuses on the importance of customer survivability during a blackout. In this context, they discuss the concept of microgrids. Microgrids are defined as "a group of distributed energy resources (DERs), including renewable energy resources (RES) and energy storage systems (ESS), and loads that operate locally as a single controllable entity" [32]. They can typically operate in both grid-connected and islanded modes and have a point of common coupling (PCC) with the larger grid. In this thesis, the term island grid is used to emphasize that instead of pre-defined grid areas, the dynamic formation of local operational grid areas in case of a blackout is considered. However, the characteristics and challenges of island grids and microgrids are the same.

There are three different options to integrate islanding in the distribution grid in the restoration process [37]:

1. **Use island grids in a build-together restoration.** If possible, island grids are created in parallel with the blackstart in the transmission grid, and then both grid levels are resynchronized. One problem may be that if there are too many island grids, there may not be enough load left for the TSO to reconnect and restore the transmission grid.

2. **Use island grids for a build-up restoration.** Instead of restoring the transmission system first and then the distribution system, it is done in reverse: island grids are built and then used to restore the transmission system. They can provide ancillary services such as black-start capability to the rest of the power system. This would require significant changes to the distribution networks, and whether this process is economically efficient is questionable.

3. **Use island grids as an emergency measure.** Island grids are created to reduce outage time for customers and serve critical loads during a blackout. Island grids with DER can help minimize outage time, especially for critical customers, and increase system resiliency. When the transmission system is ready to be restored, island grids can be resynchronized where possible. Otherwise, they are disconnected and reconnected in a top-down manner

coordinated by the TSO. This concept is also in line with the vision of the TSOs [1], [2].

This thesis focuses on option (3). Island grids are used as a resilience measure in the event of long-lasting, wide-area power outages where the restoration of the transmission grid takes time. Integrating active island grids into any further restoration process is not considered.

2.2 Distribution Grid Restoration with Island Grids

The steps for restoring island grids differ slightly from the current restoration process described in Section 2.1.1.

Step 1: Preparation of the system is similar. Any faults in the part of the system to be restored must be identified and, if necessary, repaired, the available generation and load situation must be analyzed, and, especially if the island grid area is not predefined, a restoration sequence must be defined.

The second and third steps of the current restoration process are merged into one **Step 2: Restore generation and load**, since in the distribution grid, there is no separation between transmission and distribution, and usually no switching equipment is available to separate loads from lines [40]. The authors in [12] present a case study on the possibility of local load coverage with DER. The results show that it is not possible to cover all loads at all times with only these DERs and that the longer the time horizon for load coverage, the less load can be restored. This means that a choice has to be made as to which loads should be supplied in case of a blackout. However, they only consider HV-connected units participating in the restoration process due to the assumed unreliable controllability of MV and LV generation units, meaning that a significant part of generation flexibility is left out.

Finally, the last **Step 3: Synchronization with other island grids** (Step 4 in the current restoration) is the same but optional and depends on whether the synchronization of island networks is part of the islanding strategy (which requires synchronization equipment at the distribution level) or whether the emergency islands remain separate from each other.

To implement islanding in the distribution system, several requirements must be met. The following subsections describe the requirements in more detail, distinguishing between technical requirements, communication and automation requirements, and human factors.

2.2.1 Technical Requirements

Figure 2.2 shows an example distribution grid with an islanded grid area, depicting different types of load and generation and the technical requirements necessary to restore the island grid.

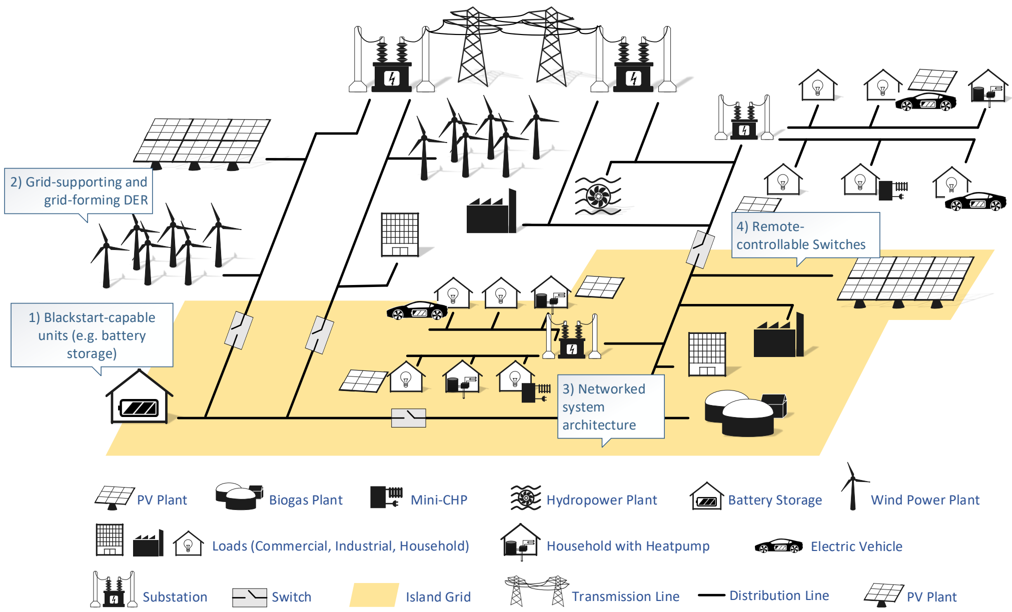

Fig. 2.2.: Illustration of distribution grid with island grid and technical requirements (own design)

One of the most critical requirements is the presence of **1) Blackstart-capable units** (BCU) in the distribution system. As explained in Section 2.1, BCU should not only be able to start from a shutdown state without an external power supply but also regulate frequency and voltage. Possible BCU in the distribution grid could be CHP plants, simple diesel generators, or battery storage (possibly co-located with wind or solar PV, as described in Section 2.1.2). Since BCU would mark the starting point for a restoration process, their placement and size can impact the islanding approach's effectiveness and is an optimization problem in itself (see, e.g., [78]).

Since the BCU in the distribution grid are too small to restore a significant amount of load, they must be coordinated with other DERs. In general, the amount of distributed generation will increase, as seen in the example of solar PV. Figure 2.3

shows the total newly installed capacity of Solar PV worldwide per year from 2016 to 2023. The total increase is divided into utility-scale, commercial and industrial, and residential PV. It can be seen that the amount of newly installed residential and commercial and industrial PV has increased in recent years and is likely to continue to grow, indicating that a significant amount of generation will be installed in distribution grids.

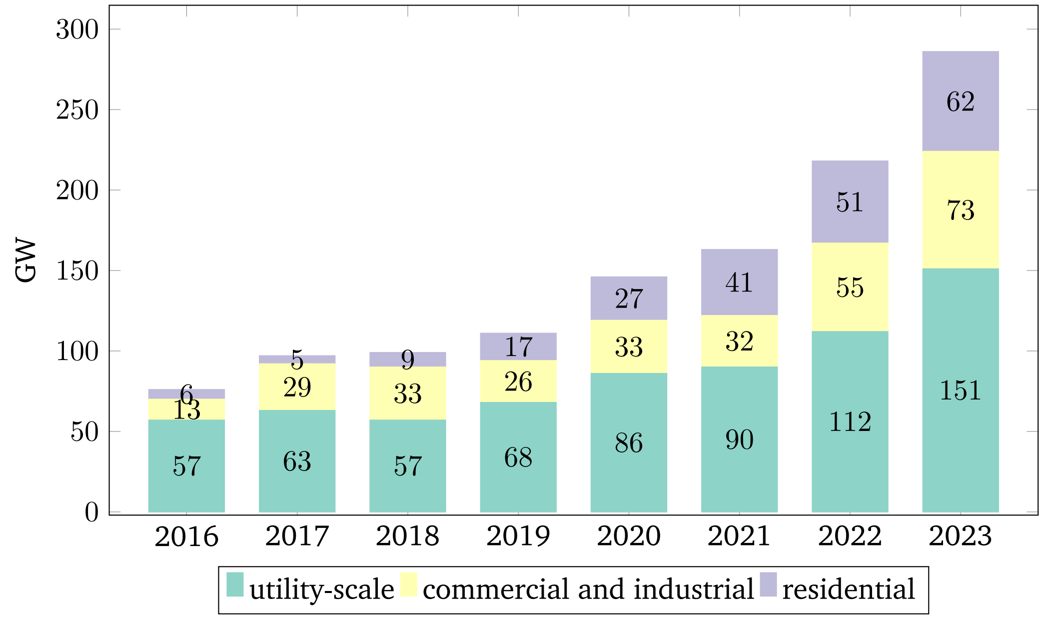

Fig. 2.3.: Increase of Solar PV power capacity compared to previous year (based on [49])

Three different control modes can be defined for DER: (1) grid-following, (2) grid-supporting, and (3) grid-forming [10]. Grid-following is the control mode of most DERs today. During restoration, they start with an active and reactive power of zero and increase it based on fixed specifications of the grid operator (e.g., a predefined gradient). As a rule, they only start feeding into the grid when the frequency has stabilized. Grid-supporting DER can help stabilize the frequency during initial restoration, e.g., through faster and more detailed adjustment of feed-in or virtual inertia. Finally, grid-forming DER can regulate both frequency and voltage and are therefore highly important for stabilizing the island grid. While most DER today have only one form of control mode – grid-following – future restoration and especially islanding will require both **2) grid-supporting and grid-forming DER**.

A critical factor for the stability of an island is the balance of generation and load and the ability to maintain that balance [88]. If the region exported rather than imported electricity before the blackout, maintaining the balance would be easier, as it would only be necessary to reduce generation and not disconnect loads. The ability to form island grids is likely to vary by geographic region, depending on the level of DER penetration. If an area can't form island grids due to insufficient generation, the DER should be operated in a grid-following mode that does not interfere with the standard, top-down restoration process.

In contrast to the transmission system, the distribution system is traditionally not networked but built in a radial structure. To isolate damaged components and reconfigure the distribution system in the event of islanding, a more **3) networked system architecture** as well as **4) remote-controllable sectionalizing switches** are required [88]. Where in the grid to place remote-controllable switches (or to upgrade existing switches to be remote-controllable) to support an islanding restoration process best can be described as a separate optimization problem. The goal is to minimize the number of switches needed while satisfying various constraints and is relevant during grid planning (see, for example, [58], [106]).

2.2.2 Communication and Automation

As described in the introduction, there are three steps to island grid restoration: (1) system preparation, (2) generation and load restoration, and (3) synchronization with other island grids. All three steps require communication. In particular, the second step, where the actual island grid is formed, involves several important control tasks that rely on the communication system. These control tasks can be divided into primary, secondary, and tertiary levels, corresponding to the hierarchical structure of the control reserves in the conventional power system [38]. In the following, the different levels are briefly described in the context of island grid restoration, based on [90].

The **Primary Control** encompasses all fast processes necessary to maintain the stability of the island grid, such as voltage and frequency control. The control actions are highly time-critical (with latency requirements in milliseconds) and, therefore, usually performed with a communication-less approach, such as droop-based control or virtual inertia. After voltage and frequency have been stabilized by primary control, the **Secondary Control** takes over to restore voltage and frequency to the defined limits. Secondary control functions are usually handled with either centralized or distributed approaches, requiring information exchange through a communication network. While Secondary Control is not as time-critical as Primary Control, the communication speed can still directly influence the performance. Finally, **Tertiary Control** is responsible for non-critical tasks such as power flow optimization.

However, before the actual island grid is built and all of these control tasks become relevant, step (1), the preparation of the system and planning of the restoration process, must be performed. The careful coordination between the BCU, DERs, loads, and remote-controllable switches required to restart the islanded grid also uses communication and is the focus of this thesis.

Figure 2.4 shows the communication infrastructure required for a centralized island restoration process. **1) The availability of real-time knowledge of current load and generation in the control room** is crucial in determining optimal switching sequences and coordinating the restoration process. Today, however, detailed load data is not available in the control room, especially information on load behavior after reconnection [70]. For example, thermostatically controlled loads would start up simultaneously, especially during a prolonged outage, creating a very different load profile from normal operation. When reconnecting a household with rooftop PV, the load will be connected before the generation starts, so it is critical to know how much load there is to balance it with the generation units that are already active. This also includes an **2) Accurate weather forecast**, which is necessary to estimate the generation of RES.

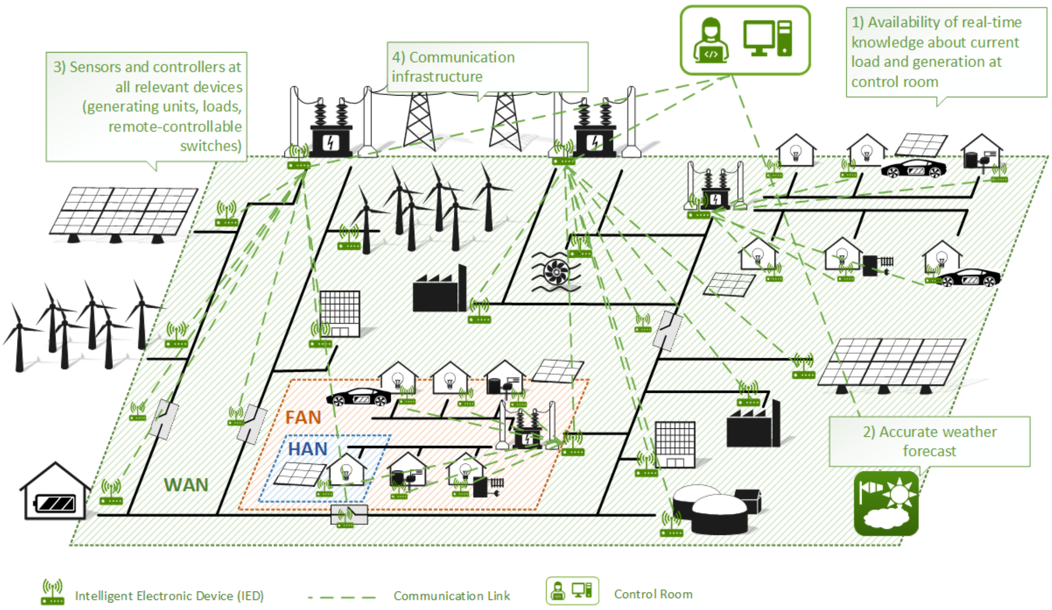

Fig. 2.4.: Illustration of distribution grid with island grid and communication and automation (own design)

This requires **3) Sensors and controllers on all relevant devices**, such as generating units, loads, and remote-controllable switches. These intelligent electronic devices (IEDs) should also be able to perform local primary control. In Germany today, DER units have different communication requirements depending on their size. DER units with a rated power of less than 30 kW connected to the low-voltage (lV) grid are not largely remote-controllable under current regulations. Larger DER units have active power reduction requirements that are often implemented using public communications technology. However, these units' availability and timing behavior in the event of a major blackout is not yet assured. DER units of several hundred kW typically communicate directly with the grid operator's supervisory control and data acquisition system. The grid operator is responsible for specifying the requirements for blackout secure communication channels. The authors in [40] list several commands that DERs should be able to receive and implement, including activation or deactivation of the restoration mode, nominal values for active and reactive power, and adjustment of the droop control curve, which automatically adjusts the active power output based on the current frequency. To transfer data from IEDs to the control room and vice versa, the **4) communication infrastructure** should reliably connect a large number of customers and field devices over a large coverage area. This connection should have low latency and high data rate while ensuring interoperability between different communication networks and the reliability of the data transfer [4].

The communication network can be divided into different hierarchical layers. There exist various definitions for the layers in literature. In the following, the definition from Kuzlu et al. is used, based on the U.S. communication system [54]. Here, the authors define three different layers, which are also shown in Figure 2.4: Home Area Networks (HAN), which cover customer premises; Field Area Networks (FAN), which transmit data from a large number of customers to substations and Wide Area Networks (WAN), which are responsible for applications like wide-area control, monitoring and protection. Each layer has different requirements for coverage range and data rate, which are summarized in Table 2.2.

Tab. 2.2.: Requirements for data rate and communication range for different levels of communication hierarchy according to [54]

	HAN	FAN	WAN
Coverage range	1 - 100 m	100 m - 10 km	10 - 100 km
Data rate	1 - 100 kbps	100 kbps - 10 Mbps	10 Mbps - 1 Gbps

Different communication technologies are possible for each level, both wired and wireless [90]. While wired technologies can provide reliable connections with low interference and high speed with fiber optics, they are difficult to scale. They can also be inflexible regarding their topology. Wireless technologies such as Wi-Fi are cheaper and easier to scale but are susceptible to interference. Cellular networks such as 3G, 4G, or 5G would be provided by third-party facilities and can cover large areas, but are expensive when service level agreements are defined to ensure the required quality of service. Wireless technologies are generally recommended for most smart grid applications due to their lower cost, higher flexibility, and faster deployment [54]. Which communication networks are used in island restoration depends on the size of the island grids and the restoration approach. Small island grids with a decentralized approach may only use the FAN network. At the same time, larger island grids or a centralized approach coordinated by the system operator may also use the WAN. Regardless of the type of communication layer used and the technologies installed, one of the most critical aspects of the communication infrastructure is its ability to withstand the blackout, which will be discussed in Section 2.3.

2.2.3 Regulatory and Social Aspects

Although not the focus of this thesis, the regulatory and social aspects of an islanding restoration process must also be considered when designing the restoration process. Figure 2.5 shows some additional elements that need to be in place besides the technical and communication requirements.

As discussed in Section 2.1.2, the DSO will get a more active role in the future restoration process because a significant part of the grid flexibility is located within its grid area. This requires new coordination paradigms between DSO and TSO during restoration, especially when using the described islanding approach. Islanding needs to be integrated into the normal restoration process, and **1) Coordination between DSO and TSO** needs to be defined accordingly. Since the island grids considered here are not all expected to be synchronized with the higher-level network or even expected to restore the system from the bottom up, the coordination is not too different from today. The primary responsibility for restoration will continue to lie with the TSO, who has a complete overview of the grid and coordinates with neighboring TSOs. DSOs have a supporting role but are allowed to restore their grid as much as possible using the island grid approach as long as it does not contradict the requirements given by the TSO. A **2) Automated interface between SOs** must facilitate the interaction between the different grid levels.

The future digitalized energy system is a so-called socio-technical system, which is shaped not only by technical but also by social factors [3]. Technology and society evolve in parallel and influence each other, e.g., public awareness of the climate crisis can lead to the development of new products such as electric vehicles, which in turn affect public awareness. In the context of island grids in the distribution system,

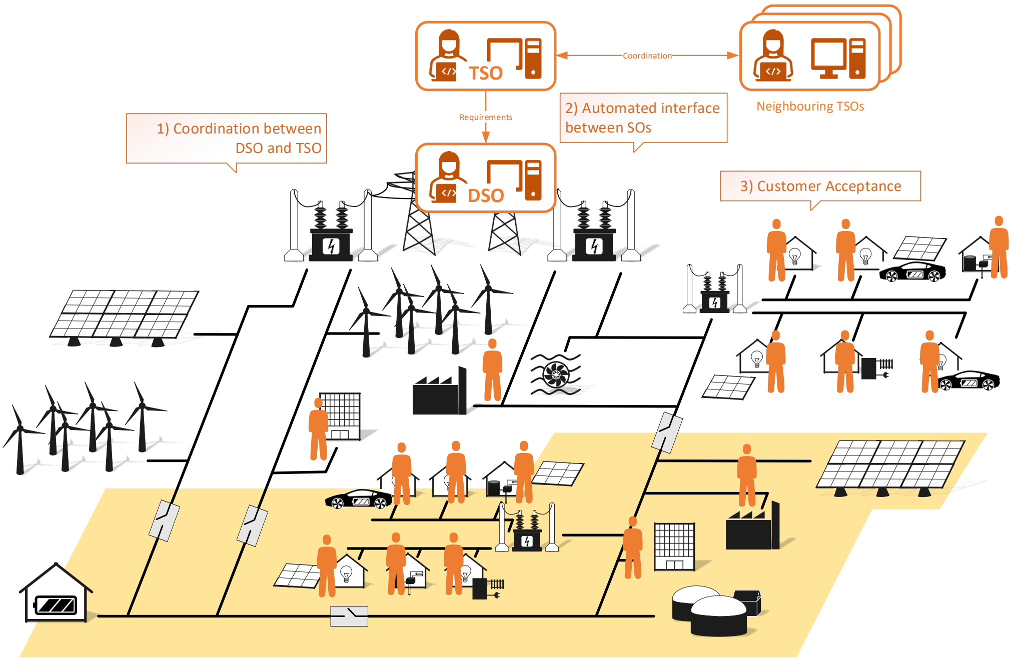

Fig. 2.5.: Illustration of distribution grid with island grid and organizational and social requirements (own design)

customer decisions significantly impact its effectiveness. The more flexibility is installed in a given area with, e.g., rooftop PV, EV charging stations, and heat pumps, the easier it will be to form balanced island grids. The installation of DER for island restoration needs to be incentivized, especially if customers should be encouraged to install DER that benefit the system more than they benefit themselves [19]. In the case of restoration, DER must act "altruistically" and not seek to maximize personal profit. In addition, if critical customers such as hospitals are to be prioritized in island restoration, the resulting island grid may not include the parts of the grid that customers - who provide flexibility - would prefer. Customers need to accept and trust the decisions of the grid operator as to where the island grid is created. This requires a general level of **3) Customer Acceptance** in the restoration process.

The *Energiesysteme der Zukunft – ESYS (Future Energy Systems)* project develops options for actions for policymakers. In their project "Resilience of digitalized energy systems," they emphasize the importance of involving private actors in designing and implementing resilience measures such as islanding [3]. They offer various ideas on how this participation could be achieved, for example by establishing a stakeholder forum to address the interests of private actors and to raise awareness of the influence of private actors. The challenge here – especially in the context of grid restoration – is to find a balance between which measures are so critical that they should be mandatory, e.g., forcing customers to provide their complete flexibility for the restoration process, and which measures can be implemented through incentives.

2.3 ICT Behavior during Emergencies

As described in Sections 2.1.2 and 2.2.2, the ICT system plays a vital role in future restoration in general and in islanding in particular. This includes the restoration process and general crisis management in case of a major blackout, e.g., coordination between first responders, repair crews, government, etc. Therefore, the power system and the ICT system are interdependent: almost all components of the ICT system depend on the power supply to function, which is not available during a major blackout, and at the same time, the power system depends on the functions of the ICT system to coordinate the restoration process.

The extent to which the ICT infrastructure is affected by the blackout depends on the technology used and the measures taken to mitigate the effects of the blackout on communication. A functioning ICT infrastructure is critical to successful restoration and is, therefore, the focus of the 2030 grid restoration target by TSOs [2]: All relevant components are expected to have a dedicated – independent of public infrastructure – blackout-resistant communication infrastructure that system operators can use to coordinate the restoration process. Blackout-resistant, in this case, means that the communication infrastructure can provide sufficient functionality in the event of a blackout and can automatically restore communication when the grid is restored without manual intervention. The relevant entities to be connected are different TSOs, TSO and underlying DSO, TSO to substations, and TSO to generation units. Essential communication links between actors, such as blackstart units, should also be redundant. Due to the decentralization of generation, power system restoration will become more complex, negatively impacting the expected restoration time. Therefore, the time for communication infrastructure to withstand the effects of a blackout should be increased from 24 hours to 72 hours in Germany [2].

For the island grid restoration considered in this thesis, it is not assumed that a blackout-resistant, dedicated communication infrastructure is in place for all participating elements at the distribution grid level. Estimating the concrete effects of a blackout on the communication infrastructure of the island grid is not trivial since a) it is not yet clear what kind of communication technologies will be used, and b) even if this were known, "there are no current, systematic and scientifically backed data surveys on the possible consequences of a power blackout for the »information technology and telecommunications« sector," as the authors state in [79]. Therefore, the impact of a widespread blackout on the ICT system will be described on a more general and abstract level.

The authors in [34] propose a separation of the ICT part of power systems into two different layers: The *physical layer*, which consists of the communication infrastructure, and the *application layer*, with the software necessary for management and protection. The power supply from the power system to the ICT system is part of the physical layer. The topology is designed in a hierarchical setup with HAN, FAN, and WAN, as described in Section 2.2.2. Figure 2.6 depicts the different levels and their respective infrastructure elements. Edge routers are part of the so-called access network, which connects the end devices to the core network responsible for wide-area communication [79].

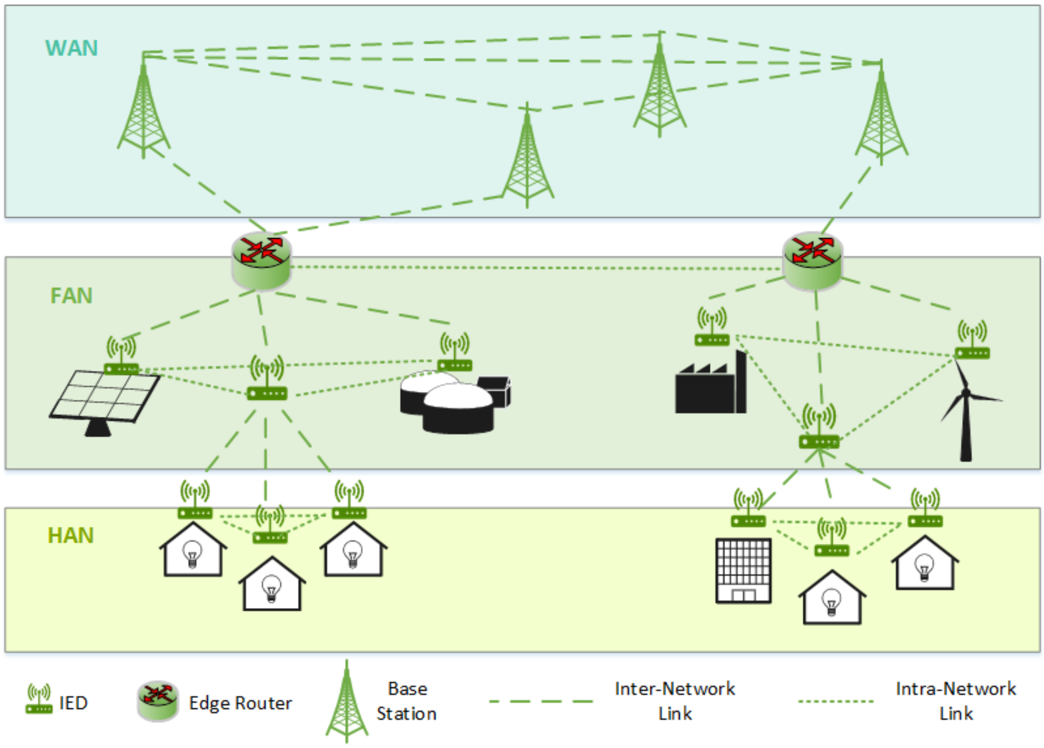

Fig. 2.6.: Illustration of ICT hierarchy levels, based on [79]

The technology used at each level can be wired, wireless, or a combination. It is also possible to have a strictly hierarchical network with only links between networks or to allow direct communication between devices within the same network. All these choices impact communication availability in the event of a blackout. Unless battery backup is installed, all devices at all levels require power to operate and are, therefore, directly affected by a blackout. The higher the hierarchy level, the more critical the communication infrastructure is because, for example, a failure of the core network would affect more customers than an access network outage. As a result, core networks are typically better protected against power outages than access networks. End devices in the home sector do not necessarily have backup batteries (such as DSL routers or computers). However, the IEDs used to monitor and control loads and generation in an islanded grid are assumed to have battery backup. This leaves only the access and core networks as critical points. Battery backup for the access network can last anywhere from 15 minutes to 8 hours, while for the core network, it can last from 8 to 48 hours, even up to 3 or 4 days [79].

2.3.1 Effects of Power System Blackout on Communication

Whether or not two devices can communicate during a blackout depends on their proximity and the failure level. Figure 2.7 shows the effects of device failures on different levels (end device, access network, and core network) for varying levels of proximity of communicating end devices in the network (same HAN, different HAN but same FAN and different FAN). Naturally, communication between two devices can only be established if both devices are active, so a failure of either end device would always result in no established connection. This underlines the importance of device-level battery backup to ensure communication during power outages. A failure of the overlying HAN or FAN access routers would only affect the

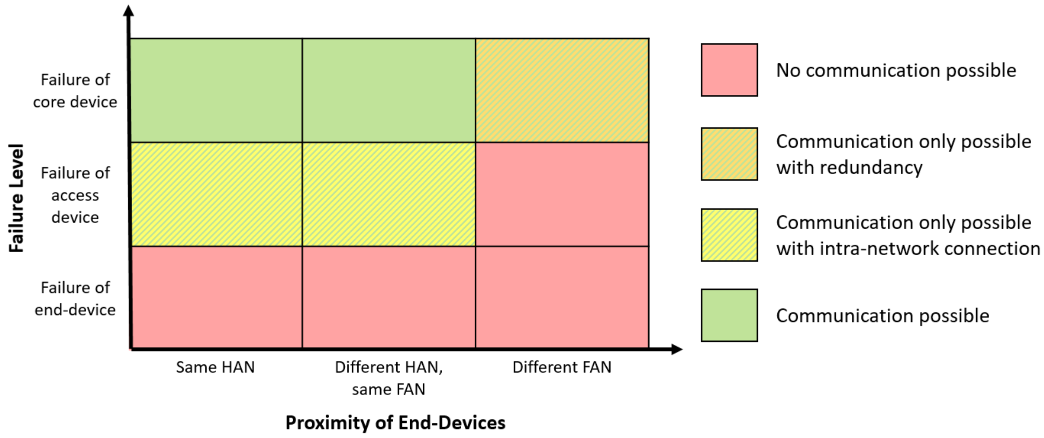

Fig. 2.7.: Effects on end-to-end communication between two devices, assuming intra-network connections (own design)

communication between devices on the same HAN or FAN network if there is no intra-network communication. However, access and core routers are critical if two devices are on different FANs. While access routers typically don't have redundancy, the core network is meshed, so the failure of a single device may not result in a loss of connectivity [79]. However, even with redundant routing paths, there is no guarantee that communication can be conducted as in normal operation. The failure of parts of the networks can lead to an overload of the remaining links, which causes congestion [79]. This, in turn, can cause jitter, packet loss, or increased latency. Moreover, increased usage of devices can also cause the battery backup to drain faster than anticipated.

From an end-device point of view, it is unknown how long the communication will last because the state of the battery backup is unknown. This means the communication can also degrade or even fail in the middle of the communication if the access device fails or becomes overloaded.

2.3.2 Effects of Communication Failures on Island Grid Restoration

As described in Section 2.2.2, communication between the various relevant devices is critical to enabling island grid restoration. Failure of the communication system directly affects the performance of the restoration service. The exact communication requirements of the service depend on its implementation (e.g., centralized vs. distributed), but the negative effects of congestion or no connection at all must be dealt with either way. From the perspective of the restoration process, several difficulties need to be addressed, such as:

- No available information on generation/load/switch status
- Inability to control devices before power is restored to the area (i.e., it is not possible to change setpoints)
- Working with outdated information on certain elements of the network
- Long response time of elements
- Uncertainty about whether or not control commands will be executed

This can generally be summarized as a higher-than-usual level of uncertainty and, therefore, increased difficulty in ensuring a stable and secure restoration process. In conclusion, it is not sufficient to rely on emergency power supply and ICT system robustness against blackouts when performing island grid restoration; it is also necessary to consider the impairment of the communication system. At the same time, restoring different parts of the grid would also restore parts of the ICT system, thereby improving communication between devices.

2.4 Automated Island Grid Restoration

Automated restoration processes can assist the DSO in the complex task of creating an island grid. Various approaches can be found in the literature, with different focuses and methodologies. This chapter aims to provide an overview of the diversity of related work based on a selection of papers. Two levels are defined to cluster the related work. The first one uses the considered state of the ICT system, following the use case description in [63]. Here, the authors describe different use cases for self-healing of so-called organic distribution systems and distinguish between three ICT service levels: acceptable, impaired, and unacceptable. In the case of acceptable ICT performance, self-healing schemes can be implemented using any control strategies that require communication. For self-healing under degraded ICT, it is necessary to evaluate the limited control options and, for example, allow operational limit violations to prevent a blackout. Finally, if the ICT service level is unacceptable, this corresponds to a blackout in the communication network, where other means of communication must be activated, or local control strategies must be used for self-healing. Using these three use cases as a base, the related work is classified into the following three categories:

1. Communication-based restoration approaches under fully functioning ICT (see Section 2.4.1)
2. Communication-based restoration approaches under impaired ICT (see Section 2.4.2)
3. Communication-less approaches (see Section 2.4.3)

The second level for clustering the related work is the approach used for restoration, namely centralized or distributed. In centralized approaches, a central controller collects data from all relevant elements, performs an optimization to find optimal set-points and switching sequences, and then sends back control signals. In distributed approaches, neighboring controllers exchange information (such as active/reactive power or switch states) to find an optimal solution. The solution to the problem is parallelized, and the system's behavior results from individual actions. In particular, MAS are used for distributed control strategies [110].

Table 2.3 summarizes some advantages and disadvantages of centralized vs distributed restoration algorithms. While central approaches usually give the best results, they are sensitive to single-point-of-failure, in which case the whole restoration can not be performed [90]. However, distributed approaches are robust against individual communication failures while providing good enough solutions.

Tab. 2.3.: Advantages (blue text) and disadvantages (orange text) of central and distributed restoration based on [110]

	Central Restoration	Distributed Restoration
Comm. load	Fewer messages necessary	Coordination requires more messages
Comm. distance	Long-distance communication links to control center are required	Data communication distances are much shorter
Data security	Data security is easier to ensure	Security of data in distributed algorithms is often a problem
Solution quality	Usually gives best solution to the problem	Might not find the optimal solution
Efficiency	Using one expensive super-machine for not much better results	Using many inexpensive machines provides a good performance/cost ratio
Reliability	Single point of failure	If one controller fails, the whole system will be able to survive, possibly with reduced performance
Scalability	Each new device requires changes in control room	Incremental expansion is possible, only local updates required
Complexity	The control center has to solve a large number of tasks with many variables	Distributed control divides the task into several subtasks, which are processed concurrently in a distributed manner

At the end of the Section, the research gap will be briefly summarized based on the presented related work.

2.4.1 Communication-based Restoration Approaches under Fully Functioning ICT

The restoration approaches described in this Subsection all require communication and assume a fully functional ICT system.

Central Approaches: The authors in [27] present a rule-based optimization algorithm for finding a switching scheme to restore a distribution grid after a disaster with multiple faults. The most critical nodes are always connected first; network radiality, voltage limits, and load limits are considered constraints. Relevant data such as network topology, load, and generation are continuously transferred from

IEDs to a database and used by the algorithm during a blackout. If monitoring or controlling a field device is impossible due to ICT failures, the corresponding node is excluded from the restoration process.

While the authors in [107] also consider multiple faults in the grid, they formulate the restoration as a constrained optimization problem, intending to maximize the amount of restored load weighted by their priority and a set of dynamic, generation resource, and topological constraints. They assume that parts of the distribution system have already been stabilized in different microgrids with some additional generation. Now, it should be decided which of the areas in blackout should be connected. They use a Matlab MILP solver to find a solution to the optimization problem and determine a restoration path. It is not mentioned where the necessary information is assumed to come from. Still, since the dynamic performance of DER is used to solve the problem, it seems that the authors assume the availability of current information on generation, load, and faults in the grid.

In [26], the authors focus on the multi-objective part of the restoration problem and consider a secondary objective besides maximizing the restored load, namely minimizing the switching costs. For this purpose, each switch is assigned a coefficient that considers the switch's current position and the switching costs themselves, which depend on whether the switch is remote-controlled or not. The Minimum Spanning Tree is used to solve the problem and find optimal island networks.

Another relevant aspect is considered by the authors in [18], who not only plan the recovery for static load values but also develop a sequential service restoration strategy with different restoration steps over a given time horizon. They note that identifying the ideal horizon length is not straightforward since, with a larger horizon length, the computation time grows exponentially. In contrast, small horizon lengths may get stuck in local optima. Therefore, they propose to use the rolling horizon method for online use, where the restoration algorithm is repeatedly run for short horizon lengths, always using the system configuration from the previous iteration as the initial condition. For information collection, the paper assumes an outage management system that collects data from the advanced metering infrastructure and field measurements through the SCADA system, which is considered to be functional.

Distributed Approaches: The authors in [85] developed an agent-based restoration approach for a low-voltage microgrid using online information about generation and load. Generation units and load are represented by agents that know the active power, connection situation, readiness for restoration, and predefined priority.

Agents can only exchange information with their neighbors in the grid. However, it is assumed that only one generation unit is grid-forming and acts as a blackstart capable unit, while the rest are grid-following. In a different approach, the authors in [16] formulate the restoration problem as a knapsack problem and assume that each load and generator can be connected individually, with no specific focus on blackstart-capable units. This allows a very dynamic creation of a microgrid.

The uncertainty of load and generation during island grid restoration is an important issue, especially considering that due to the small size of islands, it is challenging to compensate automatically for forecast errors. The authors in [91] consider island grid restoration as a multi-objective problem with maximizing the restored load (considering priorities), minimizing the number of switching operations and considering the maximum likelihood estimation of solutions. The optimal restoration sequence is found for the entire estimated outage duration. The problem is solved using a heuristic rule-based algorithm as a single-objective weighted sum. The authors also mention that information can be updated during restoration, e.g., about the cause of the outage, but do not link it to the improving ICT system. The authors in [92] also focus on the uncertainty of DER during restoration and propose an artificial neural network to predict the power output of PVs. The agents represent not individual units but feeders, zones, and switches. It is explicitly stated that communication is assumed to be reliable and fault-free. In [84], the authors do not consider uncertainty from forecast errors but evaluate the trade-off between reliability and load balancing of the islanded grid during restoration. Reliability, in this case, refers to the possibility that components may fail during restoration and that if components fail, loads can be redistributed so that the system does not go back into a blackout state. They use the Wolf Pack algorithm to solve the optimization problem.

Finally, instead of balancing generation and load, the authors in [86] also consider another aspect of island grid restoration: The protection system of island grids has to be adapted based on the topology. Therefore, they introduce an adaptive protection strategy that selects one of several pre-recorded protection settings. The agents are organized in a hierarchical setup, with the final decisions being made on the highest level.

2.4.2 Communication-based Restoration Approaches under Impaired ICT

The restoration approaches described in this subsection require communication but consider different levels of possible failures in the ICT system. It is shown that there is literature for both centralized and distributed approaches that consider the possibility of communication degradation in their design and offer various solutions to ensure the robustness of the restoration algorithm against communication failures. However, none of the related work investigates how PS restoration can restore the ICT system and how this in turn can support PS recovery. Similarly, restoring the ICT system itself is not considered an objective, especially in the distributed approaches.

Central Approaches: The authors in [7] do not address islanding in distribution networks but explicitly study the interdependence of the power system and the communication network during restoration. Their communication system is assumed to have only on/off states with no intermediate degradation levels. Figure 2.8 shows the model used to describe the interdependencies. At the beginning of the restoration, the power and ICT systems are assumed to have one source node each (SA and SB), which is self-sufficient in terms of both power and communication and from which the restoration process starts. The gray lines represent the power supply, and the green dotted lines represent the communication links.

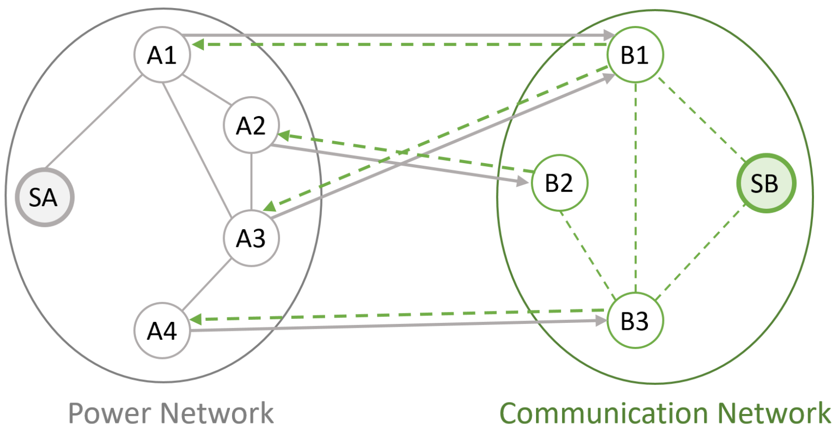

Fig. 2.8.: Illustrative example of interdependent networks from [7]

A node in either system is now only considered functional if it has both power and communication links to the source node or another functional node. In the restoration process, one PS node is restored per time step. A PS node can only be restored if at least one of the connected communication links is available. The ICT system is restored in parallel by allowing the restoration of communication links when one of the connected communication nodes is energized. At each time step, an optimization algorithm selects the node(s) to restore. The model was tested only for a small network size (14-bus power system and 9-node communication network). The authors conclude that by considering interdependencies, resources can be adequately utilized along with appropriate time management, and restoration failures can be avoided.

The authors of [81] consider the interdependency of ICT and the power system not during the restoration process but for the merging of two neighboring island grids. They assume a highly flexible network where all loads and lines are switchable and operational. The communication network is modeled by assigning a communication node to each power system node and adding links between all nodes where communication can be established. This view abstracts from any underlying ICT infrastructure and considers only the logical communication links. When both nodes are powered, the link between them is functional. This means nodes can only communicate if they are already part of an island. The optimal switching sequence to merge islands is calculated centrally, using the weighted average restored load over the planning horizon as the objective.

The authors in [109] take it a step further and analyze the stable operation of an existing islanded microgrid under random communication failures. The focus here is on synchronous voltage control of DERs in a microgrid, which requires information from sensors to be sent to a central controller, which performs the optimization and then sends adequate control commands back. They investigate both directions of this communication failure and develop several solutions to handle them, for example, an observer and controller who can take over in case of sensor failure and a prediction compensation part that uses predicted data to accomplish the control process of the controller.

Distributed Approaches: The authors in [29] developed a hybrid centralized-decentralized multi-agent framework for service restoration in smart distribution systems with DERs. The hierarchical agent architecture consists of three levels. The first level is load agents at the buses that can monitor load and generation and open switches to disconnect the bus. The second level is feeder agents at each feeder that negotiate with other feeders to restore service in case of an outage using a fuzzy rule-based system. On the third level are regulator agents at the substation transformers that can adjust the transformer tap if necessary. Communication failures are not considered as a result of the blackout, and only between two agents, not on a larger scale. The authors describe various measures to deal with these communication failures, such as a waiting period and resending of messages and backup solutions where messages are sent through other agents.

The authors in [30] take a similar approach to communication failures. They also consider three types of agents: substation control, load control, and restoration. The restoration agents and load control agents create a system behavior corresponding to a distributed version of Prim's algorithm, which creates multiple minimum spanning trees until the set of de-energized nodes is empty or the trees can no longer grow. Timers are used as triggers if agent messages are lost, making the approach robust against local communication failures. The authors in [108] develop an agent-based restoration framework that combines min-consensus, max-consensus, and bias-min-consensus algorithms to restore critical loads. They claim it is robust to topology changes, communication delays, and packet loss and can operate in an unreliable communication network. However, communication only fails for single messages, not extended periods, and there is no correlation between communication failures and the blackout.

The authors in [61] focus on the communication failures of individual agents during the restoration process. They have four different types of agents on the same structural level in the agent architecture which cooperate to accomplish the restoration task. The four agent types include bus agents, feeder bus agents, tie-switch bus agents, and DG bus agents. In case of detected communication failure of an agent, three fault-tolerance measures are implemented, including 1) assuming failed agents as uncontrollable loads and using recently recorded information for load estimation, 2) changing the identity of failed feeder bus agents to simple bus agents as they cannot act as feeder agents anymore, and 3) replacing the decision authority with the next healthy agent at the downstream side.

The authors in [36] consider only one type of agent, namely zone agents, which represent a bus with all connected loads, DERs, and switches, called a control zone. The zone agent is responsible for monitoring during normal operation and taking control actions during fault situations, such as fault isolation or restoration. The authors consider communication failures only during fault isolation and not restoration. Each zone agent checks all communication links by periodically sending beacons to its neighbors. It switches to a backup protection mechanism if it detects a communication failure.

The authors in [66] go into more detail about possible communication failures, explicitly stating that they expect communication systems to fail partially or wholly due to insufficient backup power. They also state that this is why centralized control architectures are unsuitable for island restoration in the distribution system: the longer the distance to be communicated, the more likely communication failures are. They then take a different approach to ensuring robustness against communication failures: Instead of determining the restoration steps online during the blackout, restoration is prepared in advance during normal operation when communication systems are fully functional. A controller is equipped with the resulting contingency plans and determines which contingency exists and whether a blackstart is feasible in the event of a blackout. A mixed hierarchical-distributed architecture with four types of agents is used to develop the contingency plan: Distributed generation and storage agents and tie agents at the lowest level, a microgrid control agent at the higher level, and a multi-microgrid coordinator agent at the highest level. While information is exchanged within and between all levels, control commands are only sent top-down from the microgrid control agent to the underlying agents. In the event of a power outage, the microgrid control agent checks to see which agents it still has a functional communication link with and only considers those to take part in the restoration process.

2.4.3 Communication-less Restoration Approaches

The restoration approaches described in this subsection can function without the communication infrastructure, relying on local measurements and predefined control mechanisms. These approaches are the most advanced regarding technology readiness, as they only require little additional ICT infrastructure in the distribution grid to be tested in field trials. However, communication-less approaches can only work if the islanded network itself has been designed in detail in advance and tested with simulation. This can be particularly difficult with fluctuating DER, as more or less power may be available during the blackout depending on the situation, allowing more or less loads to be connected.

Central approaches: The project *LINDA* investigated how to create a stable island grid with one blackstart capable unit as a grid-forming inverter and the other DERs in the grid as grid-following generation that can be used as an emergency measure [96]. No additional communication or control infrastructure should be installed at the DERs to reduce costs. Instead, the DER should be controlled via droop control, using frequency and voltage to "communicate" with the DER. The characteristic of the DER is assumed to be fixed as defined by the grid codes, i.e., only the leading power plant's $P(f)$ characteristic curve can be changed as required. To determine this curve, the feed-in capacity of the DER in the grid area must be known. This means the approach only works for a predefined grid area, not dynamically created island grids. A field test was conducted with a hydroelectric power plant as the black-start unit, 185 PV systems, and 400 households. A stable island grid was maintained for four hours.

The project *NETZ:KRAFT* investigated the question of how to adapt concepts for grid restoration with renewable energies and, in this context, also looked at the approach of using DER for island grids [40]. To this end, they conducted several case studies. One case study investigated the islanding of a real 20kV grid section with a biogas plant, a diesel-powered mobile emergency power supply, and distributed PV generation. Using the $P(f)$ characteristic curve, communication-free active power management is possible in the islanded grid. Switching operations can also be performed manually if they are not remote-controllable. However, they conclude that a blackout-resistant communication infrastructure is required for optimal integration of DER in grid restoration.

Distributed Approaches: The authors in [25] propose a fully distributed control architecture that is not used directly for restoration but for coordinating DERs in an islanded microgrid. The DERs are controlled by their decision units, which rely only on local measurements and information. No communication channels are required because the DERs use a voltage-frequency bus signaling method to transmit information the decision units need for optimal coordination.

While communication-less approaches can work well for the primary control level, the authors in [93] state that secondary control strategies for microgrids require communication between DERs. They, therefore, combine distributed proportional droop control and distributed integral control with distributed averaging algorithms to achieve precise frequency regulation, active power sharing, and a tunable trade-off between voltage regulation and reactive power sharing in an islanded grid. This requires all elements to communicate with each other, at least after the island grid has been energized.

2.4.4 Research Gap Summary

As seen from the previous sections, the aspects to be considered in automated island grid restoration and the approaches used for it are manifold. To show how the work

Tab. 2.4.: Related Work and Research Gap

	FR-1 blackstart with MAS	FR-2 fault-tolerant	FR-3 ICT as objective	FR-7 interdependencies of PS and ICT system
[60, 16, 11]	X	X	X	X
[49, 10, 54]	✓	X	X	X
[62, 57, 26, 15, 55]	X	✓	X	X
[48, 23]	✓	(✓)	X	X
[53]	✓	X	X	(✓)
[4, 46, 17]	X	✓	X	✓
[18, 19, 61, 37, 39]	✓	✓	X	X

in this thesis adds to the existing work in this area, Table 2.4 groups all presented works according to their fulfillment of the functional requirements defined in section 1.4. For clarity, not all functional requirements are listed here, but only those most relevant to the investigation of the hypothesis in this thesis. A check mark indicates that the requirement is fulfilled, an "X" indicates that it is not fulfilled, and the check mark in brackets represents partial fulfillment.

It can be seen that using agent-based approaches for black start and ensuring fault tolerance towards degraded ICT is quite common. However, most approaches do not consider the interdependencies between power and ICT systems and the resulting ICT degradation and recovery due to the blackout and its influence on the restoration process. In addition, no approach has yet considered ICT restoration as a separate objective in the restoration process.

2.5 Combinatorial Optimization Heuristic for Distributed Agents

The restoration algorithm developed in this Thesis is based on the *Combinatorial Optimization Heuristic for Distributed Agents (COHDA)* [44]. COHDA can solve optimization problems in a fully distributed way by splitting up the search space among distributed agents, thereby performing an asynchronous search in the global search space. Agents are connected through a communication overlay, which can have an arbitrary topology if it forms a connected graph. Agents only communicate with those agents who are their neighbors in the communication overlay and store the information they have about the system in their so-called *working memory*.

COHDA was initially developed for day-ahead planning of active power provision in a VPP, where each agent picks a schedule for its unit such that a global target is met together while also considering any local constraints the unit might have. During the negotiation, agents now perform the following three steps [45]:

1. (perceive): An agent a_i receives a message κ_j from a neighbouring agent a_j. This message κ_j contains the target profile ζ, the system's believed current configuration Ω_j, and the current solution candidate γ_j. The current configuration Ω_j contains the most up-to-date information agent a_j has about other agents' schedule selections. At the same time, γ_j comprises a collection of schedules that a_j has encountered at any point and is the best-known combination of schedules concerning the target profile ζ. Receiving agent a_i now updates its working memory based on the information he got from a_j. This includes storing the target ζ – if not already known – and checking Ω_j for new information. Each schedule selection in Ω_j is stored along with an internal counting variable that allows agent a_i to check whether the selected schedule of an agent in Ω_j is newer than the one in Ω_i and, if yes, updating it accordingly. Finally, γ_i might be replaced with γ_j if the latter either contains more agents or has a better result regarding the target schedule.

2. (decide): After updating its working memory, agent a_i now selects the best schedule for its unit based on the information he has about other agents' choices and updates Ω_i with it. At this point, local constraints or objectives can also be considered. Agent a_i then checks if the resulting system configuration Ω_i would give better results than the current best-known solution candidate γ_i. If yes, a new solution candidate is created. Otherwise, the selected best schedule is discarded, and agent a_i reverts to the schedule selection stored in solution candidate γ_i, which is still the best-known solution.

3. (act): Only if agent a_i has changed any component in its working memory, it sends a message to all of its neighbors in the communication overlay, with $\kappa_i = (\zeta, \Omega_i, \gamma_i)$

COHDA has been proven to converge, terminate, and be scalable and robust regarding different communication topologies and message delays [45]. This makes it an interesting choice to apply to the island restoration problem.

COHDA has already been used for different use cases, for example, for decentralized coalition formation, where two interlaced COHDA instances are used to identify the best assignment of an agent to a coalition as well as solving a predictive scheduling optimization within this coalition [14]. The authors in [76] analyze the effects of two different communication infrastructures – CDMA 450 and LTE Advanced – on the performance of COHDA in a regionalized ancillary service market (rAS), considering both undisturbed and disturbed communication scenarios. The disturbance scenarios included base station failures, congestions by increased traffic, and interferences triggered by a jammer. COHDA was used to schedule a VPP for regional ancillary services, setting a time constraint of 5 minutes for one negotiation and considering gate closure time for trading. They conclude that negotiation time has to be improved for these small timeframes so that the temporal requirements of rAS can be guaranteed even in case of communication disturbances.

COHDA has also been extended to solve multi-objective optimization problems using different approaches. The authors in [15] already used COHDA for building island grids in the distribution system. They are using a combination of lexicographic optimization and a weighted sum approach. The agents first try to minimize the distance between generation and load in the island (to ensure a balanced island grid) and then try to maximize the size of the island, the number of neighbors, and load priority. The authors in [74] use COHDA for the scheduling of the power consumption of smart buildings and considered in total four optimization goals: (1) cost optimization in terms of own consumption, (2) minimization of the peak load, (3) minimization of electricity costs and (4) minimization of behavioral adaptation efforts. All objectives are scalarized into a single objective function, using a monetization approach to solve this.

In [56], the authors extended COHDA for the first time to solve multi-objective optimization problems by creating a Pareto front. For this purpose, the S-Metric-Selection Evolutionary Multiobjective Algorithm (SMS-EMOA) concepts were integrated into COHDA. Instead of a single schedule, each agent has to choose a set of schedules, one for each solution point on the Pareto front. The agents then jointly optimize the Pareto front, using the S-metric (or hypervolume) to compute the performance of the front. This work was later extended in [94] to be more extensible and flexible for various multi-objective optimization problems. Both multi-objective benchmark functions and an example use case for an optimization problem in CPES were used to demonstrate the effectiveness and ease of use of MO-COHDA.

3 Agent-based Blackstart

This chapter introduces the first artifact of the thesis, the restoration algorithm. First, the assumed blackstart-capable system architecture, the multi-objective optimization problem, and the agent architecture are described. Based on this, the agent-based algorithm is introduced, and its convergence is proven. Finally, the issue of how to adequately represent and measure ICT performance is discussed.

3.1 Blackstart-capable Power System Architecture

The restoration algorithm developed in this thesis has been designed for a specific scenario with certain assumptions, shown in Figure 3.1. A MV network of a future CPES is considered. Various MV loads, MV generation, or LV networks (with their loads and generation) can be connected to each MV substation. While the number and placement of DER are not defined, it is assumed that there is a high level of DER in the grid, enough to serve most of the loads. In addition, at least one DER must have blackstart-capability to initiate the restoration process.

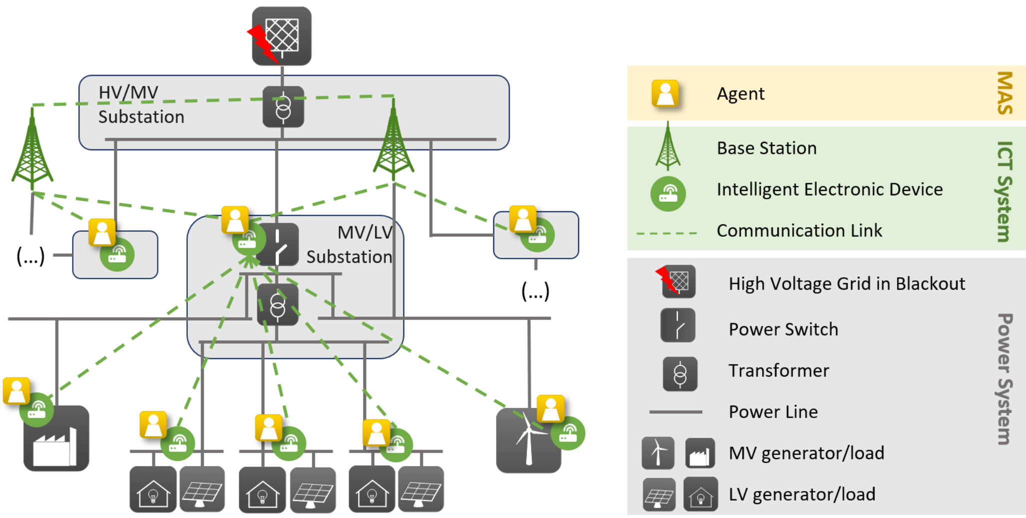

Fig. 3.1.: Blackstart-Capable PS architecture

Power lines connect the substations, and two different types of switches are assumed between the substations. The first is tie-line switches, which already exist today and can be used to connect two feeders to reroute power in case of faults in the distribution grid. They are open during normal operation and closed only when necessary. The second type of switch is the sectionalizing switch, which can divide a feeder into smaller parts. In research dealing with the future structure of distribution grids, especially concerning microgrids, it is often assumed that these sectionalizing switches are between every two nodes (see, e.g., [24], [51], [82], [89]). This assumption was adopted for this thesis. The sectionalizing switches are closed during normal operation. While some researchers also assume that switches can disconnect individual loads (see, for example, [17], [57]), this option is not considered here; if a substation is part of an island grid, then all elements connected to that substation are also part of the island grid. Switches always come in pairs, one at each substation. To connect two substations, both switches must be closed; to disconnect, only one switch needs to be opened. All switches are assumed to be remote-controllable and, regardless of their state before the blackout, will go to their "default" state when a blackout occurs (i.e., open for tie-line and closed for sectionalizing switches).

Island grids can now be created around the blackstart capable units by opening and closing switches to connect or disconnect different grid parts. If there is enough generation within the island to match the loads, the island is considered stable, and all loads are served. IEDs are needed to coordinate this balancing. They are placed at all relevant points required for the restoration process. This includes any controllable element (LV and MV level generators, switches) and loads for monitoring. Generators can receive setpoints through the IED to reduce or increase power (or even shut down the element entirely). Switches can be opened or closed. Current consumption can be measured for loads.

In the initial blackout situation, neither load nor generation is available and, therefore, cannot be measured. To have any knowledge about the system, it is, therefore, relevant to store the last known measurement on the one hand and to have a possible forecast of the generation/load for the next hours on the other hand. This knowledge is also needed during normal operation, e.g., for (re)dispatch planning. The described architecture assumes that this knowledge is available at the individual IEDs for their respective element.

The ICT system is not defined by concrete technologies but in an abstract form. A wireless hierarchical communication infrastructure is assumed, based on the information described in Section 2.2.2. Figure 3.2 shows the general architecture of the ICT system. The three base stations, BS1, BS2, and BS3, each correspond to a communication cell that establishes communication between all IEDs within this communication cell when the respective base station is active. For an IED to communicate with another IED outside of the communication cell (e.g. IED6 to IED12), it is necessary that the neighboring base station is also active and has established a communication overlay with the IED's base station. An IED can be part of more than one communication cell (see IED4, IED8, and IED9). The process of establishing communication links between IED and BS or between BS and BS is not considered in detail.

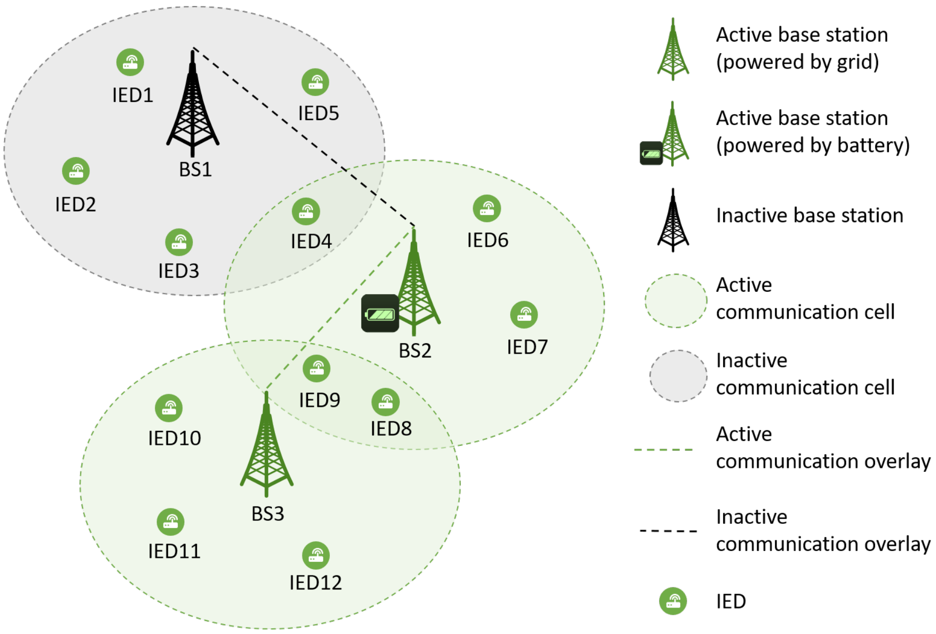

Fig. 3.2.: ICT architecture overview

All base stations are connected to the grid for power supply and are considered normal loads. If the substation they are connected to is part of an island grid, the base station is functional and can perform communication tasks (see BS3). However, if it is in the blackout part of the grid, it needs a battery backup to be functional (see BS2). The same is true for the IEDs. Due to their small size, IEDs are assumed to have sufficient battery backup throughout the restoration process. Base stations, however, may either have no battery backup at all, or it may be depleted during the blackout phase, leaving the base station inoperable until it becomes part of an island grid. IEDs within an inactive communication cell (see IED1 to IED5) can not communicate, even if the IEDs themselves are active. An agent-based algorithm can now coordinate and plan a restoration sequence using the combination of IEDs and base stations for communication. Agents can be placed on each IED and exchange messages using all available communication links.

3.2 Formalization of the Restoration Problem

The interconnected system examined in this thesis is modeled following the graph-based approach from [69]. Here, the authors define two types of nodes and four types of edges to achieve a graph representation of the different relations and dependencies between the power and ICT system. This representation is adapted for the specific wireless communication system model that was described in Section 3.1. Figure 3.3 shows the graph model with the different nodes and edges. The ICT system is described by base station nodes and communication links for inter-BS communication and intra-BS communication. The power system is characterized by aggregated grid segments, lines between the grid segments, and the power supply to the base stations in the ICT system. In the following, the formal definition of the graph model will be described.

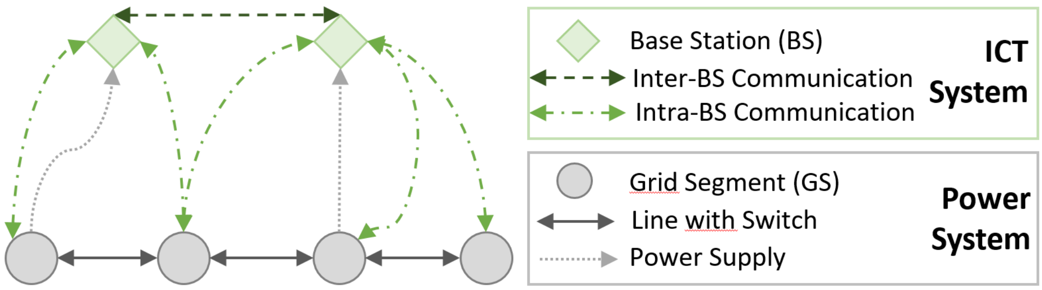

Fig. 3.3.: Graph model of interconnected PS and ICT system (based on [69])

Interconnected system graph G consists of two different sets of nodes (V_e, V_c) and four different sets of edges (E_s, E_b, E_p, E_g). The nodes V_e describe a set of grid segments. A grid segment $v_i \in V_e$ can consist of one or more power system buses enclosed by two or more switches (exception: if a grid segment is at the end of the line, it only has one switch). In the context of island grid forming, it can be assumed that a grid segment can either be fully part of an island grid or be fully disconnected. Hence, this aggregated view was chosen. Each $v_i \in V_e$ is defined by an aggregated generation schedule w_i^P and an aggregated load schedule w_i^L, which are vectors of mean power generation/consumption values for defined time intervals. The generation is described with negative values and load with positive values according to the passive sign convention. The respective schedule is filled with zeros if a grid segment has no generation or load connected. One grid segment, which has a blackstart capable unit connected to it, is the defined starting point of the restoration process and is named v_{start}.

The edges $E_s := \{\{v_x, v_y\} | v_x, v_y \in V_e \text{ and } x \neq y\}$ define the set of power lines between the grid segments. On each power line $e_i \in E_s$, there is a switch s_i, which is described by its respective switch state with $s_i = \begin{cases} 0 & \text{when the switch is open} \\ 1 & \text{when the switch is closed} \end{cases}$

If the switch for an edge is open, the respective edge gets removed from E_s. That means the switch states define which edges exist in the graph.

The second type of node, V_c, represents the base stations (BS). The communication links between two BS (inter-BS communication) are defined by edges $E_b := \{\{v_x, v_y\} | v_x, v_y \in V_c$ and $x \neq y\}$. Unless the BS has an emergency battery, it draws power from the respective grid segment it is connected to and can, therefore, only be active if the node is part of an island grid. This dependency is modeled by the edges $E_p := \{(v_x, v_y) | v_x \in V_e, v_y \in V_c\}$, which represent the BS power supply and are the only edges that are not bidirectional. Finally, the coverage area of the BS is modeled as the set of edges $E_g \to \{\{v_x, v_y\} | v_x \in V_e, v_y \in V_c\}$, which represent the communication between power system nodes via the BS (intra-BS communication).

Based on this, two subgraphs can now be derived from G: The island grid $I = (V_e^I, V_c^I, E_s^I, E_p^I)$ and the communication topology (in the following called "overlay") activated by this island grid $O = (V_e^O, V_c^O, E_b^O, E_g^O)$. Grid segments and BS are represented as nodes in both graphs, while edges are divided into power lines and communication links and are only part of either the island grid or the overlay. It should be noted that $V_c^I = V_c^O$ as long as emergency batteries are not considered, meaning that a base station can only be part of the overlay if it is also part of the island grid. However, $V_e^I \neq V_e^O$ is possible since the coverage area of a BS can stretch beyond the current island grid, enabling communication to grid segments that are themselves not part of the island grid yet.

The assignment of nodes and edges to the island grid graph I is defined as follows:

(1) $v_{\text{start}} \in V_e^I$

(2) $V_e^I = \{v_i |$ there is a path $(v_i, ..., v_{\text{start}}) \in E_s\}$

(3) $E_s^I = \{\{v_x, v_y\} | v_x, v_y \in V_e^I\}$

(4) $E_p^I = \{(v_x, v_y) | v_x \in V_e^I\}$

(5) $V_c^I = \{v_i |$ there is a path $(v_i, ..., v_{\text{start}}) \in E_p^I \cup E_s^I\}$

Definition (1) states that the grid segment with the blackstart capable unit is always part of the island grid. Definition (2) adds all those grid segments to the island grid, with a power line connection to the blackstart capable unit. That means that a) there has to exist a connection in the grid in general, and b) this connection is not interrupted by any of the switches being open. Definition (3) also adds all the power lines between the connected grid segments to the island grid. Definition (4) now considers the power supply to the base station and adds all those power supply lines where the respective grid segment is part of the island grid. This means that the power supply is active. Finally, based on the active power supply, definition (5) adds all the base stations to the island grid, which also have a connection to the starting grid segment.

Based on this, the communication overlay O can be defined as well:

(1) $v_{\text{start}} \in V_e^O$

(2) $V_c^O = \{v_i | v_i \in V_c^I\}$

(3) $E_b^O = \{\{v_x, v_y\} | v_x, v_y \in V_c^O\}$

(4) $E_g^O = \{\{v_x, v_y\} | v_y \in V_c^O\}$

(5) $V_e^O = \{v_i |$ there is a path $(v_i, ..., v_{\text{start}}) \in E_g^O \cup E_b^O\}$

Like the island grid, the starting grid segment is always part of the overlay, as it is assumed to have blackout-resistant communication. Otherwise, the restoration process could not start. Definition (2) states that all BS in the island grid are also part of the overlay. Definition (3) defines that when two base stations are part of the overlay, the respective inter-BS communication link is also considered part of the overlay. Definition (4) then regards the intra-BS communication links for the grid segments and states that all links connected to a base station, which is in the overlay, are also part of the overlay. It is important to note that the respective grid segment does NOT have to be part of the island grid, yet it is possible to communicate to grid segments outside the island. Finally, definition (5) states that all those grid segments are part of the overlay that have a connection in the overlay to the blackstart capable unit.

Only two optimization variables are considered for changing the island grid and overlay. First, the state of all the switches on the power lines can be used to change the island grid's composition; second, the generation schedules w_i^P can be adapted to match the load in the island grid. For a summary of all previously described elements, see Table 3.1.

After modeling the interconnected system, the actual optimization problem can now be defined, which aims at the optimal configuration of island grid I and the

Tab. 3.1.: Notation for problem formalization

Interconnected Power and ICT System	
$G = (V_e, V_c, E_s, E_b, E_p, E_g)$	Interconnected System Graph with both power and ICT system
$v_i \in V_e = (w_i^P, w_i^L)$	Grid segment with aggregated generation and load schedule
$v_{\text{start}} \in V_e$	Starting point for restoration
$v_i \in V_c$	Base station (BS)
E_s	Switches between grid segments
E_b	Inter-BS communication links
E_p	Power supply from grid segment to BS
E_g	Intra-BS communication links
Island Grid	
$I \subset G = (V_e^I, V_c^I, E_s^I, E_p^I)$	Island Grid
$O \subset G = (V_e^O, V_c^O, E_b^O, E_g^O)$	Communication overlay
Optimization Variables	
$w_i^L \in \mathbb{R}_0^+$	Load schedule
$w_i^P \in \mathbb{R}_0^-$	Generator schedule
$s_i = (0, 1)$	State for switch on power line $e_i \in E_s$

respective overlay O. The first objective f_1 focuses on the island grid and is to maximize the sum of all loads connected to all grid segments in the island grid:

$$\max f_1 = \left(\sum_{i=1}^{|V_e^I|} r_i \cdot w_i^L \right) \tag{3.1}$$

The parameter r_i describes the weight of load schedule w_i^L and can be used to prioritize critical loads. The choice of weight depends on the implementation.

The second objective f_2 is to maximize the "goodness" of the overlay graph O. How this goodness value is defined is up for the concrete definition of which elements should be considered in the ICT performance function. An intuitive first step is to consider the number of connected grid segments in the overlay, which would lead to the following objective:

$$\max f_2 = |V_e^O| \tag{3.2}$$

If parameters like the quality of the communication links or the importance of the grid segments (for example, if a grid segment contains a large amount of generation) should also be considered, it would be possible to add weights to the respective nodes and edges in the overlay and consider this as well in the objective. In addition, it may be useful to check in detail how many individual elements (such as generators and loads) are connected to a particular grid segment in order to rate grid segments with more connected communication nodes higher.

Both objectives are subject to the following constraints. First, a switch is only allowed to close when both the grid segments it connects are part of the communication overlay. This ensures that the information about the load and generation of this grid segment is available and suitable control commands can be sent while creating the island grid.

$$e_i = 1 \Leftrightarrow \{v_x, v_y\} \in V_c^I \tag{3.3}$$

Second, for all grid segments in the island grid, the sum of generation and load needs to equal zero (with an allowed deviation $\pm\epsilon$). Imbalanced islands are invalid solutions and could not only cause another blackout but might also destroy equipment.

$$\left(\sum_{i=1}^{|V_e^I|} w_i^L\right) + \left(\sum_{i=1}^{|V_e^I|} w_i^P\right) = 0 \pm \epsilon \tag{3.4}$$

To limit the complexity, this problem formalization uses an aggregated view of the power system (aggregation of power system nodes to grid segments) and omits further constraints of power system restoration, such as maintaining voltage and line load limits in the resulting island network. However, the relevant elements for investigating the research questions and hypotheses are included, such as the interdependencies between the island grid and the resulting communication overlay. Therefore, it can be used as a valid simplification of the complex restoration problem.

Figure 3.4 uses a small example to illustrate why including ICT as a constraint alone may not be sufficient and why it needs to be explicitly considered as a separate objective. In this scenario, the power system consists of nodes A to E, which have different amounts of load and generation connected to them. Nodes B and C have already formed an island grid, which has activated base station 1. This allows communication with nodes A and D to potentially integrate them into the existing island grid (see switch closing constraint in eq. 3.3). It can be seen that the existing island has an additional 10 MW of generation, while nodes A and B have 10 and 5 MW of loads, respectively. This means connecting both nodes to the island grid simultaneously is impossible, as the balancing constraint (see eq.

3.4) could not be satisfied. If only objective f_1 (see eq. 3.1) is considered, the obvious choice would be to connect node A, which would restore the most load. However, although connecting node B would restore less load, it would activate base station 2. This would allow communication with the additional node E and possibly further extension of the island grid in the next restoration step. By considering ICT restoration as a separate objective, these two trade-off solutions could be identified, and – depending on the priorities of each objective – the second solution could also be chosen.

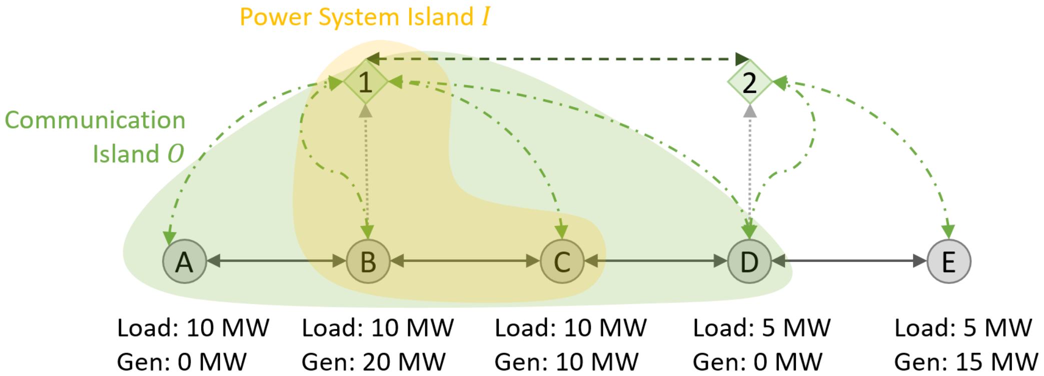

Fig. 3.4.: Example scenario to show trade-off between objectives f_1 and f_2

3.3 Agent Architecture for Blackstart Algorithm

A MAS is used to solve the optimization problem described in Section 3.2. In this thesis, it is assumed that the only task of the agents is to create a restoration plan in case of a major blackout. Any necessary coordination during normal operation or of the resulting island grid is not considered.

Agents represent the different elements described in Section 3.1 and formalized in Section 3.2. These include loads, generators, switches from the power system, and also base stations from the ICT system. Agents are divided into two types: *Switch Agents* and *Unit Agents*. Switch Agents can make decisions about opening/closing switches, defining the topology of the power system and thus creating island networks. It is important to note that Switch Agents do not represent individual switches but rather an entire substation with all the switches connected. This means that a Switch Agent is placed at each substation and can decide whether this substation should be connected or disconnected from the neighboring substations. However, the decision to connect two substations is not made by one agent alone: Since there are two switches on the line, one on each bus, both agents representing the two substations must agree to close their switch. As long as one switch remains open, the substations will remain disconnected.

While Switch Agents define the composition of island grids, Unit Agents represent all the elements that would be part of the island grid and, therefore, determine the island grid's properties. This includes loads, generators, and base stations, which can be seen as a load with additional information. Therefore, agents are placed at all these elements. It is assumed that all loads are uncontrollable, including base stations, which don't have any control options. Unit agents representing loads or base stations can only provide information about their respective elements (amount of predicted load and characteristics of the base station, such as how many nodes are within the communication cell) without the ability to adjust anything during the restoration process. This means that balancing generation and load within the island grid falls solely on those Unit Agents, which represent the generators. Here, the agents know the flexibility of their unit, possibly the forecast for generation (in the case of weather-dependent units), and can define schedules with setpoints for their units. Depending on the complexity of the problem definition, any agent's knowledge and control abilities could be extended. For example, Unit Agents representing loads could also know about their priority, or agents representing base stations could also change settings in the ICT system.

Table 3.2 summarizes the agent types and the elements they represent, which knowledge and control options they have, and to which variable from the optimization problem they belong.

Tab. 3.2.: Overview of different agent types

	Switch Agent	Unit Agent	
Represents	MV substation	Load/Generation	ICT
Knows	Current state of switch(es)	current and forecasted load/generation, for generation: flexibility	Buses connected to the base station
Controls	open/close switch	generation: setpoints for unit	-
Variable	s_i	w_i^L, w_i^P	$v_i \in V_c$

The two types of agents are separated during the optimization process to handle different parts of the optimization problem. While Switch Agents negotiate to find the optimal island grid configuration that maximizes the objectives, Unit Agents negotiate to optimize the properties of the resulting island network (in this case, minimizing the difference between generation and load). Along with this separation between types, agents are also separated by their distance from each other. This means that agents representing elements closer to each other communicate more with each other than agents representing elements further away, resulting in a *holonic* structure or *holarchy*. Holarchies are similar to hierarchical architectures with the difference that the parts are autonomous and not dependent on decisions of a higher level of control [98]. In a holonic MAS, the agents form groups of so-called holons, where each holon represents a self-contained system on the lower level while at the same time acting as a participant in the system on the higher level. The lowest level is called an atomic holon, which can not be divided further. This allows the reuse of control logic at each level and will enable holons to continue operating autonomously even if the connection to other holons is lost [77]. In the case of the power system, the use of holonic MAS can be an excellent way to manage a large number of fluctuating DERs and active consumers by having them represented as atomic holon agents and then grouping them into a hierarchy for monitoring, ensuring flexibility and scalability [48].

Some definitions of holonic MAS emphasize the complete autonomy of agents, allowing them to leave a holon at any time and join other holons, keeping the structure of the holarchy fully dynamic [33]. However, this only makes sense if the underlying system represented by the holonic MAS is also dynamic. For example, in the case of a VPP with dynamically changing generating units, it may be possible for the representing agents to change from one holon to another. It is also common, however, to represent the energy system in a holonic structure based on its regional aspects, following the structure of the energy system with the interconnected system as a whole at the highest level, down through regions, cities, and neighborhoods to individual generating units and consumers [98]. This view is also used for the restoration problem; therefore, the holons are fixed, and agents are not allowed to switch between them.

In recent years, the term "cellular energy systems" has been coined by the *Verband der Elektrotechnik Elektronik Informationstechnik – VDE* (Association for Electrical Electronic Information Technologies). They define an energy cell as a collection of operating equipment for various forms of energy, where the balancing of generation and consumption within the energy cell and coordination with neighboring cells is organized through an energy cell management [101]. It is emphasized that these cells exist not only on one level but can also be arranged in a hierarchy, leading to a generic system architecture consisting of similar cell structures on all levels. This definition is very similar to that of a holarchy. However, in this thesis, the term holarchy is used as it is more prominent in the context of agent architectures. Moreover, the term holarchy emphasizes the collaboration of the agents during system restoration since balancing load and generation is not limited to individual holons but should happen across the whole holarchy.

Figure 3.5 shows the holonic MAS used for system restoration. The top-level holon consists of all the Switch Agents representing all the substations in the system. Since, in the case of a blackout, it is assumed that there is no connection to the control room, no higher-level holons are considered here. Below this, the holons of all loads, generators, and base stations connected to the respective substations are placed. This level is a mixture of atomic holon agents – such as agents representing MV loads or generators – and more holons for LV feeders. Below this level, there are now two possibilities: If there are more switches in the LV grid, and it is possible to disconnect certain LV grid parts, another level of Switch Agents follows. Otherwise, the connection is made directly to the lowest level, which consists of the individual households and power plants in the low-voltage network. Either way, the lowest level always consists of only atomic holon agents.

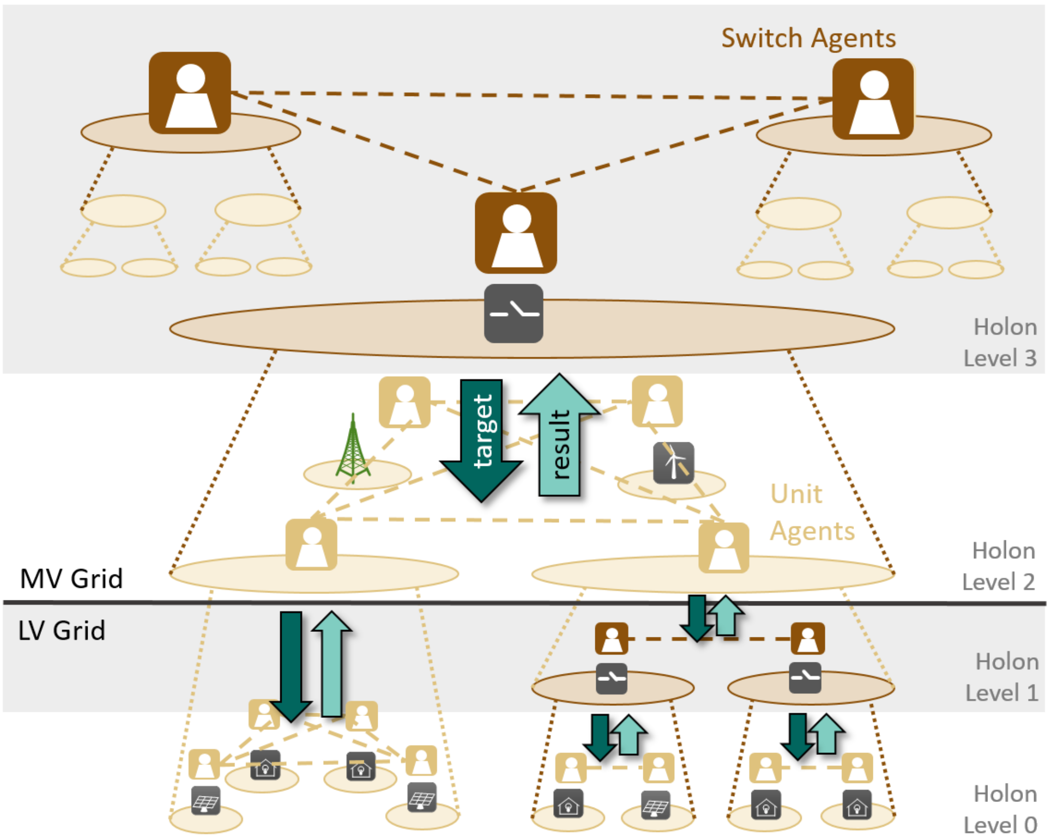

Fig. 3.5.: Holonic Agent Architecture

There is always only one type of agent within a level. As mentioned above, different types of agents are responsible for different parts of the optimization problem, which they solve by communicating with other agents within the same holon. Switch Agents try to maximize the restored load and ICT while considering the constraint of balancing load and generation. Unit Agents try to minimize the distance to a target schedule. The determination of the optimal switching sequence and island balancing is considered a combined optimization problem since the decisions for each part affect the decision for the other part: A switch can only be closed if the resulting island grid has balanced generation and load, while at the same time, the flexibility provisioning required for balancing depends on the switch configuration, as it defines which loads are part of the island. Therefore, all levels exchange the results of their respective optimizations, which will be the target schedule for the current island configuration by the Switch Agents and the restored load, ICT, and island balance by the Unit Agents.

For communication from the lower to the upper holon level, a specific agent is always chosen from the lower holon to receive the results from the upper level and to send back the results from its level. This agent is the so-called "speaker" of the holon and can be either a Switch Agent or a Unit Agent. In addition to being responsible for this exchange of information, the agent participates in the negotiations within its holon. Therefore, any agent can become the speaker. In this thesis, the speaker on the highest holon level is always the Switch Agent representing the bus with the blackstart capable unit, since it makes sense to start the restoration process there. For the underlying holons the speaker is always chosen randomly.

Another notable role of an agent is the so-called "aggregator," which describes a non-atomic Unit Agent that does not represent a single generator or load but rather an entire low-voltage grid, for example. This agent has no control options but only represents the aggregated LV node in the negotiation within its holon. While the placement of agents within holons is fixed, agents can appear/disappear dynamically during the restoration process, thereby expanding the holons themselves. The restoration process could be initiated at any hierarchical level and in any holon and propagate upwards or downwards.

It should be noted that the MAS implemented in this thesis assumes a strict hierarchy of the underlying power system, where a node of a lower voltage level has only one connection to the higher voltage level (e.g., an LV grid is always connected to exactly one MV node). In reality this is not always the case, especially on higher voltage levels it is common to have more than one connection to the external grid. In this case, the holon would have two connections to higher-level holons and receive targets from two Switch Agents. This is possible as long as several conditions are met:

- **Both Switch Agents are part of the same coalition:** In this case, both Switch Agents are aiming to build the same island grid and will, therefore, agree on the same solution to implement. This ensures that the underlying holon does not receive conflicting instructions on how much generation to provide.
- **The two options for connecting the same underlying holon to an island grid can be distinguished:** When one of the Switch Agents has already closed the switch to connect itself and the underlying holon to the island grid, the other would not directly impact the composition of the island grid by closing its own switch as well (thereby connecting the same grid part at two points to the island grid). In this case, it must be ensured that the second Switch Agent can determine whether closing or opening the switch is the better option, for example, by considering load flow or defining rules for whether more than one connection to the grid is preferred.

In the following, the case of two (or more) connection points will not be considered further.

3.4 Blackstart Algorithm

The basic idea of the restoration algorithm is that it is impossible to recover the entire system in one step since not all information is initially available due to the degraded ICT system. By creating a first island grid, ICT infrastructure is restored further, allowing the existing island grid to be extended. This results in a cascading restoration behavior, where restoring the power system enables the restoration of the ICT system, which in turn improves the restoration of the power system.

Figure 3.6 shows the concept of this cascading restoration process. After a blackout, a communication overlay is created using the available ICT infrastructure. The agents now use this communication overlay to coordinate with all other reachable agents and try to find an optimal island grid. If this is not possible – for example, because there is not enough generation to feed the loads, even in a small area – the restoration process is over. If a valid solution is found, it is implemented in the power system by controlling switches and generation units accordingly. If the restored grid area also contains ICT infrastructure elements that can improve the communication overlay, the restoration process is repeated: the communication overlay is updated, and the agents start the optimization process again, possibly to find a larger island grid. If there is no new ICT infrastructure and, therefore, no new information for agents, the restoration process is also complete. It is important to note that the current concept of the restoration algorithm does not plan to remove nodes after they have become part of an island grid. This means that in each restoration step, the island can only grow, not shrink. Only the restoration algorithm for the MAS (outlined in red) is developed in detail. The creation of the communication overlay or the implementation of the resulting island grid is beyond the scope of this thesis.

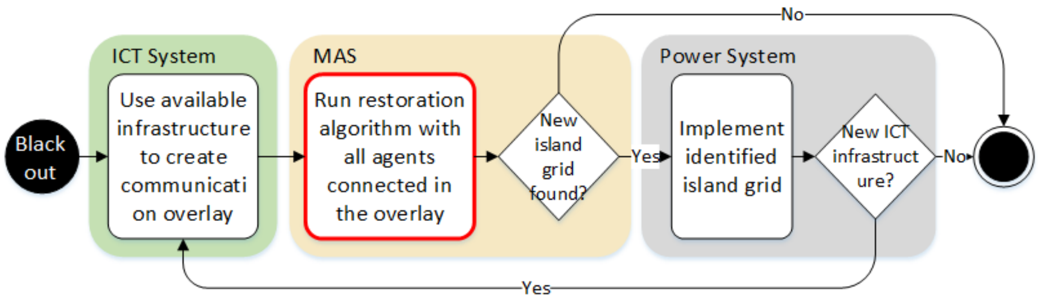

Fig. 3.6.: Basic Concept for Cascading Restoration Process

As mentioned previously, the Switch Agents determine the switch configuration, and the Unit Agents balance the generation and load. Both types of agents use a version of COHDA to solve their respective optimization problems. Figure 3.7 shows the basic optimization process from the perspective of a single Switch Agent and a single underlying Unit Agent and explains the two intertwined COHDA instances. The basic COHDA process has already been described in 2.5, so the focus is on how COHDA was adapted to solve the island restoration problem.

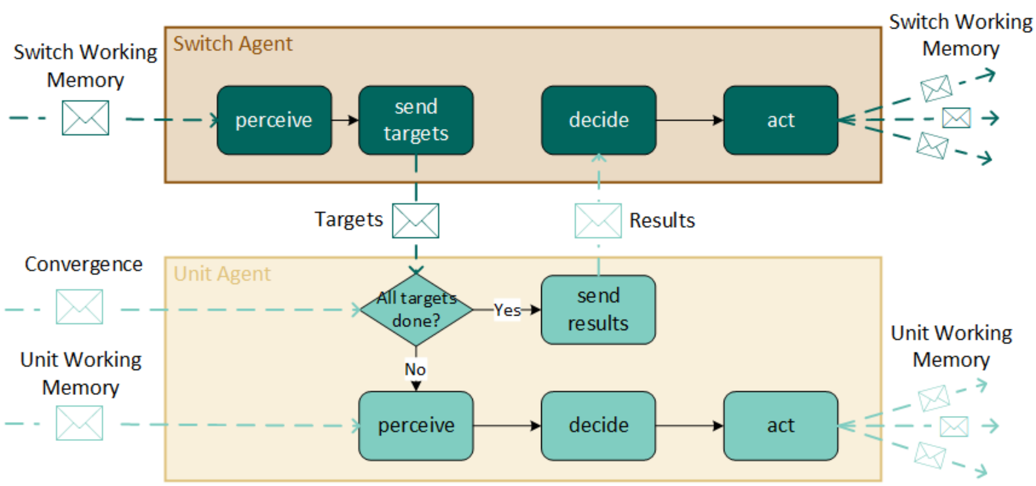

Fig. 3.7.: Intertwined COHDA instances between Switch Agent and Unit Agent

Switch Agent Optimization: All Switch Agents in one holon level are part of the same COHDA instance. They exchange information through working memories. A switch working memory contains the state of all switches controlled by the Switch Agents that have already participated in the negotiation and aggregated information about the grid nodes connected to the switches. This aggregated information includes the total load and generation connected to the node and information about the ICT infrastructure at that node (the exact information depends on how the ICT performance calculation is defined). The restoration process begins when the Switch Agent, representing the node with the blackstart capable unit, sends the first working memory to its neighbors. When a Switch Agent receives a Switch Working Memory, it performs the following steps:

1. *Perceive*: It starts with the usual perceive step of COHDA. Here, a counter is used for the agent to identify new information about switch states or nodes and to replace it accordingly in its working memory.
2. *Send Targets*: The next step would be for the Switch Agent to decide which switches to open or close, thereby connecting or disconnecting the substation it represents from neighboring nodes. However, the Switch Agent must know whether the resulting island grid is balanced to make this decision. It, therefore, triggers its underlying holon to attempt to balance the island grid by sending a target schedule for the specific island configuration. The target is created by summing the aggregated load and generation values of all nodes that would be connected in this configuration. This target can be 0 at any time step if the island is balanced, or it can be negative or positive if excess or less generation is available. A Switch Agent usually controls more than one switch, resulting in different possible combinations, each resulting in different island grids. Furthermore, in the case of multi-objective optimization, not just one solution may be optimized, but a Pareto front of solutions. Therefore, the Switch Agent creates not one but all possible targets for all the different decisions it can make and sends them to the speaker of the underlying holon.
3. *Wait*: The Switch Agent must now wait until it receives the underlying holon's results before proceeding with COHDA. However, it can still receive new Switch Working Memories and send new targets to the underlying holon during this time.
4. *Decide*: Finally, when the Switch Agent receives the results, it can perform its local optimization and select the best switch configuration(s) for the objective(s). Following the usual COHDA procedure, it then checks whether the

new best solution found is better than the current candidate solution and, if so, replaces it; otherwise, it reverts to the old one.

5. Act: All new information and the final decision of decide are then sent to all neighboring Switch Agents.

Unit Agent Optimization: Unit Agents perform optimization only within their holon and not with all other holons at the same level. Only the Unit Agents connected to the same agent at the higher holon level participate in the negotiation. This ensures local communication between agents and limits the number of agents participating in a negotiation. The process is as follows:

1. *Start COHDA (only Speaker)*: When the speaker agent receives a (list of) target(s), it takes the first one and starts a normal COHDA negotiation.
2. *perceive, decide, act*: The optimization process here is very similar to the "classic" COHDA, since the Unit Agents act like a VPP that tries to meet a target schedule. The only difference is the participation of agents representing the ICT infrastructure, which only add their information to the working memory without optimizing anything themselves.
3. *Convergence (only Speaker)*: Each time a negotiation is finished, the speaker checks if there are still unused targets. If so, a new negotiation is started. The convergence is detected by an external observer agent, which informs the speaker through a convergence message.
4. *Send Results (only Speaker)*: Once a solution has been found for all targets, the Speaker sends all the results and their respective targets back to the Switch Agent that triggered it. The Unit Agents are now passive until they are triggered again with new targets.

This process can be repeated on more levels if there are more holon levels. For example, if a Unit Agent is an aggregator for an LV grid, instead of going directly from perceiving to deciding, it would also trigger the lower-level holon with the current target and wait for the result before continuing its participation in the negotiation.

Multi-objective problem-solving: Two different objectives are considered when determining the optimal island grid configuration: maximizing the restored load and maximizing the restored ICT infrastructure (see Section 3.2). This means that Switch Agents have to consider multiple objectives during their optimization.

The authors in [23] suggest that the ideal procedure for solving multi-objective optimization problems should be to (1) "find multiple trade-off optimal solutions with a wide range of values for the objectives" and (2) "select one of the obtained solutions using higher-level information." The higher-level information is usually non-technical, qualitative, and based on experience and can help rank the objectives' importance. This ideal approach is more systematic, practical, and less subjective than transforming the multi-objective problem into a single-objective problem (e.g., with a weighted-sum approach). Therefore, the multi-objective problem in this thesis is solved using the Pareto method.

As described in Section 2.5, COHDA has already been extended to solve multi-objective problems with Pareto fronts. The generalized approach of [94] is now used and adapted to the restoration problem. Figure 3.8 shows the multi-objective optimization process with MO-COHDA and the two intertwined COHDA instances from the perspective of a Switch Agent. Instead of a single island configuration, a Switch Agent maintains a set of island configurations in its working memory, where each configuration is a solution point on the Pareto front. As usual for COHDA, the SystemConfig contains the most recent information from all other agents, while the Candidate has the best currently known solution – in the case of MO-COHDA, the currently best known Pareto front. The performance of a Pareto front is defined by its hypervolume, the size of the area between the Pareto front, and a reference point that should have very poor performance values in all objectives. In a maximization problem, this could be the zero point or a point slightly below zero. The challenge here is to ensure that the performance values can never be worse than the reference point, so it is essential to know what the lowest (in case of maximization) or highest (in case of minimization) performance values for each objective can be.

After updating the memory in perceive, the Switch Agent moves on to decide. As explained earlier, this process is split into two parts: Creating the search space and the actual decide step.

Create Search Space: A Switch Agent represents an entire power system node but has no information about that node initially stored. It must, therefore, gather information from the lower-level holon of Unit Agents. In this setting, the Switch Agent is not allowed to make decisions for individual units or even have full knowledge of their flexibility, all of which should remain with the Unit Agents. This requires the Switch Agent to ask for every switching decision: "If the island grid were to look like this, what would be your schedule choices and what would the resulting ICT system

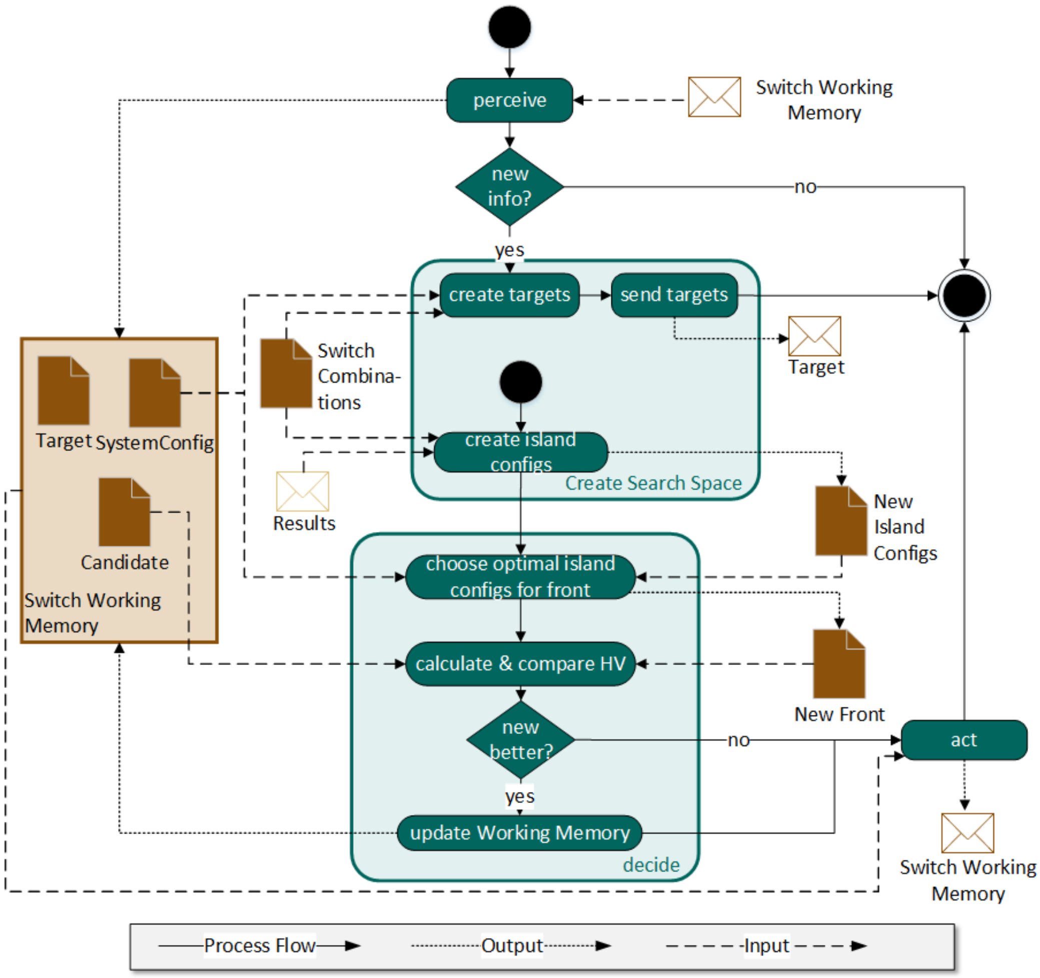

Fig. 3.8.: Detailed view of the algorithm from Switch Agent perspective

look like?" to its lower level holon, thereby creating the search space for its current decision. This involves the following steps:

1. *Create targets*: A switch is only allowed to close if both nodes that the switch would connect are already part of the SystemConfig, i.e., information about generation, load, and ICT is available on both nodes. If this is not the case, a switch must remain open. The Switch Agent now takes all allowed switch combinations and proceeds to combine all switch combinations with all solution points in the current SystemConfig, creating several new possible island configurations. It calculates the target schedule for each configuration, i.e., how much power must be produced/consumed in each time step to balance the resulting island grid.

2. *Send targets*: The Switch Agent now filters out all identical targets and sends the final list of targets to the speaker of the lower-level holon to initiate the restoration process.
3. *Create Island configs*: Once the Switch Agent receives back the results of the lower-level negotiations, it can create new island configurations by updating the switch states according to the possible switch configurations and changing the node information based on the results of the lower level negotiation for the specific target assigned to that switch combination. The Switch Agent has now created a list of new solution points.

Decide: With all the information collected, the Switch Agent can proceed with the actual decide step. This includes:

1. *Choose optimal island configs*: The Switch Agent has all the solution points from the current SystemConfig, plus any newly created points. The goal is to reduce the number of points back to the predefined number of solution points. This is done following the process of MO-COHDA, where the solution point with the smallest contribution to the hypervolume is removed until the desired number of solution points is reached [94]. The hypervolume is calculated using the performance values of each objective. This part can easily be extended with more objectives or constraints, thereby fulfilling the non-functional requirement of Extensibility. After this process, the Switch Agent has created a new optimal Pareto front.
2. *Calculate & Compare HV*: The Switch Agent calculates the hypervolume of the new front and compares it to the current Candidate's hypervolume, representing the best Pareto front so far. If the hypervolume is larger, a better front has been found.
3. *Update Working Memory*: The front in the candidate gets replaced, and the agent updates all its switching choices and node information in the SystemConfig based on the new front.

3.5 Proof of Convergence of Blackstart Algorithm

The basic COHDA has been formally proven to converge by Christian Hinrichs in [45]. In this section, the same approach will be used to show that the restoration algorithm, despite the changes compared to the basic COHDA, still converges, thus fulfilling the non-functional requirement of guaranteed convergence. While this section provides an informal summary of the convergence proof, a detailed version is given in Appendix A.1.

The convergence proof is done under a set of assumptions that must be satisfied for the convergence proof to work. These assumptions are also considered and adapted for the convergence proof of the restoration algorithm:

- Every identifier of an agent is unique such that a lexicographic ordering on the set of agents exists.
- The search space of each agent is finite.
- Only agents connected to the agent that starts the restoration in the communication overlay can participate in the restoration process. This ensures that the communication graph of agents is connected.
- Agents are only allowed to participate in the negotiation if the communication links they use are sufficiently stable so that no message loss can occur. If the quality of a communication link degrades during restoration to the point where messages are lost, the respective agent must be removed from the restoration process.

All interlaced COHDA instances in the holonic architecture need to converge for the restoration algorithm to converge. Therefore, the convergence is investigated for three different types of agents:

1. Convergence of *atomic agent*: A Unit Agent with no further holon levels underneath them can directly make its decisions without waiting for the results from lower levels with single-objective COHDA. Atomic holons are, by default, only Unit Agents because Switch Agents, even on low voltage, have a holon with Unit Agents underneath them.
2. Convergence of *non-atomic agent with single-objective optimization*: This describes Unit Agents aggregating a lower-level holon. They must wait for the lower-level negotiation to converge and use single-objective COHDA.
3. Convergence of *non-atomic agent with multi-objective optimization*: Finally, Switch Agents with lower-level Unit Agent Holons underneath them have to wait for the convergence of these holons and use MO-COHDA.

Within one negotiation, there can be a mixture of atomic agents and non-atomic single-objective agents, e.g., Unit Agents representing MV generating units and Unit Agents representing an aggregated LV grid, which are connected to the same MV bus and, therefore, part of the same holon and the same negotiation. On the other hand, non-atomic multi-objective agents can never be in the same holon as the other two types of agents, i.e., they only negotiate with agents of the same type within a COHDA instance. The following sections briefly summarize the convergence proof for all three types of agents.

3.5.1 Atomic Agents

Hinrichs defines three predicates as the base for the convergence proof and uses the convergence stairs reasoning approach from [28] to prove that they will all consecutively hold within a finite timespan. The three predicates are:

$\mathcal{A}_1$ All agents have complete working memories, i.e., they have information about all other agents stored.

$\mathcal{A}_2$ A final solution candidate is found that cannot be improved by any agent.

$\mathcal{A}_3$ The working memories of all agents are identical, and thus, the heuristic terminates with the final solution candidate.

The proof for $\mathcal{A}_1$ uses the behavior of COHDA as a base. Following *perceive*, *decide*, and *act*, agents always add their own information to the working memory when they receive it for the first time and do not remove it again at any point. Additionally, when an agent receives a working memory that contains information about another agent it has not yet stored in its own working memory, it will always add this information. That means, as long as there is no message loss and all agents are connected – which are two of the previously defined assumptions – within a finite amount of time, all agents will have participated in the negotiation at least once, adding their information to the working memory, which in turn gets distributed to all other agents.

To prove $\mathcal{A}_2$, Hinrichs shows how once $\mathcal{A}_1$ holds, a solution candidate at an arbitrary agent is only replaced when the agent either finds a better solution or has found the same solution but has a higher agent id. In that case, the solution gets stored with the higher agent ID, which requires the assumption of lexicographic ordering of agent IDs mentioned previously to be fulfilled. That means the solution quality can only increase, not decrease, over the whole agent system. Since one of the assumptions is a finite search space for each agent, the number of possible solution candidates is also finite. This results in the agents reaching a (local) optimum in a finite amount of time, which individual agents cannot improve anymore.

Finally, $\mathcal{A}_3$ follows after $\mathcal{A}_2$ holds true. In this case, at least one agent has found the final solution candidate and the information has to be spread among all other agents. When an agent receives the final solution candidate for the first time, it will include it in its working memory and then send it to all its neighbors. Within a finite amount of time, the information will have reached all agents in the negotiation. Once an agent knows the final solution candidate, it will stop sending messages since any message it receives will not give it new information. This means that the system will terminate within a finite amount of time.

For a more detailed derivation of the convergence proof, see [45]. Atomic agents have behavior identical to the algorithm described by Hinrichs et al. in [45]. Consequently, the convergence proof for negotiation between only atomic agents is the same as the convergence proof for basic COHDA. **This means that any negotiation consisting only of atomic agents would always converge** (if the assumptions are met).

3.5.2 Non-atomic Agents with Single-objective Optimization

For non-atomic agents with single-objective optimization, the most significant difference to the basic COHDA is the break between *perceive* and *decide*. If the agent has made any changes to its working memory in *perceive*, the target for the lower-level holon is created and sent, triggering the COHDA process there. The agent must now wait for the result of this negotiation to include the schedule in its schedule selection, then follow the same *decide* and *act* steps as in the basic COHDA process. This requires some changes to the original COHDA convergence proof.

Most importantly, it must be shown that a non-atomic agent can still process a message in a finite time despite waiting for the lower-level negotiation to finish. To simplify the proof, let's consider a holon layer of non-atomic agents with only atomic agents below. For atomic agents, convergence was already proved in section 3.5.1, meaning that in a finite amount of time, a non-atomic agent would receive the result of the negotiation and be able to continue with its *decide* and *act* processes. Based on this, $\mathcal{A}_1$ (all agents have complete working memories) still holds after a finite amount of time since non-atomic agents have the same behavior of adding information to working memory and incorporating new information they have about other agents.

Regarding $\mathcal{A}_2$ (a final solution candidate is found), the process of replacing solution candidates only if they have a higher performance value or the respective agent has a higher ID is the same. All that remains to be shown is that the finite search space assumption also holds for non-atomic agents. A non-atomic agent with single-objective optimization has no initial search space since it represents a set of underlying Unit Agents. It builds its search space with each result it receives from the underlying negotiation. As long as the underlying atomic agents have a finite search space (and thus a finite set of solutions they can send), the non-atomic agent will also have a finite search space. Based on this, $\mathcal{A}_2$ also holds for non-atomic agents.

Since it was shown that messages are still processed within a finite amount of time, $\mathcal{A}_3$ (the heuristic terminates with a final solution candidate) also holds. **This means that any negotiation of non-atomic agents with single-objective optimization would always converge.** This convergence proof also extends to mixed negotiations with atomic and non-atomic agents with single-objective optimization since the interaction between the agents is identical. Non-atomic agents might just take longer to reach the *act* step of COHDA, as they have to wait for the lower level result in between.

For a more detailed derivation of the convergence proof for non-atomic agents with single objective optimization, see Appendix A.1.1

3.5.3 Non-atomic Agents with Multi-objective Optimization

Non-atomic agents with multi-objective optimization are similar to those with single-objective optimization concerning the separation of *perceive*, *decide*, and *act*. However, there are several differences:

1. Agents do not try to find one single solution but a set of non-dominated solutions. Therefore, a set of solutions has to be optimized in parallel, and agents must choose their decision variables for each solution.

2. Agents have two different variables they can choose: the bus data from the lower level result and the switch states.

3. While bus data can only be chosen from a single agent (since a bus is represented by exactly one Switch Agent, as described in section 3.3), switch data can be chosen by the two agents who represent the buses that the switches connect. That means two agents control the same variable.

4. Agents do not always send a single target to the lower level but can also send a set of targets and, therefore, receive a set of solutions from which they can choose.

However, all of these differences can be integrated into the convergence proof of non-atomic agents with single-objective optimization. Despite the increased complexity, agents still process messages in a finite amount of time. While an agent can send more than one target to the lower level, the total number of targets to be sent in one message is still limited by the number of different possible switch combinations and the number of solution points, both of which are finite. The targets will be processed by either non-atomic agents with single-objective optimization or atomic agents, both for which convergence has already been shown. That means the agent will receive a set of results from which it can choose in finite time and proceed with *decide* and *act*.

For $\mathcal{A}_1$ (all agents have complete working memories), while data integration is more complex due to the set of solution points and the two different variables, it is still ensured that each agent gathers information about all other buses and switches in the negotiation in a finite amount of time.

Also, $\mathcal{A}_2$ (a final solution candidate is found) will still hold. First, comparing two solution candidates still relies on a single value, namely the hypervolume of the Pareto front in the solution candidate and – if this is identical – the agent ID. Second, there is a limited number of possible island configurations and a limited number of potential bus data (based on the possible schedules the agents connected to this bus can choose from). This means the search space of agents is also still finite. Agents can only create a finite number of different solution points to change the Pareto front, which means there is a finite number of different sets of non-dominated points. This ensures that there will be a solution candidate that no agent can improve further.

Finally, $\mathcal{A}_3$ (the heuristic terminates with a final solution candidate) also holds true. Since each switch is stored in the solution candidate with only one switch state, it can never happen that two agents controlling a switch assume different states for it. That means, based on the fact that agents still show the behavior of only answering messages if they changed something in their system state or solution candidate, the final solution candidate found through $\mathcal{A}_2$ will be distributed among all agents until they all have the same solution candidate and stop sending messages.

It can be concluded that any negotiation of non-atomic agents with multi-objective optimization would always converge. This shows that each of the three different agent behaviors introduced at the beginning of section 3.5 would lead to convergence, and therefore, the restoration algorithm itself will always converge. For a more detailed derivation of the convergence proof for non-atomic agents with multi-objective optimization, see subsection A.1.2.

3.6 Measuring ICT performance in Optimization Problem

Measuring the ICT performance of an island grid is a prerequisite for considering its maximization as an objective, as described in Equation 3.2. A simple approach would be to take the number of connected components in the ICT system as the performance measure and aim to maximize it. This assumes that ICT connectivity is binary; either it is fully present, and the component can be used as usual, or it is unavailable. However, as described in Section 2.3, failures in the communication system can have further effects than just the inability to communicate between two components, especially in the context of the islanding process. Therefore, when trying to maximize ICT performance, it could be helpful to consider not only the connectivity of components as a binary variable (connected/not connected) but also the state of the components. Different levels of ICT failures can then be classified into different *ICT states*, which can be used to describe the performance of individual components in more detail than just their connectivity. The goal is then to maximize the number of connected components and improve their state.

This section presents an approach for deriving states of agents in the restoration algorithm for this purpose. It is based on the authors in [52], who introduced a concept for classifying the performance of so-called Smart Grid Services (SGS) into different states based on the properties of the ICT system. The idea is that each SGS has requirements on the ICT system that can be categorized into three properties: *Availability*, *Correctness*, and *Timeliness*. Availability is defined as the functionality of a component at a specific time instant, correctness is defined as "the closeness of a measurement to its true value (ground truth)," and timeliness is defined as "the total time lapse between transmission and reception of measurements and control signals." A SGS that satisfies all three properties is "fully functional." In [71], the authors have used these properties to show the influence of different ICT faults on each of the properties. The results are shown in Table 3.3. With this concept, changes in the three properties can represent different failures.

Changes in the properties of the ICT system result in changes in the performance of the SGS, which may differ from the expected and desired behavior. However, devia-

Tab. 3.3.: ICT faults and their categorization for Correctness (C), Timeliness (T) and Availability (A) after [71]

ICT faults	Affected Components	C	T	A
Cyber Attack	All except links	√		√
Congestion or Overload	All		√	
Loss of power	All except links			√
Hardware failure	All			√
Hardware partial failure	All except links	√	√	
Device software complete or partial failure	All except links		√	√

tions from the desired behavior do not necessarily mean the SGS is not functional. Depending on the service, it is also possible for it to exhibit behavior that cannot be considered "fully functional" but is not a "complete failure" and still provides valuable results to the power system. This is due to the concept of "graceful degradation", where a service does not jump directly from "fully functional" to "complete failure" but goes through one (or more) intermediate step(s) [104]. Based on this, the authors define three states for all SGSs: *normal*, *limited*, and *failed*, which reflect how the system operator can use that service. A normal state means the service is fully functional and can be used as intended. A limited state means that the service has partial performance degradation and should be used cautiously. A failed state means that the service is no longer functional, and the system operator should focus on restoring its functionality [72]. Different behaviors of an SGS can now be categorized into one of these states, and the correctness, timeliness, and availability properties can be used to define when an SGS is in which state. While normal and failed states are easy to determine, the limited state is up to the concrete design and definition of the service. It may also be possible to define multiple levels of the limited state if necessary [72].

For distributed services, such as the agent-based restoration algorithm, the challenge in defining states is accounting for the emergent effects between agents. It is impossible to determine in advance how an individual agent's failure will affect the service's overall performance. Therefore, in this thesis, the state concept for SGS is not used for the whole restoration algorithm but rather at the level of individual agents, assuming that each agent is its own SGS.

An agent in a *limited* state can offer a reduced performance compared to its normal behavior but still participate in island restoration. This limited performance can either be designed by the agent itself (e.g., using historical data as a fallback option when real data is not available) or be a consequence of the limitations of the ICT system (e.g., a longer time to respond to messages due to increased delay in communication links). Again, it should be noted that the fact that individual agents are in a limited state does not necessarily mean that the entire restoration service shows limited performance. A good example is the increased response time of agents due to delays in communication links. In [13], it was shown that having agents postponing their local optimization randomly in COHDA (making them so-called "lazy") – which is similar to messages getting delayed – can improve the performance of COHDA. Similar effects could also occur for the restoration algorithm. This makes it particularly difficult to define an overall state for the whole algorithm and why the focus here is only on individual agents.

Since each agent represents a component of the power system that is relevant to the restoration process, not only the number of participating agents but also their state should be used to calculate the ICT performance of an island system. In this regard, the following two questions must be answered:

1. How many states beyond *normal*, *limited* and *failed* can an agent have? Should there be several gradients of limited?
2. How is a particular state defined from ICT perspective? What has to happen in the ICT system for an agent to be in a specific state?

The following sections discuss these questions with the aim of deriving a general concept for the ICT states of agents in the restoration algorithm.

3.6.1 ICT States of Agents

In general, both Switch Agents and Unit Agents perform the following tasks in the restoration algorithm:

- **Monitor:** Agents observe the current state of their component and other relevant aspects associated with it, such as weather forecast information.
- **Process:** This includes all tasks necessary for the negotiation, such as processing messages following the steps of the algorithm described in Section 3.4.
- **Control:** This task is only relevant for agents representing controllable components, such as Switch Agents and Unit Agents representing generating units. It describes the ability to control and change the component's settings.

- **Communicate:** In the context of the restoration algorithm, this task describes explicitly the ability of an agent to communicate with the agent that represents the blackstart-capable unit and thus start the recovery process, i.e., the agent can send and receive messages from the blackstart capable agent.

Using these tasks as a base, it is now possible to define different states for agents based on whether or not each task can be completed. To limit the number of states in this example, task completion is considered binary, i.e., whether the task can be fulfilled. However, it would be possible to create more detailed states by considering partial task fulfillment, e.g., limited controllability.

Table 3.4 shows all combinations of fulfilled and unfulfilled tasks, along with the resulting states. Here, "Com" refers to communication, "P" to process, "M" to monitor, and "C" to control. Combinations, where monitoring is worse than controlling, are unrealistic and therefore excluded from the table. Controlling is assumed to be always as good as monitoring since both need a connection to the required component. All combinations where the communication or the processing task is impossible can be categorized into the state **non-responsive**. When an agent is in this state, the associated component is non-existent from the point of view of the restoration algorithm since no information about it is available. If the agent can perform processing and communicate with other agents, but monitoring and control are impossible, the respective agent can be considered as **addressable**. In this state, the agent can still participate in the restoration process and either provide general information about its component based on historical data or inform other agents about its existence. If the agent can only monitor the component, the state is referred to as **observable**. In this case, the agent has up-to-date information about the element and can communicate this information to the restoration process but cannot control the component. This is already the best state for agents representing generally uncontrollable components, such as loads. Finally, if all tasks can be performed, the agent can be considered **flexible**, which is the best possible state for agents representing generating units and switches and means that all functions can be used for restoration.

These states can only describe atomic agents representing a single component. For non-atomic agents, the state would also depend on the state of the lower-level agents, which can be mixed (e.g., some lower-level agents might be in a flexible state and some only in an addressable state). To adequately describe this case for the aggregating agent, it may be necessary to define more in-between states.

Tab. 3.4.: ICT States for Agents in Restoration Algorithm

Com.	P	M	C	State Name	State Description of respective component
0	0	0	0	non-responsive	No reliable information whatsoever of a component is available
0	0	1	0		
0	0	1	1		
0	1	0	0		
0	1	1	0		
0	1	1	1		
1	0	0	0		
1	0	1	0		
1	0	1	1		
1	1	0	0	addressable	Static information regarding its built or installed capacity or last known state may be inquired
1	1	1	0	observable	Dynamic information regarding its current and last known demand or generation or state may be inquired
1	1	1	1	flexible	The component is observable and offers assured flexibility or ancillary services as well as a forecast for a given/defined period into the future

3.6.2 Relation between ICT Failures and ICT States of Agents

To calculate an island grid's ICT performance value it is necessary to derive ICT States for agents in a potential – not yet existing – island grid. Therefore, the relationship between the current state of the ICT system and its effect on the previously described tasks that the agents perform must be defined.

Figure 3.9 shows a simplified overview of all the ICT infrastructure an agent uses to fulfill its aforementioned tasks. In total, there are a maximum of 5 different ICT elements an agent uses:

- The **component** the agent represents. This can be a switch, generating unit, or load in the power system or an ICT node from the communication system.
- The **agent** itself. It can either be a switch or a Unit Agent.
- The **link between the component and the agent**. This element is optional, as it is also possible that the agent is directly located at the component. In this case, their communication link is not considered a separate element.
- The **speaker agent** who starts the restoration process and triggers the agents.
- The **link between the speaker agent and the agent**. This link doesn't have to be direct but can also be through other agents.

The curly brackets show which elements are required for which of the different tasks. This means that for a specific task, the respective elements must fulfill the requirements described by the element's availability, timeliness, and correctness values.

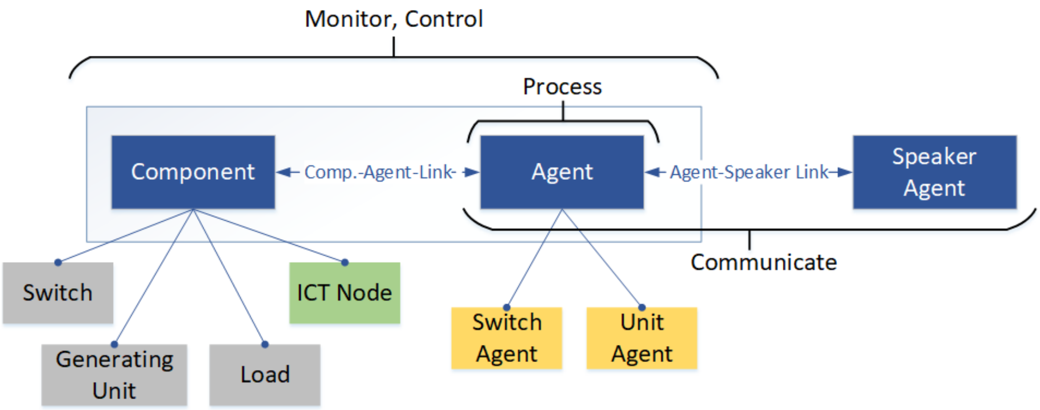

Fig. 3.9.: ICT System components of agents

All of these elements can be affected by failures in the ICT system, which can be defined as changes in their availability, timeliness, and correctness properties, as previously shown in Table 3.3. Since only a binary view has been used to describe task fulfillment, the properties are also considered binary, i.e., if the required values for availability, timeliness, or correctness are not met, the respective element is considered to have failed. In summary, the states can be derived as follows:

1. Determine each element's expected availability, timeliness, and correctness values.
2. If any of the values does not meet the requirements, the element is considered to have failed.
3. If any element required for a task is considered failed, the whole task is not functional.
4. Depending on how many tasks are expected to be non-functional, the state can be derived according to Table 3.4

3.6.3 Integration into the Blackstart Algorithm

First, to integrate this approach into the restoration algorithm, the **states of agents need to be determined by the algorithm**. The ICT system is represented by special Unit Agents that represent one base station and have knowledge about this one ICT node. As soon as a new base station is connected to a potential island grid by a Switch Agent's decision, it is now necessary not only to deduce how many new agents would be connected but also to (re)evaluate the state of all agents that would be part of this island grid. This includes agents that are not part of the current negotiation. Each agent representing a base station would require a detailed representation of the ICT system and other agents' ICT requirements to perform the previously listed steps for deriving an ICT state. How to keep the information as distributed and abstracted as possible to maintain the advantages of the distributed algorithm remains to be investigated.

Second, the **ICT performance of an island grid needs to be calculated considering the ICT states of agents**. One option could be to consider the number of connected components in the island grid (as suggested in the Formalization in Section 3.2) and additionally assign a weight g between 0 and 1 to each agent based on its state, leading to the following objective function:

$$\max f_2 = \left(\sum_{i=1}^{|V_e^O|} g_i \right) \tag{3.5}$$

However, this would mean that an island with many agents in a lower state might have the same ICT performance as an island with fewer agents in the best state – whether this is desirable behavior or not is to be investigated. Another option would be to consider not just the state of agents but also their type, e.g., an agent that represents a generator in the best state is considered more important than an agent that represents a load agent in the best state.

Incorporating the concept of ICT states into the restoration algorithm may also **require changes in the agents' behavior based on state changes** and not just an adaptation of the objective functions. If only flexible (or observable in the case of loads) agents can participate in the negotiation, nothing needs to be changed. However, allowing agents in limited states to participate means anticipating the adverse effects of this on the restoration and having a resilience measure in place to handle it. For example, the information provided by an agent in an addressable state would come with uncertainty that must be accounted for, possibly by maintaining additional flexibility reserves or allowing only a limited number of "addressable" agents in the islanded network.

3.7 Chapter Summary

This chapter introduces the agent-based restoration algorithm (artifact 1). The highlights of this chapter are as follows:

- A Blackstart-capable power system architecture has been presented. It considers an MV grid with connected MV generators, MV loads, LV networks, remote-controllable switches between every two nodes, and at least one blackstart-capable unit. Each power system element has an IED on which agents are placed. Communication between the IEDs is assumed via a wireless infrastructure using base stations to form communication cells. The restoration algorithm has been developed for this power system.
- The island grid restoration problem has been formally described. It is a multi-objective optimization problem with two objectives (maximizing the

restored load and the restored ICT) and two constraints (connecting only observable/controllable power system nodes to the island grid and balancing generation and load).

- Following the structure of the power system architecture, the MAS has been defined. Switch agents and Unit Agents represent all relevant power system elements and are arranged in a holonic structure to manage the large number of components involved in the restoration process. The optimization problem is divided into two parts: while the Switch Agents optimize the two objectives, the Unit Agents aim to satisfy the balancing constraint.
- Finally, the complete restoration algorithm has been described. It consists of two interlaced COHDA instances, where the Switch Agents use a version of MO-COHDA adapted to the restoration problem. A cascading restoration process has been achieved by repeating the restoration whenever new agents are activated.
- Guaranteed convergence (NFR-1) has been formally proven by extending the convergence proof of the original COHDA. In addition, the extensibility (NFR-2) of the algorithm concerning additional objectives or constraints has also been shown.
- The idea of using ICT states of agents as a performance measure for ICT restoration has been introduced. ICT states allow for a more nuanced view of ICT degradation than simply distinguishing between "functional" and "not functional" agents. To form a new island, the ICT performance of connected agents should be calculated. Some first approaches for defining and including these states in the restoration algorithm have been presented.

4 Proof of Concept of Blackstart Algorithm

This chapter presents a first proof of concept for the restoration algorithm to verify that the developed algorithm meets the previously defined functional requirements (see Section 1.4). It is split into two parts: a proof of concept for a single-objective version of the algorithm and one for the full multi-objective version.

The chapter is structured as follows: Section 4.1 describes the co-simulation setup, which is one of the artifacts of this thesis and was used for all evaluations. Section 4.2 describes the evaluation of the single-objective algorithm, including the scenarios, the experimental design, and the results. Finally, Section 4.3 describes the first evaluation of the multi-objective restoration algorithm, including scenarios, design of experiments (DoE), and results. The co-simulation setup and the evaluation of the single-objective algorithm have been published in [95], and the corresponding sections in this thesis (namely Sections 4.1 and 4.2) use parts of that paper, extended where necessary. These literal citations are not marked in the sections. The Section 4.3 is entirely unpublished.

Table 4.1 gives an overview of all the functional requirements, whether they are fulfilled or not, and in which section the fulfillment of the requirement is discussed.

The following sections will show the fulfillment of all requirements except functional requirement (4). The fulfillment of requirement (4) is given by the holonic agent architecture described in the previous chapter, which allows for the consideration of multiple voltage levels in a hierarchical fashion.

4.1 Co-Simulation Setup

For executing the experiments, a co-simulation approach was used with the following three simulators:

- *mango*[1] for the implementation of the MAS

[1]https://gitlab.com/mango-agents/mango, (v0.1)

Tab. 4.1.: Overview of Functional Requirements

Requirement	Fulfilled	Section
The restoration algorithm should:		
(1) Restore a distribution grid from blackout state by solving the optimization problem using a heuristic	√	4.2
(2) Be fault-tolerant (impaired ICT system)	√	4.2
(3) Consider ICT system in the optimization problem	√	4.3
(4) Consider multiple voltage levels (hierarchical structure)	√	3.3
The simulation setup should:		
(5) Co-simulate the MAS with power and communication system	√	4.1
(6) Consider all relevant characteristics of the systems needed for evaluation in the context of a simplified scenario	√	4.1
(7) Consider the interdependencies of power and communication system during restoration	(√)	4.1
(8) Provide sufficient logging & visualization results needed for evaluation	√	4.1

- *pandapower*[2] for the SimBench power grid
- *NetworkX*[3] for the ICT system.

The coupling of these three simulators was simplified by using the semi-automatic scenario configuration tool *midas*[4], which allowed easy creation of different scenarios and changing of parameters using already available simulation models and is based on the co-simulation platform *mosaik*[5].

Figure 4.1 depicts the data exchange between the simulators. The power system simulator is initialized with grid data from a pandapower grid model. The ICT system is modeled as a graph with IEDs, substation routers, and base stations as nodes in *NetworkX*. Communication links are designed as weighted edges, with the weight representing the delay of the respective link. While these delay values are always static for one simulation step, they can also be changed during the simulation to represent improvements (or deterioration) of delay values during restoration. The specific delay values depend on the ICT scenario and/or the desired objective of the evaluation (e.g. testing extreme cases).

At the beginning of each simulation step, the power system simulator sends data about available buses to the ICT system simulator, which then updates its network

[2]http://www.pandapower.org (v2.5.0)
[3]https://networkx.org (v2.5)
[4]https://gitlab.com/midas-mosaik/midas (v1.0)
[5]https://mosaik.offis.de (v2.6.0)

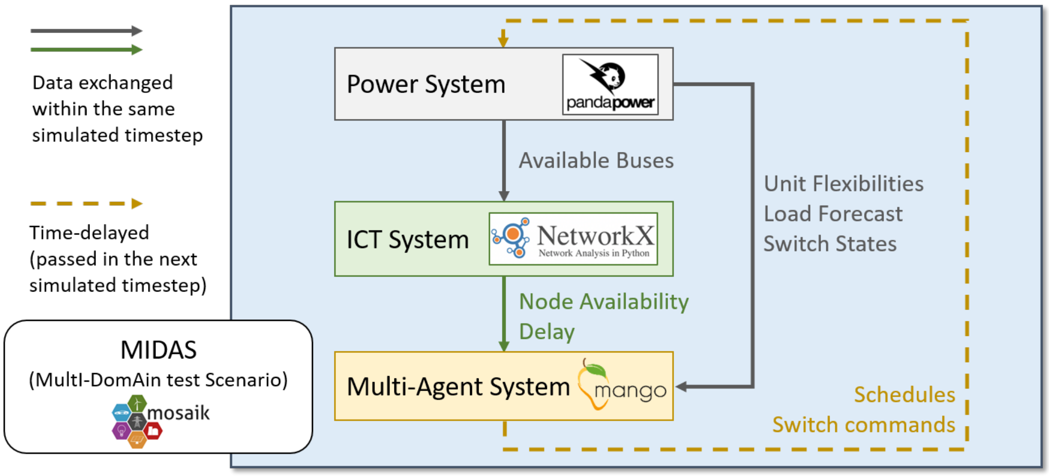

Fig. 4.1.: Data exchange between simulators

representation accordingly. A bus is considered available when it is part of an island grid. A communication network node is only part of the current network graph if it has battery backup or is connected to an available bus. The MAS then receives information about the availability of the communication nodes, which directly translates into which agents are reachable and the delay between them. This information is necessary for the agents to know who to contact during the restoration process and how long messages would be delayed. In addition, the agents receive the unit flexibilities, load forecasts, and switch states for their respective components. As uncertainties of renewables and loads are not considered in this thesis, this data corresponds to the real behavior of both units and loads. However, midas already includes a feature to add a normal distributed random noise to the data coming from the power system simulator, which could be used to mimic the fluctuating behavior of renewables. Based on all this information, the MAS performs the restoration described in Section 3.4.

A simulation step is set to 15 minutes and corresponds to a restoration step of the MAS. This means there is no time simulation of the MAS; it is assumed that a restoration process can always be completed within a 15-minute interval and that there are no changes in the ICT system between restoration steps. This also means that the previously defined delay values in the ICT system cannot directly influence the power system, as the time-critical operations during the restoration process are not modeled. However, the communication delay in the ICT system is still relevant to the MAS as it defines the order in which the agents receive messages and can, therefore, influence the outcome of the restoration process. The loads and generators also do not change during the restoration steps. This simplifies the simulation and focuses on the general analysis of the developed restoration algorithm and comparing different versions.

At the end of a simulation step, the resulting unit schedules and switch states are sent to the power system simulator, which then updates the grid and starts the next simulation step. By modelling the power system in pandapower, a load flow calculation of the resulting island grid would be possible to analyze potential violations of grid parameters. However, this was not considered in this thesis.

An observer agent is used to collect the results from the agents. The observer agent knows all agents and is known by all agents and not only keeps track of the convergence of the system but also counts the number of messages exchanged, collects the final results of a restoration step of the agents, and stores them in a CSV file after each recovery step. The parameters stored by the observer include the timestamp of the start of a new restoration process (not a new restoration step, but a whole new run of the restoration, starting from step 1), the current number of the restoration steps in the ongoing restoration, the ID of the island grid (which is relevant if several islands are being recovered in parallel), the amount of load and generation in the island grid, the number of buses connected in the ICT system, the number of messages divided into switch messages and unit messages, the number of buses connected, the list of buses connected, the performance values of the result and the total number of negotiations performed. This setup fulfills the functional requirements (5) to (8):

5. All three systems are simulated as required
6. The simulation setup represents the infrastructure of both power and ICT systems with generation, load, switch states, delays, and availability.
7. The interdependencies between the systems are modeled, with the ICT system adding/removing ICT nodes based on available power system nodes. The agents can only communicate if the underlying ICT infrastructure is available. In the basic setup, the degradation is only considered binary; ICT nodes are either available or unavailable. More levels of degradation can be added, such as changing the delay values based on changes in the ICT system. However, this has to be done manually and is not automatically considered in the setup. This requirement is, therefore, only partly fulfilled.
8. Logging is done by the observer.

Using the co-simulation setup, the general evaluation process is the same for both the proof of concept and extended evaluation. Figure 4.2 gives an overview of the evaluation setup used in this thesis. Based on the objective of the evaluation, the ICT scenario, the power system scenario, and the evaluation parameters are defined, together with an appropriate design for experiments. The MAS is derived from the ICT and PS scenarios (as it is predefined which elements have to be represented by agents, see Section 3.3). The chosen evaluation parameters and their variation for each scenario defined by the design of experiments result in the parameterization of these variable parameters. These variable parameters may also include some aspects of the restoration algorithm itself, such as the exact definition of the objective function or the approach used by the agents in their local optimization. The scenarios, the MAS setup, and these parameter settings are then fed into the evaluation platform to run the complete evaluation scenarios. The measured KPIs also depend on the aim of the evaluation and the chosen DoE. As previously explained, the KPIs are collected and stored by the observer agent. Finally, the results are investigated and interpreted

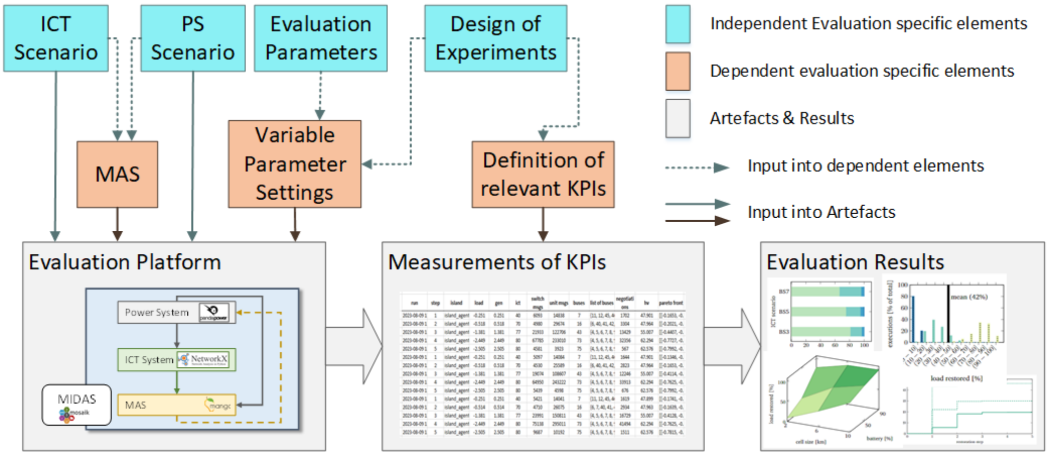

Fig. 4.2.: Evaluation Setup

4.2 Single-objective Blackstart Algorithm

This first evaluation aimed to test the restoration algorithm's general functionality and assess the impact of ICT impairments on the solution quality. To focus on the iterative restoration process of the power and ICT systems and the interaction of the agents, this first evaluation considers only single-objective optimization with the sole objective of restoring the load. Therefore, the solution quality is defined as a percentage of the maximum load restored using the available generation capacity.

4.2.1 Scenarios

To show the impact of ICT impairment on power system restoration, the limiting factors should only come from the interconnected ICT system. Therefore, the requirements for the power system scenario are:

- High penetration of DER capable of serving all loads
- High number of switches for increased flexibility in island formation

To satisfy these requirements, the SimBench *1-MV-rural–2* scenario (Figure 4.3 was chosen [67]. It is a static benchmark grid for a future rural MV scenario. Only one grid level was considered in the evaluation, with aggregated LV generations and loads as on an MV bus. The grid has 90 (aggregated) LV loads, 5 MV loads, 90 (aggregated) LV generators (PV), and 11 MV generators (PV, Wind, Hydro, and Biomass) distributed over 93 buses arranged in an open ring topology. The Simbench grid model contains two switches on every line (one per bus). They are considered to be open during the initial blackout situation. The grid has eight feeders, of which two can be connected by a tie-line, resulting in 4 separate grid segments, potentially resulting in 4 island grids. In each grid segment, one of the generating units is assumed to be blackstart-capable, which serves as the starting point of the restoration. SimBench provides time-series for generation and load for one year in 15-minute intervals, based on which the agents make their decisions. Uncertainty in the generation forecast is not considered since the restoration is only done for an interval of 15 minutes, during which the forecast is assumed to be sufficiently reliable. To be able to supply all loads with DER, a day with a high generation-to-load ratio was chosen. It is assumed that all DERs can be flexibly controlled by giving setpoints anywhere between zero and the forecast value.

Figure 4.3 also shows the concept of the ICT scenarios designed by Anna Volkova [95]. Due to the rural grid structure, the network is assumed to be primarily represented by a cellular network with base stations. The core network is not considered and assumed to be unavailable due to the wide-area blackout. Instead, the base stations establish direct communication links between each other. Each base station contains a circular communication cell of a specific size and a binary status of battery availability. A base station is always co-located with a power system node from which it receives its power supply. When the communication cells overlap, the two respective base stations have a communication link between them to allow communication between base stations. Base stations are manually placed on the network following the power lines so that all nodes are covered by at least one communication cell, and there is a continuous communication overlay between the

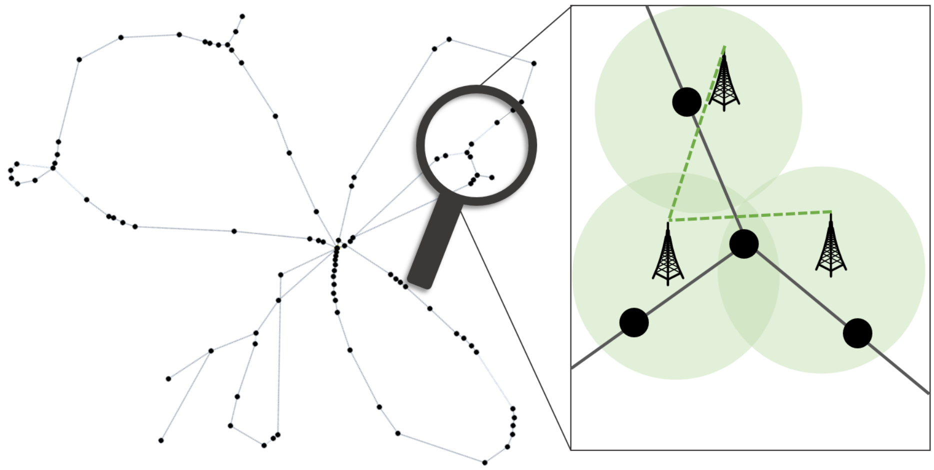

Fig. 4.3.: Scenario single-objective evaluation

base stations, i.e., the communication cells always overlap with the neighboring cells.

The scenario has a total of 285 agents, with 192 Unit Agents and 93 Switch Agents for each of the 93 buses in the Simbench grid.

4.2.2 Objective Functions

The agents use the following objective function to calculate the performance of a solution. Let $I = \{\Omega^L, \Omega^G\}$ be a potential island grid with $\Omega^L = (\omega_1^L, \omega_2^L, ..., \omega_m^L)$ being the set of m loads and $\Omega^G = (\omega_1^G, \omega_2^G, ..., \omega_n^G)$ being the set of n generators connected to the island grid. A load ω_i^L is a vector of length o which corresponds to the length of the load schedule and describes the load values for each timestep. The same is the case for a generator ω_j^G. Only active power is considered.

With only one objective, the only goal is to maximize the restored load in the island grid, which means the performance of an island grid I can be formulated as:

$$g(I) = \sum_{k=0}^{o} \sum_{i=0}^{m} \omega_{ik}^L \tag{4.1}$$

However, there is also the island balance constraint, which has to be considered. The island balance $h(I)$ describes the difference between generation and load in each timestep and can be defined as:

$$h(I) = \left| \sum_{k=0}^{o} \left(\sum_{i=0}^{m} \omega_{ik}^{L} - \sum_{j=0}^{n} \omega_{jk}^{G} \right) \right| \tag{4.2}$$

This constraint is now integrated into the calculation of the performance of an island I, resulting in the objective function $f(I)$:

The performance σ for a solution x is then calculated as

$$f(I) = \begin{cases} -|h(I)| & \text{when } |h(I)| > 0 + \epsilon \\ g(I) & \text{otherwise} \end{cases} \tag{4.3}$$

This means that when the island grid is balanced, the amount of load in it is used as a performance value, and for imbalanced islands, the negative extent of the imbalance is used as the performance value. This allows to also compare the performance of invalid solutions but ensures that valid solutions are always better than invalid ones.

4.2.3 Design of Experiments and Methodology

From a distributed restoration perspective, the state of the ICT network immediately after an outage is characterized by architectural and QoS parameters. Architectural parameters are given by the interconnected ICT and power system model. They include the number of physically available and powered ICT nodes, the average size of the communication cells, and the placement of the ICT relative to the power grid. Since the co-location of power and ICT nodes is manually defined for each scenario, only battery backup availability and cell size are variable parameters to consider. QoS is defined as the assurance provided by the communication network to deliver a set of measurable service parameters such as *delay*, *jitter*, *available bandwidth*, and *packet loss*. For this evaluation, the focus was only on the delay parameter.

To summarize, the impact of three factors on the MAS-based restoration service performance is investigated: (1) the number of available ICT nodes (base stations with battery supply), (2) the size of communication cells, and (3) the delay. For the experimental setup, a Box-Behnken-Design was chosen to study the effect of the three factors and their interdependencies [39]. The values of the three factors are shown in Table 4.2 and are described as follows:

- **Cell Size**: The values of cell sizes are chosen based on the power grid scenario and current state of the art. Owing to power line lengths of < 6 km in the selected SimBench scenario, the smallest cell size is considered to be 2 km. Based on an open data analysis performed by Anna Volkova [95], the medium cell size is selected as 6 km. Finally, large cell size is considered 10 km per state of the art of LTE technology [47]. Cells are placed manually to create one ICT scenario for each cell size.

- **Battery Supply**: According to [31], more than 30% of the batteries installed at the base stations might be faulty, discharged, or nearly dead. Thus, it is assumed that a minimum level of degradation will always be present, choosing 90% of available battery backup as the highest possible value. On the other hand, a minimum value of 10% of available batteries is assumed to enable basic restoration and 50% as the medium value to achieve uniform coverage of the response surface. Batteries are placed randomly at the base stations for each scenario and each simulation run.

- **Delay**: To receive delay values, Anna Volkova used OMNeT++ [6] simulation to retrieve delay values for the scenario [95]. Based on this, three levels of communication impairment are defined: normal (10-20 ms), slightly degraded (20-100 ms), and severely degraded (200-500 ms). The degraded network behavior is set up in the following way: Communication links start with an initial delay according to the scenario and get updated to the next best state after each restoration step, representing the increasing availability of the ICT system as well as increasing stability of communication links along the restoration progress. This also applies to the links that appear during the restoration process, newly powered buses, and consequently connected base stations. To simulate the impact of delay variations, delay values are assigned randomly with uniform distribution for the communication links based on the defined range.

Tab. 4.2.: Factor variations

	-1	**0**	**+1**
Cell size	2 km	6 km	10 km
Battery backup	10%	50%	90%
Delay	200-500 ms	20-100 ms	10-20 ms

[6] https://omnetpp.org/ (v5.6.2.)

Based on the Box-Behnken-Design, the three factors have three levels each, resulting in a total of 13 different scenarios. Table 4.3 shows all the scenarios executed in the evaluation.

Tab. 4.3.: Simulated scenarios with factor combinations

Scenario	Battery	Cell Size	Delay
S1	10%	2 km	20-100 ms
S2	90%	2 km	20-100 ms
S3	10%	10 km	20-100 ms
S4	90%	10 km	20-100 ms
S5	10%	6 km	200-500 ms
S6	90%	6 km	200-500 ms
S7	10%	6 km	10-20 ms
S8	90%	6 km	10-20 ms
S9	50%	2 km	200-500 ms
S10	50%	10 km	200-500 ms
S11	50%	2 km	10-20 ms
S12	50%	10 km	10-20 ms
S13	50%	6 km	20-100 ms

The variation in the initial conditions from the random placement of batteries and the delay values mandates the need for repeated simulation runs. To determine the number of simulation runs required per scenario to achieve the desired level of precision in the results, the approach described in [8] is followed. An initial sample of R_0 simulation runs is conducted, and the standard deviation S_0 is derived. Using Equation 4.4, the necessary number of simulation runs R is calculated for a chosen confidence interval of α and an allowed error ϵ.

$$R \geq \left(\frac{t_{\alpha/2,R_0} \cdot S_0}{\epsilon}\right)^2 \tag{4.4}$$

The parameters α and ϵ are defined as 0.05, and the start value $R_0 = 20$ is set for each scenario. For $t_{\alpha/2,R_0}$, the respective t-value from the Student's t-distribution table is selected. After executing the calculated R simulation runs per scenario, all results have a confidence value of ≤ 0.05.

4.2.4 Results

In this section, the evaluation results are presented and discussed. As a benchmark, scenarios with 100% battery backup and no delay were tested for all three cell sizes, which always resulted in 100% load restored. This implies that any degradation in load restoration observed henceforth is a consequence of impaired ICT.

Effect of Cell Size, Battery and Delay on Restored Load

Figure 4.4 shows the observed impact of cell size, battery availability, and delay on the restored load. Each point marks the mean restored load of all scenarios with the respective factor variation, i.e., -1, 0, and 1 (see Tables 4.2, 4.3). The dashed line marks the total mean of all scenarios at 63% of load restored, showing that the algorithm, in general, is capable of restoring a distribution grid from a blackout state to a certain extent and also doing so under an impaired ICT system, thereby fulfilling the functional requirements (1) and (2).

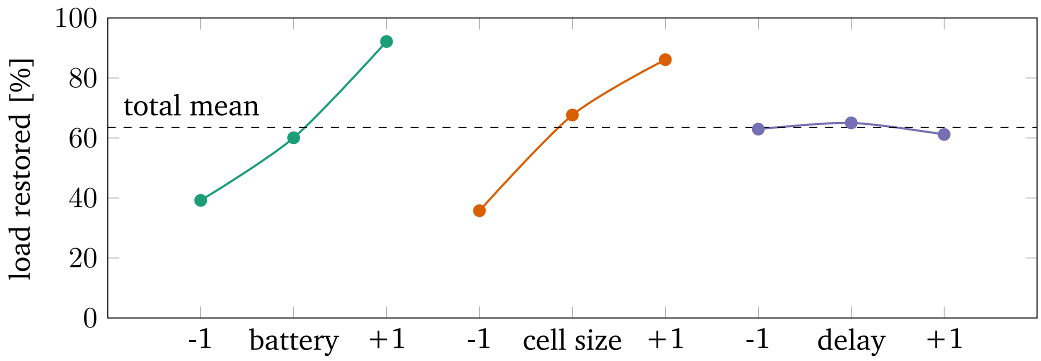

Fig. 4.4.: Effect of battery, cell size and delay.

Battery: The results show that the number of initial available base stations strongly affects the mean restored load. For the lowest battery backup availability of 10%, 40% of loads are restored, whereas 92% of loads are restored for 90% battery backup. While this effect was expected, it still raises the question of whether this dependency on initially available batteries can be reduced by considering ICT in the objective function.

Cell size: From 35% for 2 km cell size, the mean restored load reaches 86% for 10 km cell size, showing that with increasing cell size, more load gets restored. This has two main reasons: First, larger cell sizes offer a larger initial communication overlay for the restoration service even with less battery availability. As explained in Section 4.2.1, the communication system structure follows the power system structure, which means agents on neighboring power system nodes are connected in one communication cell and, hence, can form an island grid. Second, larger cells tend to overlap more, which enables the cascading restoration.

Delay: In contrast to cell size and battery, the delay does not significantly affect the restored load and was, therefore, not considered in further evaluation. This can be attributed to the already proven robustness of COHDA against message delay, which also applies to the multi-level version used in the proposed restoration algorithm. However, it should be noted that this only applies to the here-used steady-state simulations and not necessarily to time-critical operations with strict latency requirements.

Effect of Battery Placement on Restored Load

Owing to the random placement of batteries, the amount of restored load differs in each scenario execution. This effect is summarized in Figure 4.5, showing the distribution of results for different cell sizes. The black line marks the mean restored load of all simulations runs in all scenarios for the respective cell size. In Figure 4.5c, it can be observed that in the 10 km cell size scenario, the spread for all levels of battery backup availability is relatively small with a minimum of $(60 - 70]\%$ and a maximum of $(90 - 100]\%$. This is due to the higher amount of overlapping cells, which makes the restoration process more robust against base station unavailability.

However, the spread in the restored load is larger for 2 km and 6 km cell size – not only for all levels of battery backup availability but also within one individual level. Figure 4.5b, for example, shows that in the case of 50% available battery backup, in the worst case, only $(40 - 50]\%$ of the load gets restored, and in the best case, it is up to $(90 - 100]\%$ (i.e. double the amount of restored load). This effect is more pronounced in the 2 km cell size scenario, as shown in Figure 4.5a. Even with 90% available battery backup, the possible restored load varies between $(50 - 60]\%$ to $(90 - 100]\%$. Additionally, a stronger separation between the different battery levels can be observed. With minimal overlap of cells in the 2 km scenario, there is less redundancy in the communication and fewer options for cascading restoration, i.e., agents, which are not initially available through battery backup, cannot participate in the restoration process.

Cascading Restoration Behaviour

The algorithm's cascading restoration behavior, which allows the extension of initial islands after parts of the ICT system have been restored, could be observed in all scenarios. Figure 4.6 shows the mean restored load for the restoration steps for different initial available battery backup and cell sizes. For the battery backup, the

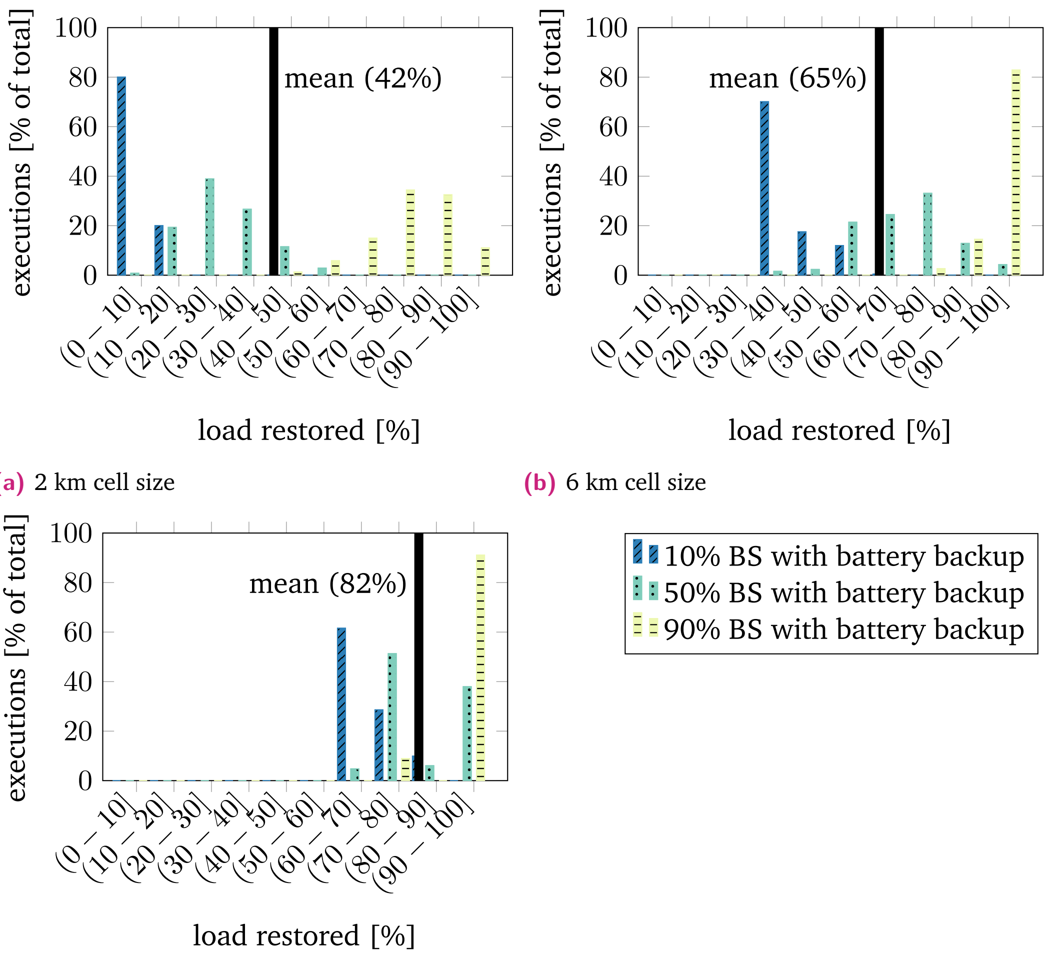

(a) 2 km cell size

(b) 6 km cell size

(c) 10 km cell size

Fig. 4.5.: Distribution of load restored per scenario execution for different numbers of batteries in different cell sizes

most substantial effect can be observed in the case of 10% battery backup: While in the first step, only 11% of the load gets restored, it increases to 36% in the second step, showing the advanced connectivity of agents after the first island grids are formed. The higher the amount of initially available base stations, the shorter subsequent restoration steps get. This is because the more base stations are initially available, the higher the chance they can form a connected communication overlay. Even with 90% of battery initially available, the mean restored load after the final restoration step is only 92% instead of 100%. The limiting factor here is the structure of the ICT system: Cascading restoration is only possible when cells sufficiently overlap for a base station to be within range of a neighboring cell, and it is energized when the agents in the adjacent cell become part of an island grid. The cascading restoration also does not compensate for less battery backup availability.

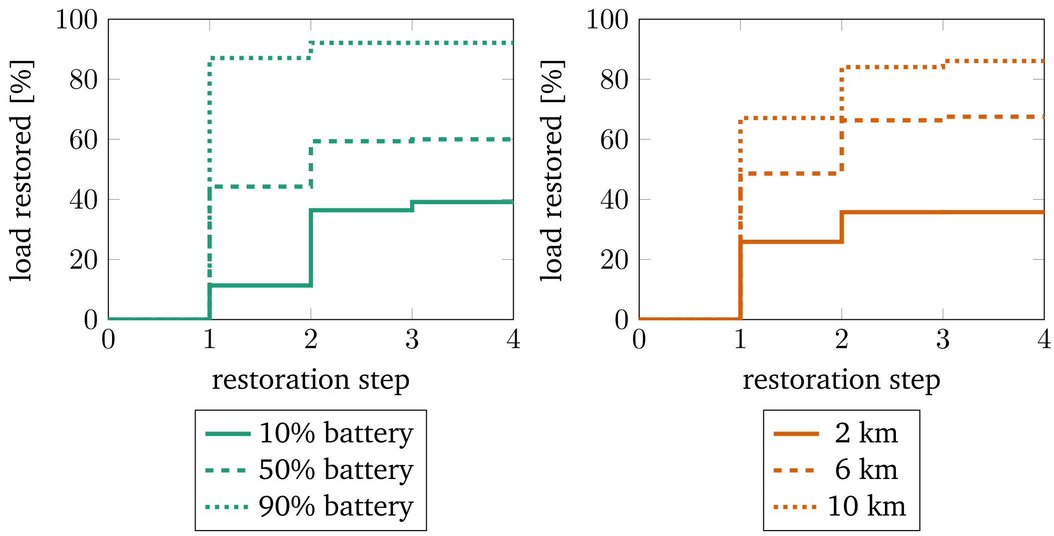

(a) Battery Backup

(b) Cell size

Fig. 4.6.: Effect of different parameters on algorithm convergence

Figure 4.6b shows the restoration steps for different cell sizes. Here, the 2 km cell size offers only limited cascading restoration behavior due to the limited overlapping of cells in this scenario. Both the 6 km and 10 km scenarios show similar behavior, with an additional 20% of load being restored after the first restoration step.

Interdependencies Between Cell Size and Battery Backup

Figure 4.7 shows the correlation between battery and cell size. The highest mean restoration of 99% can be observed for the combination of both parameters' best values, the 10 km cell size and 90% battery backup availability. However, the positive effect of a bigger cell size and a higher battery backup is reduced when the other value is increased. This suggests that with more overlapping cells, a high initial availability of base stations is less critical and vice versa, i.e., with a higher amount of initial available base stations, a scenario with small cell size and less overlapping can also be efficiently restored. It can also be seen that both factors can compensate for each other: Scenarios with 2 km cell size and 90% battery provide equally good results as scenarios with 10 km cell size and 10% battery backup.

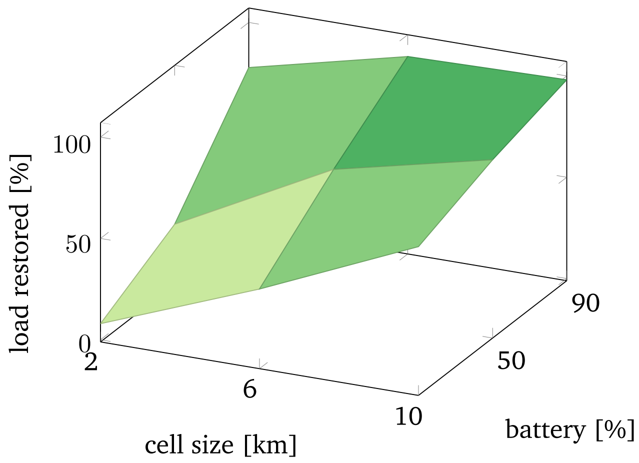

Fig. 4.7.: Surface plot for battery and cell size

4.2.5 Key Findings & Discussion

The key findings of this initial evaluation of the single-objective optimization restoration algorithm are as follows:

- The co-simulation setup works as required, allowing flexible algorithm evaluation.
- The algorithm itself works, including the interaction between the agents.
- The algorithm shows the expected cascading restoration behavior even without ICT in the objective function simply by modeling the interdependencies of ICT and the power system and using automatically re-energized parts of the ICT system to extend existing islands.
- Increased delay has no impact on algorithm performance
- The total load that can be restored still depends heavily on the initial ICT available, especially for smaller communication cells. The presence of certain nodes is also relevant for maximizing the amount of restored load.

However, due to the single objective, the interdependency between power and ICT is not explicitly considered in the decisions. After setting up the evaluation environment and ensuring the general functionality of the algorithm, the next step was to extend it to multi-objective optimization and consider ICT in the restoration process.

4.3 Multi-Objective Blackstart Algorithm

The multi-objective evaluation aimed to test the impact of ICT in the objective function on the overall performance of the restoration algorithm. Instead of a single solution, a set of Pareto optimal solutions is generated, and one is selected to continue the restoration process. In addition, different forms of constraint handling were discussed and tested.

4.3.1 Scenarios

To understand and analyze the multi-objective restoration process in detail, a smaller scenario was chosen for the initial evaluation. Figure 4.8 shows the three interconnected power and ICT scenarios used for the evaluation. The power system is the CIGRE medium-voltage 14-bus system with DERs, with additional switches placed between every two buses to provide maximum flexibility for islanding. The DER units are scaled to the load so that the entire grid can be restored at any time with fully functional ICT. The total generation for all scenarios is 15.95 MWh, and the total load is 14.75 MWh. The loads are modeled as static while generating units can be flexibly scaled between a maximum value and zero.

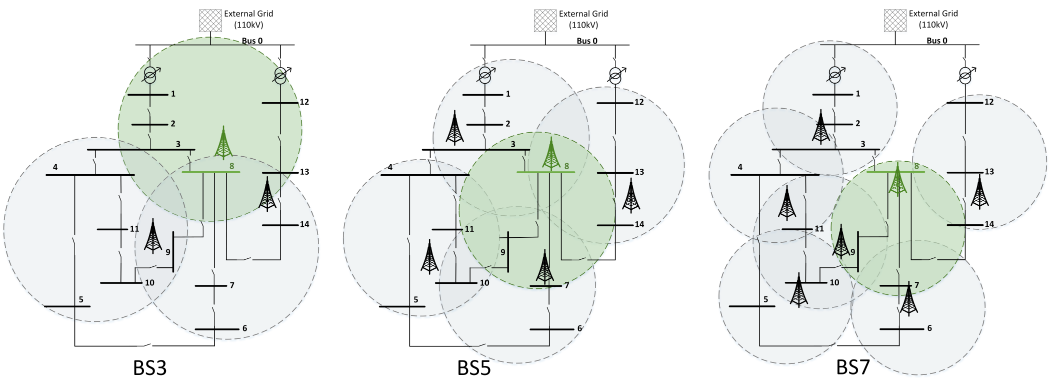

Fig. 4.8.: CIGRE-MV testgrids with 3, 5 and 7 Base Stations

The wireless ICT infrastructure proposed in [95] (also used for the single-objective evaluation) was considered for the ICT system. It consists of base stations (BS) that allow communication between all agents within their respective communication cells. Each BS is powered by one of the buses and, unless equipped with a battery backup, is only active when the bus is part of an island grid. Agents are executed on Intelligent Electronic Devices (IEDs), which are located either directly at the generating units or at substations and are considered to have battery backup.

As shown in Section 4.2.4, communication cell size can impact restoration performance. Three different ICT scenarios have been defined which differ in the size of their cells and, consequently, in the total number of BSs. The authors in [102] have developed a methodology for quantifying the geospatial relationships between the power system and ICT nodes and found that for cellular networks, the median number of power system nodes in a communication cell ranges from 8 for rural areas to 56 in urban areas. However, to achieve different scenarios for the CIGRE medium voltage grid, the number of buses was reduced to 3 for the smallest cell and 6 for the largest cell.

All scenarios represent the moment after a blackout, with all switches open and all buses in a blackout state. The starting point for restoration is always *bus 8* (marked in green), to which a blackstart capable unit is assumed to be connected. This bus is the most connected in the grid with four neighboring buses, which allows different island grids to be created in the first restoration step. To enable the initial restoration step, the base station connected to bus 8 is considered to have a functional battery backup, while all other base stations do not have a battery. The initial communication cell for each ICT scenario is also highlighted in green. In the following, the three ICT scenarios are named *BS3*, *BS5*, and *BS7*.

Regarding the agents, each scenario has 28 Unit Agents and 14 Switch Agents, with an additional 3, 5, and 7 ICT agents representing the base stations in the respective scenarios.

4.3.2 Objective Functions

In the multi-objective case, the definition of an island I (see Section 4.2.2) is extended to $I = \{\Omega^L, \Omega^G, \sigma\}$, where Ω^L and Ω^G are still the set of loads and the set of generators in an island grid, and σ is the number of buses connected in the communication overlay for this island grid. This is used as the ICT performance measure since a connection in the communication overlay allows the agents representing the respective node to participate in the restoration process. Note that this number may be larger than the number of buses in the island grid since the communication overlay may be larger than the island grid. The agents now have to consider two equally important objectives; one is to maximize the restored load:

$$\max f_1(I) = \sum_{k=0}^{o} \sum_{i=0}^{m} \omega_{ik}^{L} \tag{4.5}$$

And the second one is the maximization of the restored ICT:

$$\max f_2(I) = \sigma \tag{4.6}$$

The question now is how to consider the island balancing constraint:

$$g(x) = \left| \sum_{k=0}^{o} \left(\sum_{i=0}^{m} \omega_{ik}^{L} - \sum_{j=0}^{n} \omega_{jk}^{G} \right) \right| = 0 \tag{4.7}$$

For handling this constraint in the optimization, three different approaches have been tested:

(1) Hard constraint: This is the approach that was used in the single-objective evaluation (see Section 4.2.2). If the island balance exceeds 0, the value replaces the performance values calculated in f_1 and f_2. This means that solutions that violate the constraint will always have a lower performance value than the solutions that satisfy the constraint. When comparing two solutions that violate the constraint, the smaller violation is preferred. However, this approach resulted in a premature convergence in local minima, especially for small scenarios with high flexibility in generation. If the agents can create a balanced island early in the negotiation, all imbalanced solutions are discarded for the rest of the negotiation, even though they might be necessary intermediate steps to create a larger island. Consequentially, Switch Agents representing a load bus would not connect to the balanced island grid, even though excess generation is left. To solve this problem, the constraint handling needed to be relaxed to allow constraint violations throughout the negotiation while ensuring that the final solution fulfills the constraint.

(2) Increasing Penalty: The second approach, therefore, aims at encouraging agents to explore more areas of the solution space. A penalty function $p(I) = g(I)^2$ was subtracted from the objective functions (f_1 and f_2) with a weight w_p:

$$f_x p(I) = f_x(I) - w_p \cdot p(I) \tag{4.8}$$

This weight is initially set to zero but is then increased by the speaker during the negotiation. While the weight is zero, solutions that violate the constraint are not penalized, encouraging agents to add as many nodes as possible to the island grid, irrespective of potential imbalances. With the increasing penalty, imbalanced solutions are rated worse, and the algorithm converges towards an optimal and balanced solution. Additionally, Unit Agents representing generators initially publish their maximum possible generation to inform other agents about available generation capacities. The challenge of this approach is that the performance values have to be re-calculated throughout the negotiation whenever w_p gets changed. While the first results looked promising, it also became apparent that tuning the weight parameter would be a challenge. Depending on the number of agents participating, the increase could happen slower or faster to ensure that the algorithm always converges to valid solutions.

(3) Additional Objective: The third approach uses the multi-objective algorithm by including the constraint as another objective. Only when choosing the final solution from the Pareto front is this objective considered a hard constraint again, and only solutions that fulfill the constraint can be chosen. It results in a third objective function:

$$f_3(I) = g(I) = \left| \sum_{k=0}^{o} \left(\sum_{i=0}^{m} \omega_{ik}^{L} - \sum_{j=0}^{n} \omega_{jk}^{G} \right) \right| \tag{4.9}$$

With this approach, the algorithm converges towards valid and optimal solutions. For the evaluated scenarios, this approach worked well and is therefore used in the remainder of this thesis. However, one drawback is that the final Pareto front can have invalid solutions.

4.3.3 Design of Experiments / Methodology

In addition to different cell sizes, another relevant parameter influencing the restoration process is the distribution of load and generation in the scenario. To create different distributions, loads and generating units were placed randomly for each ICT scenario using different seeds – except the blackstart capable bus 8, which had fixed load and generation. Using these various test scenarios, the complete multi-objective restoration algorithm described in Section 3.4 was then run with (a) only objective functions f_1 (see Eqn. 4.5) and f_3 (see Eqn. 4.8) and (b) with objective functions f_1, f_2 (see Eqn.4.6) and f_3. These two versions will be referred to from now as *MOO2* (restoration without ICT) and *MOO3* (restoration with ICT), respectively.

Figure 4.9 shows the process of evaluating the scenarios with different seeds and sorting them into four categories (C1 to C4) according to the algorithm's performance. The performance is defined as the total restored load in the final restoration step. The goal of this process is to identify whether there are scenarios where MOO3 (with ICT) performs better than MOO2 (without ICT) and, if so, to identify the characteristics of these scenarios. The steps shown in Figure 4.9 are explained below:

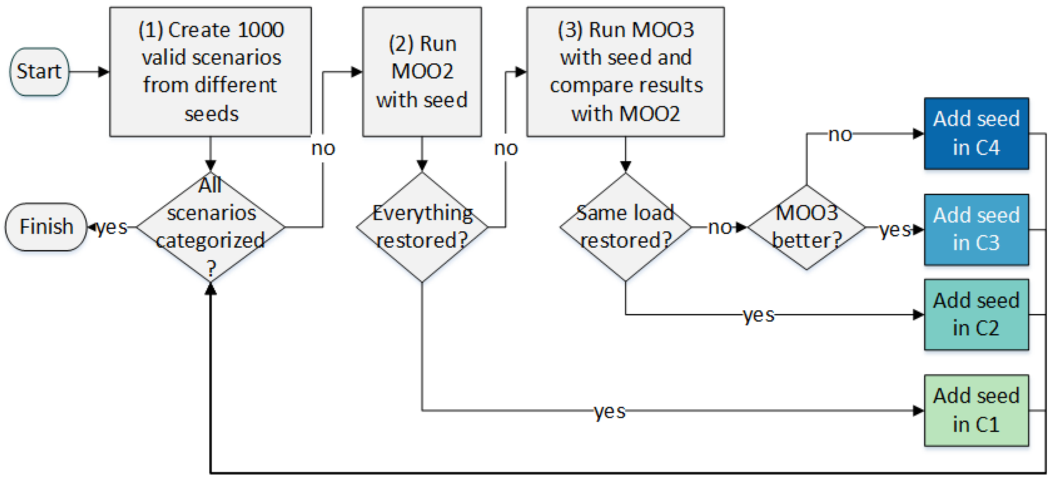

Fig. 4.9.: Process to sort scenarios into different categories

Step 1 – Identification of valid scenarios: Each seed creates a different random load-generation-scenario, which is considered valid if it fulfills the following three criteria: (1) Every bus that has a BS connected to it should have a non-zero load since the BS itself would be considered as a load. (2) Every bus needs at least a non-zero load or generation; otherwise, it is not considered a separate bus. (3) Considering the initial available buses, at least one restoration step should be possible, meaning at least two buses should be able to connect to form an island grid. Otherwise, a scenario is considered unsolvable. Based on these criteria, 1000 valid scenarios have been created for each ICT scenario to conduct the evaluation.

Step 2 – Evaluate performance with MOO2: In this step, each valid seed is tested using MOO2, i.e. restoration without ICT. This algorithm is run with $x = 5$ (number of solution points on the Pareto front), which was arbitrarily chosen considering the trade-off between performance and computational time. In case of variations in results, the best result (regarding the total restored load) is considered for further evaluation. Those seeds, for which MOO2 manages to restore the whole grid, are categorized into C1. These scenarios seem to be trivial enough that considering ICT in the objective function can not provide any improvement.

Step 3 – Evaluate performance for restoration with ICT: Here, MOO3 (restoration with ICT) is run with those seeds where MOO2 does not manage to restore all loads, also with $x = 5$. The weights for choosing the final solution from the Pareto front are $w_1 = 0.7$ for f_1 (restored load) and $w_2 = 0.3$ for f_2 (restored ICT). These weights, chosen exemplary, indicate that load restoration is prioritized, but ICT is also included in the optimization. The results from MOO3 are obtained and compared to those from MOO2, using the final restored load for comparison. Based on the results, the seeds are then sorted into the three remaining categories: same (C2), MOO3 better (C3), and MOO2 better (C4).

4.3.4 Results

This section presents the results of the multi-objective evaluation. In addition to testing the general functionality of the multi-objective restoration algorithm, it also serves as a first investigation of the hypothesis that restoring more ICT will result in more load restoration.

Constraint Handling

The experimental setup described in Section 4.3.1 was also used to compare the different approaches for constraint handling (see Section 4.3.2), namely single-objective with hard constraint (SO), single-objective with increasing penalty (Penalty) and multi-objective with the constraint as the second objective (MOO2). For 20 random valid scenarios distributed among the three different ICT scenarios BS3, BS5, and BS7, each constraint handling approach has been run 50 times, and the average performance (in % of restored load) and standard deviation have been determined. SO restores 26% load on average with a standard deviation of 0%. The penalty approach manages to restore around 62% load on average with a standard deviation of around 10%, showing a greater variety of possible results. A behaviour like this would require the restoration algorithm to be repeated several times to ensure that the best possible solution is found. Finally, MOO2 can restore an average 73% load with 0% standard deviation, thereby giving consistently good results.

Figure 4.10 shows the exemplary results for one of the seeds for BS3. The boxplots show the distribution of the final restored load for 50 simulation runs for each of the three constraint handling approaches. It can be seen that SO – while not having any variation in the results – converges to a local minimum and only manages to restore around 13% of load, even though the specific scenario allows 100% load restoration (as can be seen from the results of the other constraint handling approaches). With Penalty, the optimal solution could sometimes be found, but the median is at around 64% and the standard deviation around 12%. On the contrary, considering the constraint as a second objective in MOO2 results in no variation and a reliable convergence to the optimal solution, i.e., 100% of the load is restored in all cases. Therefore, this approach shows the best results.

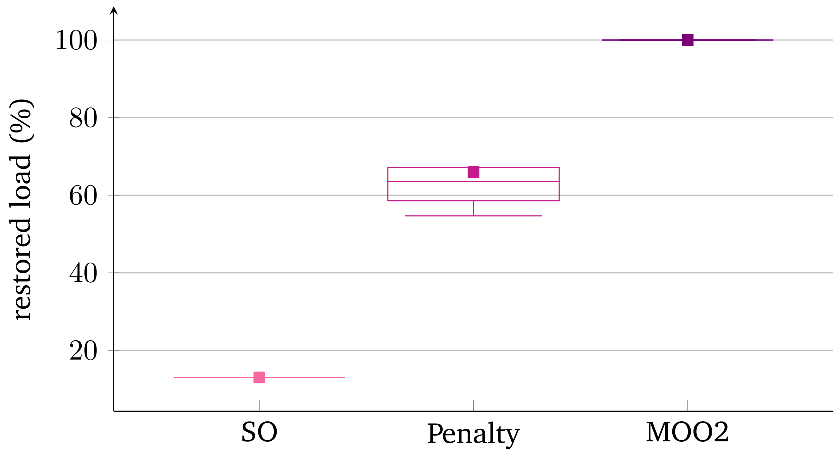

Fig. 4.10.: Boxplot of final result values for different constraint handling approaches for a BS3 example scenario

Category Distribution

The bar plots in Figure 4.11 show the distribution of the 1000 valid scenarios over the different categories for each ICT scenario. **C1** is the largest category for all three ICT scenarios, from around 66% for BS7 to 81% for BS3. This suggests that, in general, ICT impairment only weakly influences the evaluation scenarios. Since the BS are close to each other, (nearly) every restoration step offers the possibility to restore more BS. In BS3, every fifth; in BS5, every third; and in BS7, every second bus has a BS connected to it. At the same time, the total number of buses to choose from in each restoration step is relatively small (maximum of 6 buses per communication cell in the BS3 scenario). Therefore, the chances that base stations get restored automatically by restoring load are high.

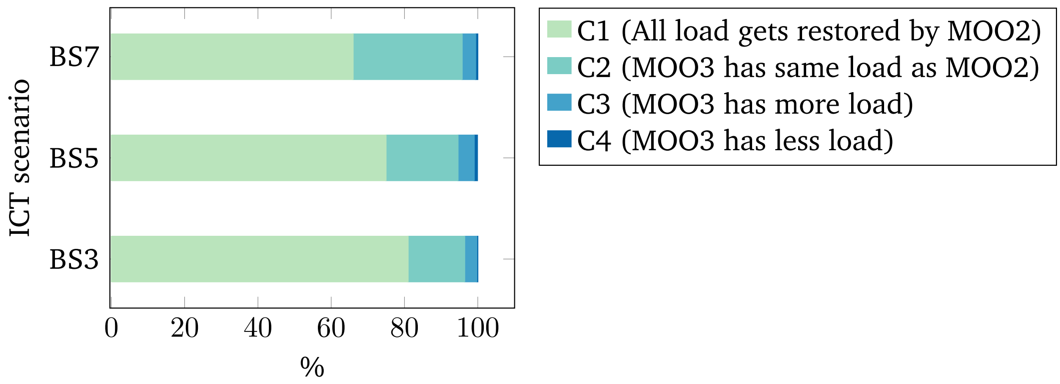

Fig. 4.11.: Categories distribution for different ICT scenarios

C2 is the second largest category (15% in BS3 to 30% in BS7), suggesting that – in addition to the impaired ICT – the distribution of load and generation can also prevent full restoration in these scenarios. For example, if most generation units are outside the initial communication area, relevant flexibility is unavailable in the restoration process. In this case, considering just the ICT in the objective function does not improve the restoration. The sum of categories C1 and C2 is 96% for BS3, 95% for BS5 and 96% for BS7. With more base stations, more scenarios shift from C1 to C2 because smaller cell sizes lead to more complex scenarios. Consequentially, an unfavorable distribution of generation and load (e.g., the majority of generation covered by those communication cells that can only be restored in a later restoration step) can not be compensated, resulting in more unsolvable scenarios.

C3 is the most relevant category in the context of the investigated hypothesis. It makes up around $3-4\%$ of all seeds and will be analyzed in more detail in the following.

C4 scenarios are outliers, which make up less than 1% of all the scenarios. It must be noted that, due to the small number of scenarios in C4, it is impossible to draw conclusions on the cases where MOO3 performs worse than MOO2. Further experiments have shown that just by increasing the number of solution points x on the Pareto front (from $x = 5$ to $x = 10$), the performance of MOO3 improves to level with MOO2, thereby shifting the seeds from C4 into C2, resulting in less than 0.4% of all seeds in C4.

Since all scenarios are run with a version of the multi-objective restoration algorithm, from the overview, it can be concluded that the algorithm can solve multi-objective problems, with ICT as one of the objectives, thereby fulfilling the functional requirement (3). Moreover, the distribution of seeds in the different categories shows that by considering ICT, the performance of the restoration algorithm improves and does not worsen (since C4 is negligible).

Restoration path in C3

Figure 4.12 shows the average cumulative results of all scenarios in C3 per step in the iterative restoration process for the different ICT designs. The blue lines show the restored load (light blue for MOO2, dark blue for MOO3), while the dotted red lines show the restored ICT (light red for MOO2, dark red for MOO3). It can be seen that all three ICT scenarios exhibit similar behavior: In step 1, the values of MOO2 (without ICT) and MOO3 (with ICT) for both restored load and ICT are nearly the same. In step 2, MOO3 restores more ICT than MOO2, while the restored load is the same for both. Only from step 3, MOO3 restores significantly more load than MOO2 and continues to do so for the subsequent steps, while the restoration in MOO2 stagnates.

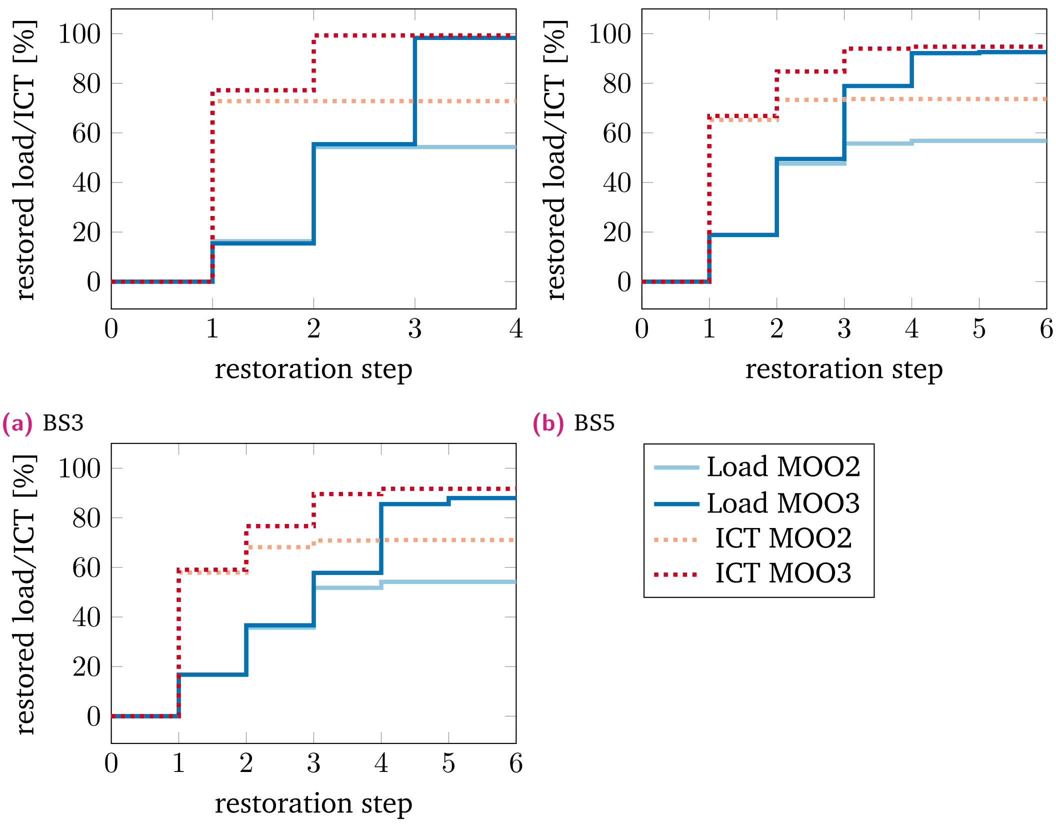

(a) BS3

(b) BS5

(c) BS7

Fig. 4.12.: Average cumulative result values of all scenarios in C3 for each restoration step of different ICT designs

For example, in step 1 for BS5 in Figure 4.12b, the restored load is around 19% for both MOO2 and MOO3, and the restored ICT is around 65% for MOO2 and 67% for MOO3. In step 2, the restored load for MOO2 and MOO3 is 48% and 49%, respectively, whereas the restored ICT shows a significant difference with 73% for MOO2 and 85% for MOO3. In step 3, MOO2 only manages to restore 56% of load, while MOO3 restores 79%. In steps 4 and 5, MOO2 stagnates at 57% restored load, and MOO3 restores a total load of 93%. This shows that considering ICT in the optimization problem improves the performance of the agent-based restoration algorithm.

Detailed results for category 3

To analyze the influence of ICT in the objective function in more detail, the seeds from C3 have been further categorized based on the restoration step, in which MOO2 (without ICT) and MOO3 (with ICT) differ for the first time. This resulted in $2-3$ different subcategories for C3. Table 4.4 shows exemplary results for the subcategory where the first difference between MOO2 and MOO3 occurs in restoration step 2.

Tab. 4.4.: Comparing average cumulative restored load and ICT values in % for MOO2 and MOO3 for one subcategory of C3

		Step1		Step2		Step3		Step4		Step5	
		MOO2	MOO3	MOO2	MOO3	MOO2	MOO3	MOO2	MOO3	MOO2	MOO3
BS3	Load	15.12	15.12	57.79	55.56	57.79	97.85	-	-	-	-
	ICT	76.19	76.19	76.19	99.11	76.19	99.11	-	-	-	-
BS5	Load	18.39	18.39	52.91	51.38	57.07	82.53	57.07	93.63	-	-
	ICT	68.88	68.88	72.96	86.48	72.96	95.41	72.96	95.41	-	-
BS7	Load	17.15	17.15	44.24	43.35	47.26	54.51	47.58	79.34	47.58	81.62
	ICT	58.65	58.65	63.16	74.44	63.91	85.71	63.91	87.22	63.91	87.22

This table summarizes the cumulative average restored load and ICT values for all seeds in this subcategory, for both MOO2 and MOO3, considering all three ICT scenarios (BS3, BS5, and BS7). In step 2 of each ICT scenario (marked in yellow), MOO3 restores slightly less (around $1-2\%$) load than MOO2 but restores significantly more ICT (around $11-23\%$). This shows a trade-off between restoring load and ICT at this restoration step. By including ICT in the objective function, these trade-off solutions are included in the Pareto front and can then be selected depending on the weights for each objective. Consequently, it can be observed that MOO3 manages to restore more load in each subsequent step, while the restoration process for MOO2 converges prematurely. The reason is that there is no new information available that could be used to extend the existing island grid. The same behavior could also be observed for all the other subcategories, where the difference between MOO2 and MOO3 occurs in an earlier or later restoration step.

4.3.5 Key Findings & Discussion

The key findings of this first evaluation of the restoration algorithm with multi-objective optimization are the following:

- The multi-objective restoration algorithm works as required.
- Out of the 1000 seeds considered for creating different distributions of load and generation, in $3-4\%$ of the cases, MOO3 restored more load than MOO2.
- It was shown that there can be a trade-off between restoring load and restoring ICT and that restoring more ICT in the intermediate restoration step can improve the overall load restoration. This supports the hypothesis.

However, only a small subset of the total number of tested scenarios reflects relevant use cases. Therefore, as a next step, larger and more complex scenarios should be studied. This will also test the approach's scalability.

4.4 Chapter Summary

This chapter describes the first proof of concept of the restoration algorithm. The co-simulation setup (artifact 2) is also presented in this context. The results are summarized as follows:

- The co-simulation setup used to evaluate the restoration algorithm uses *mango* for the implementation of the MAS, *pandapower* for the power grid, and *NetworkX* for the ICT system. These three simulators are combined using the semi-automatic scenario configuration tool *midas*, which is based on the co-simulation platform *mosaik*. It was shown that all FRs for the simulation setup are fulfilled.
- In the first evaluation cycle, the algorithm was tested with single-objective optimization using the 93-bus rural MV Simbench network. Cell size, battery backup, and communication delay are variable parameters, and their influence on the restoration process is analyzed using a Box-Behnken experimental design. The results show that the algorithm can restore the grid under degraded

ICT, satisfying FR-1 and FR-2. However, the initially available ICT greatly influences how much load can be restored. Furthermore, it can be seen that increased delay does not affect the algorithm's performance.

- In the second evaluation cycle, the complete multi-objective restoration algorithm was tested using the 14-bus CIGRE MV network. Three different ICT scenarios and random placement of generation and load are used. ICT performance is measured as the number of power system nodes connected in the ICT overlay. This satisfies FR-3 (consideration of ICT in the optimization problem). Different forms of constraint handling for the multi-objective case are compared. Based on the findings, the island balancing constraint is considered a separate objective to allow the agents to also consider invalid solutions. The algorithm with ICT in the objective function is compared with a version of the algorithm that does not consider ICT. The results show that, at least in some cases, the hypothesis that restoring ICT instead of load at an earlier restoration step can improve the overall load restoration is true.

5 Evaluation of Blackstart Algorithm

This chapter describes an extended evaluation of the multi-objective restoration algorithm. This evaluation aimed to use larger and more complex scenarios to investigate the hypothesis in more detail and also to analyze the non-functional requirements: effectiveness (amount of restored load), efficiency (restoration time and communication complexity), robustness (effectiveness and efficiency under a degraded ICT system), and scalability (effectiveness and efficiency under different numbers of PS nodes).

The chapter is structured as follows: Section 5.1 describes the scenarios, including the power system, the interconnected ICT system, the MAS, and a first approach to integrating the concept of ICT states into the scenario. Section 5.2 then describes the design of experiments and methodology used in the evaluation. The evaluation is conducted in the same co-simulation platform previously described in Section 4.1. In Section 5.3, the first results are presented with a focus on the non-functional requirements. Further results are presented in Section, 5.4, focusing on the hypothesis. The key findings of all results are discussed in Section 5.5.

5.1 Scenarios

The general idea of creating the scenarios was not only to have a larger number of nodes but also to include more design parameters to create a variation of different scenarios. This would allow an analysis of the characteristics of scenarios where MOO3 performs better, worse, or identical to MOO2 and to draw conclusions under which circumstances considering ICT in the objective functions has an advantage. This section first describes the power system scenario and its parameters, then the ICT scenario and its parameters, and the associated agent system. Finally, an idea for integrating the concept of ICT states into the specific scenarios is described to allow a more detailed view of impaired ICT than just "connected" or "not connected."

5.1.1 Power System

The power system scenarios use two slightly modified medium voltage grids from the Simbench benchmark dataset [68]. Figure 5.1 shows the selected grids, one with rural (Simbench code "1-MV-rural–2") and one with urban (Simbench code "1-MV-urban–2") characteristics. Additional power lines have been added to ensure that all grid parts are connected with no connection through the external grid, theoretically allowing the creation of one single island grid over the entire grid area. The Simbench networks have switches between every two nodes in the network, assuming that most of them are closed during normal operation. All switches are considered to be remote-controllable for maximum flexibility in the recovery process. The Simbench dataset distinguishes three development scenarios for each grid: today's network, a near-future network, and a far-future network. They differ in the number and type of DERs. For this evaluation, the far future grid was used, which substantially increases DERs and includes heat pumps and electric vehicles.

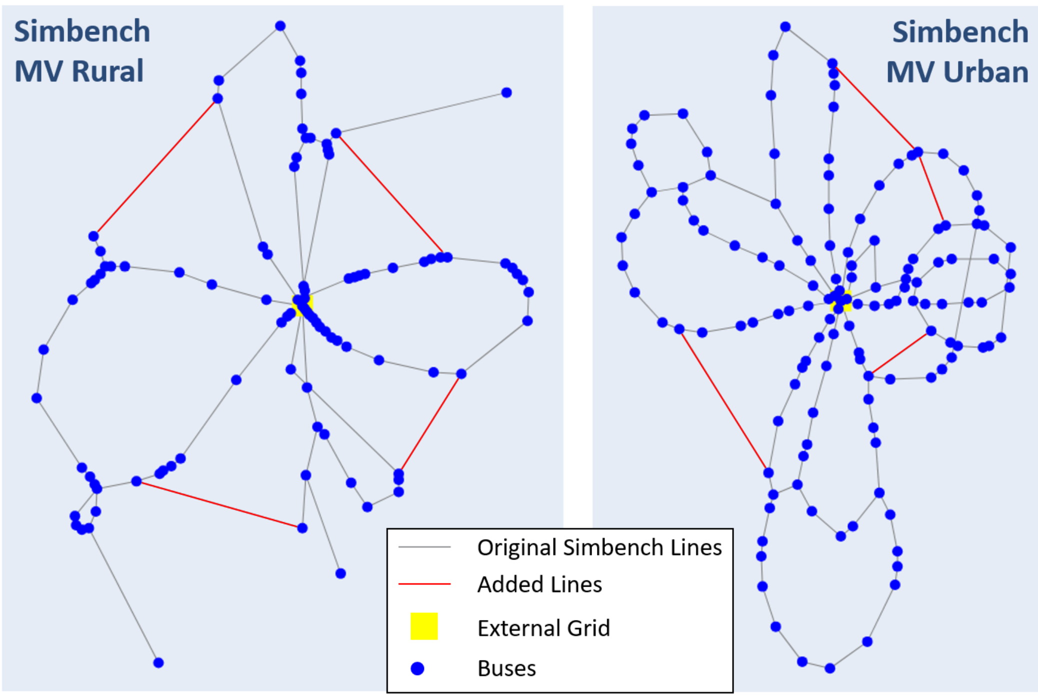

Fig. 5.1.: The two Simbench power grid models used in the evaluation

The Simbench grids come with time series data for all loads, generation, and storage units for one year with a 15-minute resolution. The time series have been aggregated to simplify the evaluation and create average days for three seasons (summer, winter, and transition) and three different day types (weekday, Saturday, and Sunday). This reduces the number of distinct days from the whole year to only nine different kinds of days. All days of the year were categorized into one of the nine categories (e.g., "Winter-Sunday" or "Transition-Weekday"). Then, the average value of each 15-minute interval of all days in a category was calculated. For an overview of the aggregated time series values, see Appendix A.2.

Since the evaluation is only for a single restoration process, there is only one starting point for the restoration in the grid, which is considered fixed (bus 45 in the rural grid and bus 86 in the urban grid). The blackstart capable unit required to initiate the restoration process is assumed to be connected to this bus. Since the optimal placement of these blackstart capable units is not part of this thesis, it does not vary throughout the evaluation.

5.1.2 ICT System

To date, there are no benchmark models for ICT systems. Since the ICT system is usually designed according to the communication requirements of the respective area, the ICT infrastructure was modeled for this thesis on top of the previously described power system, using its structure as a basis. As in the proof of concept, a fully wireless ICT infrastructure with base stations and communication cells was used. Instead of focusing on ICT-related parameters such as range and density when designing the scenario, parameters were used to describe the relationship between the power system and the ICT system. The goal was to test various ICT scenarios and see their impact on restoration. The authors in [102] used two parameters to describe the relationship between the PS and the ICT system: The number of ICT nodes within the coverage area of a power system node and the average number of power system nodes within the coverage area of ICT nodes. In this paper, these two parameters have been slightly modified to describe the relevant relationship: how many cells a single PS bus falls into (*cells per bus* - cpb) and how many buses are within a communication cell (*buses per cell* - bpc). Figure 5.2 visually explains these two parameters. The cpb value is always calculated for a power system node, checking how many cells this bus is within, and the bpc value is calculated for each base station, checking how many buses are within its communication cell.

A *low* and a *high* setting have now been defined for both parameters. This results in four combinations of low/high settings for both the rural and urban PS scenarios, resulting in eight different ICT scenario types. Since the cell size and the amount of cell overlap in an ICT grid can vary from base station to base station, a range of values was defined instead of a fixed value. Table 5.1 gives an overview of the parameter ranges for all eight scenarios. The value for bpc has been calculated as

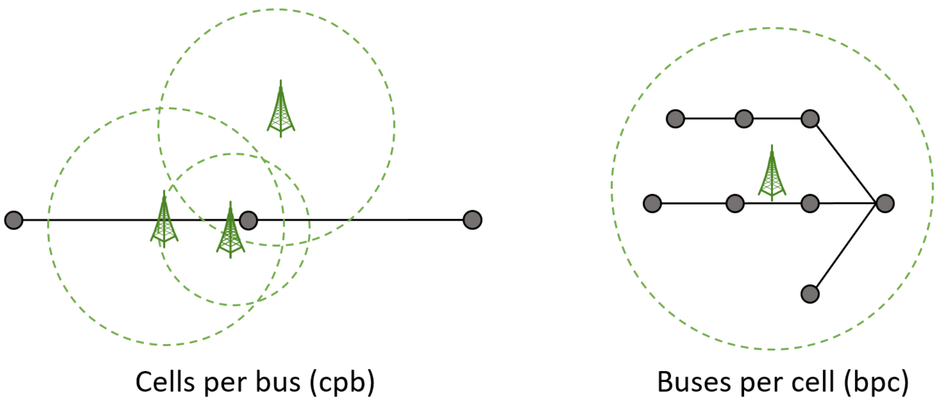

Fig. 5.2.: Explanation of the ICT parameters cpb and bpc

a percentage of the total number of busses in the network that should be within a communication cell, with the low setting between 10% and 20% and the high setting between 30% and 40%. This should ensure that even larger cells cover less than half of the network to keep the restoration problem challenging and to ensure the need for a gradual restoration process. The actual cpb and bpc values for a scenario are calculated using the median of all cpb and bpc values. This allows for outliers (which is important considering that the distribution of buses in the network is not uniform) but ensures that most buses and base stations fall within the required cpb and bpc values. The number of base stations and their cell ranges have been varied to achieve the respective cpb and bpc values. The cell ranges are roughly based on the cell ranges identified in [102] for LTE communication cells. The number of was determined for each of the 8 ICT scenarios.

Tab. 5.1.: Overview of ICT parameters

scenario id	cells per bus	buses per cell	cell ranges (m)	number of bs
rural_low_low	1-3	10-19	2500-7000	19
rural_low_high	1-3	29-39	5000-10000	10
rural_high_low	5-7	10-19	2500-7000	30
rural_high_high	5-7	29-39	5000-10000	22
urban_low_low	1-3	14-27	800-1500	19
urban_low_high	1-3	41-54	1100-1800	10
urban_high_low	5-7	14-27	800-1500	30
urban_high_high	5-7	41-54	1100-1800	22

With these parameters set, concrete ICT scenarios were created for each scenario type by placing the fixed number of base stations with random cell ranges on the respective power grid scenario. To determine the cpb and bpc values, knowing the distance between the PS nodes and the base stations is essential. The Simbench grids come with the x and y coordinates of the nodes, but these are only for visualization of the grid and are, therefore, scaled-down and do not correspond to the distance between the nodes. To determine an approximate scaling factor, the following steps were taken for each pair of busses connected by a line:

1. Calculate the haversine distance between the two buses.
2. Compare with the given line length and calculate the required scaling factor so that haversine distance = line length.

This process assumes that a line is a direct connection between two buses and that the line length in Simbench is based on accurate data, unlike coordinates. Using this method, the average scaling factor was determined to be 5.156 for the rural network and 1.279 for the urban network. These scaling factors were then used to calculate distances within the ICT system. With this, it is now possible to place base stations with communication cells (using the maximum and minimum coordinates of the Simbench grid as the boundaries of the grid area) and calculate which PS buses would fall within that communication cell.

The placement of base stations was not done completely randomly but followed the distribution of PS buses by assigning weights to different areas of the network. The aim was to encourage placing base stations in areas with more PS buses since the ICT system is usually more developed in densely populated areas. This was done as follows:

1. Divide the grid area into 5 x 5 sections of equal size.
2. Count the number of buses within each section and assign a weight to this section according to the number.
3. When placing a base station, randomly select a section using the weights.
4. Within the section, place the base station completely random.

Once the base station is assigned a random cell size within the given range, the next step is to connect it to the PS to receive power. This is done by identifying the buses closest to the base station and assuming that one of these buses will be its power supply. This process is repeated until the defined number of base stations has been placed. The resulting scenario is then checked to ensure that the median cpb and bpc values meet the requirements, that all PS buses are covered by at least one cell, and that the overlay between the BSs forms a connected graph. Given the various ways to place base stations, 10 scenarios were created for each ICT scenario type.

5.1.3 Agents

As described in Section 3.3, there are two main types of agents: Switch Agents and Unit Agents. Each load, generator, and base station in the scenarios is represented by a Unit Agent, while each bus (and the switches connecting that bus to neighboring buses) is represented by a Switch Agent. Forecasting of all loads and generation is assumed to be ideal, i.e., the agents know the time series of their respective loads or generation, and the unit will not deviate from this time series. While all loads are assumed to be uncontrollable, all generating units can be flexibly reduced below the respective value from the time series. This reduces the types of flexibility representations required by the agents. Table 5.2 shows the number of agents for all four ICT scenario types for rural and urban grids, sorted in ascending order of total number of agents.

Tab. 5.2.: Overview of number of agents per ICT scenario

	# of Switch Agents	# of Unit Agents (load/gen)	# of Unit Agents (ICT)	# of total agents
rural_low_high	93	192	10	295
rural_low_low	93	192	19	304
rural_high_high	93	192	22	307
rural_high_low	93	192	30	315
urban_low_high	133	267	10	410
urban_low_low	133	267	19	419
urban_high_high	133	267	22	422
urban_high_low	133	267	30	430

5.1.4 ICT States

The ICT scenarios introduced in Section 5.1.2 are designed to have overlapping communication cells. Following the description in Section 3.6, it is possible to describe the effect of ICT impairment on the restoration algorithm in terms of *ICT states*. Three different communication states of PS nodes can be defined in the scenarios with overlapping cells, as shown in Figure 5.3. First, when all communication cells are active, all PS nodes are expected to be in a normal state. Normal state is defined as the ability of the agents representing the PS node to participate normally in the restoration process without any limitations. Second, when no cells are active, the respective PS nodes are non-responsive. In this case, the agents cannot participate in the restoration process. Third, if cells are partially active, the PS nodes are in a degraded state, meaning that the respective agents can participate in the restoration process but might not be fully functional.

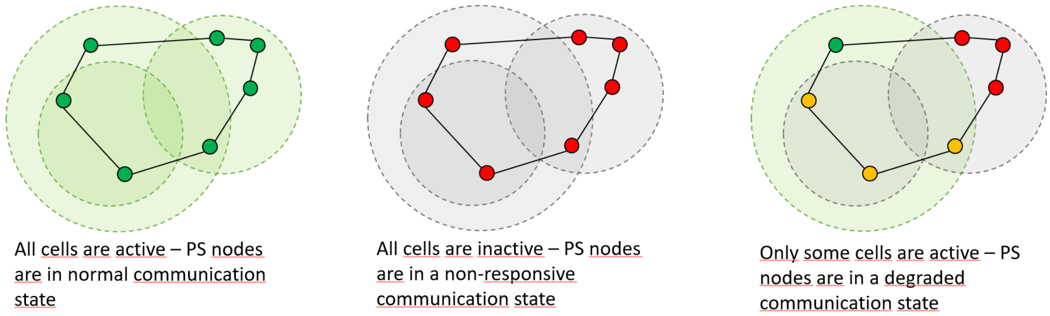

Fig. 5.3.: Example of different ICT States when considering overlapping cells

This degraded state aims to reflect the difference between a fully operational communication system and one that is limited due to the ongoing restoration process and, therefore, only partially functional. The question here is how to define the effect of the limited states on the restoration process. With the abstracted simulation of both ICT and PS, it is difficult to specify precisely what effect it would have if, for example, a PS node had only 2 out of 5 cells available for communication. In Section 3.6, ICT states are defined using the availability, timeliness, and correctness properties of the different ICT elements an agent needs. These include the component that the agent represents, the agent itself, the speaker agent that starts the restoration, and the communication links between all these elements. Due to the abstract representation of the ICT system, the focus in this evaluation is only on the communication links and not the components. Both the agent and the component it represents are assumed to be functional throughout the restoration, and the only constraints are from the unavailable base stations (and corresponding communication cells) that need to be restored.

As noted in Section 3.6, communication links have only availability and timeliness properties. Fewer cells could decrease availability (links are sometimes interrupted), increase timeliness (messages take longer to reach), or both. On an abstract level, it can be said that not yet fully functional communication links result in increased uncertainty in the restoration process. For example, agents initially involved in the negotiation might drop out during island formation and not deliver the promised generation, or aggregating agents do not have specific information about the load and generation from the lower level because of unstable links. For agents not placed at their component, this could also mean that they cannot reliably monitor the component and have to make decisions based on outdated information. One option to handle this increased uncertainty is to account for more buffer of generation capacity to have more flexibility in case of unexpected events during the restoration process. This means that agents representing generation units do not offer their full flexibility but reduce it depending on the level of degradation in the communication system.

As a first approach in this evaluation, the ICT states are represented as weights between 0.0 and 1.0, assigned to each PS node depending on how much the ICT system is restored. A weight of 1.0 means that all the agents that represent a component connected to this PS node are in the *flexible* state, i.e., active and fully functional. In contrast, a weight of 0.0 means that no communication cell is available, preventing any communication to and from that PS node and leaving all respective agents in the *non-responsive* state. Therefore, the number of available cells is used to measure how much of the ICT system is restored.

Two versions of ICT states will be compared in this evaluation. The first version corresponds to the approach used in the first multi-objective evaluation (see Section 4.3). In this version, even one available communication cell creates fully functional communication between the nodes, allowing the agent to offer full flexibility. This means two solutions can have the same ICT performance value if one does not restore any additional ICT and the other only restores redundant cells in an area already fully covered by active cells. This version is described by the keyword **Binary**. For the Binary ICT states, the following equation is used to calculate the weight w_{bin} for a bus n:

$$w_n^{bin} = \begin{cases} 1.0 & \text{if } c_{now} > 0 \\ 0.0 & \text{else} \end{cases} \tag{5.1}$$

The parameter c_{now} describes the current number of active cells for a bus (basically the current cpb value). Once a single cell is available, the bus will be assigned the best possible weight (i.e., 1.0).

The second version of ICT states is assumed to have a linear relationship between the availability of communication cells and available generation flexibility. With each additional cell, communication improves linearly until it reaches the best possible state when the maximum number of cells is active. Each agent can have a different number of states depending on how many cells it belongs to. Although simplistic, this approach increases the limiting effect of ICT impairment on PS restoration. It, therefore, can be used to analyze the effect of stronger ICT dependency on the performance of the restoration algorithm. This version will be described by the keyword **Linear**. For the Linear ICT states, the weight should more accurately reflect the state of ICT restoration. The weight w_{lin} for a bus n is calculated with the following equation:

$$w_n^{lin} = \frac{c_{now}}{c_{max}} \tag{5.2}$$

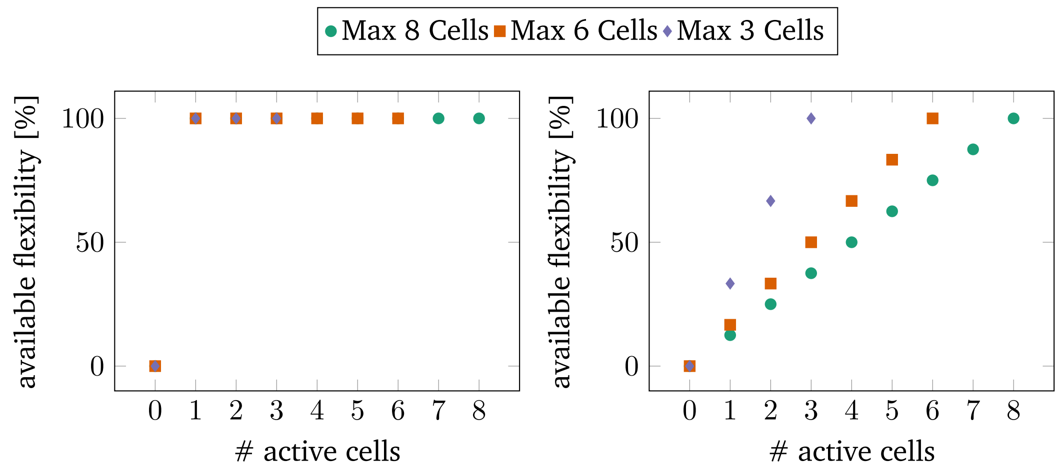

(a) Binary

(b) Linear

Fig. 5.4.: Generation flexibility reduction based on available communication cells for different two ICT States concepts

In this case, c_{max} is the cpb value in normal operation for a bus, meaning the maximum number of cells that cover the bus. Each Switch Agent must know the c_{max} and c_{now} values for all connected buses to calculate these weights and the ICT performance value. The ICT performance of an island grid is then calculated using the weighted number of connected buses.

The effects of degraded states on the agents are then represented by reducing a unit's maximum value in the time series, using the weights of the Linear ICT states to calculate how much of the maximum value the agent can offer. However, the flexibility of control is not affected, and an agent can still choose any value between the (reduced) maximum value and zero at any time step. Figure 5.4 shows examples of the resulting curves for both weight calculation approaches, using three different c_{max} values.

5.2 Design of Experiments and Methodology

The PS and ICT scenarios described previously have several variable parameters that must be combined for each simulation, resulting in a large parameter space. Monte Carlo simulation draws random samples from the parameter space and averages the results. The scenarios are created using the Halton sequence (a quasi-random sequence) to ensure uniform space coverage. A value is defined for each parameter between 0 and 1 in the Halton sequence. Since the parameter values are discrete and not continuous, each value is assigned a range between 0 and 1, depending

Tab. 5.3.: Variable parameters in Halton sequence

variable	factor	range in Halton sequence
time of year	winter	$0.0 \leq x < 0.333$
	transition	$0.333 \leq x < 0.666$
	summer	$0.666 \leq x < 1.0$
time of week	weekday	$0.0 \leq x < 0.333$
	Saturday	$0.333 \leq x < 0.666$
	Sunday	$0.666 \leq x < 1.0$
time of day	01:00	$0.0 \leq x < 0.25$
	07:00	$0.25 \leq x < 0.5$
	13:00	$0.5 \leq x < 0.75$
	19:00	$0.75 \leq x < 1.0$
ICT scenario	ICT_0	$0.0 \leq x < 0.1$
	ICT_1	$0.1 \leq x < 0.2$
	ICT_2	$0.2 \leq x < 0.3$
	ICT_3	$0.3 \leq x < 0.4$
	ICT_4	$0.4 \leq x < 0.5$
	ICT_5	$0.5 \leq x < 0.6$
	ICT_6	$0.6 \leq x < 0.7$
	ICT_7	$0.7 \leq x < 0.8$
	ICT_8	$0.8 \leq x < 0.9$
	ICT_9	$0.9 \leq x < 1.0$
Batteries (amount)	only initial	$0.0 \leq x < 0.333$
	35%	$0.333 \leq x < 0.666$
	70%	$0.666 \leq x < 1.0$
Batteries (placement)	close to initial BS	$0.0 \leq x < 0.333$
	far from initial BS	$0.333 \leq x < 0.666$
	evenly distributed	$0.666 \leq x < 1.0$

on the total number of values per parameter. Table 5.3 shows all the variable parameters and their assigned ranges. There are three parameters for both PS and ICT scenarios.

For PS, time of year and time of week are considered, which have already been described in the context of the aggregated time series used. In addition, the time of day is considered, representing the time the restoration process starts. Here, four different times were chosen to include different load and generation behavior (e.g., in the evening, there is a load peak but less or no PV generation, depending on the time of year – see time series in Appendix A.2).

The ICT parameters include the specific ICT scenario and the number and placement of batteries. As described in Section 5.1.2, ten scenarios have been created for each ICT scenario type, with different base station placements. The value in the Halton sequence defines which base station setting is used for a concrete scenario. Three values were chosen for the number of base stations with batteries: only initial means that only the base station connected to the blackstart capable bus has a battery backup. The 35% and 70% refer to the percentage of all base stations in the network that have batteries. To make the scenarios not too simple to solve, the highest percentage was chosen to be well below 100%.

Another relevant parameter is the placement of batteries, which determines which base stations exactly are functional in the event of a blackout and which require power before their respective communication cell would be activated. While it is assumed that the first base station to start the restoration process will always have a battery, other base stations may not. To reduce the amount of randomness in the scenario and to have a more structured approach, three different versions of battery placement have been defined using the initial base station as a reference: 1) close to the initial base station, 2) far from the initial base station, 3) evenly distributed. In this case, the distance is not defined by the Haversine distance between the base stations but instead as the number of PS nodes between the base stations in the power grid. This is based on the fact that for two base stations to become part of the same island grid, all the power system buses between them – including the two to which they are connected – must become part of the island. The more buses between a base station and the initial base station, the longer it would take for that base station to become part of the island. The batteries are now placed as follows:

1. For each base station, calculate how many buses it is away from the initial base station.
2. Sort all base stations in a list by this number (from least to most).
3. Use this list to distribute the batteries. In the "close to initial" case, all batteries are placed on the base stations at the beginning of the list. In the "far from initial" case, they are placed at the end of the list. For "evenly distributed," they are distributed throughout the list.

Figure 5.5 shows the entire evaluation process. It is similar to the one described in Section 4.3.3. Each parameter combination from the Halton sequence is combined with both rural and urban grids and all four ICT types, resulting in 8 scenarios per parameter combination. These scenarios are then run for both Binary and Linear ICT states described in Section 5.1.4, for both the algorithm without ICT objective (MOO2) and with ICT objective (MOO3). For MOO3 there is an additional parameter because weights are used to select the final solution from the Pareto front after each restoration step. For a scenario restoration, the same weight is always used from a list of defined weights: [(0.9, 0.1), (0.7, 0.3), (0.5, 0.5), (0.3, 0.7), (0.1, 0.9)]. Which of the defined five different weights is chosen depends on the id of the scenario in the Halton sequence by calculating $id\%5$ and using the result to select the weight on the list. Each scenario is repeated five times to account for the variation in results due to the heuristic behavior of COHDA. Only the best result is used to compare the results. The final number of individual scenarios run is 3208 for Binary and Linear ICT States. This corresponds to 401 Halton sequence IDs. Based on the comparison results, the scenarios are sorted into one of 4 categories. These are C2 (MOO2 and MOO3 have the same result), C3 (the result of MOO3 is better than that of MOO2), C4 (the result of MOO3 is worse than that of MOO2), and invalid (neither MOO2 nor MOO3 manages to form an island grid). The C1 category, also introduced in Section 4.3.3, is not considered here.

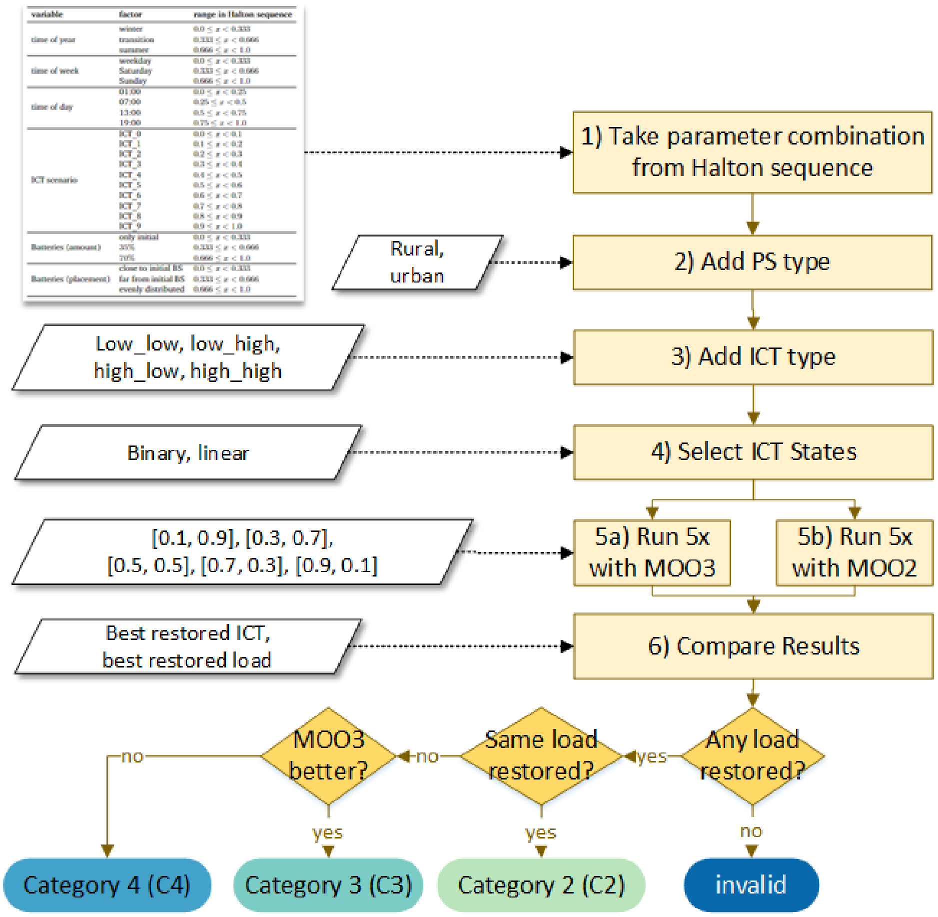

Fig. 5.5.: Evaluation Process

The experiments were conducted on three virtual machines with 3.40GHz CPUs, one with four cores and two with eight cores. The smaller VM always ran three scenarios in parallel, while the other two ran seven. The agents themselves were not executed in multiple processes but in a single process, which can also slightly distort the algorithm's behavior compared to how it would be in a real distributed system.

5.3 Results – Non-Functional Requirements

This section presents the results for analyzing the fulfillment of non-functional requirements, focusing on the differences between MOO2 and MOO3. The results are separated between rural and urban scenarios, as these are two completely different grids with different structures, generation, and load distributions.

5.3.1 Effectiveness

The effectiveness of the restoration algorithm can be measured by checking how much load and ICT are restored in each scenario. While load restoration is the main objective, ICT is used as a secondary measure of effectiveness. Load and ICT are not measured as absolute values but as a percentage of the maximum possible restored load/ICT. For the maximum load value, the total load and generation in the system are compared, and either the total load – if there is equal or more generation – or the total generation is used as a reference. For the maximum ICT value, the total number of nodes in the grid is used. In both cases, it can not be guaranteed that these values reflect the true optimum of a specific scenario. Since the ICT scenarios were designed randomly, there might not always be a restoration sequence that can incrementally restore all load and ICT. Therefore, the theoretical 100% restored load (and ICT) used as a reference may only be achieved in some cases. The optimal solution may be even lower in the Linear setting due to generation limits. However, since the focus is more on comparing different versions of the algorithm and less on absolute performance values, this approximation is sufficient.

There are 1604 scenarios in total for the urban grid and the same amount for the rural grid. Out of the five repeated runs of one scenario, only the one with the best results regarding restored load/ICT is used for the analysis to compare the best runs of MOO2 and MOO3. Figure 5.6 shows the restored load for both the Binary and Linear ICT states settings. The median (line) and the mean (diamond) are shown. In general, it can be seen that the range of how much load is restored is extensive, showing how the differences in the scenarios resulting from the parameter variations affect the final result. It can be seen that there is little difference between MOO2 and MOO3 in the rural grid for both Binary and Linear. In the Linear ICT states, slightly less load is restored (median of about 65% for Binary and 52% for Linear). This makes sense if one considers that in the Linear ICT states, generation is more constrained by impaired ICT.

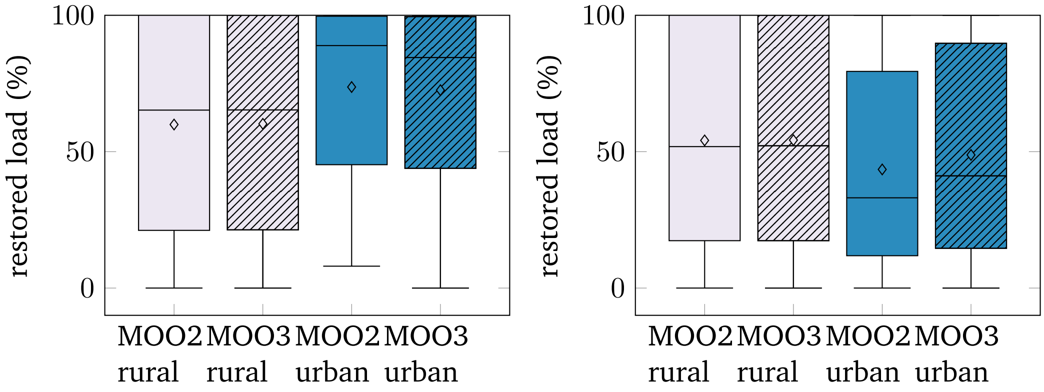

(a) Binary ICT States

(b) Linear ICT States

Fig. 5.6.: Boxplots for restored load per scenario

For the urban scenarios, there are more visible differences between MOO2 and MOO3 and between the Binary and Linear ICT states. The urban scenarios are generally restored more effectively in the Binary setting (see Figure 5.6a). In addition, the median value of MOO2 is 89%, and the median value of MOO3 is slightly lower at 85%, showing that MOO3 seems slightly less effective than MOO2 in load restoration in these scenarios. These observations are reversed for the Linear ICT states (see Figure 5.6b): first, less load is restored in the urban scenarios than in the rural scenarios, and second, MOO3 performs slightly better than MOO2 (41% vs. 33%).

Figure 5.7 shows the results for effectiveness in terms of restored ICT. First, it can be seen that in the rural scenarios, MOO2 and MOO3 have almost identical results, similar to the restored load. Overall, slightly more ICT is restored than load, which makes sense considering that the communication overlay is usually larger than the island grid unless the entire grid is restored. The urban scenarios again show differences between MOO2 and MOO3. It is interesting to note that in both settings, Binary and Linear, MOO3 performs better than MOO2 with a median of 59% vs. 47% in the Binary setting (see Figure 5.7a) and a median of 40% vs. 24% in the Linear setting (see Figure 5.7b).

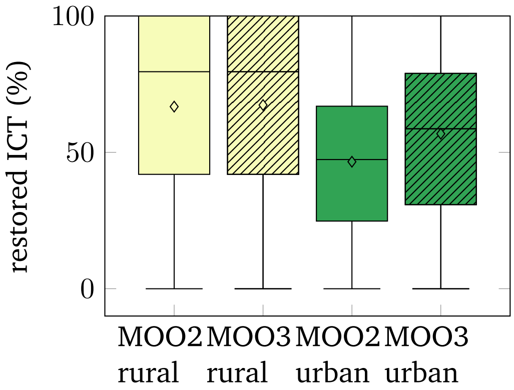

(a) Binary ICT States

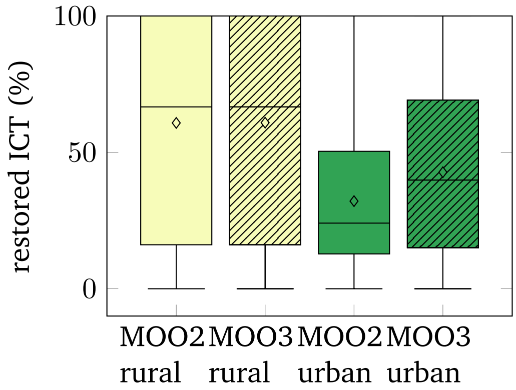

(b) Linear ICT States

Fig. 5.7.: Boxplots for restored ICT per scenario

5.3.2 Efficiency and Scalability

Efficiency and scalability are considered together because the differentiation between the rural and urban scenarios shows how efficiency changes with an increased number of nodes. In the following, the number of messages, the execution time, and the number of negotiations are considered for efficiency measures. The values are always calculated for an entire restoration process, not just a single restoration step. If a restoration consists of several restoration steps, the values of each step are summed up.

Figure 5.8 shows the number of messages for all scenarios with the Binary ICT States setting, divided by agent type (Switch Agent or Unit Agent), grid type (rural or urban), and algorithm (MOO2 or MOO3). Outliers are not considered. It can be seen that there are visible differences between urban and rural grids and between switch and unit messages. Urban scenarios have a higher message load than rural scenarios. This makes sense, considering that urban scenarios have, on average, slightly over 100 agents more than rural scenarios. Unit Agents exchange more messages (within the same grid type category) than Switch Agents. This is because the restoration at the lower level is triggered many times in just one decide-step of the higher level Switch Agent (see Section 3.4). However, while messages between Switch Agents are exchanged over long distances, Unit messages are exchanged between agents that represent physically close entities.

In all cases, the Median of MOO3 is higher than the Median of MOO2, with the smallest difference for the rural switch messages (5.732) and the highest for the urban unit messages (43.984). This reflects the higher complexity of optimizing three instead of two objectives.

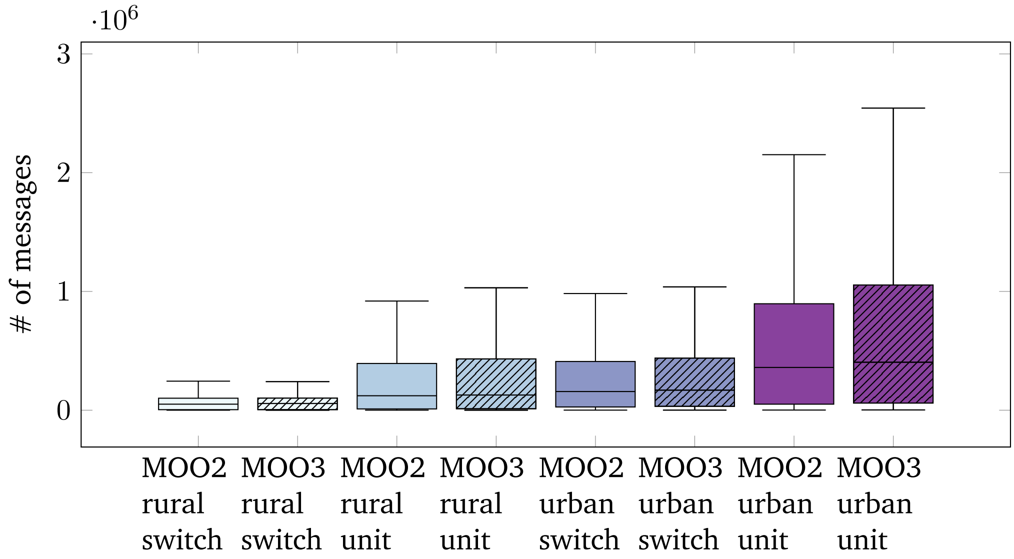

Fig. 5.8.: Boxplots for number of messages for Binary ICT States

Figure 5.9 shows the number of messages for the Linear ICT States setting. Overall, a behavior similar to the Binary setting can be observed. The main distinction is that in the urban scenarios, the difference between the Median number of messages between MOO2 and MOO3 is much larger than in the Binary setting (61.413 instead of 11.709 for switch messages and 163.086 instead of 43.984 for unit messages). This could be because of the limiting effect of degraded ICT on generation, making it more difficult to find a balanced island grid.

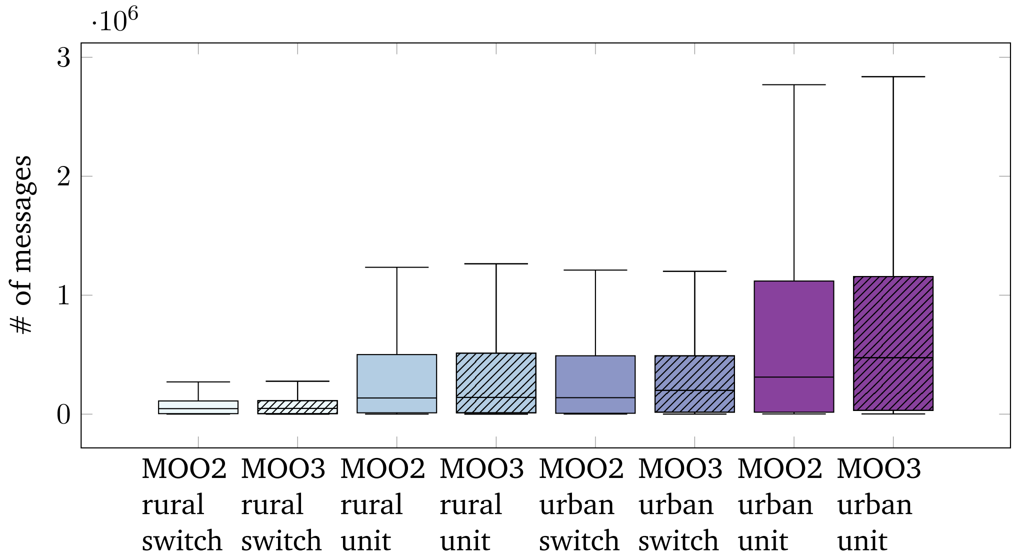

Fig. 5.9.: Boxplots for number of messages for Linear ICT States

Figure 5.10 shows the boxplots for the execution time of all scenarios. The purpose of showing the execution time here is to show how long the simulation took and to identify differences between the different grid types and algorithms. It is difficult to draw conclusions about the restoration time of real grids because the agents would be executed on different machines and run in parallel, influencing the runtime.

It can be seen that the execution time of the urban scenarios is much higher than that of the rural scenarios for both Binary and Linear ICT states. This could be because there are not just more agents in the scenario, but the agents are also closer together, so even with less ICT initially available, more agents can participate in the negotiation. For rural scenarios, the runtime of MOO2 and MOO3 is similar (difference in Median of 2 minutes for Binary ICT states and 1 minute for Linear ICT states). For urban scenarios, there is a significant difference (the Median of MOO3 is 27 minutes higher than of MOO2 in the Binary setting and 68 minutes higher in the Linear setting). Also, the variation is larger, with some scenarios of MOO3 requiring up to 10 hours to complete. This could be due to the higher complexity in the local optimization with three objectives instead of 2, increasing the time until convergence. It matches the observations from the number of messages.

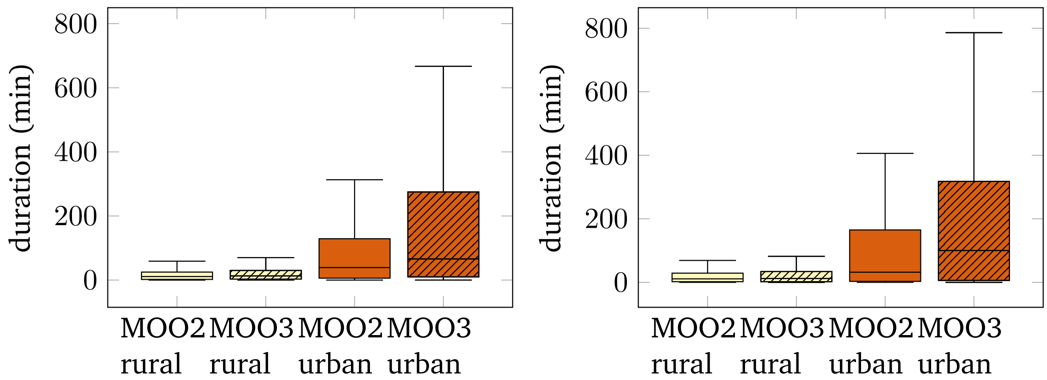

(a) Binary ICT States (b) Linear ICT States

Fig. 5.10.: Boxplots for duration per scenario

The only difference between the Binary ICT States (Fig. 5.10a) and Linear ICT States (Fig. 5.10b) is that the urban scenarios of MOO3 take longer (Median of 66 minutes for MOO3 in the Binary setting vs Median of 100 minutes in the Linear setting). This also matches the observations from the number of messages, where the Linear ICT States setting requires more message exchange and, therefore, has a longer execution time.

Figure 5.11a shows the total number of negotiations performed for an entire restoration process (i.e., all restoration steps) per scenario. The negotiations count both switch negotiations and unit negotiations. In a restoration process, the Switch Agents have as many negotiations as there are steps since a restoration step is precisely one negotiation of the Switch Agents. Therefore, the majority of negotiations are between Unit Agents. The results are consistent with the number of messages: in the urban scenarios, there are more negotiations and, therefore, more messages exchanged.

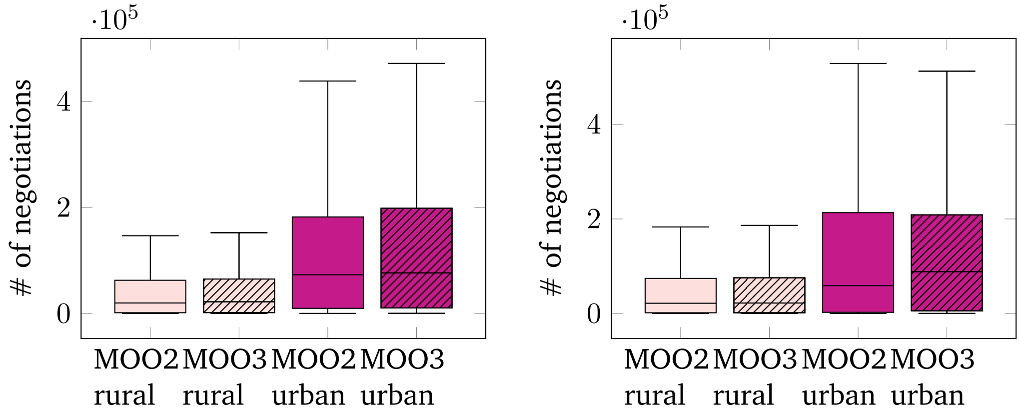

(a) Binary ICT States

(b) Linear ICT States

Fig. 5.11.: Boxplots for total negotiations of restoration process

5.3.3 Robustness

To evaluate the robustness, the algorithm's effectiveness in terms of load and ICT restoration with different levels of initially available ICT is analyzed. For the different ICT levels, the three available battery backup parameter settings are used: "only initial," "35%," and "70%." For these settings, both rural and urban grids have 544, 524, and 536 scenarios, respectively.

Figure 5.12 shows the relationship between initially available ICT and restored load for rural and urban scenarios in the Binary ICT States setting. It can be seen that the urban scenarios (Figure 5.12b) appear to be more robust to initially impaired ICT, with only minor variations between the different levels of battery availability (Median ranges between 83% and 91% for both MOO2 and MOO3). For the rural scenarios (Figure 5.12a), however, there seems to be a dependency between how much load can be restored and the initially available ICT. For "only initial" the Median of both MOO2 and MOO3 is at 21%, for "35%" the Median is at 62% and finally, for "70%" available battery the Median is at 100%, meaning in this case in most scenarios all of the load gets restored. In both rural and urban cases MOO3 does not have an advantage over MOO2 and shows very similar results.

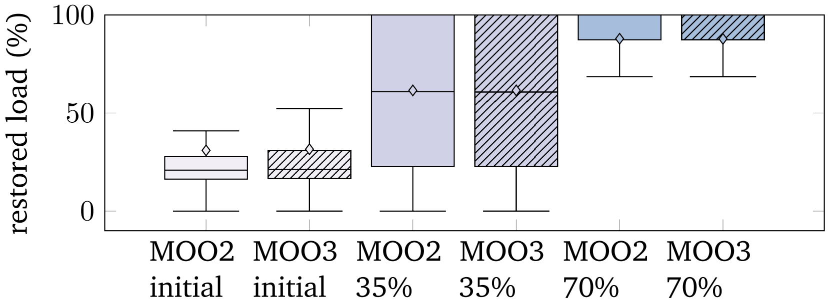

(a) Rural

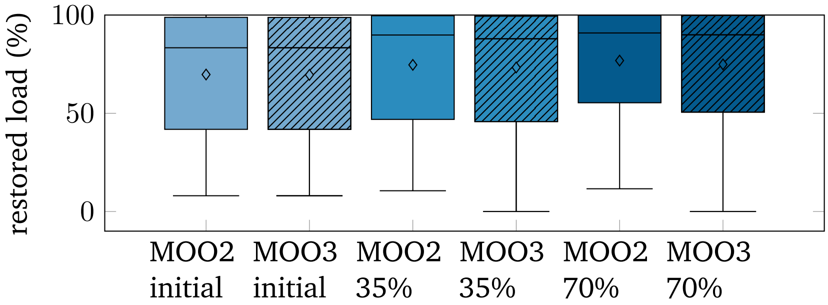

(b) Urban

Fig. 5.12.: Boxplots for restored load for different levels of initial battery availability per scenario in Binary ICT States

Figure 5.13 shows the same analysis for the restored ICT. For the rural scenarios, the results look very similar to the restored load, with a clear dependence on the initial available ICT and no difference between MOO2 and MOO3. For urban scenarios, dependency seems less strong, although more initial ICT leads to more total restored ICT. The Median of MOO2 in urban scenarios increases from 34% in the "only initial" case to 61% in the "70%" case. For MOO3, it increases from 44% to 77%, showing there is a difference between MOO2 and MOO3, with MOO3 always restoring slightly more ICT than MOO2.

Another interesting observation is that when comparing the Median of restored load and restored ICT for the urban scenarios, much more load is restored than ICT. This is a result of the scenario design: In the urban grid, there is not enough generation to serve all loads in most of the season/week/day combinations (for further details, see Appendix A.2), which means that only a smaller percentage of load can be restored anyway, which is used here as the reference value to calculate the percentages. For the restored ICT, however, the reference value is the total number of buses in the grid. This means that the results show that even though fewer nodes in the network are connected via communication to participate in the restoration process,

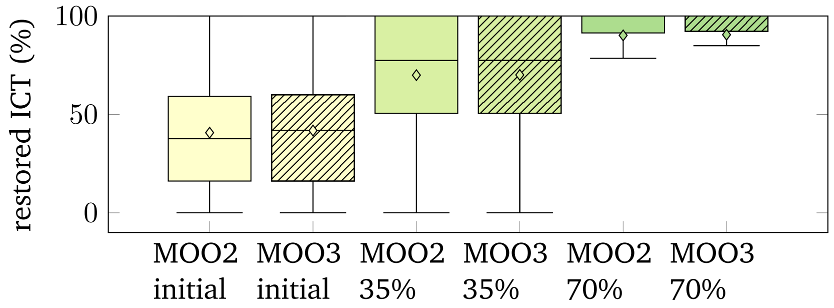

(a) Rural

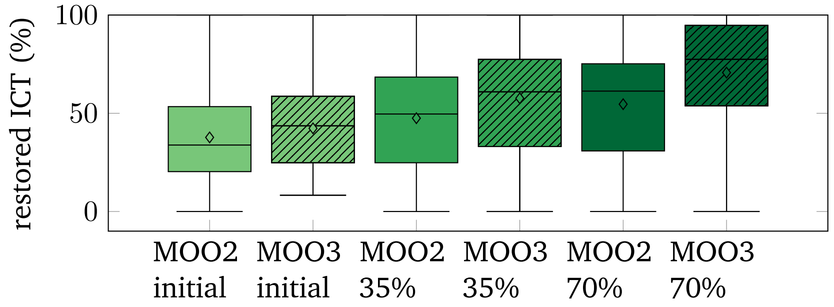

(b) Urban

Fig. 5.13.: Boxplots for restored ICT for different levels of initial battery availability per scenario in Binary ICT States

they still manage to restore most of the load that can be restored with the available generation.

Figures 5.14 and 5.15b show the same results for the Linear ICT States setting. Again, the rural scenarios show the same behavior with a strong dependence on the initial available ICT and no difference between MOO2 and MOO3. However, Figure 5.14 shows that in the Linear urban scenario – unlike the Binary urban scenario – MOO3 seems to have a slight advantage over MOO2 in terms of how much load is restored. This advantage is largest with "35%" ICT initially available: Here, the median of restored load for MOO3 is around 10% higher than for MOO2 (as opposed to a difference in Medians of around 5% for the other two cases). Regarding robustness, the Linear ICT States show the same dependence on the initially available ICT as the Binary states.

5.4 Results – Hypothesis

The first impression from evaluating the NFRs is that MOO3 has no advantage over MOO2 in terms of restored load in the Binary setting. In contrast, it has a positive

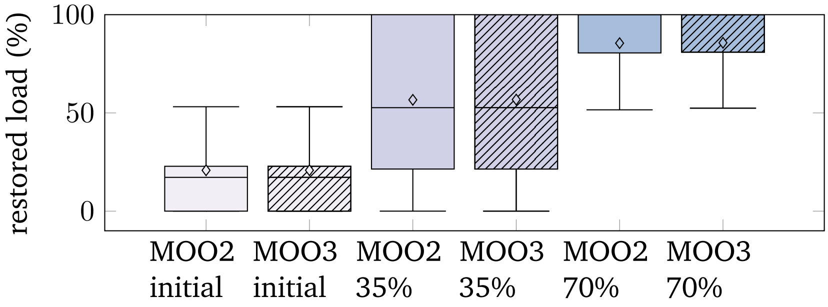

(a) Rural

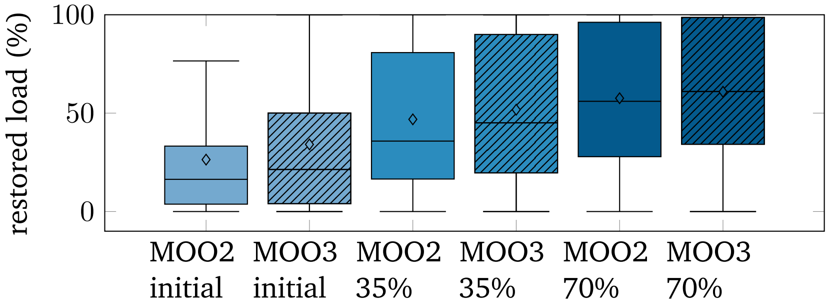

(b) Urban

Fig. 5.14.: Boxplots for restored load for different levels of initial battery availability per scenario in Linear ICT States

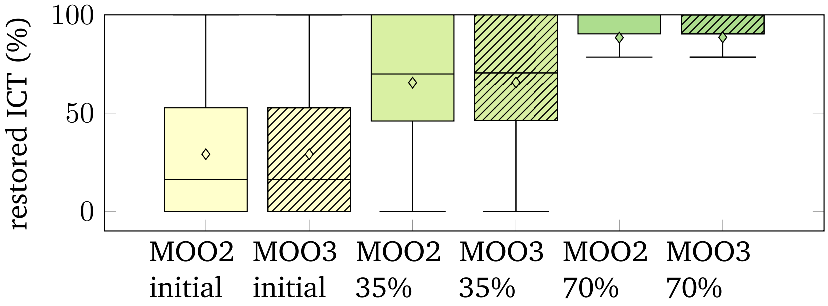

(a) Rural

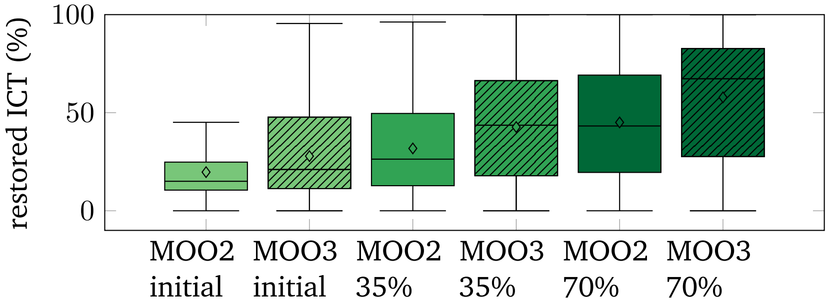

(b) Urban

Fig. 5.15.: Boxplots for restored ICT for different levels of initial battery availability per scenario in Linear ICT States

effect in the Linear setting, at least for urban scenarios. For both Binary and Linear ICT States, MOO3 restores more ICT in the urban scenarios. In this section, the results will be analyzed in more detail to investigate whether the hypothesis that more ICT restoration leads to more load restoration is true.

5.4.1 Category Distribution

The purpose of classifying the scenarios into categories is to a) get an idea of how often MOO3 has a better solution than MOO2 and b) identify characteristics of scenarios where this is the case, as well as characteristics for the other categories. Figure 5.16 shows the category distribution for both ICT states, using the maximum restored load as a reference for comparison. It can be seen that for the majority of scenarios (more than 60%), the best results of MOO2 and MOO3 are identical. This means that MOO2 and MOO3 find the same optimal solution in most scenarios. The number of invalid scenarios increases significantly between the Binary ICT states (less than 1%) and the Linear ICT states (around 10%). This is due to the limitation of generation, which in some scenarios is reduced so much that not even an initial island network can be formed.

The most interesting categories in terms of the hypothesis are C2 and C3. Here, it can be seen that in the Binary setting, not only are there very few scenarios where MOO3 has an advantage over MOO2 (only 8.56%), but there are more than twice as many scenarios where the results are worse when ICT is considered as an objective (20.48%). This changes when the reduction of generation flexibility is introduced in the Linear setting: Here, the C3 category is slightly larger than C2 with 17.71% vs. 11.21%.

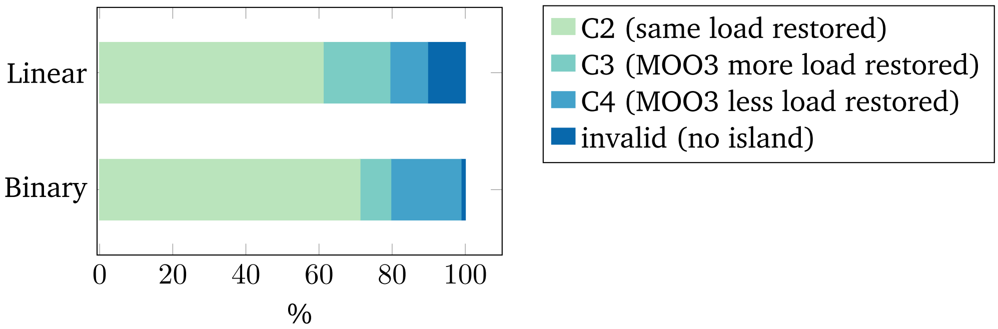

Fig. 5.16.: Categories distribution for different ICT scenarios using max restored load as reference

Figure 5.17 shows how the category distribution changes when the maximum restored ICT is considered for comparison instead of the maximum restored load.

The C2 category is slightly reduced but still makes up the majority of scenarios. However, hardly any scenarios fall into the C4 category, with only about 1% of the total scenarios for both Binary and Linear settings. Instead, the C3 category is much larger, with 32.81% and 24.43% respectively. This means that in almost all cases where the result is not the same or invalid, MOO3 manages to recover more ICT. This shows that the basic functionality of including ICT as an objective – namely, improving ICT restoration – seems to work. However, the increase in ICT restoration does not always affect power system restoration positively.

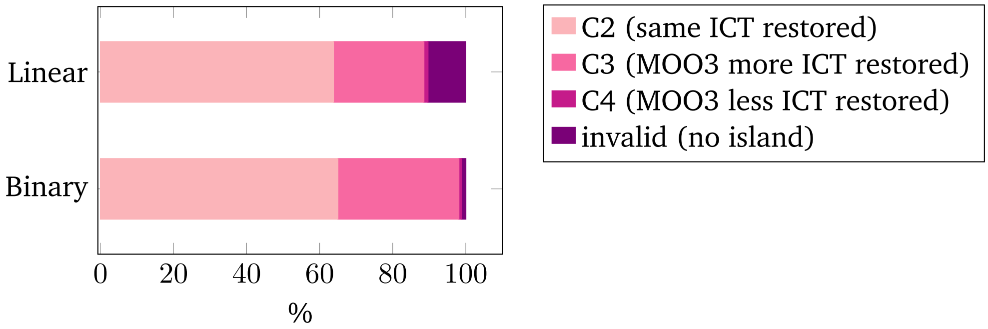

Fig. 5.17.: Categories distribution for different ICT scenarios using max restored ICT as reference

Convergence of Category Distribution

The convergence of the category distribution was checked to estimate how many parameter combinations from the Halton sequence are needed to obtain a meaningful result. One scenario ID in the Halton sequence corresponds to 8 scenarios, run with all combinations of PS type and ICT type (see Section 5.2). Figure 5.18 shows the convergence of the category distribution values over the number of scenario IDs from the Halton sequence for Binary and Linear ICT states. The category distribution values are calculated at fixed intervals, every 20 IDs. The red line is the "convergence point" and marks the scenario ID where the difference between two subsequent checkpoints in all categories is less than 0.5% and remains less than 0.5% for all subsequent points. This means that running more scenario IDs does not lead to significant changes in the category distributions after this point.

For both ICT states, this point is between 100 and 120 IDs, while 401 IDs have been run in total per setting. This means that it can be assumed that the results are meaningful and that running more scenarios would not have changed the category distribution significantly.

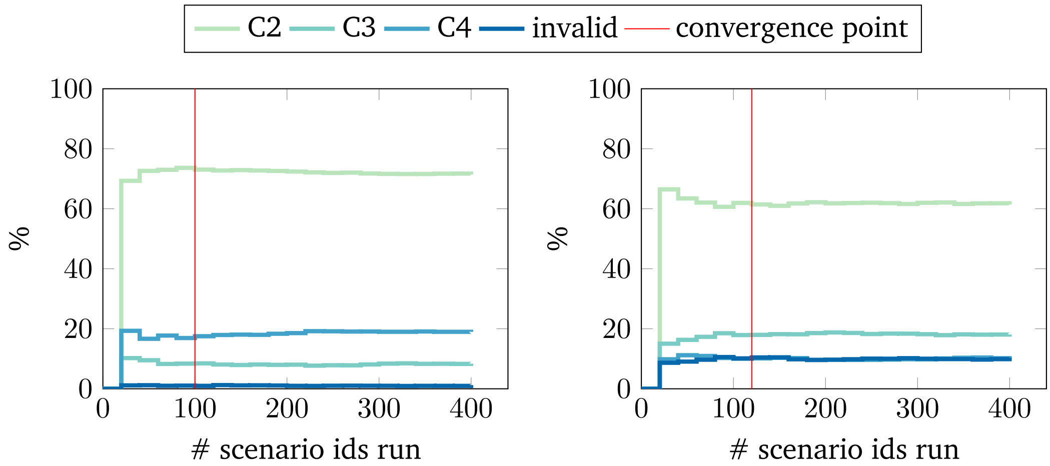

(a) Binary

(b) Linear

Fig. 5.18.: Category distribution at different number of scenario ids run for different ICT States

5.4.2 Analysis of Various KPIs per Category

To learn more about the variation in the restoration process in the different categories, the following relevant KPIs have been identified and analyzed:

- Variation of results per category – Out of 5 runs, how many results differ?
- Difference between the results – How big is the difference between the best and worst result in 5 runs?
- Number of scenarios with Pareto choice – How many scenarios in MOO3 have at least two valid solutions with a trade-off between restoring load and restoring ICT?
- Number of restoration steps – How often is the restoration process repeated before the island grid can not be extended further?

Table 5.4 shows the mean, standard deviation, and median (in parentheses) for all these KPIs for Binary (B) and Linear (L) ICT states, separated by category and MOO2 and MOO3 results. The first column shows the number of different results in 5 runs. It can be seen that, in general, for all the ICT state variants and all the categories, for both MOO2 and MOO3, the average number is greater than 1. This shows that, due to the heuristic behavior of MO-COHDA, the algorithm does not always converge to the same solution. Especially in the C3 and C4 categories, it can be seen that more than half of the runs reach different results on average. The C2 category, on the other hand, seems to have less variation, with a median of 1,

Tab. 5.4.: Average and standard deviation and Median in brackets for different KPIs per category

			# of different results in 5 runs	max diff between results in 5 runs in %	scenarios with Pareto choice in %	# of restoration steps
B	C2	MOO2	$1.67 \pm 1.09(1.0)$	$1.05 \pm 5.74(0.0)$	-	$2.4 \pm 1.16(2.0)$
		MOO3	$1.48 \pm 1.0(1.0)$	$1.22 \pm 9.0(0.0)$	0.01	$2.4 \pm 1.15(2.0)$
	C3	MOO2	$3.2 \pm 1.35(3.0)$	$2.13 \pm 4.73(1.0)$	-	$1.99 \pm 0.8(2.0)$
		MOO3	$3.37 \pm 1.33(4.0)$	$5.85 \pm 16.69(1.93)$	0.03	$2.32 \pm 1.0(2.0)$
	C4	MOO2	$3.4 \pm 1.3(4.0)$	$1.86 \pm 2.67(1.2)$	-	$1.95 \pm 0.69(2.0)$
		MOO3	$3.0 \pm 1.46(3.0)$	$7.2 \pm 21.02(1.4)$	0.03	$2.02 \pm 0.64(2.0)$
L	C2	MOO2	$1.66 \pm 1.18(1.0)$	$2.1 \pm 9.46(0.0)$	-	$2.25 \pm 1.35(2.0)$
		MOO3	$1.47 \pm 1.05(1.0)$	$1.17 \pm 8.77(0.0)$	0.01	$2.16 \pm 1.24(2.0)$
	C3	MOO2	$3.27 \pm 1.48(3.0)$	$12.82 \pm 20.27(1.85)$	-	$2.17 \pm 1.26(2.0)$
		MOO3	$3.99 \pm 1.17(4.0)$	$19.91 \pm 29.96(3.75)$	0.01	$3.24 \pm 1.28(3.0)$
	C4	MOO2	$3.63 \pm 1.27(4.0)$	$11.46 \pm 19.76(2.05)$	-	$1.95 \pm 1.19(2.0)$
		MOO2	$3.06 \pm 1.41(3.0)$	$10.75 \pm 24.01(1.63)$	0.01	$1.98 \pm 1.02(2.0)$

suggesting that most scenarios have the same result in all five runs. This may also explain why scenarios end up in the C2 category: They seem to have properties that reduce the number of optimal solutions the algorithm can find, regardless of whether 2 or 3 goals are considered. Therefore, MOO2 and MOO3 are more likely to find the same solution.

The second column shows the maximum difference in % of total load restored between two results in 5 runs. For those scenarios where all runs have the same final result, this value would be 0. To calculate the percentage, the maximum possible load that can be restored for the specific scenario was used as the 100% value. For the C2 category, the difference seems to be very small in most scenarios, with an average between 1% and 2% and a median of 0, consistent with the observations from the number of runs with a different result. The maximum difference variation for the C3 and C4 categories is more significant in both Binary and Linear ICT states. This shows that the heuristic does not always find similarly good solutions and could mean that the C3 and C4 scenarios are more complex and the algorithm gets stuck in local minima more easily. However, the median difference between the best and the worst solution is still small (< 4%) even for the C3 and C4 categories, suggesting that the algorithm finds similar solutions in most cases.

The number of scenarios with a Pareto choice is only relevant for MOO3 scenarios since MOO2 has only one objective (after eliminating all invalid scenarios where the island balance objective is not 1). For each restoration step of each run, it was checked whether there are at least two valid solutions, A and B, in the final Pareto front, where for solution A, the restored load is higher than in solution B. In contrast, the restored ICT is lower than in solution B. A solution is valid when the island balance objective is 1. Then, the scenarios where this is the case were counted, and the percentage of total scenarios was calculated. As seen in Table 5.4, the occurrence of such scenarios is very rare (less than 0.05% of scenarios). It shows one of the problems of using the constraint of island balance as an objective: the resulting Pareto front not only considers trade-off solutions between ICT and load but also for island balance, which can be invalid.

Finally, the last column shows the number of restoration steps. It is noticeable that in nearly all cases, the median number of steps is 2. This means that in the scenarios of the C3 and C4 categories, the difference between MOO2 and MOO3 does not come from one algorithm being able to perform more restoration steps than the other but rather from the choice they make during the same number of restoration steps. It also shows that the scenarios created are unsuitable for testing a longer restoration process with many restoration steps. The more restoration steps there are, the more significant the difference between MOO2 and MOO3. Since restored ICT can only show its benefit during the subsequent restoration step, the chances of ICT being beneficial for load restoration increase when the recovery process takes more time.

5.4.3 Distribution of Scenario Characteristics

The following sections present the distribution of the different variable parameters (see Table 5.3) for the different ICT states and categories. The aim is to examine whether specific scenario characteristics can be used to decide which category a scenario would belong to.

Results for Binary ICT States

Figures 5.19, 5.20, and 5.21 show the distribution of all scenario characteristics for Binary ICT states. Many of the parameters in each category have an almost even distribution of the different possible variables. This means these parameters do not significantly influence whether a scenario belongs to the respective category. In Figure 5.19 for C2, the only parameter that seems to have a significant influence is the grid type, as most scenarios in C2 belong to the rural grid (68.69%). This shows that MOO2 and MOO3 are less likely to find different optimal points in the rural grids, as shown previously (see Section 5.3.1). This could be explained by the less meshed structure of the rural network and the larger distance between nodes, resulting in a smaller number of different restoration paths that the algorithm could take. In addition, the time series for the rural grid has much more generation compared to the available load (see Appendix A.2). Almost every time step, there is enough generation to serve all the loads, plus some excess generation. The same reason could explain why the "only initial" case occurs slightly more often than the other two cases for the battery amount parameter: With less initial communication available, the options for grid restoration are reduced, and it is more likely that MOO2 and MOO3 start on the same restoration path and then follow it.

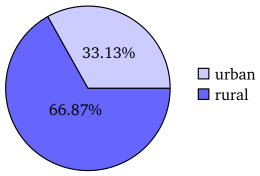

(a) grid type

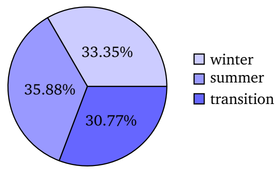

(b) time of year

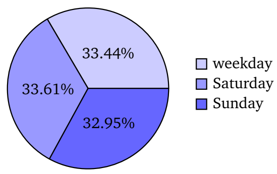

(c) time of week

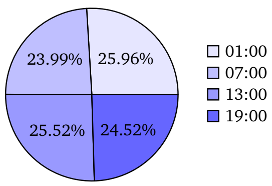

(d) time of day

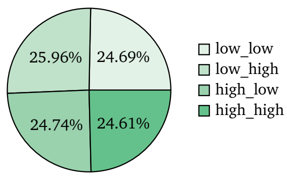

(e) ICT type

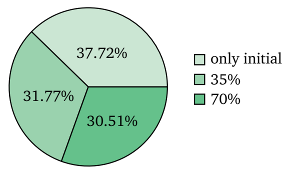

(f) battery amount

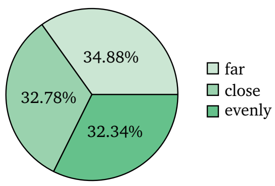

(g) battery placement

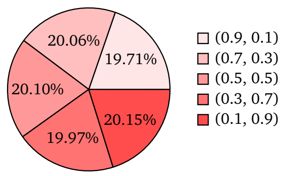

(h) weights

Fig. 5.19.: Parameter Distribution for Binary **C2**

The results are similar for C3 (see Figure 5.20). Only the grid type seems to have a significant influence, with 90% of the scenarios belonging to the urban grid type, which is a noticeable difference from the C2 category. In the urban grid, there is less generation than the load for most of the time steps in all time series. This could mean that the restoration algorithm cannot simply restore all available nodes in one restoration step but has to make a decision, which in turn depends on the objectives considered. Similarly, the "only initial" value of the battery amount parameter has the least occurrence in the scenarios. This can be explained with the same argumentation as for the C2 category: A higher amount of initially available battery backup allows more options for island grid forming, and only then can it make a difference whether the decision is made concerning only load restoration or load and ICT restoration.

In the ICT type parameter, it can also be seen that the one with the lowest occurrence is the "high_low" value. This refers to scenarios with a high median cpb value and a low median bpc, which means that the cells are small, but there are many of them, so each bus is covered by several cells. In this case, when a node is added, and more base stations are restored, the number of buses covered by these base stations is generally smaller, and all the buses would be close together and (direct) neighbors in a power line. This would lead to less flexibility in the restoration process, as there are no different restoration paths to choose from.

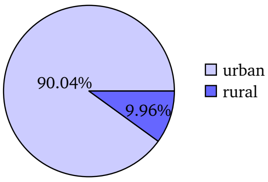

(a) grid type

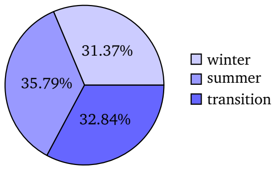

(b) time of year

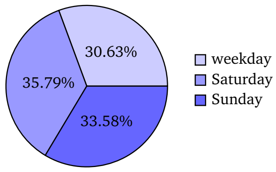

(c) time of week

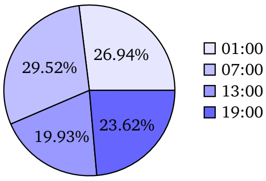

(d) time of day

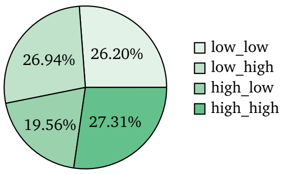

(e) ICT type

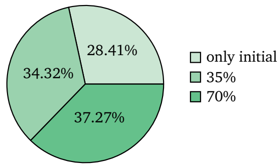

(f) battery amount

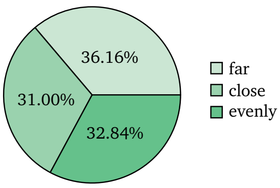

(g) battery placement

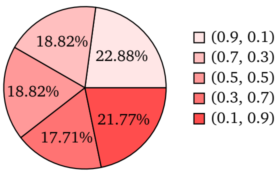

(h) weights

Fig. 5.20.: Parameter Distribution for Binary **C3**

Finally, Figure 5.21 shows the parameter distribution for all scenarios in the Binary C4 category. Here, the urban grid type is even more evident in the majority with 97.50%. This supports the previous observation that differences between MOO2 and MOO3 are mainly observed in scenarios with the urban PS type. Some other interesting observations can be made. For example, time of year seems to be a relevant parameter in this category, with summer being the parameter value with the lowest occurrence (19.84%). The summer time series has the highest amount of generation due to the feed-in from PV units and is the only time series for the urban grid where there are some time steps with more generation than load, meaning that all load can be restored. For these scenarios, the results of MOO2 and MOO3 do not differ; therefore, they are more likely to end up in the C2 category. The same applies to scenarios with the "only initial" value in the battery amount parameter, which is only 19.53% for the C4 category. With less ICT initially available, the algorithm's choices are reduced, and both MOO2 and MOO3 are more likely to choose the same path.

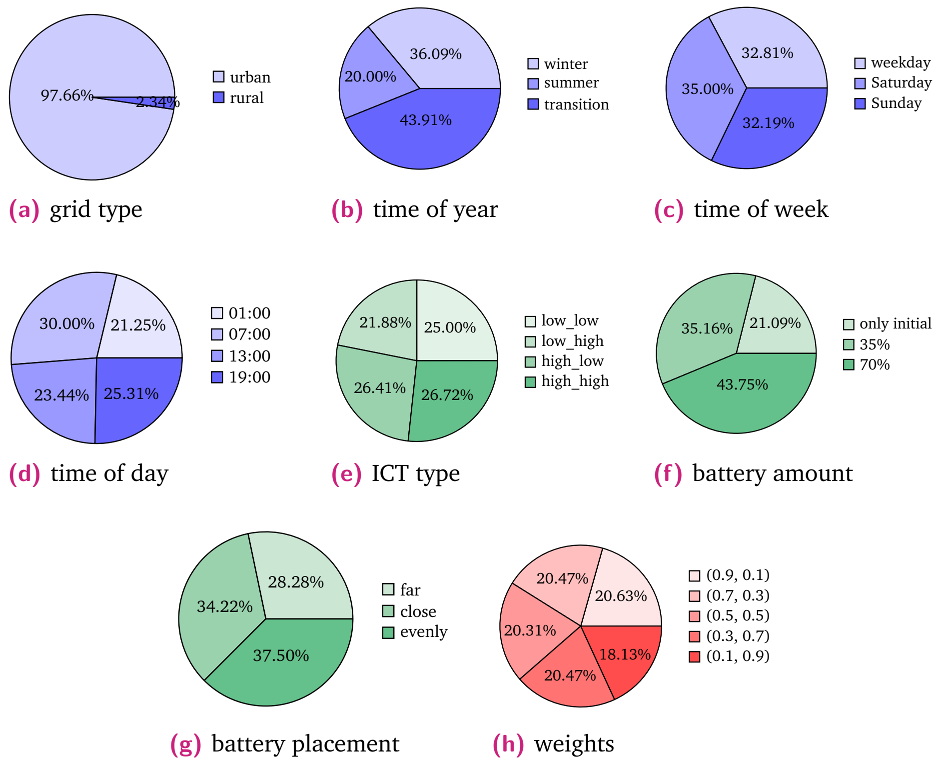

Fig. 5.21.: Parameter Distribution for Binary **C4**

It can be seen that for none of the categories, the weight parameter seems to have a significant influence. This can be explained by the results in Section 5.4.2, where it was shown that only in very few cases the final Pareto front has more than one valid solution. Without a set of solutions to choose from, the weights obviously do not influence the allocation to the different categories.

Results for Linear ICT States

For the Linear setting, only those results are shown where the difference between the lowest and highest occurrence of a parameter value is at least 10%, to focus only on those parameters with a relevant difference between values. The only parameter that meets this criterion for the C2 category of Linear ICT states is the grid type, which can be seen in Figure 5.22. Equally to the Binary C2 category, most scenarios belong to the Rural network type with 67.92%.

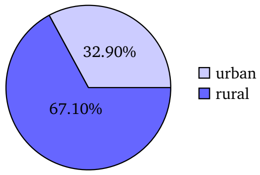

(a) grid type

Fig. 5.22.: Parameter Distribution for Linear **C2**

Figure 5.23 shows the relevant parameters for the C3 category of Linear ICT states. Again, the urban grid type is the most prominent with 91.13%. In the time of year parameter, it is noticeable that summer scenarios seem to occur less (only 11.70%). As mentioned before, for the C4 category with Binary ICT states, the main difference between the summer time-series and the other two for urban grids is the fact that there are intervals with more generation than load, allowing for an easier restoration process. It is interesting to note that while in the Binary case, the time of year was not a relevant parameter in the C3 category, this is the case in the Linear setting. For the time of week parameter, the weekday value appears less frequently than the other two, with 26.77%. Weekdays in the time series provide the highest load, combined with the reduced generation flexibility in the Linear ICT states; this might lead to fewer options for restoration (potentially even invalid scenarios).

Regarding the ICT parameters, battery amount and placement show a difference of more than 10% between the smallest and largest percentage values. Here, scenarios with only battery backup at the initial base station and a battery placement close to the initial starting points are less common. Both parameters potentially reduce the amount of different optimal restoration paths: On the one hand, only initial available battery reduces the number of initial restoration steps. On the other hand, if the available battery backup is placed close to the initial base station, nearly all available communication can already be used in the first restoration step. Both cases potentially reduce the benefits of explicitly considering ICT in the restoration process.

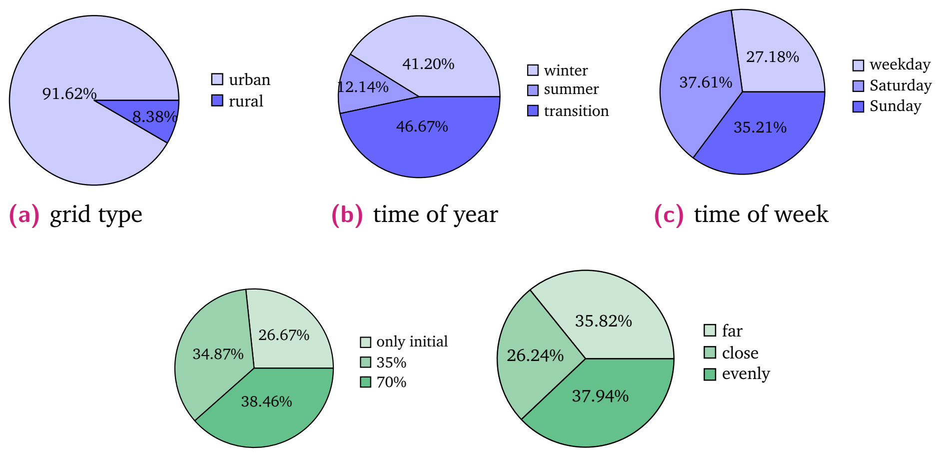

(a) grid type (b) time of year (c) time of week

(d) battery amount (e) battery placement

Fig. 5.23.: Parameter Distribution for Linear **C3**

Finally, Figure 5.24 shows the parameter distribution for the C4 category of Linear ICT states. Grid type and time of year show the same behavior as for the C3 category, with urban being the most common PS type with 96.56% and summer being the least common season with only 18.59%. However, different distributions can be observed for battery amount and battery placement. Regarding battery amount, in around half of the scenarios in C4, 70% of base stations have battery backup. Scenarios with only initial are rare with only 14.69%. This means that if there is a lot of initial ICT available, considering ICT in the objective does not seem to support PS restoration anymore, at least in the case of Linear ICT states. For the battery placement, most scenarios in C4 have the batteries either close or evenly distributed; only 19.22% of the scenarios have the base stations with batteries far away from the initial one. This is consistent with the observation of the battery amount parameter: It seems that when the ICT scenario itself is "easy," due to a large amount of available battery that is either close to the starting point or at least evenly distributed over the network, considering ICT as an additional objective does not improve load restoration, but rather limits it, possibly due to the unnecessary focus on ICT restoration when there is already enough ICT available to restore the maximum amount of load.

5.4.4 Influence of Battery Backup

A closer look at the influence of the battery backup parameters is relevant to further analyze potentially relevant scenario characteristics that could indicate the benefits of MOO3 during restoration. This includes the amount and the placement of battery backup at base stations.

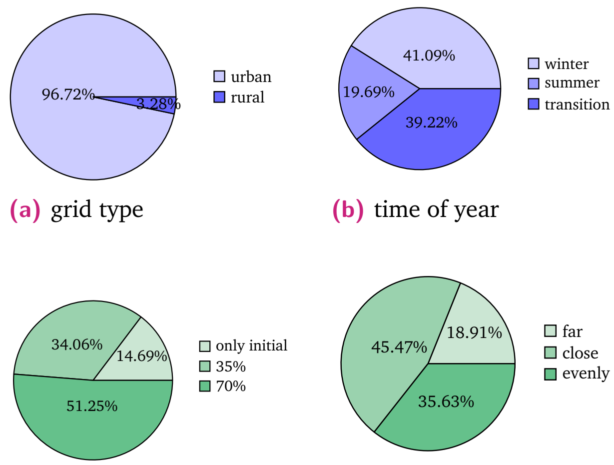

(a) grid type

(b) time of year

(c) battery amount

(d) battery placement

Fig. 5.24.: Parameter Distribution for Linear **C4**

Figure 5.25 shows for the Binary ICT States setting which battery parameter combinations are more likely to lead to scenarios with different possible restoration paths and for which parameter combinations MOO3 is more likely to have a positive effect on the amount of restored load.

First, Figure 5.25a shows for all combinations of these two parameters what percentage of scenarios have the same result regarding restored load (C2) and what percentage of scenarios have different results (C3 or C4). The parameter combinations have been sorted using the percentage of scenarios in C2 as a reference. It can be seen that with 70% of battery backup and an even distribution of the batteries across the grid, the percentage of scenarios where there is a difference between MOO2 and MOO3 is the highest (around 36%), while for those scenarios where only the initial base station is active, the percentage is the lowest (around 19%).

Second, Figure 5.25b shows for those scenarios where there is a difference between MOO2 and MOO3, how they are distributed among the C3 and C4 categories for all battery parameter combinations, sorted by increasing percentage of C3. The parameter combination with the lowest amount of scenarios in C3 (meaning that MOO3 has the least positive effect with only around 23% of scenarios in C3) is the same as the parameter combination with the lowest amount of scenarios in C2. On the other hand, the parameter combination where MOO3 is most likely to have a positive effect (with around 37% of scenarios in C3) is the same combination with the highest amount of scenarios in C2.

Figure 5.26 shows the same results for the Linear ICT states. Here, the differences in the amount of scenarios where MOO3 has a better result are more pronounced,

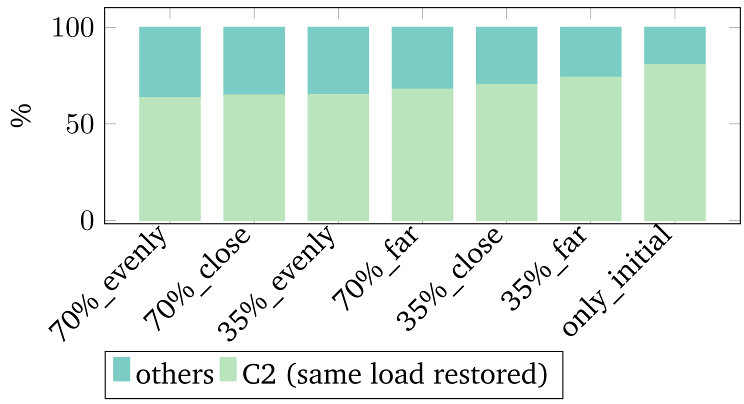

(a) C2 and others (out of all scenarios)

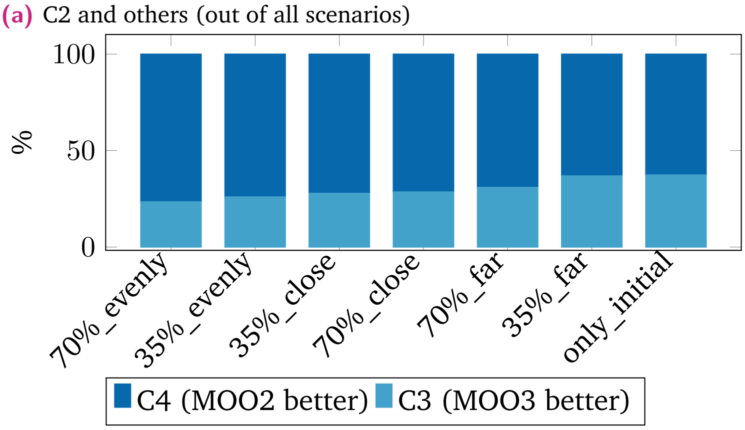

(b) C3 and C4 (out of scenarios in "others")

Fig. 5.25.: Distribution for different combinations of ICT parameters with Binary ICT States

as can be seen in Figure 5.26b with only about 33% of scenarios for the parameter combination with the lowest effect (70% battery backup and close to the initial base station) up to about 83% in the parameter combination with the highest effect (only initial).

In general, the results for both Binary and Linear ICT States show that the concrete ICT scenario significantly influences the effectiveness of MOO3. At the same time, the combination of battery parameters also influences whether MOO2 and MOO3 find different restoration paths. Interestingly, in both cases, the parameter combination with the lowest number of scenarios that are not in C2 also has the highest number of scenarios in C3 and vice versa. This indicates that it can be challenging to identify those scenarios where MOO3 is most likely to have a positive effect in a structured way.

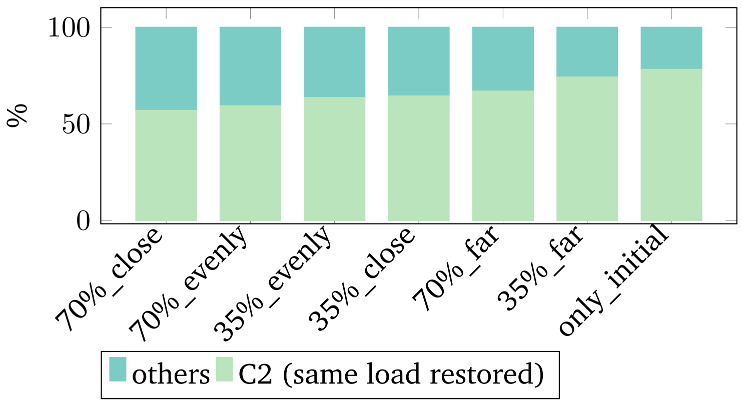

(a) C2 and others (out of all scenarios)

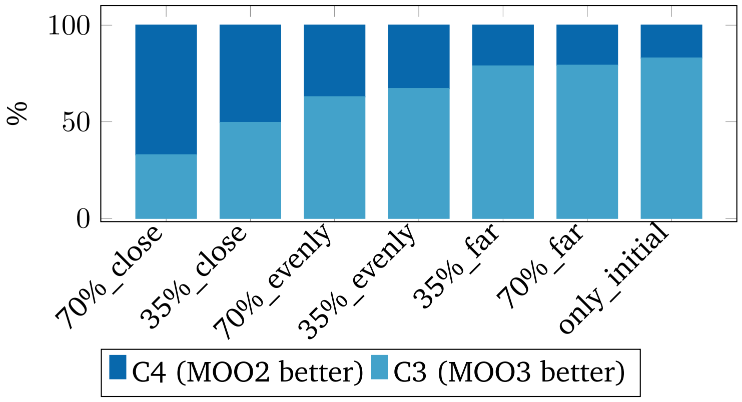

(b) C3 and C4 (out of scenarios in "others")

Fig. 5.26.: Distribution for different combinations of ICT parameters with Linear ICT States

5.4.5 Cumulative Average Restoration Path

This section examines and compares the average cumulative restoration paths for the different categories between MOO2 and MOO3. This should give additional information on the differences in the behavior of the two algorithm versions.

Results for Binary ICT States

Figure 5.27 shows the average cumulative restoration path for both MOO2 (lighter colors) and MOO3 (darker colors) in the Binary ICT States setting. Both load (solid line) and ICT (dotted line) restoration are shown. The number of restoration steps on the x-axis is always based on the scenario with the highest number of restoration steps. However, as identified in Section 5.4.2, most scenarios have only two restoration steps. This is also reflected in the restoration paths, as most of the restoration occurs in the first step, with a much smaller increase in the second step and only a marginal increase in all subsequent steps.

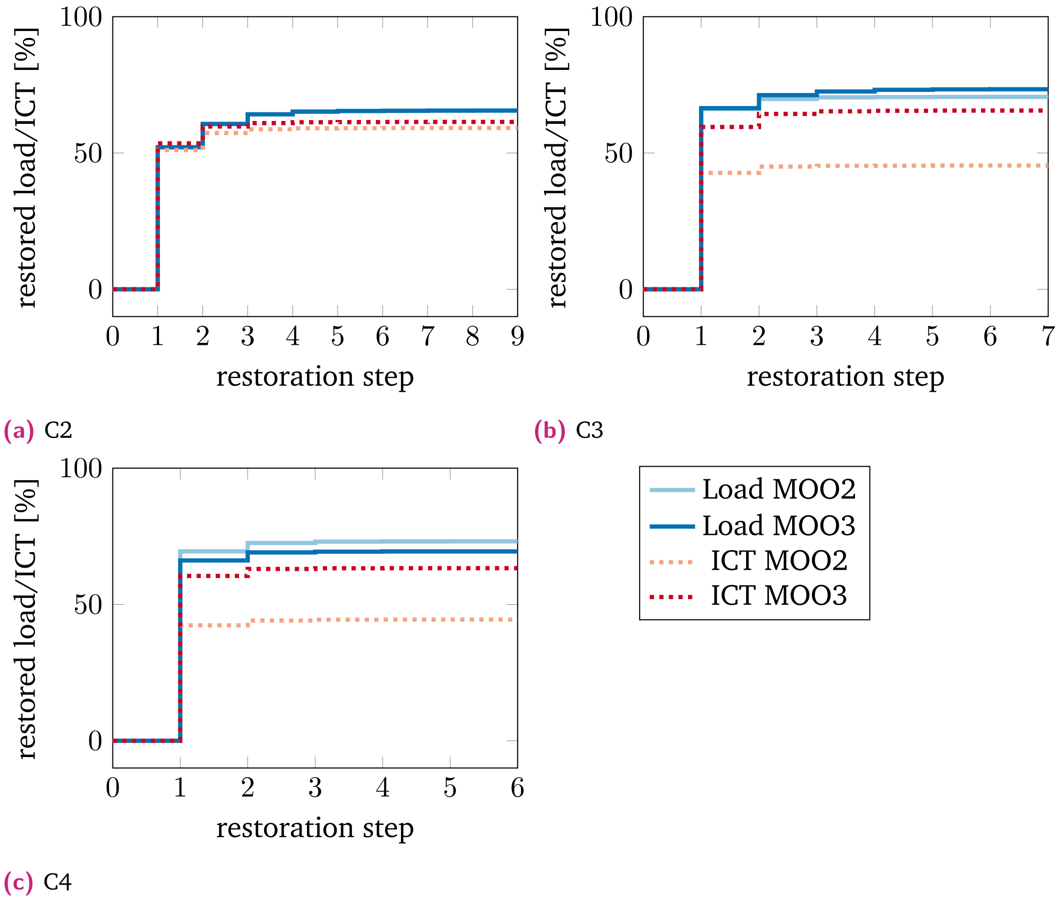

Fig. 5.27.: Average cumulative result values of all seeds per category in Binary Scenarios

It can be seen that the amount of ICT restored is always higher for MOO3, even in the C2 category. This shows again that considering ICT in the objective function positively impacts the total amount of ICT restored. The load restoration in C2 is nearly the same in each restoration step, which shows that each point in the restoration path is the only optimal point that both MOO2 and MOO3 find. How it is possible that the restored load is the same and only the restored ICT is slightly higher in MOO3 can be explained by the load distribution in the Simbench grids: There are only a few load types that are repeated at each node, i.e., there can be several combinations of different nodes that would result in the same total load for the respective island grid. While MOO2 focuses only on the load value and only randomly restores ICT, MOO3 also includes ICT in the decision process.

In the C3 and C4 categories, there are differences in load restoration. In both cases, one version of the algorithm (MOO3 for C3 and MOO2 for C4) restores more load in the first step and continues to do so in the following steps. However, the differences between the load recoveries are very marginal: In C3, MOO3 restores on average 73.16% of the load and MOO2 70.74% in the last restoration step, and in C4 it is 71.26% for MOO3 and 74.59% for MOO2, i.e., they are only about 3% apart. Depending on the overall situation, it could be said that the marginal difference in restored load is worth almost 20% more restored ICT in category C4.

Results for Linear ICT States

Figure 5.28 shows the average cumulative restoration path for the Linear ICT States setting. Several differences can be observed when comparing these results with the Binary setting. First, the total load restored is slightly less than in the Binary setting for MOO2 and MOO3 in all categories. The difference between the maximum restored load is largest in C2 with around 12% and between $4-5\%$ for both C3 and C4. This shows that the reduced generation from the limited ICT affects the whole restoration process, and even MOO3 cannot "catch up" with the restoration process without this limitation. The same is true for the restored ICT, with a difference of around 5% for C2, around 1% for C3, and around 9% for C4.

Second, the amount of load that gets restored after the first restoration step in the C3 and C4 categories is more in the Linear setting. It ranges from around 13% (MOO3 in C4) to even around 36% (MOO3 in C3), while for the Binary scenarios, it is only between 3% (MOO3 in C4) and 7% (MOO3 in C3).

Finally, the C3 restoration path shows some more differences. The difference between the restored load of MOO2 and the restored load of MOO3 is nearly 19%.

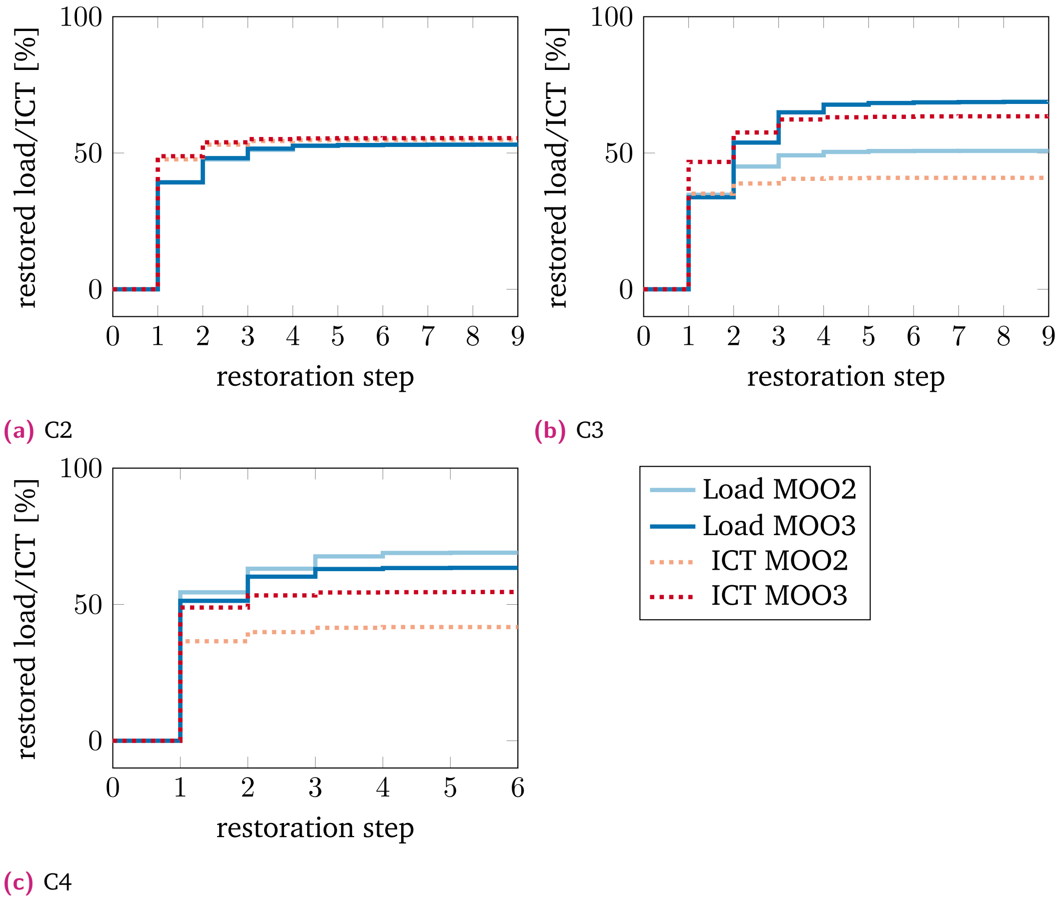

Fig. 5.28.: Average cumulative result values of all seeds per category in Linear Scenarios

That means that in the Linear ICT states setting, for those scenarios where MOO3 has an advantage over MOO2, that advantage is more significant. In the C4 category, on the other hand, the difference between the restored load of MOO2 and MOO3 ends up being only around 5%.

5.4.6 Detailed Restoration Paths

Previously, only the average cumulative restoration paths were shown. To gain a deeper understanding of the differences in the restoration process between MOO2 and MOO3, the restoration paths were examined at a more granular level. For each scenario, the result of each restoration step in terms of restored ICT and load is compared between MOO2 and MOO3 and classified accordingly. Figure 5.29 shows an overview of this classification. A total of 9 different classes can be distinguished with this approach. A restoration path can then be defined by performing this classification for each step and creating a sequence of classes. If the same class occurs in two steps in a row, it is combined into a single entry to focus only on the different occurrences of the step classes during the restoration.

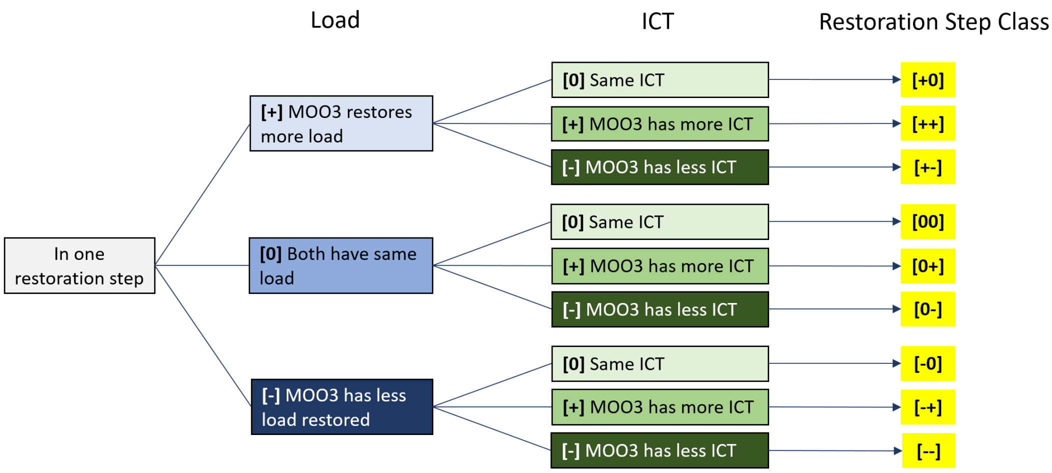

Fig. 5.29.: Explanation of step classification based on result comparison

According to the hypothesis, the scenarios in C3 should have a $[-+] \rightarrow [++]$ sequence. This sequence represents that by restoring less load and more ICT in an earlier step, more load and more ICT can be restored later, showing the importance of ICT availability for load restoration. The following tables show the most common restoration paths for all three categories for Binary and Linear ICT state settings. Only those paths that occur in at least 1% of the scenarios in at least one of the two ICT state settings are listed in the table. Paths that differ from each other by only one [00] step class at the beginning are considered equal and combined. The path with the highest occurrence for each ICT State setting is marked in yellow.

Table 5.5 shows the most common restoration path types for the C2 category. Most scenarios for the Binary and Linear ICT settings have the same restored load and ICT in each restoration step, meaning that both algorithms take the same restoration path. The second most common path for the Binary setting is for MOO3 to have the same restored load as MOO2 but more restored ICT. This is also reflected in the cumulative average restoration path shown in Figure 5.27a, where the line for restored ICT for MOO3 is slightly higher than for MOO2.

Tab. 5.5.: Most common restoration path types for C2

pathtype	Binary	Linear
['00']	79.63%	84.85%
['0+'], ['00', '0+']	12.90%	2.14%
['0+', '00'], ['00','0+', '00']	2.98%	0.46%
['+0', '00']	1.18%	2.65%

Table 5.6 now shows the restoration path types for the C3 category. Here, the most common restoration path is different for Binary and Linear ICT states: In the Binary setting, MOO3 restores more ICT and load in most scenarios, while in the Linear setting, the expected behavior from the hypothesis can be observed. In the Binary setting, this expected restoration path type occurs in only 10.19% of all scenarios in the category. For both ICT states, the most common restoration path type only accounts for about 60% of all scenarios, leaving 40% to fall into other categories. This shows that while there is a dominant path type for the category, other types are also relevant, and the scenarios in this category can not be reduced to a specific restoration behavior of the two algorithms.

Finally, Table 5.7 shows the restoration path types for C4. For both Binary and Linear, the most common path type is where MOO3 restores more ICT but less load, corresponding to the first half of the expected behavior. For these scenarios, the increase in ICT restoration does not directly translate into an increase in load restoration, i.e., the additional ICT does not help to expand the existing island grid. For these scenarios, the lack of ICT availability is not the limiting factor, but rather the availability of generation.

Tab. 5.6.: Most common restoration path types for C3

pathtype	Binary	Linear
['++'], ['00', '++']	59.78%	14.87%
['+0'], ['00', '+0']	18.82%	4.96%
['-+', '++'], ['00', '-+', '++']	9.96%	52.48%
['0+', '++'], ['00', '0+', '++']	5.90%	4.10%
['-0', '+0'], ['00', '-0', '+0']	1.85%	3.59%
['-0', '++']	0.74%	2.56%
[-0,-+,++]	-	2.05%
['++', '-+', '++']	-	1.37%
['-+', '+0']	-	1.20%
['--', '++']	-	1.03%
['-+', '++', '+0']	-	1.03%
['++', '+0']	-	1.03%
['+0', '-+', '++']	-	1.03%

Tab. 5.7.: Most common restoration path types for C4

pathtype	Binary	Linear
['-+'], ['00','-+']	86.22%	58.31%
['-0'], ['00','-0']	4.21%	13.90%
['+0','-0'], ['00','+0','-0']	2.59%	0.60%
['--'], ['00','--']	2.27%	6.65%
['++','-+'], ['00','++','-+']	1.78%	3.02%
['-+','++','-+']	-	3.93%
['-0','-+']	-	1.21%
['-0','++','-+']	-	1.21%

5.5 Key Findings and Discussion

From both the NFR analysis (see Section 5.3) and the hypothesis analysis (see Section 5.4), the following key findings and discussion points can be summarized:

- Only in 30% (Binary), respectively 40% (Linear) of the scenarios MOO2 and MOO3 find different optimal solutions regarding restored load for the restoration process. This shows that for most of the defined scenarios, **restoring ICT and restoring load do not seem to be conflicting objectives** (see Section 5.4.1).
- Especially in the **rural scenarios**, there is **no difference between MOO2 and MOO3** with regards to how much load or ICT gets restored (see Section 5.3.1).

- In the **urban scenarios, MOO3 is more efficient in restoring ICT**, which is precisely what it is supposed to do (see Section 5.3.1). Also, when looking in detail at the differences between MOO2 and MOO3 in those scenarios where MOO2 restores more load, it can be seen that the restored load is only marginally less while the restored ICT is much more (see Section 5.4.5). This means that in the context of multi-objective optimization and the goal of finding trade-off solutions, the solution found by MOO3 could still be considered better.
- However, **restoring more ICT does not automatically have a positive effect on the amount of load that gets restored**, as stated in the hypothesis. Only in around 0.87% (Binary) and around 10.4% (Linear) of the total scenarios does the expected behavior from the hypothesis – that by restoring more ICT and less load in an earlier step, more ICT can get restored later – occur (see Section 5.4.6).
- The initially available ICT is still highly relevant, and **MOO3 is not capable of canceling out the negative effect from having less initial ICT** available (see Section 5.3.3).
- While some parameter values could be identified that occur more or less frequently in those scenarios where MOO3 gives better results than MOO2, it was not possible to conclusively define which characteristics decide whether a scenario can benefit from MOO3 or not (see Section 5.4.3).

Conclusion: The hypothesis is true for some scenarios but is relevant only in a few cases. While MOO3 works as expected and can find solutions different from MOO2, which restore more ICT in the grid, this behavior does not have the desired positive effect on load restoration. However, the additional restored ICT can have positive effects in case of a blackout beyond load restoration. For example, it can be used to inform the general public, which is essential in the event of a disaster. The authors in [65] conducted a study using scenario planning and role-playing exercises to investigate people's possible reactions and expectations of government during a hypothetical 3-day blackout. The results show that a lack of information is a major problem for people affected by the blackout and dramatically increases their anxiety and feelings of uncertainty. Restoring ICT – especially in areas still in blackout – and thereby increasing the ability of people to communicate is therefore still crucial in long-lasting blackouts, even if it might not directly help to restore more load. This aspect should also be considered when evaluating the usefulness of the approach.

Moreover, the differences in results between Binary and Linear ICT States show that with changes in the definitions of ICT performance and effects of ICT on the restoration process, MOO3 can become more relevant.

5.6 Chapter Summary

This chapter presents an extensive evaluation of the restoration algorithm, which analyzes the remaining NFRs and the hypothesis in more detail. The highlights of the chapter can be summarized as follows:

- Large evaluation scenarios were introduced with several variable parameters for both the power system and the ICT system part. They are based on two Simbench MV networks, one rural (with 93 buses) and one urban (with 133 buses). Variable parameters include season, time of week, and time of day. Different ICT scenarios are created using a systematic approach to vary cell size and number of base stations, as well as the number and placement of batteries. Finally, two versions of ICT performance measurement are tested, one that only considers the number of connected nodes in the overlay (Binary) and one that also considers the state of these nodes based on how many communication cells are restored (Linear).
- Monte Carlo simulation with a Halton sequence was used to identify parameter combinations for each scenario. The scenarios are executed for the algorithm with (MOO3) and without (MOO2) ICT and then compared and sorted into categories.
- The effectiveness, efficiency, scalability, and robustness of MOO2 and MOO3 were measured and compared. The results for rural scenarios are generally very similar for all NFRs, while the urban scenarios show more differences. It is noteworthy that MOO3 is more efficient in restoring ICT, which confirms that the algorithm works as expected.
- Regarding the hypothesis, it seems to be valid only for a minority of scenarios, even if only those scenarios where there is a difference between MOO2 and MOO3 are considered. When comparing the Linear and Binary ICT performance calculation, the hypothesis is true more often in the Linear setting. Of all the scenario characteristics, only a few have an impact on whether the results of MOO2 and MOO3 are the same or different, including grid type, season, and battery placement.

6 Conclusion

This chapter presents a summary of the scientific contributions of this thesis in Section 6.1 and then concludes with an outlook on potential fields of future work derived from the findings of this thesis in Section 6.2.

6.1 Summary

The electric power system is safety-critical. A widespread blackout has severe implications for almost all aspects of daily life, including communications, transportation, water supply, and food supply. Therefore, rapid system restoration ("blackstart") is crucial. This blackstart process faces new challenges from the ongoing energy transition: The growing number of distributed energy resources (DER) is increasing system complexity. A so-called "smart grid" with advanced information and communication technology (ICT) can help manage this complexity but also increase the interdependencies between the energy and ICT systems. At the same time, these changes open up new opportunities for grid resilience. For example, generation capacity from DERs can be used to create island grids in the distribution system - small, autonomous clusters of generation and load that operate separately from the rest of the grid, thereby reducing customer outage time in the event of a blackout.

Deciding on the optimal composition of island grids can be described as an optimization problem with the goal of maximizing the amount of restored load while ensuring frequency stability by balancing generation and load within the island. This involves determining the states of power switches that connect or disconnect parts of the grid and coordinating the power generation of controllable units to match the consumed load within the island grid. Intelligent automated restoration services can help solve this problem by using the ICT system to gather the necessary information, make decisions, and send control commands to the appropriate elements. However, since the ICT system relies on the power system for power supply, the blackout will likely affect it. This requires these restoration services to be robust to an impaired ICT system. Distributed multi-agent systems (MAS) are not only capable of solving complex optimization problems in a reasonable time but can also dynamically adapt to changing communication infrastructure, making them an efficient strategy for various power system services.

While agent-based restoration algorithms are already a popular concept in the literature, most approaches either ignore the impact of a blackout on the ICT system, assuming it is fully functional, or focus only on the robustness of agents against link failure and message loss. The interdependencies of the power and ICT systems during a blackout with a MAS have yet to be considered. This PhD project aims to fill this gap by investigating the parallel restoration of power and ICT systems and the hypothesis that prioritizing the restoration of the ICT system can increase the total amount of restored load. To this end, the restoration process will be considered a multi-objective optimization problem, where the amount of restored load and the restored ICT infrastructure is maximized.

The thesis then answers the research question, „How to blackstart an ICT-reliant distribution system with high DER penetration using MAS? “. In detail, the following sub-research questions are answered:

1. How to design the MAS considering ICT impairment?
2. How to formulate the (multi-objective) optimization problem considering the impairment and the restoration of the ICT system?
3. How to implement the optimization problem in the designed MAS?
4. How to test and validate the developed MAS using a co-simulation framework?

Two main artifacts are developed. The first is an **agent-based restoration algorithm for the distribution system** capable of solving the multi-objective optimization problem. The algorithm is based on the Combinatorial Optimization Heuristic for Distributed Agents (COHDA). COHDA was originally developed for day-ahead planning of active power supply and has been proven to converge, terminate, and be robust to unsteady communication networks and different network topologies. In addition, COHDA has been extended to perform multi-objective scheduling with an approximation of the Pareto front (MO-COHDA). MO-COHDA is adapted to the specific use case so that the agents generate a set of Pareto-optimal island grid configurations that reflect the trade-off between load and ICT restoration. To ensure the stability of the resulting island, the balance between load and generation within the island is imposed as a hard constraint. The agents then select a solution from the Pareto front and implement the corresponding island grid.

Agents represent different elements in the power system, such as loads, generators, and remote-controllable switches. A wireless ICT infrastructure with base stations and communication cells is assumed. Using the initially available ICT infrastructure, agents communicate with each other to exchange information and, following the MO-COHDA process, find an optimal island configuration. Once implemented, additional ICT infrastructure is activated along with additional agents so that more agents can participate in the next restoration step. This allows for an iterative restoration process, further expanding the existing island. This process is repeated until no further restoration is possible. It is formally shown that this algorithm has guaranteed convergence.

The second artifact is the implementation of this algorithm in a simulation environment, **co-simulating the MAS, the power system, and the ICT system**. This is used for extensive evaluation to prove the algorithm's performance, robustness, efficiency, and scalability. The simulation environment uses the co-simulation platform mosaik, which allows combining models and simulators to create large-scale Smart Grid scenarios. The restoration algorithm is implemented using mango, a Python library for MAS, coupled with pandapower for power system simulation and NetworkX, a complex network library, for ICT system simulation.

Two evaluations were conducted using different design of experiments (DoE) methods. First, the fulfillment of the functional requirements of both artifacts is demonstrated with a proof of concept. Second, the hypothesis is examined in more detail, and the fulfillment of the non-functional requirements is presented. Specifically, the effect of considering ICT restoration as a separate objective in the optimization problem on the overall performance (in terms of total power system load restored) of the agent-based restoration algorithm is studied by comparing a version of the algorithm with ICT as an objective (MOO3) and without (MOO2). Two different versions of ICT states for calculating ICT performance are tested: a binary one where power system nodes are either fully available or unavailable (Binary) and a linear one where power system nodes may be available, but the connected generators have limited flexibility as long as the ICT infrastructure is not fully restored (Linear). Relevant KPIs are measured, such as the restored load and ICT infrastructure per restoration step and the number of messages exchanged by the agents.

The results show that for the scenarios tested, there is only a minority of scenarios with a difference between MOO2 and MOO3 regarding restored load. This indicates that ICT and load restoration are not conflicting objectives for the defined scenarios in most cases. Only a few scenarios show the behavior expected from the hypothesis that by prioritizing ICT over load restoration in an earlier restoration step, the later steps allow for more load restoration. However, MOO3 still works as expected and restores more ICT than MOO2. This can still support crisis management in case of a blackout to keep the population informed or coordinate between different restoration teams. It can also be seen that in the Linear ICT states setting, MOO3 is more efficient than MOO2 in a larger number of scenarios, showing that the definitions of ICT performance and the effects of ICT on the restoration process significantly impact the overall usefulness of the approach.

6.1.1 Influence of Design Choices

Having presented the results, it is important to note that these findings are specific to the technologies and methods employed. Different choices could yield different conclusions. In the following section, this thesis's four main design choices are presented, and how a change in each could influence the results is discussed.

Wireless Communication: The most important design choice in the scenario definition is the use of wireless communication technologies. The overlapping communication cells allow an iterative restoration process and communication with parts of the grid that are not yet part of an island since the active communication network can be larger than the island grid. This iterative restoration behavior may no longer be possible if the wireless communication infrastructure is replaced by a wired-only communication infrastructure. Substation routers may be directly connected and can only communicate when both routers are active. A wired communication infrastructure may, therefore, require that nodes that are not yet connected in the communication overlay be included in the restoration process. This introduces new challenges, such as the increased uncertainty of connecting nodes that cannot communicate or receive control commands before they are included in the island network.

(MO-)COHDA: (MO-)COHDA was the chosen optimization algorithm to solve the two intertwined optimization problems at the Switch Agent and Unit Agent levels. The results of each optimization are exchanged between the different holon levels. It would be possible to keep this general agent architecture but replace (MO-)COHDA with another algorithm. Since the optimal solutions for the evaluation scenarios are unknown, it is difficult to estimate how much the restoration performance can be improved in general. Also, to identify more suitable algorithms, performing a fitness landscape analysis of the scenarios would be helpful. Since COHDA is known to get stuck in local optima, an algorithm capable of escaping local optima might lead to better results if the fitness landscape has many of them. Another aspect is the relatively large number of messages required by COHDA. While this could be reduced with an optimized communication overlay, other algorithms may use fewer messages in general.

Multi-Objective Optimization: There are several ways to solve multi-objective optimization problems, and finding a set of Pareto optimal solutions is only one of them. Instead, it is possible to use a weighted sum or lexicographic approach. In the weighted sum approach, load restoration and ICT restoration are assigned a weight according to their priority. In the lexicographic approach, one of the goals is considered more important, and only if two solutions are equal in the first goal is the second goal used to distinguish. The lexicographic approach would help in those scenarios where restoring more ICT does not directly lead to more restored load. Focusing on load recovery first and ICT recovery second could reduce the number of scenarios in the C4 category. However, for those scenarios where restoring more ICT and less load in the first step leads to more restored load in later steps, this approach would lead to worse results. The weighted sum approach could work in this case, especially since the restored ICT was often much more than the limit on the restored load. Using a simpler optimization approach would reduce the runtime of the algorithm and could produce similarly good results. In both cases, the question remains how to handle the island balancing constraint.

ICT performance measure: Two design aspects are involved here: The first is how to compute the performance of the ICT restoration objective. The second is how to model the effect of ICT impairment on the restoration algorithm to represent the adverse effects of an incomplete communication system adequately. In the evaluation, two different versions were tested (Binary and Linear ICT states). The results already showed how a difference in ICT performance measurement and modeling of ICT impairment significantly impacts the algorithm's performance. Therefore, the exact modeling and definition of the interdependencies and the ICT performance measurement are critical to evaluating the algorithm's effectiveness in general. More detailed modeling may show a stronger relevance for MOO3 than the evaluation results have shown.

6.2 Future Work

This section presents several promising future research opportunities to further investigate the impact of ICT on power system restoration that have been identified from the findings and insights of this thesis.

Modeling the Effect of ICT Impairment: This thesis primarily focuses on the positive impact of prioritized ICT restoration on power system restoration. However, the differences between the Binary and Linear ICT States underscore the importance of defining the concrete negative impact of ICT impairment on power system restoration. In the Binary ICT States, impaired ICT leads to the unavailability of certain power system nodes in the restoration algorithm, while in the Linear states, it causes a reduction in available generation. Both versions are abstract models, and a more detailed study is necessary to understand the exact behavior of the ICT system during power system restoration and its concrete effects on the power system restoration. A comprehensive overview of possible effects was provided in Section 2.3.2.

Extending the ICT Performance Metric: There is a need to enhance the performance metric to better capture the intricate interdependencies between power and ICT system restoration. One approach could be to refine the concept of *ICT states* that reflect the quality of communication and thus the level of controllability of the respective power system element. A first approach was presented in Section 3.6. However, this approach is still on a theoretical level and only considers binary effects of failures. The possible states should be refined with more detailed in-between states and then thoroughly tested. It might also be relevant to evaluate ICT nodes in terms of which PS nodes are connected to them (so that, for example, a base station that connects fewer nodes, but all of which are generation units, gets priority in the communication system over connecting a grid area that consists only of loads). Also, from an ICT perspective, different ICT nodes might have different criticality, e.g., dependency between different ICT nodes, and critical nodes have to be restored first. Another interesting possibility is to look not only one step into the future (e.g., how the restored ICT will help in the next restoration step) but several steps, e.g., how many neighboring base stations a newly added base station would have.

Reduce dependency on initially available ICT: In the current approach, a PS node can only participate in the restoration process if the node itself is already part of the communication island. For this to work, specific requirements are placed on the ICT infrastructure; for example, in the case of wireless ICT, the overlapping of cells is such that the communication island is always larger than the PS island. However, there are also scenarios where the cells do not overlap perfectly, or in the case of wired scenarios, where the node itself has to be part of the PS island to be part of the communication island (unless it has battery backup). One idea to reduce this dependency is to either allow agents to have some information about neighboring nodes to decide if they can become part of the island network or not or to not place agents directly at the nodes but use them like virtualized network functions: All agents start in an area with available communication, no matter what network elements they represent, and then use historical data to decide about the island network. Once their node becomes part of the island grid, the agent can be migrated there and continue to monitor and control its element from there.

Additional objectives and constraints: With the multi-objective restoration algorithm, it is also possible to study the effect of other objectives, such as maximizing the amount of generation flexibility in the island or minimizing the uncertainty of the solution. Especially uncertainty in load and generation is a major challenge in managing an island grid since even small changes in the forecasted load or generation can cause instability and should, therefore, be considered in the optimization problem. Other constraints from both the power system and the ICT system (e.g., line loading, voltage limits, bandwidth limits) should also be considered so that the resulting island grid can have a stable operation. This could be done entirely by the agents, which would also require that all necessary information is distributed (e.g., each agent would have to be aware of current flows, thermal line limits, or node voltages to perform a load flow calculation). Or one could follow the concept of organic computing and introduce an observer and a controller into the system, which would check the final island network for these constraints and, if they are violated, trigger another negotiation with different parameters (e.g., limiting the amount of generation in a specific network area).

Adaptive objective function: The results show that the consideration of ICT is not relevant for every scenario and, within the C3 scenarios, not even in every restoration step. It should be investigated if it is possible to know at the beginning of a restoration step, based on specific characteristics of the scenario, whether ICT should be considered in the objective function so that the objectives can be chosen dynamically. This would allow the optimization to be only as complex as necessary.

Include dynamic part of power system restoration: Currently, the system is only considered in a steady state and focuses on planning the restoration process rather than performing it. However, the actual process would most likely have more stringent requirements on the state of the ICT system, which should also be considered when planning the island grid.

Include persisting disturbances: Until now, the power grid and the ICT infrastructure have been assumed to be fault-free and fully functional (once power is restored). This may not be the case, as the faults that caused the outage may still be present. Therefore, the restoration process should consider that there may be infrastructure damage in either the distribution network, the ICT system, or both.

Robustness to failures during restoration: Extending the previous point, not only could there be persistent failures in the systems, but it could also happen that previously functioning parts fail, both in the energy system and the ICT system. The recovery algorithm could be extended to handle such failures, such as the sudden disappearance of agents involved in a negotiation.

Allow restoration of parallel islands: This requires multiple starting points in the grid and coordination between the speakers of each island on when and how to merge neighboring island grids. It would also present new challenges for measuring ICT performance, as the restoration of ICT on one island could also positively impact the creation of a neighboring island, which should be taken into account.

Include the whole grid in the performance value: So far, only the current island grid is evaluated in the objective functions, i.e., all nodes connected to the blackstart capable node according to the current switch states are considered. This means that the switching decisions of Switch Agents that are not direct neighbors of the current island do not influence the performance value. It is worth investigating whether a "remaining network value" can improve performance when nodes not yet part of an island try to balance themselves.

Bibliography

[1] 50Hertz, Amprion, TenneT, and TransnetBW, *1. ergänzung zum maßnahmenkatalog der vier deutschen übertragungsnetzbetreiber mit regelzonenverantwortung zum netzwiederaufbauplan gemäß artikel 4 absatz 2 buchstabe c sowie artikel 23 absatz 4 buchstabe c eu-vo 2017/2196*, Accessed: 2024-07-24, 2024 (cit. on pp. 3, 23).

[2] 50hertz, amprion, tennet, and transnetbw, "Weißbuch netz- und versorgungswiederaufbau 2030," Tech. Rep., 2022, p. 32 (cit. on pp. 19, 21, 23, 31).

[3] acatech/Leopoldina/Akademienunion, *The resilience of digitalised energy systems. options for reducing blackout risks (series on science-based policy advice)*, Apr. 2021 (cit. on pp. 3, 29, 30).

[4] E. Ancillotti, R. Bruno, and M. Conti, "The role of communication systems in smart grids: Architectures, technical solutions and research challenges," *Computer Communications*, vol. 36, no. 17-18, pp. 1665–1697, 2013 (cit. on p. 28).

[5] G. Andersson, P. Donalek, R. Farmer, *et al.*, "Causes of the 2003 major grid blackouts in north america and europe, and recommended means to improve system dynamic performance," *IEEE transactions on Power Systems*, vol. 20, no. 4, pp. 1922–1928, 2005 (cit. on p. 2).

[6] A. Ansaria, "Analysis of ukraine power grid cyber-attack 2015," *World Journal of Advanced Engineering Technology and Sciences*, vol. 11, no. 1, pp. 410–412, 2024 (cit. on p. 2).

[7] P. M. Baidya and W. Sun, "Effective restoration strategies of interdependent power system and communication network," *The Journal of Engineering*, vol. 2017, no. 13, pp. 1760–1764, 2017 (cit. on pp. 5, 39).

[8] J. Banks, J. II, B. Nelson, and D. Nicol, *Discrete-Event System Simulation*. Jul. 2009 (cit. on p. 90).

[9] Z. Bie, Y. Lin, G. Li, and F. Li, "Battling the extreme: A study on the power system resilience," *Proceedings of the IEEE*, vol. 105, no. 7, pp. 1253–1266, 2017 (cit. on pp. 2, 3).

[10] M. Braun, *Beiträge erneuerbarer energien beim netzwiederaufbau*, `https://r8.ieee.org/germany-pes/wp-content/uploads/sites/169/2018/11/02-IEEE_Kassel_180925_EE_NWA_Braun.pdf` [Accessed: 10.04.2024], 2018 (cit. on p. 25).

[11] M. Braun, J. Brombach, C. Hachmann, *et al.*, "The future of power system restoration: Using distributed energy resources as a force to get back online," *IEEE Power and Energy Magazine*, vol. 16, no. 6, pp. 30–41, 2018 (cit. on pp. 1, 16, 17).

[12]M. Braun, C. Hachmann, and J. Haack, "Blackouts, restoration, and islanding: A system resilience perspective," *IEEE Power and Energy Magazine*, vol. 18, no. 4, pp. 54–63, 2020 (cit. on pp. 3, 23).

[13]J. Bremer and S. Lehnhoff, "The effect of laziness on agents for large scale global optimization," in *Agents and Artificial Intelligence: 11th International Conference, ICAART 2019, Prague, Czech Republic, February 19–21, 2019, Revised Selected Papers 11*, Springer, 2019, pp. 317–337 (cit. on p. 74).

[14]J. Bremera and S. Lehnhoffa, "Decentralized coalition formation with agent-based combinatorial heuristics," *REGULAR ISSUE*, p. 13, 2017 (cit. on p. 45).

[15]H. Buhl, T. Dombrowski, E. Hogen, *et al.*, "Ein algorithmus für den wiederaufbau eines smart grid nach einem blackout," *INFORMATIK 2017*, 2017 (cit. on p. 46).

[16]J. P. Carvalho, M. Shafie-khah, G. Osório, E. Rokrok, and J. P. Catalão, "Multi-agent system for renewable based microgrid restoration," in *2018 International Conference on Smart Energy Systems and Technologies (SEST)*, IEEE, 2018, pp. 1–6 (cit. on p. 38).

[17]L. Che and M. Shahidehpour, "Adaptive formation of microgrids with mobile emergency resources for critical service restoration in extreme conditions," *IEEE Transactions on Power Systems*, vol. 34, no. 1, pp. 742–753, 2018 (cit. on p. 48).

[18]B. Chen, C. Chen, J. Wang, and K. L. Butler-Purry, "Sequential service restoration for unbalanced distribution systems and microgrids," *IEEE Transactions on Power Systems*, vol. 33, no. 2, pp. 1507–1520, 2017 (cit. on p. 37).

[19]C. Chen, J. Wang, and D. Ton, "Modernizing distribution system restoration to achieve grid resiliency against extreme weather events: An integrated solution," *Proceedings of the IEEE*, vol. 105, no. 7, pp. 1267–1288, 2017 (cit. on pp. 22, 30).

[20]L. Clarke, Y.-M. Wei, A. D. L. V. Navarro, *et al.*, "Energy systems," in *Climate Change 2022: Mitigation of Climate Change. Contribution of Working Group III to the Sixth Assessment Report of the Intergovernmental Panel on Climate Change*. Cambridge, UK and New York, USA: Cambridge University Press, 2022 (cit. on pp. 18, 19).

[21]Council of European Energy Regulators (CEER), *Ceer benchmarking report 6.1 on the continuity of electricity and gas supply - data update 2015/2016*, Accessed: 2021-08-02, 2018 (cit. on p. 2).

[22]B. H. Czock, H. Diers, and P. Schnaars, "Versorgungssicherheit mit strom in einer kalten dunkelflaute-szenarien für 2030," *Zeitschrift für Energiewirtschaft*, vol. 47, no. 1, pp. 32–37, 2023 (cit. on p. 20).

[23]K. Deb, "Multi-objective optimization," in *Search methodologies*, Springer, 2014, pp. 403–449 (cit. on p. 64).

[24]D. K. Dheer, O. V. Kulkarni, S. Doolla, and A. K. Rathore, "Effect of reconfiguration and meshed networks on the small-signal stability margin of droop-based islanded microgrids," *IEEE Transactions on Industry Applications*, vol. 54, no. 3, pp. 2821–2833, 2018 (cit. on p. 48).

[25] N. L. Díaz, J. C. Vasquez, and J. M. Guerrero, “A communication-less distributed control architecture for islanded microgrids with renewable generation and storage,” *IEEE Transactions on Power Electronics*, vol. 33, no. 3, pp. 1922–1939, 2017 (cit. on p. 43).

[26] S. Dimitrijevic and N. Rajakovic, “Service restoration of distribution networks considering switching operation costs and actual status of the switching equipment,” *IEEE Transactions on Smart Grid*, vol. 6, no. 3, pp. 1227–1232, 2015 (cit. on p. 37).

[27] A. Dognini, A. Sadu, A. Angioni, F. Ponci, and A. Monti, “Service restoration algorithm for distribution grids under high impact low probability events,” in *2020 IEEE PES Innovative Smart Grid Technologies Europe (ISGT-Europe)*, IEEE, 2020, pp. 237–241 (cit. on p. 36).

[28] S. Dolev, “Self stabilization,” *Journal of Aerospace Computing, Information, and Communication*, vol. 1, no. 6, pp. 253–255, 2004 (cit. on pp. 68, 181).

[29] A. Elmitwally, M. Elsaid, M. Elgamal, and Z. Chen, “A fuzzy-multiagent service restoration scheme for distribution system with distributed generation,” *IEEE Transactions on Sustainable Energy*, vol. 6, no. 3, pp. 810–821, 2015 (cit. on pp. 4, 5, 40).

[30] M. Eriksson, M. Armendariz, O. O. Vasilenko, A. Saleem, and L. Nordström, “Multiagent-based distribution automation solution for self-healing grids,” *IEEE Transactions on industrial electronics*, vol. 62, no. 4, pp. 2620–2628, 2014 (cit. on pp. 5, 41).

[31] X. Fan, F. Wang, and J. Liu, “On backup battery data in base stations of mobile networks: Measurement, analysis, and optimization,” in *Proceedings of the 25th ACM International on Conference on Information and Knowledge Management*, ser. CIKM ’16, Indianapolis, Indiana, USA: Association for Computing Machinery, 2016, 1513–1522 (cit. on p. 89).

[32] M. Farrokhabadi, C. A. Canizares, J. W. Simpson-Porco, *et al.*, “Microgrid stability definitions, analysis, and examples,” *IEEE Transactions on Power Systems*, vol. 35, no. 1, pp. 13–29, 2019 (cit. on pp. 11, 22).

[33] C. Gerber, J. Siekmann, and G. Vierke, “Holonic multi-agent systems,” 1999 (cit. on p. 57).

[34] M. Ghorbanian, S. H. Dolatabadi, M. Masjedi, and P. Siano, “Communication in smart grids: A comprehensive review on the existing and future communication and information infrastructures,” *IEEE Systems Journal*, vol. 13, no. 4, pp. 4001–4014, 2019 (cit. on p. 32).

[35] A. Gloe, C. Jauch, and T. Räther, “Grid support with wind turbines: The case of the 2019 blackout in flensburg,” *Energies*, vol. 14, no. 6, p. 1697, 2021 (cit. on p. 19).

[36] L. Guan, H. Chen, and L. Lin, “A multi-agent-based self-healing framework considering fault tolerance and automatic restoration for distribution networks,” *IEEE Access*, vol. 9, pp. 21 522–21 531, 2021 (cit. on p. 41).

[37] Y. Guo, E. Torabi-Makhsos, G. Rossa-Weber, *et al.*, “Review on network restoration strategies as a part of the restoregrid4res project,” in *15. Symposium Energieinnovation*, vol. 1, 2018, pp. 1–8 (cit. on p. 22).

[38] U. O. Handbook, “Policy 1: Load-frequency control and performance,” *final version: v3. 0*, 2009 (cit. on p. 26).

[39] N. A. Heckert, J. J. Filliben, C. M. Croarkin, *et al.*, “Handbook 151: Nist/sematech e-handbook of statistical methods,” 2002 (cit. on p. 88).

[40] W. Heckmann, H. Becker, C. Hachmann, *et al.*, “Netz: Kraft. netzwiederaufbau unter berücksichtigung zukünftiger kraftwerksstrukturen. öffentlicher abschlussbericht,” 2019 (cit. on pp. 23, 28, 43).

[41] I. Helsloot and R. Beerens, “Citizens’ response to a large electrical power outage in the netherlands in 2007,” *Journal of Contingencies and Crisis Management*, vol. 17, no. 1, pp. 64–68, 2009 (cit. on p. 2).

[42] P. Hinkel, D. Henschel, M. Zugck, *et al.*, “Control center interfaces and tools for power system restoration,” in *International ETG-Congress 2019; ETG Symposium*, VDE, 2019, pp. 1–6 (cit. on p. 21).

[43] C. Hinrichs, S. Lehnhoff, and M. Sonnenschein, “Cohda: A combinatorial optimization heuristic for distributed agents,” in *International Conference on Agents and Artificial Intelligence*, Springer, 2013, pp. 23–39 (cit. on p. 8).

[44] C. Hinrichs, S. Lehnhoff, and M. Sonnenschein, “Cohda: A combinatorial optimization heuristic for distributed agents,” in *Agents and Artificial Intelligence: 5th International Conference, ICAART 2013, Barcelona, Spain, February 15-18, 2013. Revised Selected Papers 5*, Springer, 2014, pp. 23–39 (cit. on p. 44).

[45] C. Hinrichs and M. Sonnenschein, “A distributed combinatorial optimisation heuristic for the scheduling of energy resources represented by self-interested agents,” *International Journal of Bio-Inspired Computation*, vol. 10, no. 2, pp. 69–78, 2017 (cit. on pp. 45, 66, 69, 175, 176).

[46] C. Hinrichs and M. Sonnenschein, “Evaluation guidelines for asynchronous distributed heuristics in smart grid applications.,” in *EnviroInfo*, 2014, pp. 365–372 (cit. on p. 10).

[47] H. Holma and A. Toskala, *LTE for UMTS: Evolution to LTE-advanced*. New York, NY, USA: John Wiley & Sons, 2011 (cit. on p. 89).

[48] S. Howell, Y. Rezgui, J.-L. Hippolyte, B. Jayan, and H. Li, “Towards the next generation of smart grids: Semantic and holonic multi-agent management of distributed energy resources,” *Renewable and Sustainable Energy Reviews*, vol. 77, pp. 193–214, 2017 (cit. on p. 57).

[49] IEA, *Solar pv power capacity in the net zero scenario, 2015-2030*, `https://www.iea.org/data-and-statistics/charts/solar-pv-power-capacity-in-the-net-zero-scenario-2015-2030` [Accessed: 10.04.24], 2024 (cit. on p. 25).

[50] IPCC, in *Climate Change 2022: Mitigation of Climate Change. Contribution of Working Group III to the Sixth Assessment Report of the Intergovernmental Panel on Climate Change*. Cambridge, UK and New York, USA: Cambridge University Press, 2022 (cit. on p. 18).

[51]A. Kavousi-Fard, A. Zare, and A. Khodaei, “Effective dynamic scheduling of reconfigurable microgrids,” *IEEE Transactions on Power Systems*, vol. 33, no. 5, pp. 5519–5530, 2018 (cit. on p. 48).

[52]M. Klaes, A. Narayan, A. D. Patil, *et al.*, “State description of cyber-physical energy systems,” *Energy Informatics*, vol. 3, pp. 1–19, 2020 (cit. on p. 72).

[53]U. G. Knight, “Power systems in emergencies: From contingency planning to crisis management,” in Wiley-Blackwell, 2001, ch. 7 (cit. on pp. 16–18).

[54]M. Kuzlu, M. Pipattanasomporn, and S. Rahman, “Communication network requirements for major smart grid applications in han, nan and wan,” *Computer Networks*, vol. 67, pp. 74–88, 2014 (cit. on pp. 28, 29).

[55]S. Larsson and A Danell, “The black-out in southern sweden and eastern denmark, september 23, 2003.,” in *2006 IEEE PES power systems conference and exposition*, IEEE, 2006, pp. 309–313 (cit. on p. 2).

[56]S. Lehnhoff *et al.*, “Towards fully decentralized multi-objective energy scheduling,” in *2019 Federated Conference on Computer Science and Information Systems (FedCSIS)*, IEEE, 2019, pp. 193–201 (cit. on p. 46).

[57]S. Lei, C. Chen, Y. Song, and Y. Hou, “Radiality constraints for resilient reconfiguration of distribution systems: Formulation and application to microgrid formation,” *IEEE Transactions on Smart Grid*, vol. 11, no. 5, pp. 3944–3956, 2020 (cit. on p. 48).

[58]S. Lei, J. Wang, and Y. Hou, “Remote-controlled switch allocation enabling prompt restoration of distribution systems,” *IEEE Transactions on Power Systems*, vol. 33, no. 3, pp. 3129–3142, 2017 (cit. on p. 26).

[59]J. B. Leite and J. R. S. Mantovani, “Development of a self-healing strategy with multiagent systems for distribution networks,” *IEEE Transactions on Smart Grid*, vol. 8, no. 5, pp. 2198–2206, 2016 (cit. on p. 5).

[60]B. Li, S. Basu, S. J. Watson, and H. W. Russchenberg, “A brief climatology of dunkelflaute events over and surrounding the north and baltic sea areas,” *Energies*, vol. 14, no. 20, p. 6508, 2021 (cit. on p. 20).

[61]W. Li, Y. Li, C. Chen, *et al.*, “A full decentralized multi-agent service restoration for distribution network with dgs,” *IEEE Transactions on Smart Grid*, vol. 11, no. 2, pp. 1100–1111, 2019 (cit. on pp. 4, 41).

[62]L. Lindgren, *Automatic power system restoration: application of a search algorithm*. Department of Measurement Technology and Industrial Electrical Engineering ..., 2009 (cit. on p. 4).

[63]I. Loeser, M. Braun, C. Gruhl, *et al.*, “The vision of self-management in cognitive organic power distribution systems,” *Energies*, vol. 15, no. 3, p. 881, 2022 (cit. on p. 35).

[64]L. H. Macedo, G. Muñoz-Delgado, J. Contreras, and R. Romero, “Optimal restoration of distribution networks through reconfiguration and microgrid formation,” in *2020 IEEE PES Innovative Smart Grid Technologies Europe (ISGT-Europe)*, Ieee, 2020, pp. 1231–1235 (cit. on p. 4).

[65] F. Mahdavian, S. Platt, M. Wiens, M. Klein, and F. Schultmann, "Communication blackouts in power outages: Findings from scenario exercises in germany and france," *International Journal of Disaster Risk Reduction*, vol. 46, p. 101 628, 2020 (cit. on p. 149).

[66] P. McKeever, E. De Din, A. Sadu, and A. Monti, "Mas for automated black start of multi-microgrids," in *2017 IEEE International Conference on Smart Grid Communications (SmartGridComm)*, IEEE, 2017, pp. 32–37 (cit. on pp. 4, 5, 41).

[67] S. Meinecke, N. Bornhorst, L.-P. Lauven, *et al.*, *Simbench documentation - documentation version en-1.0.0*, `https://simbench.de/wp-content/uploads/2020/01/simbench_documentation_en_1.0.0.pdf`, 2020 (cit. on p. 86).

[68] S. Meinecke, D. Sarajlić, S. R. Drauz, *et al.*, "Simbench—a benchmark dataset of electric power systems to compare innovative solutions based on power flow analysis," *Energies*, vol. 13, no. 12, p. 3290, 2020 (cit. on p. 110).

[69] J. V. Milanović and W. Zhu, "Modeling of interconnected critical infrastructure systems using complex network theory," *IEEE Transactions on Smart Grid*, vol. 9, no. 5, pp. 4637–4648, 2017 (cit. on p. 50).

[70] L. Mota, A. Mota, and A Morelato, "Load behaviour prediction under blackout conditions using a fuzzy expert system," *IET Generation, Transmission & Distribution*, vol. 1, no. 3, pp. 379–387, 2007 (cit. on p. 27).

[71] A. Narayan, M. Klaes, D. Babazadeh, S. Lehnhoff, and C. Rehtanz, "First approach for a multi-dimensional state classification for ict-reliant energy systems," in *International ETG-Congress 2019; ETG Symposium*, VDE, 2019, pp. 1–6 (cit. on pp. 72, 73).

[72] A. Narayan, M. Klaes, S. Lehnhoff, and C. Rehtanz, "Analyzing the propagation of disturbances in cpes considering the states of ict-enabled grid services," in *2021 IEEE Electrical Power and Energy Conference (EPEC)*, IEEE, 2021, pp. 522–529 (cit. on p. 73).

[73] nationalgridESO, *Black start from non-traditional generation technologies*, `https://www.nationalgrideso.com/document/148201/download`, Accessed: 2023-05-08, 2019 (cit. on pp. 20, 21).

[74] M. Nebel-Wenner, C. Reinhold, F. Wille, A. Nieße, and M. Sonnenschein, "Distributed multi-objective scheduling of power consumption for smart buildings," *Energy Informatics*, vol. 2, pp. 1–19, 2019 (cit. on p. 46).

[75] A. Nieße, M. Tröschel, and M. Sonnenschein, "Designing dependable and sustainable smart grids–how to apply algorithm engineering to distributed control in power systems," *Environmental Modelling & Software*, vol. 56, pp. 37–51, 2014 (cit. on p. 13).

[76] F. Oest, M. Radtke, M. Blank-Babazadeh, S. Holly, and S. Lehnhoff, "Evaluation of communication infrastructures for distributed optimization of virtual power plant schedules," *Energies*, vol. 14, no. 5, p. 1226, 2021 (cit. on p. 45).

[77] A. Pahwa, S. A. DeLoach, B. Natarajan, *et al.*, "Goal-based holonic multiagent system for operation of power distribution systems," *IEEE transactions on smart grid*, vol. 6, no. 5, pp. 2510–2518, 2015 (cit. on p. 57).

[78] G. Patsakis, D. Rajan, I. Aravena, J. Rios, and S. Oren, "Optimal black start allocation for power system restoration," *IEEE Transactions on Power Systems*, vol. 33, no. 6, pp. 6766–6776, 2018 (cit. on p. 24).

[79] T. Petermann, H. Bradke, A. Lüllmann, M. Poetzsch, and U. Riehm, *What happens during a blackout: Consequences of a prolonged and wide-ranging power outage* (Technology Assessment Studies Series). Büro für Technikfolgen-Abschätzung beim Deutschen Bundestag (TAB), 2011, vol. 4, 256 pp. (cit. on pp. 1, 32–34).

[80] T. Petermann, H. Bradke, A. Lüllmann, M. Poetzsch, and U. Riehm, *What happens during a blackout: Consequences of a prolonged and wide-ranging power outage*, 2014 (cit. on p. 5).

[81] M. Pietsch, A. Klein, and F. Steinke, "Merging microgrids for optimal distribution grid restoration under explicit communication constraints," in *2020 Resilience Week (RWS)*, IEEE, 2020, pp. 48–54 (cit. on p. 40).

[82] S. Poudel and A. Dubey, "A two-stage service restoration method for electric power distribution systems," *arXiv preprint arXiv:2004.07921*, 2020 (cit. on p. 48).

[83] F. Prillwitz and M. Krüger, "Netzwiederaufbau nach großstörungen," *Universität Rostock, Institut für Elektrische Energietechnik, Rostock*, 2007 (cit. on pp. 16, 17).

[84] Y. Ren, D. Fan, Q. Feng, *et al.*, "Agent-based restoration approach for reliability with load balancing on smart grids," *Applied energy*, vol. 249, pp. 46–57, 2019 (cit. on pp. 4, 38).

[85] E. Rokrok, M. Shafie-khah, P. Siano, and J. P. Catalão, "A decentralized multi-agent-based approach for low voltage microgrid restoration," *Energies*, vol. 10, no. 10, p. 1491, 2017 (cit. on p. 37).

[86] F. C. Sampaio, R. P. Leao, R. F. Sampaio, L. S. Melo, and G. C. Barroso, "A multi-agent-based integrated self-healing and adaptive protection system for power distribution systems with distributed generation," *Electric Power Systems Research*, vol. 188, p. 106 525, 2020 (cit. on p. 38).

[87] L. Schröder and C. Klaue, "Eingeschneit: Schneechaos im münsterland," *Abgerufen von https://www1. wdr. de/fernsehen/heimatflimmern/sendungen/schneechaos-immuensterland-100. html*, 2021 (cit. on p. 2).

[88] N. A. of Sciences, Engineering, and Medicine *et al.*, *Enhancing the resilience of the nation's electricity system*. National Academies Press, 2017 (cit. on pp. 25, 26).

[89] M. Sedighizadeh, G. Shaghaghi-shahr, M. Esmaili, and M. R. Aghamohammadi, "Optimal distribution feeder reconfiguration and generation scheduling for microgrid day-ahead operation in the presence of electric vehicles considering uncertainties," *Journal of Energy Storage*, vol. 21, pp. 58–71, 2019 (cit. on p. 48).

[90] I. Serban, S. Cespedes, C. Marinescu, *et al.*, "Communication requirements in microgrids: A practical survey," *IEEE Access*, vol. 8, pp. 47 694–47 712, 2020 (cit. on pp. 26, 28, 35).

[91] A. Sharma, A. Trivedi, and D. Srinivasan, “Multi-stage restoration strategy for service restoration in distribution systems considering outage duration uncertainty,” *IET Generation, Transmission & Distribution*, vol. 12, no. 19, pp. 4319–4326, 2018 (cit. on pp. 6, 38).

[92] E Shirazi and S Jadid, “A multiagent design for self-healing in electric power distribution systems,” *Electric Power Systems Research*, vol. 171, pp. 230–239, 2019 (cit. on pp. 4, 38).

[93] J. W. Simpson-Porco, Q. Shafiee, F. Dörfler, *et al.*, “Secondary frequency and voltage control of islanded microgrids via distributed averaging,” *IEEE Transactions on Industrial Electronics*, vol. 62, no. 11, pp. 7025–7038, 2015 (cit. on p. 43).

[94] S. Stark, E. Frost, and M. Nebel-Wenner, *Distributed multi-objective optimization in cyber-physical energy systems*, 2024 (cit. on pp. 46, 64, 66).

[95] S. Stark, A. Volkova, S. Lehnhoff, and H. de Meer, “Why your power system restoration does not work and what the ict system can do about it,” in *Proceedings of the twelfth ACM international conference on future energy systems*, 2021, pp. 269–273 (cit. on pp. 81, 86, 89, 97).

[96] C. Steinhart, M. Finkel, M. Gratza, *et al.*, “Abschlussbericht zum verbundvorhaben linda,” 2019 (cit. on p. 42).

[97] A Sujil, J. Verma, and R. Kumar, “Multi agent system: Concepts, platforms and applications in power systems,” *Artificial Intelligence Review*, vol. 49, no. 2, pp. 153–182, 2018 (cit. on p. 4).

[98] I. Taleb, G. Guérard, F. Fauberteau, and N. Nguyen, “A holonic multi-agent architecture for smart grids.,” in *ICAART (1)*, 2023, pp. 126–134 (cit. on p. 57).

[99] UCTE, *Final report system disturbance on 4 november 2006*, `https://eepublicdownloads.entsoe.eu/clean-documents/pre2015/publications/ce/otherreports/Final-Report-20070130.pdf`, Accessed: 2024-08-01, 2007 (cit. on p. 2).

[100] Union for the Co-ordination of Transmission of Electricity (UCTE), “P5 - Policy 5: Emergency Operations,” in *UCTE Operation Handbook*, UCTE, 2010, pp. 1–46 (cit. on pp. 1, 12, 15–18).

[101] VDE Verband der Elektrotechnik Elektronik Informationstechnik e.V, *Zellulares energiesystem – ein beitrag zur konkretisierung des zellularen ansatzes mit handlungsempfehlungen*, Accessed: 2024-07-25, 2019 (cit. on p. 57).

[102] A. Volkova, J. Terzer, and H. de Meer, “Quantifying geospatial interdependencies of ict and power system based on open data,” *Energy Informatics*, vol. 4, pp. 1–12, 2021 (cit. on pp. 97, 111, 112).

[103] J. Wäfler and P. E. Heegaard, “Interdependency in smart grid recovery,” *2015 7th International Workshop on Reliable Networks Design and Modeling (RNDM)*, pp. 201–207, 2015 (cit. on p. 5).

[104] J. Wäfler and P. E. Heegaard, "Interdependency modeling in smart grid and the influence of ict on dependability," in *Meeting of the European Network of Universities and Companies in Information and Communication Engineering*, Springer, 2013, pp. 185–196 (cit. on p. 73).

[105] M. Xiang, D. Yu, W. Wang, *et al.*, "The reason analysis of holland blackout on march 27, 2015 and lessons for hunan power grid," *J. Clean Energy Technol*, vol. 6, no. 3, pp. 263–267, 2018 (cit. on p. 2).

[106] Y. Xu, C.-C. Liu, K. P. Schneider, and D. T. Ton, "Placement of remote-controlled switches to enhance distribution system restoration capability," *IEEE Transactions on Power Systems*, vol. 31, no. 2, pp. 1139–1150, 2015 (cit. on p. 26).

[107] Y. Xu, C.-C. Liu, K. P. Schneider, F. K. Tuffner, and D. T. Ton, "Microgrids for service restoration to critical load in a resilient distribution system," *IEEE Transactions on Smart Grid*, vol. 9, no. 1, pp. 426–437, 2016 (cit. on p. 37).

[108] L. Yang, Y. Xu, H. Sun, M. Chow, and J. Zhou, "A multiagent system based optimal load restoration strategy in distribution systems," *International Journal of Electrical Power & Energy Systems*, vol. 124, p. 106314, 2021 (cit. on pp. 4, 5, 41).

[109] B. Zhang, C. Dou, D. Yue, Z. Zhang, and T. Zhang, "A cyber-physical cooperative hierarchical control strategy for islanded microgrid facing with random communication failure," *IEEE Systems Journal*, vol. 14, no. 2, pp. 2849–2860, 2020 (cit. on p. 40).

[110] A. Zidan, M. Khairalla, A. M. Abdrabou, *et al.*, "Fault detection, isolation, and service restoration in distribution systems: State-of-the-art and future trends," *IEEE Transactions on Smart Grid*, vol. 8, no. 5, pp. 2170–2185, 2016 (cit. on pp. 1, 4, 35, 36).

List of Figures

List of Tables

Appendix A

A.1 Detailed Convergence Proof of Blackstart Algorithm

The following sections describe the formal convergence proof for the two new types of agents. To distinguish the newly added parts from the convergence proof directly taken from Hinrichs et al. in [45], the original convergence proof is written in Blue.

Table A.1 summarizes the elements used in the formal description.

Tab. A.1.: Notation for COHDA

Symbol	Description
$a_i \in A$	Agent
$N_i \subseteq A$	Neighbourhood of agent a_i
S_i	Set of feasible schedules of agent a_i
$\omega_i = (a_i, \theta_i, \lambda_i)$	Schedule selection of agent a_i with identifier, selected schedule and value of counting variable
$\kappa_i = (\zeta, \Omega_i, \gamma_i)$	Working memory of agent a_i
ζ	Target profile
$\Omega_i = \{\omega_j, \omega_k, ..., \}$	Believed set of current schedule selections (System Config) of agent a_i
$\gamma_i = (a_x, \Omega)$	Solution candidate of agent a_i with best known schedule selection and agent id of agent who found it

A.1.1 Non-atomic Agents with Single-objective Optimization

For non-atomic agents with single-objective optimization, the behavior is shown in algorithm 1, with the original algorithm marked in blue and the changes in black. Since the aggregator agent has no initial knowledge of its lower level holon, S_i is initially empty. If the agent has made any changes to its working memory in perceive, the target for the lower holon is created based on the difference between the agent's target a_i and the current system configuration γ_i, without the agent's own schedule choice ω_i. This target ζ^{low} is then sent to the lower level holon, triggering the COHDA process there (lines 26 to 29). The agent must now wait for the result of this negotiation τ_i to include the schedule in its schedule selection S_i, then follow the same decide and act steps as in the basic COHDA process. When an agent reaches act here, it always sends its working memory to the neighbors since it is already clear that changes have been made in the perceive step (otherwise, the agent would not even perform decide).

The following describes the convergence proof for non-atomic agents with single-objective optimisation, focusing on the differences from the basic COHDA convergence in [45].

As no message can physically be delivered in a zero timespan, we discretise real-time with a resolution of s, where s denotes the minimal amount of real-time an arbitrary message needs to be delivered, and call s a time step. We may now define *COHDA-task, result-task*, *period*, *execution* and *termination*, followed by two lemmas regarding the liveliness of the system:

- *Task*: In their initial state, agents are inactive, i.e., waiting for incoming messages. An agent can receive two different message types, a *COHDA-message* and a *result-message*. When an agent is inactive, and a message is received, the agent performs the actions depicted in Algorithm 1. Together, these actions are called a task. It is distinguished between *COHDA-task* and *result-task*, corresponding to the two types of messages an agent can receive. A task is considered as atomic, i.e., message deliveries do not interfere with running tasks, and an agent may only execute at most one task at a time. Messages that are received by an agent while being active, i.e., while executing a task, will be placed in a buffer storage and will come into effect directly afterwards. Due to possibly varying processing speeds of the machine the agent runs on, an agent may be busy executing a single task over several time steps.
  - *COHDA-task:* If an agent a_i is active and processing a COHDA-message, its currently running COHDA-task is denoted with t_i^c. A COHDA-task includes lines 1 to 30 in Algorithm 1. If the working memory κ_i of a_i is not modified during a task t_i^c, this task is called *passive*. If the working memory is modified, the agent is called *waiting*, meaning it has triggered the underlying holon and is waiting for a result-message. While waiting, an agent can still start new tasks. All buffered COHDA-messages are handled at once by concatenating their contents together.
  - *Result-task:* If an agent a_i is active and processing a result-message, its currently running result-task is denoted with t_i^r. A result-task includes lines 31 to 42 in Algorithm 1. Result-tasks in the buffer storage will be

Algorithm 1 Behaviour of an non-atomic agent a_i with single-objective optimization in the restoration algorithm

Local attributes:

S_i ▷ Set of feasible schedules (is initially empty)
λ_i ▷ Schedule selection counting variable
$\kappa_i = (\zeta, \Omega_i, \gamma_i)$ ▷ Working memory: target, system config, solution candidate

Objective functions:

$f(\gamma), f(\Omega)$ ▷ Rates γ or Ω according to the global objective function
accept(θ_i) ▷ true, iff θ_i acceptable according to local objectives

Behaviour:

if receiving message κ_j **then**
  $\zeta_j \leftarrow \zeta \in \kappa_j$ ▷ Extract target profile from message
  $\Omega_j \leftarrow \Omega_j \in \kappa_j$ ▷ Extract system configuration from message
  $\gamma_j \leftarrow \gamma_j \in \kappa_j$ ▷ Extract solution candidate from message
  $\omega_i \leftarrow \omega_i \in \Omega_i$ ▷ Extract own schedule selection from Ω_i
  $\kappa_j' \leftarrow (\zeta, \Omega_i, \gamma_i)$ ▷ Create backup of own working memory
  $K_i \leftarrow \{a_k | \omega_k \in \Omega_i\}$ ▷ Extract agent identifiers from γ_i
  $K_j \leftarrow \{a_k | \omega_k \in \Omega_j\}$ ▷ Extract agent identifiers from γ_j
  if $\zeta =$ None **then**
    $\zeta \leftarrow \zeta_j$ ▷ Store target profile
  end if
  for $\omega_k \in \Omega_i, \omega_k' \in \Omega_j$ **do** ▷ Update Ω_i
    if $\forall \omega_x \in \Omega_i : x \neq k$ **or** $\lambda_k \in \omega_k' > \lambda_k \in \omega_k$ **then**
      $\Omega_i \leftarrow (\Omega_i \backslash \{\omega_k\}) \cup \{\omega_k'\}$
    end if
  end for ▷ Replace/extend solution candidate...
  if $K_i \subset K_j$ **then** ▷ ...if the new one is larger
    $\gamma_i \leftarrow \gamma_j$
  else if $K_i \not\subseteq K_j$ **then** ▷ ...or if it contains entries from unknown agents
    $\gamma_i \leftarrow (a_i, \{\omega_k \in \gamma_i\} \cup \{\omega_k | a_k \in K_j - K_i\})$
  else if $f(\gamma_j) > f(\gamma_i)$ **then** ▷ ...or if it rates better
    $\gamma_i \leftarrow \gamma_j$
  else if $f(\gamma_j) = f(\gamma_i)$ **and** $a_x \in \gamma_j > a_y \in \gamma_i$ **then** ▷ ...or to break ties
    $\gamma_i \leftarrow \gamma_j$
  end if
  if $(\zeta, \Omega_i, \gamma_i) \neq \kappa_i'$ **then**
    $\zeta^{low} \leftarrow \zeta - (\gamma_i \backslash \{\omega_i\})$ ▷ Calculate difference from system config to target
    send ζ^{low} to lower level holon
  end if
end if
if receiving message τ_i **then**
  $S_i \leftarrow \tau_i$ ▷ Extract schedule from result
  $\omega_i' \leftarrow \omega_i \in \gamma_i$ ▷ Extract own schedule selection from γ_i
  if $\exists \theta \in S_i : f((\Omega_i \backslash \{\omega_i\}) \cup \{(a_i, \theta, \lambda_i + 1)\}) > f(\gamma_i)$ **and** accept(θ) **then** ▷ Better schedule found?
    $\omega_i' \leftarrow (a_i, \theta, \lambda_i + 1)$ ▷ Create new schedule selection
    $\lambda_i \leftarrow (a_i, (\Omega_i \backslash \{\omega_i\}) \cup \{\omega_i'\})$ ▷ Create new solution candidate
  else if $\omega_i \neq \omega_i'$ **then** ▷ Historical schedule chosen?
    $\omega_i' \leftarrow (a_i, \theta \in \omega_i', \lambda_i + 1)$ ▷ Create new schedule selection using the historical schedule
  end if
  $\Omega_i \leftarrow (\Omega_i \backslash \{\omega_i\}) \cup \{\omega_i'\}$ ▷ Update Ω_i with new schedule selection
  send $(\zeta, \Omega_i, \gamma_i)$ to neighbours ▷ Always publish working memory to neighbours
end if

handled individually. At the end of a result-task an agent always sends its working memory κ_i to its neighbours.

- *Period*: Let d_{max} be a constant that denotes the maximal number of time steps a message can possibly be delayed in the system. Further, let r_{max} be a constant that denotes the maximal number of time steps an agent can possibly require to execute a task. Finally, let w_{max} be a constant that denotes the maximal number of time steps an agent has to spend in waiting before receiving a result message. Then $\rho = d_{max} + r_{max} + w_{max}$ is called a period.

- *Execution*: Let $t_s = (s_u, s_v, \dots)$ be a series of consecutive time steps. Then within each $s_u \in t_s$, an arbitrary number of distinct agents may be active executing tasks. Let $T_u = \{t_i^x, t_j^x, \dots\}$ be the (possibly empty) set of tasks that will be finished in time step s_u. Then, $e = (T_u, T_v, \dots)$ is called an execution of the system.

- *Termination*: Let e be an arbitrary execution in which every agent $a_i \in A$ finishes at least one task. If for every agent $a_i \in A$ the most recent task in e is a passive COHDA-task t_i^c and no agent has the status waiting, the system terminates with the execution of e, and e is called a terminating execution.

Lemma 0: Any agent in waiting status will receive a result message in a finite amount of time, triggering a result-task t_i^r and exiting the waiting status.

Proof: The waiting status is entered after a COHDA process has been triggered in the lower-level holon. That means a COHDA process is started there. No matter how many holon layers there are, at some point, a layer would consist only of atomic agents, and for them, convergence is proven based on the basic COHDA convergence proof. This means the result message would travel upwards, and the agent a_i would receive a result message in a finite amount of time.

Lemma 1: As long as the heuristic is not terminated, within any period of ρ time steps, at least one agent a_i is active and either finishes a COHDA-task t_i^c that is not passive and thus sending a target message to the lower level holon or finishes a result-task t_i^r and thus sending its working memory κ_i to its neighbours.

Proof: This directly follows from defs. *task*, *period*, *execution*, *termination* and the connectedness property of the communication network.

Lemma 2: As long as the heuristic is not terminated, within any $\rho \cdot |A|$ time steps every agent $a_i \in A$ finishes at least once a COHDA-task t_i^c that is not passive or a result-task t_i^r.

Proof: This directly follows from Lemma 1.

Completeness (predicate $\mathcal{A}_1$) *Theorem 3*: Within a finite amount of time steps after starting the heuristic, $\mathcal{A}_1$ will eventually hold.

Proof: Following from Lemma 2 and the integration of data in lines 9 to 20 of the behaviour in Algorithm 1, every agent in the system gains some knowledge about all other agents in the system as well as the target profile ζ within at most $\rho \cdot |A|$ time steps after starting the heuristic.

Final solution candidate (predicate $\mathcal{A}_2$) Let e be an arbitrary execution. We denote the sum of the ratings of all solution candidates in the system after executing e by:

$$h(e) = \sum_{a_i \in A} f(\gamma_i) \tag{A.1}$$

Lemma 4: The COHDA heuristic has the anytime property in the following sense: Given an execution e that implies that $\mathcal{A}_1$ holds. Then for any possible additional completion of a COHDA-task t_i^c or a result-task t_i^r of an arbitrary agent a_i the value of the function (Equation A.1) cannot decrease:

$$e' = e + t_i^c \vee e + t_i^r \Rightarrow h(e') \geq h(e) \tag{A.2}$$

Proof: We consider the formalisation of the considered tasks t_i^c and t_i^r in Algorithm 1. As the value of the function (A.1) is influenced by the modification of solution candidates only, we may focus on lines 17 to 25 for the COHDA-task and lines 33 to 36 for the result-task. Here, lines 17 to 20 can further be ignored due to the completeness induced by $\mathcal{A}_1$. In lines 21 to 22, γ_i is replaced with γ_j as the latter has a higher rating according to the objective function. This yields an increase of the value of the function (A.1). In lines 23 to 25, γ_i is replaced with an equally rated γ_j, if the identifier of γ_j's creator, say a_x, is superordinate to the identifier of γ_i's creator, say a_y, with respect to a lexicographic ordering. This is done to break ties of equally rated solution candidates, and yields an unchanged value of the function (1). Finally, in lines 33 to 36 in the result-task, γ_i is replaced with a newly created solution candidate that yields a higher rating than the existing one under the circumstance that an appropriate schedule can be found. The value of the function (A.1) increases with this action. In summary, the implication (A.2) holds with every possible execution of a task t_i^x

Lemma 5: The COHDA heuristic is deadlock-free in the following sense: Given an execution e which implies that $\mathcal{A}_1$ holds. Then with every possible non-terminating continuation e^+ of the execution e the value of the function (A.1) will eventually increase.

Proof: As described in Algorithm 1 , the value of the function (A.1) remains unchanged by a task t_i^x of an arbitrary agent a_i in the following two cases only:

1. When handling a COHDA-task t_i^c the solution candidate γ_i is kept unchanged.
2. When handling a result-task t_i^r the solution candidate γ_i is replaced by γ_j, which has the same rating but a lexicographically superordinate creator-ID.

Following Lemma 2 and the fact that the considered execution fragment e^+ is non-terminating, there may be at most $\rho \cdot |A| - 1$ consecutive time steps in e^+ in which case 1 holds for all tasks therein. Hence, within any $\rho \cdot |A|$ time steps the solution candidate of an arbitrary agent will be replaced. Moreover, due to the uniqueness of the identifiers $a_i \in A$, case 2 can only happen at most $|A| - 1$ times without introducing new solution candidates with a higher rating somewhere in between. Hence, in the worst case, a solution candidate with a higher rating will be created in $\rho \cdot |A|^2$ time steps at the latest in e^+, effectively increasing the function value (A.1).

Theorem 6: Within a finite amount of time steps after $\mathcal{A}_1$ holds, $\mathcal{A}_2$ will eventually hold.

Proof: As defined in the introduction of Section 3.5, for each agent $a_i \in A$, its respective search space S_i is finite. Hence, as a solution candidate comprises exactly one schedule element from each S_i in the system, only a finite number of possible solution candidates exists in the system. A non-atomic agent has no initial S_i itself but rather builds its search space up based on the results it receives from the lower level. However, since the search space of atomic agents is finite, the search space of the upper-level agents is also finite. Moreover, from Lemma 4 and Lemma 5 is known that, as long as the heuristic is not terminated, better solution candidates will successively be generated. It follows that eventually a solution candidate will be found by an arbitrary agent in the system, which subsequently cannot be improved any further (or replaced by another solution candidate).

Due to the *anytime* and *deadlock-free* properties, the heuristic produces better and better solutions over time, and might be stopped arbitrarily. This could easily be realised by a special signal to the agents, which forbids the creation of new solution candidates.

Also, please note that Theorem 6 neither implies completeness nor optimality. Anyway, the solution space of the optimisation problem usually is not fully enumerated in the search process. Instead, a final solution candidate can (and typically will) be found much earlier.

Termination (Predicate A3) In the following, we will denote the final solution candidate by γ^*. If an agent, say a_i, receives γ^* within a message from a neighbour, say a_j, and assigns it to its own working memory (i.e., $\gamma_i \leftarrow \gamma_j$ with $\gamma_j = \gamma^*$ according to lines 21 to 25 in Algorithm 1), we may say that a_i *knows* γ^* from this point in time on. It remains to be shown that γ^*, which is created by a single arbitrary agent at some point in time (line 36 in Algorithm 1), will subsequently spread through the system until it is known to every agent, and that the heuristic afterwards will terminate in a state where the working memories of all agents are identical (note that, due to line 40 in Algorithm 1, it suffices to reason about solution candidates rather than whole working memories to prove termination in the following).

Theorem 7: Within a finite amount of time steps after $\mathcal{A}_2$ holds, $\mathcal{A}_3$ will eventually hold.

Proof: Let e be an arbitrary execution that implies that $\mathcal{A}_2$ holds, i.e., the final solution candidate γ^* is known to at least one agent. We denote the number of agents that know γ^* after executing e by $t(e)$. Then, according to [28], we can define a variant function as follows:

$$VF(e) = |A - t(e)| \tag{A.3}$$

The domain of VF is $[0, |A|]$. Now let e_t be an arbitrary terminating execution (see defs. *execution* and *termination*) with

$$e_t = (\underbrace{T_a, T_b, ...}_{e_p}, T_m, \underbrace{T_u, T_v, ...}_{e_s}) \tag{A.4}$$

Here, the first part $e_p = (T_a, T_b, \dots)$ until T_m (excluding), is an arbitrary prefix. Let $T_m \Rightarrow VF(e_p + T_m) < VF(e_p)$, i.e., in T_m, at least one agent that didn't know γ^* in e_p, receives γ^* within a message and stores it in its working memory according to lines 21 to 25 in Algorithm 1. We denote $A_{m+} = \{a_i | t_i^c \in T_m \wedge t_i^c \text{ is not passive}\}$ as the non-empty set of those agents. We now have to show that the function A.3 monotonically decreases with every possible suffix $e_s = (T_u, T_v, \dots)$, that it eventually approaches zero, and that the system then terminates within a finite number of time steps. For this, we have to consider two cases regarding the execution $e' = e_p + T_m$:

1. $VF(e'_p) = 0$, i.e., after executing e'_p , all agents know γ^*. Following lines 26 to 29 in Algorithm 1, all agents $a_i \in A_{m+}$ will trigger the underlying holon by sending a target message and then go into waiting state. According to Lemma 0, an agent in waiting will receive a result message in a finite amount of time, thereby starting the result task. Following lines 40 to 41 in Algorithm 1, all agents $a_i \in A_{m+}$ will send a message containing their working memory to each of their neighbours. From def. *period* follows that all these messages will be received and processed within at most ρ time steps, such that $|e_s| \leq \rho$. As the receiving agents already know γ^*, all COHDA-tasks in e_s are passive, and the system terminates according to def. *termination*.

2. $VF(e'_p) > 0$, i.e., there exists an agent, say a_i, which does not know γ^* after e'_p has been executed, but which has a neighbour, a_j, who does know γ^*. Following lines 26 to 29 in Algorithm 1, a_j, after learning about γ^*, will trigger the underlying holon by sending a target message and then go into waiting state. According to Lemma 0, an agent in waiting will receive a result message in a finite amount of time, thereby starting the result task. Following lines 40 to 41, a_j sends a message with its working memory to a_i. From def. period follows that this message will be received and processed by a_i within at most ρ time steps. Let $e'_t = e'_p + e'_s$ with $e'_s = (..., T_x) \subseteq e_s)$ be the execution until the point in time in which a_i processed this message (in a COHDA-task $t_i^c \in T_x$) and thus also knows γ^*. Then, in summary, the value of the function A.3 has been decreased within at most ρ time steps after T_m, and the present distinction of cases has to be evaluated again for e'_t.

Following this recursive reasoning, as long as $VF(e) > 0$ for an arbitrary execution e, the value of the variant function will decrease within at most ρ time steps after executing e. After the variant function reaches zero, the system terminates within at most ρ time steps comprising only passive tasks.

A.1.2 Non-atomic Agents with Multi-objective Optimization

Table A.2 shows the updated notation for MO-COHDA in the restoration algorithm. The set C_i of an agent is the set of allowed switch combinations depending on which agents are part of the current system configuration Ω_i. A switch is only allowed to close if information about the other bus is available, so initially, only one combination with all switches is allowed. The lower level γ_x^{low} results contain all aggregated information from the elements connected to the bus that the Switch Agent represents, separated into load, generation, and ICT information. This separation is necessary for the different objective functions (see section 3.2), each requiring different information. Due to the multi-objective problem solving, the agents have to choose not only one result for the bus and one state for each switch but one result and one state for each solution point. Therefore, the choices for all solution points are stored in a set X_i^{bus} and X_i^{switch} for buses and switches, respectively. The system configuration Ω_i of an agent now contains one of these sets for each bus and switch that has already been added to the working memory by an agent. The target profile λ can either be 0 in every timestep (default if the Switch Agents are on the highest holon level and try to create a balanced island) or describe the value needed to reach 0 in every timestep (if there is another holon level above which a specific target was sent). In the following, those parts of the convergence proof described in subsection 3.5.2 will be analyzed that are affected by these changes, and it will be shown that they still hold.

Definitions: For a better overview, *Cohda-task* and *result-task* for non-atomic agents in the multi-objective case have been separated into two different algorithms, Algorithm 2 and Algorithm 3 respectively. Lines 1 to 43 in Algorithm 2 process a COHDA-meassge, and lines 1 to 22 in Algorithm 3 process a result message. Otherwise, the same rules as described in subsection 3.5.2 for *Task*, *Period*, *Execusion* and *Termination* apply.

Proof for Lemma 0: In addition to the proof described in subsection 3.5.2, it should be noted here that even though a Switch Agent can send more than one target at a

Algorithm 2 Behaviour of an non-atomic agent a_i in reaction to COHDA message with multi-objective optimization in the restoration algorithm

Local attributes:

C_i ▷ Set of allowed switch combinations (initially only open)
τ_i ▷ Set of results from lower level (initially empty)
$L = \{\lambda_j^{switch}, \lambda_k^{switch}, ...\}$ ▷ Switch state selection counting variables
λ_i^{bus} ▷ Bus data selection counting variable
$\kappa_i = (\zeta, \Omega_i, \gamma_i)$ ▷ Working memory: target, system config, solution candidate

Objective functions:

$F = (f_1, f_2, ...f_n)$ ▷ List of Objective Functions
$f_n(\Omega_x^{bus}, \Omega_x^{switch})$ ▷ Rates Solution point x according to objective function f_n
$HV(F, f^{ref}, \Omega)$, $HV(F, f^{ref}, \gamma)$ ▷ Calculates hypervolume of Ω or γ

Behaviour:

if receiving message κ_j **then**
  $\zeta_j \leftarrow \zeta \in \kappa_j$ ▷ Extract target profile from message
  $\Omega_j \leftarrow \Omega_j \in \kappa_j$ ▷ Extract system configuration from message
  $\gamma_j \leftarrow \gamma_j \in \kappa_j$ ▷ Extract solution candidate from message
  $\kappa_j' \leftarrow (\zeta, \Omega_i, \gamma_i)$ ▷ Create backup of own working memory
  $K_i^{bus} \leftarrow \{a_k | X_k^{bus} \in \Omega_i\}$ ▷ Extract bus identifiers from γ_i
  $K_j^{bus} \leftarrow \{a_k | X_k^{bus} \in \Omega_j\}$ ▷ Extract bus identifiers from γ_j
  $K_i^{switch} \leftarrow \{s_k | X_k^{switch} \in \Omega_i\}$ ▷ Extract switch identifiers from γ_i
  $K_j^{switch} \leftarrow \{s_k | X_k^{switch} \in \Omega_j\}$ ▷ Extract switch identifiers from γ_j
  if $\zeta =$ None **then**
    $\zeta \leftarrow \zeta_j$ ▷ Store target profile
  end if
  for $X_k^{bus} \in \Omega_i, X_k^{bus'} \in \Omega_j$ **do** ▷ Update bus data in Ω_i
    for $\omega_{k_x}^{bus} \in X_k^{bus}, \omega_{k_x}^{bus'} \in X_k^{bus'}$ **do**
      if $\forall \omega_{y_x}^{bus} \in X_k^{bus} : y \neq k$ **or** $\lambda_k^{bus'} \in \omega_{k_x}^{bus'} > \lambda_k^{bus} \in \omega_{k_x}^{bus}$ **then**
        $X_k^{bus} \leftarrow (X_k^{bus} \setminus \{\omega_{k_x}^{bus}\}) \cup \{\omega_{k_x}^{bus'}\}$
      end if
    end for
  end for
  for $X_k^{switch} \in \Omega_i, X_k^{switch'} \in \Omega_j$ **do** ▷ Update switch data in Ω_i
    for $\omega_{k_x}^{switch} \in X_k^{switch}, \omega_{k_x}^{switch'} \in X_k^{switch'}$ **do**
      if $\forall \omega_{y_x}^{switch} \in X_k^{switch} : y \neq k$ **or** $\lambda_k^{switch'} \in \omega_{k_x}^{switch'} > \lambda_k^{switch} \in \omega_{k_x}^{switch}$ **then**
        $X_k^{switch} \leftarrow (X_k^{switch} \setminus \{\omega_{k_x}^{switch}\}) \cup \{\omega_{k_x}^{switch'}\}$
        if $s_n \in \omega_{k_x}^{switch'} : s_n \in C_i$ **then**
          $\lambda_i^{switch} \leftarrow \lambda_k^{switch'}$ ▷ Update switch counter to current highest
        end if
      end if
    end for
  end for ▷ Replace/extend solution candidate:
  if $K_i^{bus} \subset K_j^{bus}$ **then** ▷ If the new one is larger
    $\gamma_i \leftarrow \gamma_j$
  else if $K_i^{bus} \not\subseteq K_j^{bus}$ **then** ▷ Or if it contains entries from unknown buses
    $\Omega_i^{merged} \leftarrow \{\{X_k^{bus} \in \gamma_i\} \cup \{X_l^{switch} \in \gamma_i\} \cup \{X_k^{bus} | a_k \in K_j^{bus} - K_i^{bus}\} \cup X_l^{switch} | s_l \in K_j^{switch} - K_i^{switch}\}\}$
    $\gamma_i \leftarrow (a_i, \Omega_i^{merged})$
  else if $HV(F, f^{ref}, \gamma_j) > HV(F, f^{ref}, \gamma_i)$ **then** ▷ Or if it rates better
    $\gamma_i \leftarrow \gamma_j$
  else if $HV(F, f^{ref}, \gamma_j) = HV(F, f^{ref}, \gamma_i)$ **and** $a_x \in \gamma_j > a_y \in \gamma_i$ **then**
    $\gamma_i \leftarrow \gamma_j$ ▷ Or to break ties
  end if
  if $(\zeta, \Omega_i, \gamma_i) \neq \kappa_i'$ **then**
    Update C_i
    create targets Z for lower level optimization
    send Z to lower level holon
  end if
end if

Algorithm 3 Behaviour of a non-atomic agent a_i in reaction to result message with multi-objective optimization in the restoration algorithm

Local attributes:

C_i ▷ Set of allowed switch combinations
τ_i ▷ Set of results from lower level
$L = \{\lambda_j^{switch}, \lambda_k^{switch}, ...\}$ ▷ Switch state selection counting variables
λ_i^{bus} ▷ Bus data selection counting variable
$\kappa_i = (\zeta, \Omega_i, \gamma_i)$ ▷ Working memory: target, system config, solution candidate

Objective functions:

$F = (f_1, f_2, ...f_n)$ ▷ List of Objective Functions
$f_n(\Omega_x^{bus}, \Omega_x^{switch})$ ▷ Rates Solution point x according to objective function f_n
$HV(F, f^{ref}, \Omega)$, $HV(F, f^{ref}, \gamma)$ ▷ Calculates hypervolume of Ω or γ

Behaviour:

if receiving message τ_i **then**
  $\tau_i \leftarrow \tau_i$ ▷ Store results
  $X_i^{bus} \leftarrow X_i^{bus} \in \Omega_i$ ▷ Extract own bus data selection from Ω_i
  $X_i^{bus'} \leftarrow X_i^{bus} \in \gamma_i$ ▷ Extract own bus data selection from γ_i
  $\mathbb{X}_i^{switch} \leftarrow X_j^{switch} \in \Omega_i : s_i \in C_i$ ▷ Extract own switch data selection from Ω_i
  $\mathbb{X}_i^{switch'} \leftarrow X_j^{switch} \in \gamma_i : s_i \in C_i$ ▷ Extract own switch data selection from γ_i
  $\mathbb{S} \leftarrow$ Create possible solution points from τ_i, C_i and the data in Ω_i
  if $\exists\{X_m^{bus}, \mathbb{X}_n^{switch}\} \subseteq \mathbb{S} : HV(F, f^{ref}, (\Omega_i \backslash \{X_i^{bus} \cup \mathbb{X}_j^{switch}\}) \cup \{X_m^{bus}, \mathbb{X}_n^{switch}\}) > HV(F, f^{ref}, \gamma_i)$ **then** ▷ Better Pareto front found?
    $X_i^{bus'} \leftarrow X_m^{bus}$ ▷ Create new bus data selection
    $\mathbb{X}_j^{switch'} \leftarrow \mathbb{X}_n^{switch}$ ▷ Create new switch data selection
    $\lambda_i \leftarrow (a_i, (\Omega_i \backslash \{X_i^{bus} \cup \mathbb{X}_j^{switch}\}) \cup \{X_m^{bus}, \mathbb{X}_n^{switch}\})$ ▷ Create new solution candidate
  else ▷ Historical data chosen?
    if $X_i^{bus} \neq X_i^{bus'}$ **then**
      $\forall \omega_{i_x}^{bus'} \in X_i^{bus'} \leftarrow (a_i, \gamma_i^{low} \in \omega_i^{bus'} x, \lambda_i^{bus} + 1)$ ▷ Create new bus data selection using the historical bus data
    end if
    if $\mathbb{X}_j^{switch} \neq \mathbb{X}_j^{switch'}$ **then**
      $\forall \omega_{i_x}^{switch'} \in \mathbb{X}_j^{switch'} \leftarrow (s_i, t_i \in \omega_{i_x}^{switch'}, \lambda_i^{switch} + 1)$ ▷ Create new switch data selection using the historical switch data
    end if
  end if
  $\Omega_i \leftarrow (\Omega_i \backslash \{X_i^{bus} \cup \mathbb{X}_j^{switch}\}) \cup \{X_m^{bus}, \mathbb{X}_n^{switch}\}$ ▷ Update Ω_i with new bus and switch data selection
  send $(\zeta, \Omega_i, \gamma_i)$ to neighbours ▷ Always publish working memory to neighbours
end if

Tab. A.2.: Notation for MO-COHDA in restoration algorithm

Symbol	Description
$a_i \in A$	Agent
$N_i \subseteq A$	Neighbourhood of agent a_i
$C_i = \{c_1, c_2, ...\}$	Set of all allowed switch combinations for agent a_i for the current κ_i
$c_m = \{(s_x, t_x), (s_y, t_y), ...\}$	Single switch combination with switch identifier and switch state
$t_x \in [0, 1]$	Switch state can be open (0) or closed (1)
$\tau_i = \{\gamma_1^{low}, \gamma_2^{low}, ...\}$	Collected solution candidates from lower level for agent a_i to choose from
$\gamma_x^{low} = (\gamma^{load}, \gamma^{gen}, \gamma^{ICT})$	Lower Level result with aggregated load, gen and ICT
$\omega_{ix}^{bus} = (a_i, \gamma_i^{low}, \lambda_i^{bus})$	Bus data selection of agent a_i for solution point x with identifier, selected solution candidate and counting variable
$\omega_{ix}^{switch} = (s_i, t_i, \lambda_i^{switch})$	Switch state selection for switch s_i for solution point x with switch combination, state and counting variable
$X_i^{bus} = \{\omega_{i1}^{bus}, ..., \omega_{in}^{bus}\}$	Bus data selections for all n solution points of agent a_i
$X_i^{switch} = \{\omega_{i1}^{switch}, ..., \omega_{in}^{switch}\}$	Switch state selections for all n solution points of switch s_i
$\kappa_i = (\zeta, \Omega_i, \gamma_i)$	Working memory of agent a_i
ζ	Target profile
$\Omega_i = ((X_j^{bus}, X_k^{bus}, ...), (X_l^{switch}, X_m^{switch}, ...))$	Believed set of all selected bus data and switch data of agent a_i
$\gamma_i = (a_x, \Omega)$	Solution candidate of agent a_i with best known set of solution points and agent id of agent who found it

time to the lower level to trigger a negotiation there, the set of targets Z created in line 40 of algorithm 2 must be finite. This ensures that while the maximum waiting time ω_{max} may be greater than ω_{max} for non-atomic single-objective agents, a waiting agent will still receive a result message in a finite amount of time. How exactly the targets in Z are chosen depends on the implementation. The maximum number of different targets is to take all allowed switch combinations in C_i, apply them to all solution points in Ω_i, calculate the island balance for each resulting island grid, and subtract it from the target λ.

Proof for Theorem 3: Data integration for non-atomic multi-objective agents is shown in lines 10 to 34 of the algorithm 2. While it is more complex due to the more complicated data structure, it still follows the same rules as the basic COHDA perceive. The data is separated into bus and switch data, and each bus and each switch has its own set of data for each solution point. The bus data is updated in lines 13 to 19 of the algorithm 2 by checking if there is information on a bus that is not yet in the working memory or if there is newer data on a bus based on the counting variable. This is done for every solution point. Lines 20 to 29 do the same for switch data. Note that since two agents can control the same switch, two agents can also increase the switch count variable. If an agent notices that the switch counting variable of one of the switches it controls is higher than the one it currently has stored, it must update it (lines 24 and 25). It can still happen that both agents a_i and a_j controlling a switch s_k have the same count variable λ_k^{switch} with different states, e.g., a_i has $t_k = 0$, and a_j has $t_k = 1$. However, when comparing the solution candidates in lines 30 to 39, only one set of solution points with s_k having a defined state (either $t_k = 0$ or $t_k = 1$) would be selected, which is then also integrated into the system configuration at the end of decide in line 20 of algorithm 3.

When comparing the solution candidates in lines 30 and 32, only the bus identifiers are needed because new switches can only exist if there is a new bus, but a new bus can not exist without a new switch. However, the switch data is updated to include new switches in line 33 when the solution candidate is updated. Overall, the data integration still ensures that each agent in the system gains some knowledge about all other agents in the system and the target profile λ within at most $\rho \cdot |A|$ time steps after starting the heuristic.

Proof for Lemma 4: Instead of evaluating individual solutions, the hypervolume of the set of non-dominated solutions is evaluated. Therefore, the sum of the ratings of all solution candidates in the system after an arbitrary execution e for the multi-objective case can be defined by:

$$h(e) = \sum_{a_i \in A} HV(F, f^{ref}, \gamma_i) \tag{A.5}$$

However, the concept still holds that a solution candidate γ_i is only replaced by γ_j – after the working memory is complete – if the latter has a higher rating according to the hypervolume, or, in the case of the same hypervolume, if the identifier of the creator of γ_j is higher than the identifier of the creator of γ_i. This is handled in lines 35 to 36 and 37 to 38 of the 2 algorithm, respectively. Finally, in lines 8 to 11 of algorithm 3, γ_i is replaced by a newly created set of non-dominated solutions that yield a higher hypervolume than the existing one, if the agent was able to identify better solution points. In summary, this means that for the multi-objective non-atomic case, the implication A.2 holds for every possible execution of a task t_x.

Proof for Theorem 6: The search space for all Switch Agents $a_i \in A$ is still finite. It consists of the possible switch combinations C_i and the lower level negotiation results τ_i. As defined before, the search space of atomic agents is always finite, i.e., the search space of the upper-level agents is also finite. Therefore, τ_i will always be finite. The number of switches controlled by an agent is finite, so the number of different possible switch combinations for the agent is also finite. Finally, the number of solution points to search is predefined and fixed, as explained in Section 3.4. New solution points are created using τ_i and C_i to replace the old agent choices in Ω_i. In the algorithm 3, this is summarized on a general level in line 7 since there could be different approaches to creating new solution points (e.g., picking only single solution points and randomly changing switch states or bus data, or creating all possible combinations). No matter the approach, the agents can only create a finite number of different solution points, leading to a finite number of different sets of non-dominated points. It follows that at some point, any agent in the system will find a solution candidate that cannot be improved upon (or replaced by another solution candidate).

Apart from these changes, the rest of the convergence proof is identical to the one described in subsection A.1.1.

A.2 Overview of Aggregated Simbench Time Series

The following subsections show the graph of the aggregated time series for both the rural and urban grid for the different time of years and time of weeks. With one time series value per 15-minute interval there is a total of 94 values for one 24-h-day (starting from 00:00 and ending at 23:45). Load and generation of the same type of year are always scaled to the same y-axis value for better comparison of the generation-load-ratio.

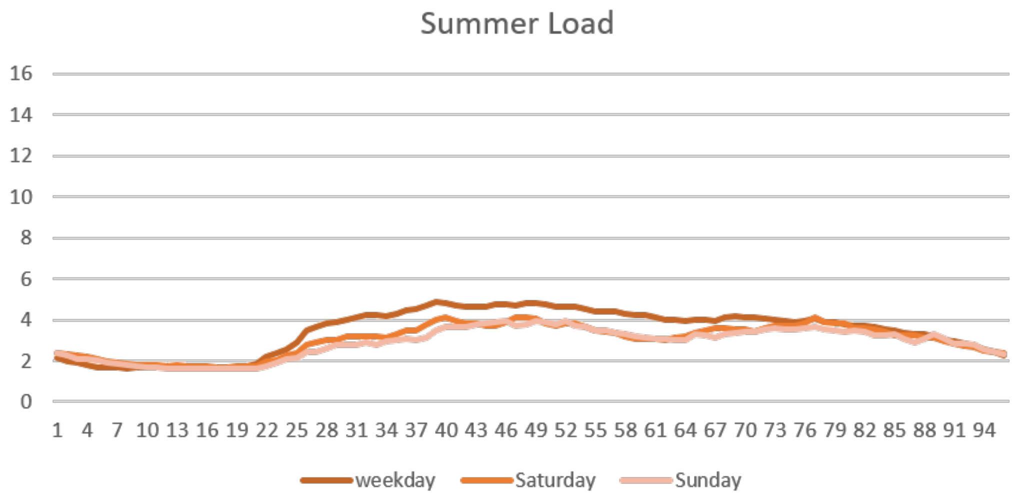

Fig. A.1.: Aggregated time series for rural summer load

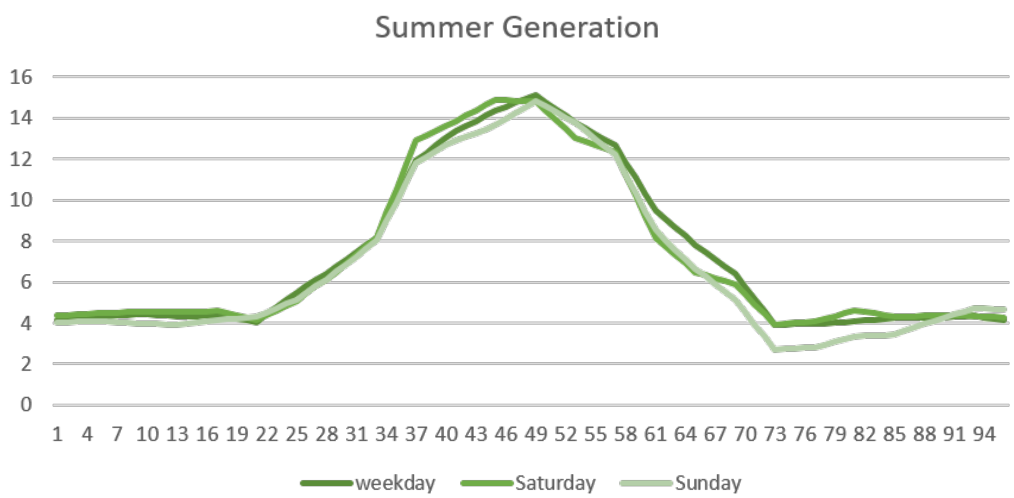

Fig. A.2.: Aggregated time series for rural summer generation

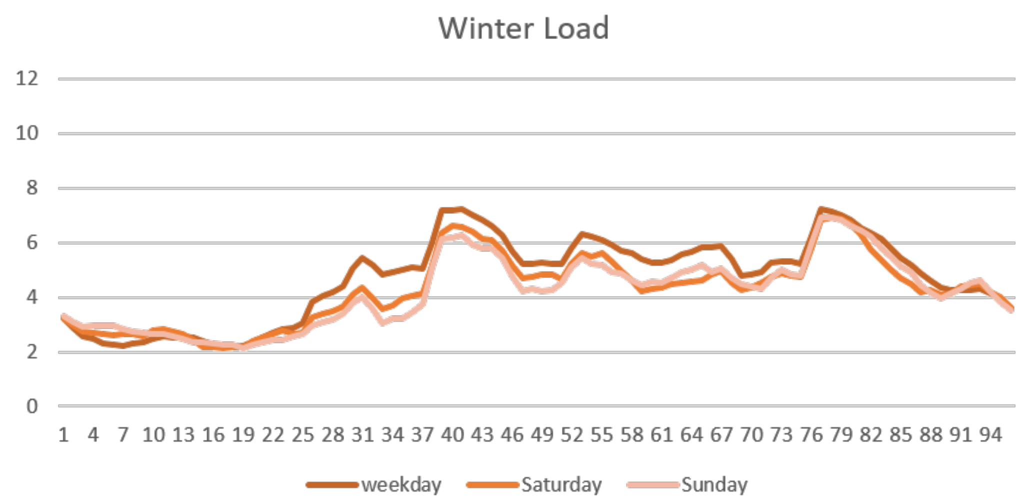

Fig. A.3.: Aggregated time series for rural winter load

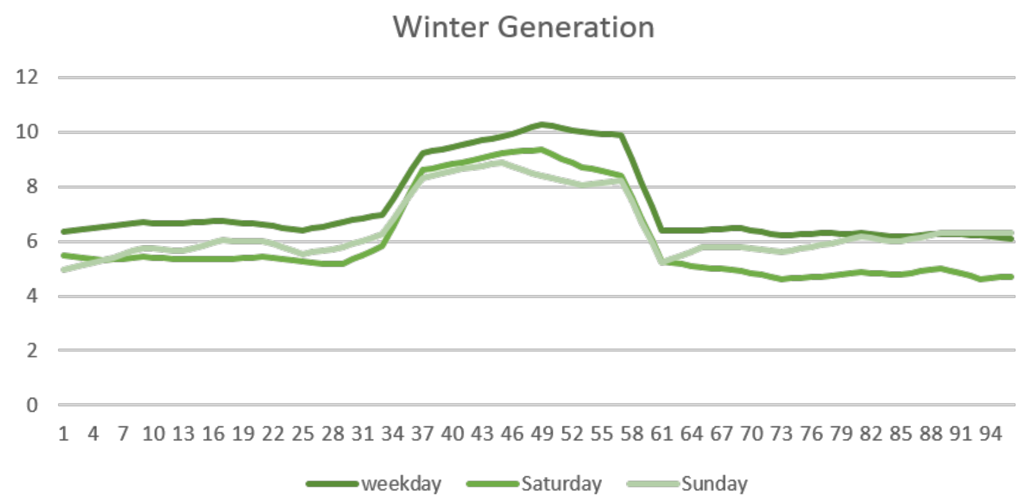

Fig. A.4.: Aggregated time series for rural winter generation

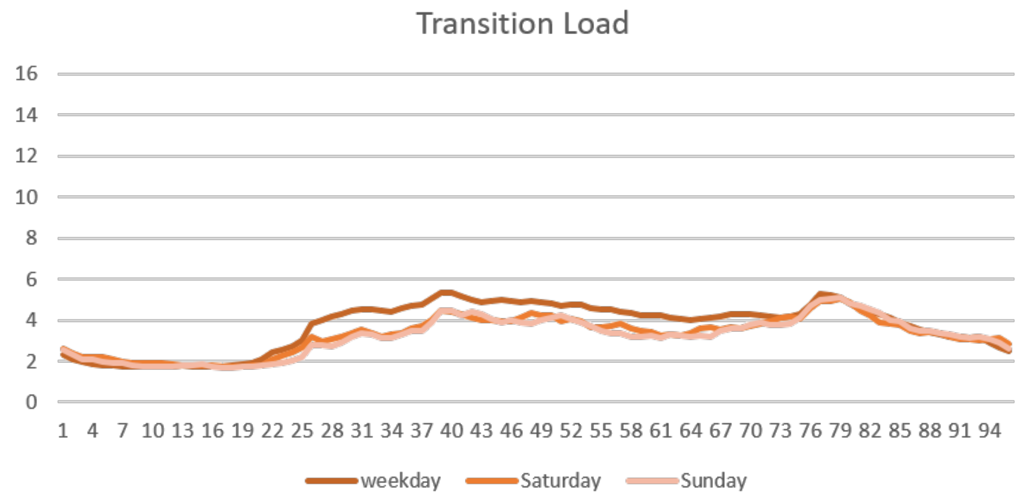

Fig. A.5.: Aggregated time series for rural transition load

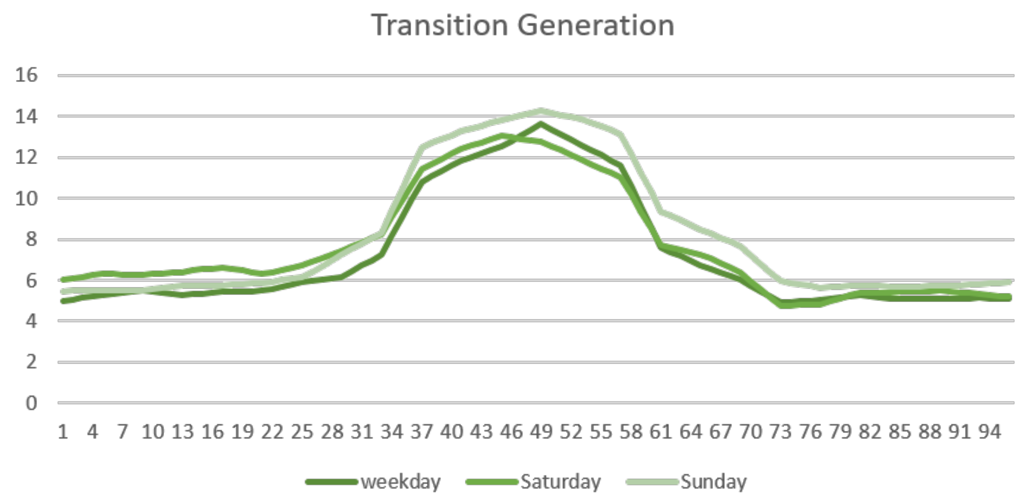

Fig. A.6.: Aggregated time series for rural transition generation

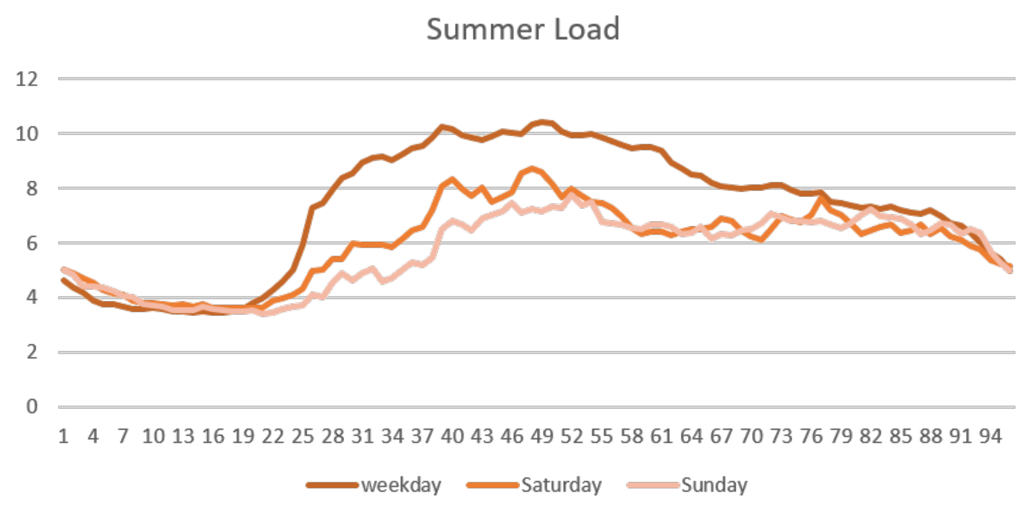

Fig. A.7.: Aggregated time series for urban summer load

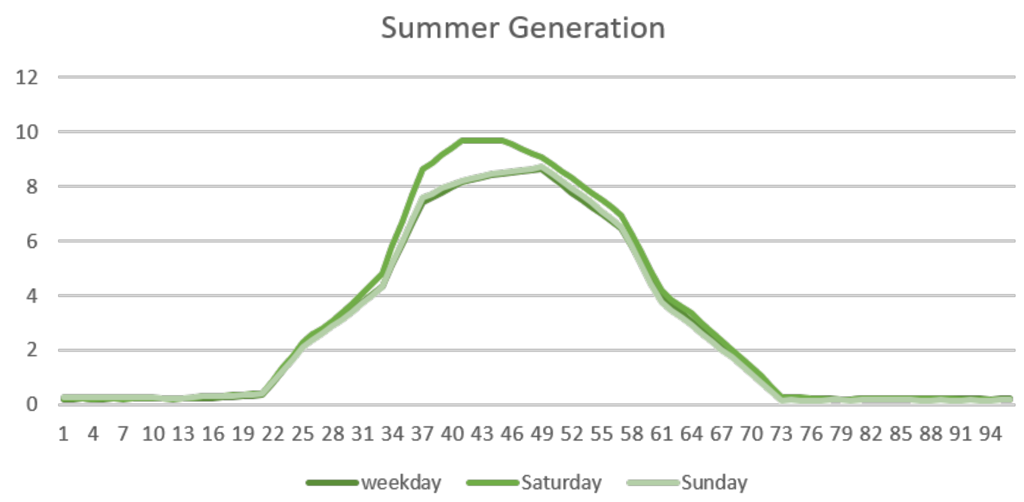

Fig. A.8.: Aggregated time series for urban summer generation

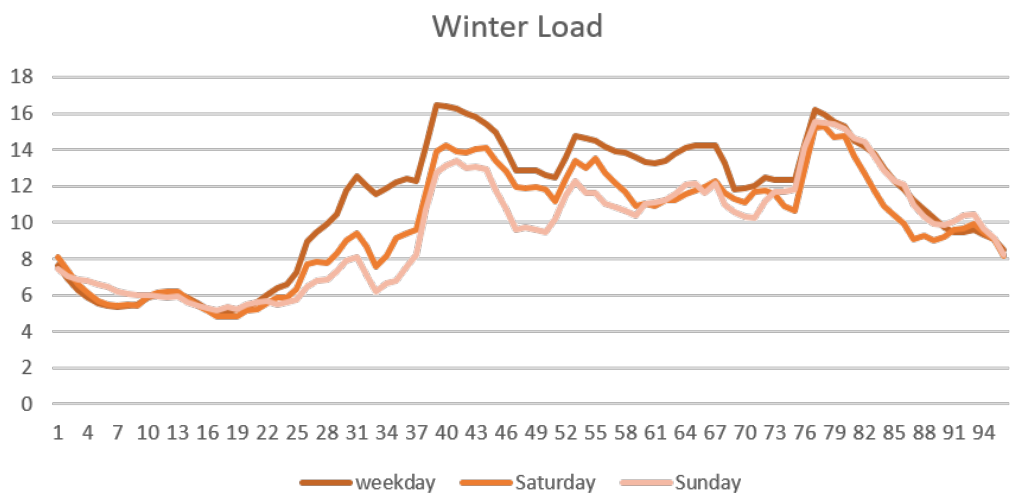

Fig. A.9.: Aggregated time series for urban winter load

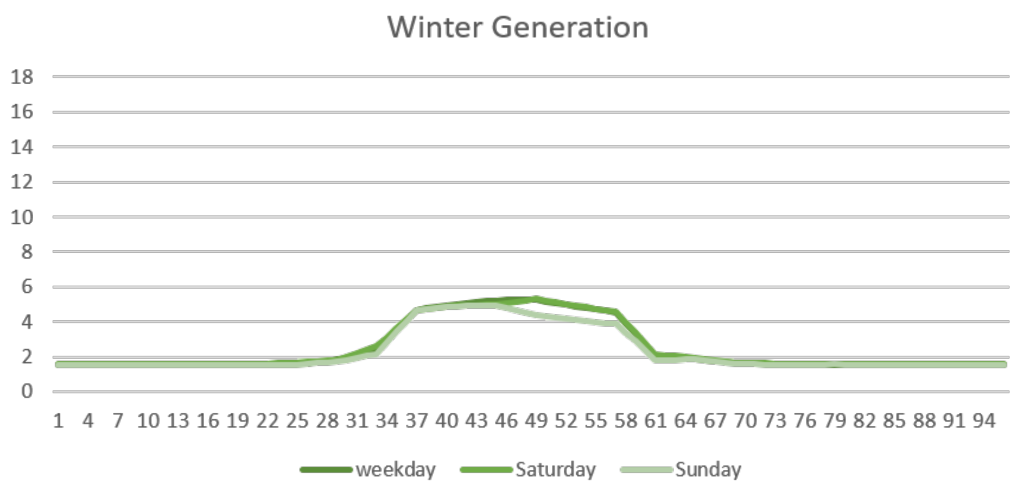

Fig. A.10.: Aggregated time series for urban winter generation

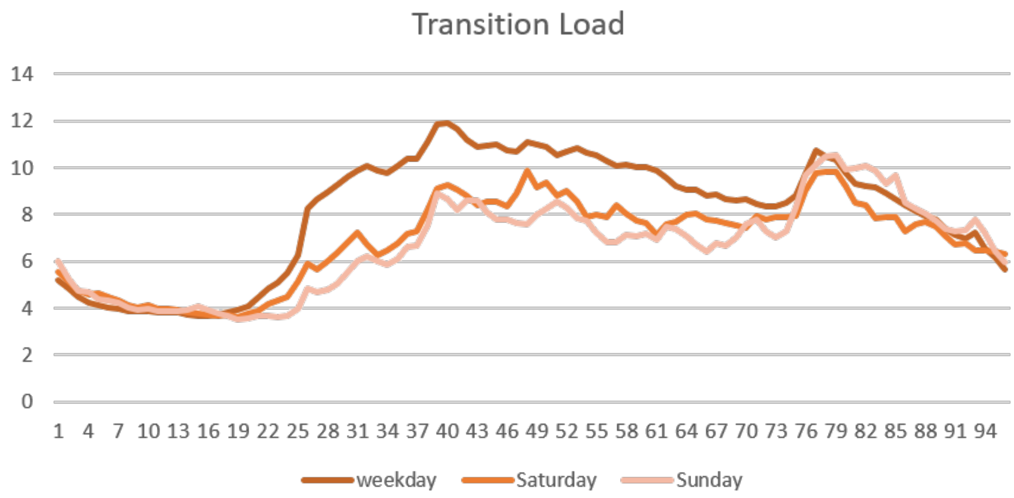

Fig. A.11.: Aggregated time series for urban transition load

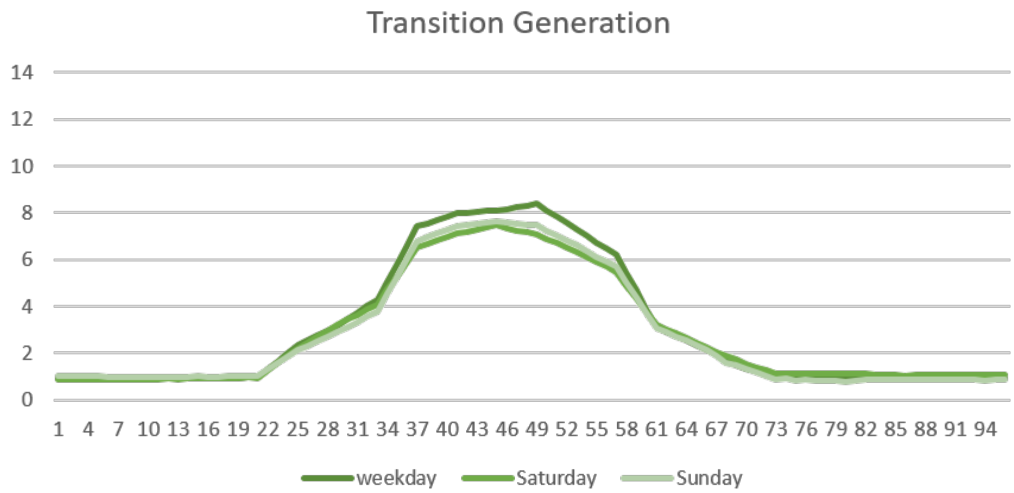

Fig. A.12.: Aggregated time series for urban transition generation

Erklärung

Hiermit erkläre ich, dass ich diese Arbeit eigenständig verfasst und keine anderen als die angegebenen Hilfsmittel und Quellen benutzt habe. Ebenso versichere ich, dass diese Dissertation weder in ihrer Gesamtheit noch in Teilen einer anderen wissenschaftlichen Hochschule zur Begutachtung in einem Promotionsverfahren vorgelegen hat.

Declaration

I declare that I have written this thesis independently and that I have used only the resources indicated. I also affirm that this dissertation has not been submitted by me, in whole or in part, to any other university for assessment in a doctoral procedure.

Oldenburg, 09. Januar 2025

Sanja Stark